UiT
THE ARCTIC
UNIVERSITY
OF NORWAY

Faculty of Science and Technology, Department of Mathematics and Statistics

On the effects of symmetry in the energy balance on a sphere

Aksel Samuelsberg

MAT-3900 Master's Thesis in Mathematics
May 2022

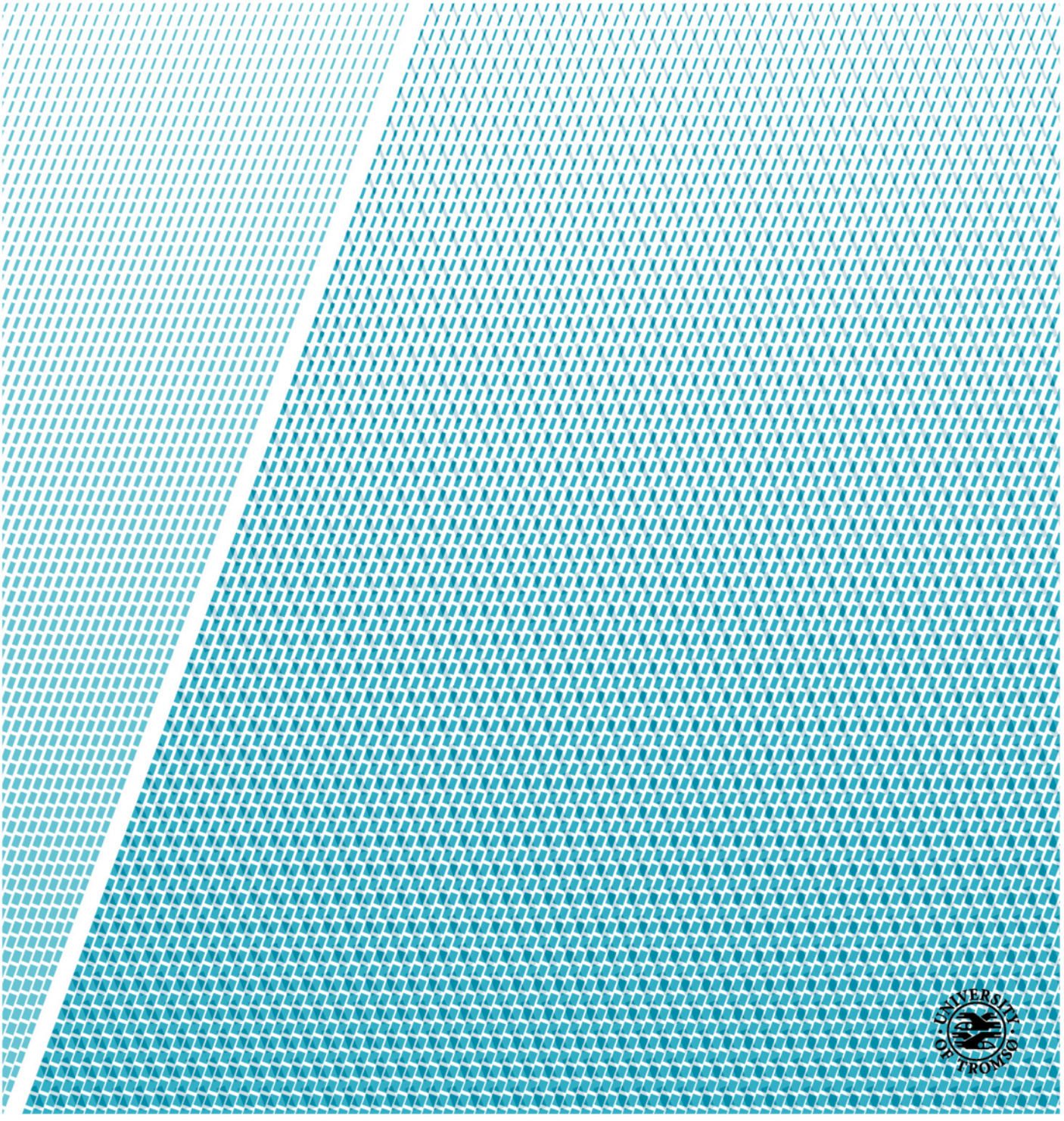

Abstract

Simple climate models have gathered much attention as they have suggested the possibility of abrupt climate change associated with tipping points. Several simple climate models are found to have multiple equilibria, but in most cases similar equilibria do not appear or become too difficult to find in complex, fully coupled earth system models. In this thesis, we investigate a simple climate model, an energy balance model on a sphere, and we highlight a possible factor in the behavioral discrepancy between many simple, low-dimensional models and earth system models. A hypothesis is put forward and investigated regarding the effects of symmetry and the presence of multiple equilibria in this simple model. A novel application of boundary integral methods in the context of energy balance models is presented, and used to find semi-analytical solutions to the stationary energy balance equation. The hypothesis is eventually refuted and a new hypothesis is formulated based on the evidence presented: Symmetry violations in energy balance models cause the steady state solutions to become more similar. This is discussed in light of earth system models and how a similar dynamic would make the detection of multiple equilibra challenging in earth system models.

Acknowledgements

First and foremost, I would like to thank my supervisor, Per Kristen Jakobsen, for guidance and ideas during this project. Your support has been priceless and you have always been available and offered your help. Without our discussions this thesis would not be the same.

I would also like to thank my office mates Alessandro Schena, Wijnand Steneker and Iver Martinsen for all the mathematical and non-mathematical discussions we have had these last two years. You have made the office a good work environment.

Table of Contents

List of Figures

1. Introduction

Headlines regarding climate change have become a familiar sight in newspaper all over the world. The Intergovernmental Panel on Climate Change (IPCC) assessment reports naturally gathers much global attention with its climate projections, produced, in part, by multi-model studies such as the Coupled Model Intercomparison Project (CMIP). These multi-model studies are comprised of an ensemble of complex climate models, *Earth system models*, that seek to simulate all relevant aspects of the Earth's climate system [5]. A complete climate model must include several physical, chemical and biological modules coupled together through physically realistic interface conditions. Such modules include an atmosphere and ocean module with hydrodynamic equations, a radiation module, a sea-ice module as well as modules of terrestrial and marine ecosystems, atmospheric chemistry and biogeochemical processes [10].

Simple climate models generally focus on describing one component of the Earths climate system, and can be valuable if they are able to replicate aspects of complex, fully coupled earth system models [18]. Simple climate models have gathered much interest as the study of them has revealed the appearance of multiple equilibria and the possibility of abrupt climate change. Among these models are the Atlantic meridional overturning circulation box model [19], energy balance models [4] [14], vegetation–atmosphere interaction in subtropical deserts [3] and the Indian monsoon box model [21]. An equilibrium, or *stationary solution*, is a solution, $\vec{x}^{\star}(t) \in \mathbb{R}^n$, to a differential equation

$$\frac{\partial \vec{x}}{\partial t} = \vec{f}(\vec{x}, t),$$

where $\vec{f}(\vec{x}^{\star}, t) = \vec{0}$ for all future and past t. If the equilibrium is stable we often call it a steady state. In a physical system, like the climate system, we expect to only observe steady states over time. An unstable equilibrium is not easily realized as any minor perturbation will drive the system away from this equilibrium and the system will, in time, settle at a stable equilibrium. Once this steady state is reached, the system will retain this state for all future time unless affected by a sufficient external factor driving the system, often called a *forcing*. If a system has multiple steady states, a sufficient forcing may drive the system from one steady state to another. If this transition coincides with the sudden appearance and disappearance of stable equilibria, a *bifurcation* phenomena has occurred and the system may experience an abrupt change.

In the study of dynamical systems, the term "bifurcation" is extremely general [20]. In this thesis we will concern ourselves with a type of local one-dimensional bifurcation that occurs when a smooth change in a parameter value of a system causes a sudden qualitative change in the solution space of the governing equation. There are many types of bifurcation, but in climate science the most iconic type of bifurcation is the *fold bifurcation*, as this is associated with dramatic effects on the climate system. The fold bifurcation, or *saddle-node bifurcation*, is a local bifurcation where an unstable equilibrium (a saddle) and a stable equilibrium (a node) coincide at, and disappear beyond, the *bifurcation point*. Bifurcation points refers to the parameter values at which the system's dynamics suddenly change. A forcing on the system is usually quantified in terms of a *bifurcation parameter*, a parameter value of the problem that triggers the sudden change. Plotting a certain state quantity, usually a state defining quantity, as a function of the bifurcation parameter,

a *bifurcation diagram* may be drawn. Figure 1 shows an example of a bifurcation diagram with two saddle-node bifurcation points, A and B. If the system in Figure 1 is assigned a bifurcation parameter lower than A, the system has one equilibrium. Increasing the bifurcation parameter beyond A, will entail a sudden qualitative change to the system, namely the appearance of two new equilibria.

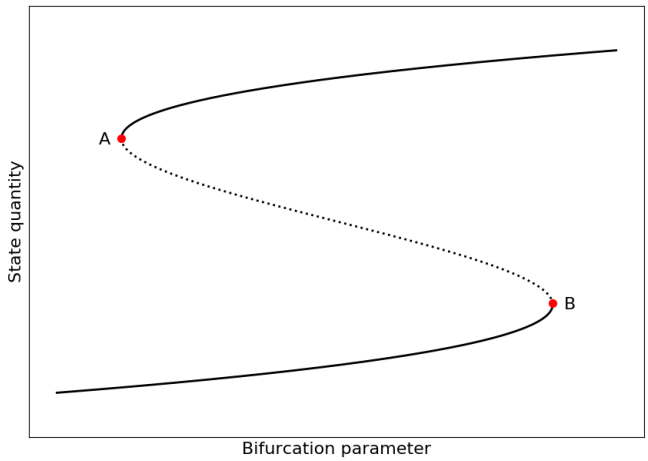

Figure 1: *A state quantity of a system in equilibrium as a function of the bifurcation parameter. Solid lines commonly indicate stable equilibria and dashed lines commonly indicate unstable equilibria.*

Let's say the system in Figure 1 is the climate system and the state variable is some quantity that gauges climate change, such as global average surface temperature. The variation of the bifurcation parameter may represents some forcing on the climate system such as radiative forcing, the change in energy flux in the atmosphere, typically caused by anthropogenic greenhouse gas emissions. If the climate system rests in some steady state in the lower branch in Figure 1 close to point B, and the bifurcation parameter is increased beyond point B, a *tipping point*, the climate system will eventually stabilize at some steady state in the upper branch, potentially causing catastrophic effect on the climate. In order to return to the initial state, the bifurcation parameter must be reduced beyond point A and the climate system must stabilize at the lower branch again before it can recover. This phenomenon is called *hysteresis*. Such tipping points and saddle-node bifurcations are common in simple, low-dimensional models and has motivated the search for similar tipping points in complex climate models.

Most earth system models seemingly do no not exhibit this multiple equilibria behavior and the identification of tipping points has largely been unsuccessful. Complex climate models are essentially a system of coupled partial differential equations, relating times rates to various state variables. Not surprisingly, only numerical solutions are available and a highly efficient computational infrastructure is necessary to find these solutions. The behaviour of these models is accessible by performing numerical runs, a time consuming process that, in general, requires supercomputers. The stability properties of these models are not very well known, only inferred from analysing the output. Equilibria are detected by running the models for a sufficiently long time for the climate

system to approach a steady state. Detecting multiple equilibria has proved difficult, the reasons for this has been discussed by Bathiany [2]: The methods for detecting multiple equilibria can be divided in two groups, interventional and diagnostic methods. A popular interventional method is to choose extreme initial conditions to see if the simulation approach a different steady state after a long time. This poses experiment design problems as it involves assumptions regarding the dependency of different state variables. Furthermore, the different time scales associated with various physical processes poses computational problems as certain state variable approach equilibrium on extremely long timescales. For example, the deep ocean thermal response is hundreds of years. Another common interventional method is to look for hysteresis. The model is ran with an increasing forcing for a sufficiently long time to hopefully enclose a tipping point, causing the climate system to not return to the initial state following an equivalent reduction in forcing. This method suffers from similar experiment design issues as the apparent lack of multiple equilibria may stem from an insufficient increase in forcing, or the forcing was not increased for sufficiently long time to induce a catastrophic bifurcation event. Diagnostic methods involves analyzing the models output and are therefore easier to apply, but tend to be even less conclusive.

So, the apparent lack of multiple equilibria in earth system models may simply stem from the difficulty in detecting them, but could symmetry play an overlooked role in the phenomenological discrepancy between complex and simple climate models? Complex climate models are naturally asymmetrical in nature due to the configuration of the Earth's continents, ocean circulations, planetary waves etc. Simple climate models often exhibits some form of symmetry and that is certainly the case in the classical installment of the model we are going to study in this thesis, the energy balance model on a sphere [14]. In its original form, the Earth's surface is idealized to a uniform medium (generally considered an ocean) and given averaged parameter values empirically chosen to fit Earth's current interglacial climate state. Energy balance models are among the simplest climate models, the time rate of the surface temperature is described in terms of a global radiative imbalance,

$$C\frac{dT}{dt} = E_{\text{in}} - E_{\text{out}}.$$

Here C is the heat capacity of the lower layers of atmosphere plus lithosphere/hydrosphere, E_{in} denotes the energy the Earth receives from the sun in the form of thermal radiation and E_{out} is the thermal energy returned to outer space.

The objective of this thesis is to investigate a simple climate model, an energy balance model on a sphere, based on the question; how does symmetry affect the dynamics of the system? Specifically, we want to investigate if asymmetry affects the presence of multiple equilibria. In section 2 we present the energy balance model we are going to study in this thesis and in section 3 we are going to find solutions to the stationary case using the boundary integral method. These solutions corresponds to a situation in which the climate system is in radiative equilibrium. Identifying these solutions will be an important intermediate step for viewing the system as a whole. The climate system on the sphere will be forced by varying the incoming energy, E_{in}. In the simplified model studied in this thesis, forcing the climate system through increasing solar irradiance, is equivalent to a forcing through increasing the greenhouse effect [17]. As we will see, for certain parameter ranges the climate system has several equilibria. It is therefore vital to assess the stability of these

equilibria. In section 4 we implement a finite difference algorithm for solving the time dependent case as this will allow us to observe how the climate system evolves in time from a given initial state. In section 5 we analyse the equilibria found in section 3 and assess their stability. This is done both through an application of the finite difference code, where a perturbed equilibrium is given as the initial condition, as well as a separate stability analysis scheme involving eigenvalues of a discrete system associated with the problem. In this section we also draw the associated bifurcation diagrams which will be informative representations of the overall climate system on the sphere. We round up the results of this thesis in section 6 and present concluding remarks regarding the affects of symmetry on the climate system on a sphere and possible future work.

2. Model

In this project we are going to study the one-dimensional energy balance model on a sphere formulated by North in 1975 [14]. The model describes the zonal mean surface temperature of a sphere, or in other words the surface temperature averaged over longitude. The surface of the sphere is described using spherical coordinates, where the polar angle is latitude, designated by θ. The latitude ranges from $\theta = 0$, the North pole, to $\theta = \pi$, the South pole. The sphere rotates on its axis just like the Earth, and it also has an obliquity. However, the sphere is assumed to be rotationally symmetrical such that averaging over long times scales the night and day cycle may be neglected and the model varies only in time and with latitude. Consequently, the temperature is constant along zonal strips around the sphere for a given time t,

$$T = T(\theta, t).$$

Meridional heat transport is built into the model by including the thermal diffusion term $-D\nabla^2 T$, ensuring that thermal energy is being redistributed across latitudes with a flux density proportional to the negative local temperature gradient and scaled by the thermal diffusion coefficient, D. With the appropriate expression of the Laplace operator in spherical coordinates the time-dependent energy balance equation takes the form

$$C\frac{\partial T}{\partial t} - D\frac{1}{\sin\theta}\frac{\partial}{\partial\theta}\big(\sin\theta\frac{\partial T}{\partial\theta}\big) = E_{\text{in}} - E_{\text{out}}.$$

Here C denotes the heat capacity of the lower layers of atmosphere plus hydrosphere or lithosphere, and although the heat capacity varies with the local medium surrounding the surface, it is assigned an average constant value. We will study a sphere both with and without a continent, but we start by considering a *water world*. In this thesis, a water world will refer to a sphere where the surface is entirely covered by water. Later on we will introduce a continent and at that point all the necessary modifications to the energy balance equation will be discussed in order to extend our analysis to include a continent. For now all of the following parameters concern a water world.

The sphere receives energy in the form of radiation from an external sun, and this energy will be modelled as

$$E_{\text{in}} = Qs(\theta)(1 - a).$$

Here Q denotes the solar constant divided by 4, as the disk capturing radiation is 4 times less than the total area of the sphere. To account for the nonuniform distribution of solar radiation along latitudes the model includes an average annual latitudinal energy distribution function, $s(\theta)$. The obliquity of the sphere will be the same as that of the Earth today and the resulting seasonal effects are built into $s(\theta)$. The albedo effect is included in the model, and a denotes the albedo. Albedo is a measure of the diffuse reflection of solar radiation and varies with surface and atmospheric conditions. The polar regions may have snow cover and a denser cloud cover, thus a greater albedo than that of water. We will therefore allow for a temperature dependent albedo,

$$a = a(T).$$

The model assumes a constant lapse rate, meaning that there will be a linear relation between the

surface temperature and outgoing energy [4]. This outgoing energy is modelled as

$$E_{\text{out}} = A + BT,$$

where A and B are constants. With this form for the incoming and outgoing energy the time-dependent energy balance equation may be formulated as

$$C\frac{\partial T}{\partial t} - D\frac{1}{\sin\theta}\frac{\partial}{\partial\theta}\big(\sin\theta\frac{\partial T}{\partial\theta}\big) + BT = Qs(\theta)(1-a) - A. \tag{2.1}$$

A full derivation of the energy balance equation (2.1) can be found in a Appendix B. Since $s(\theta)$ describes the annual energy distribution, the model must necessarily vary on the same timescale. Therefore, (2.1) describes the annual, zonal mean surface temperature. Coupling the temperature dependent albedo to the system, equation (2.1) becomes highly nonlinear. This is the ice-albedo feedback mechanism.

In order to solve the energy balance equation (2.1) we must constrain the solution using boundary conditions. We allow for no heat transport at the poles and must therefore have the following boundary conditions;

$$\lim_{\theta\to 0}\sin\theta\frac{\partial T}{\partial\theta}(\theta) = 0 \tag{2.2}$$

and

$$\lim_{\theta\to \pi}\sin\theta\frac{\partial T}{\partial\theta}(\theta) = 0. \tag{2.3}$$

In Appendix B.3 these boundary conditions are derived from physical assumptions underlying the model.

We will allow for ice/snow cover on the surface if the local temperature is sufficiently low. We model this threshold as

$$T_s(\theta, t) = T_s,$$

where T_s refers to the critical temperature for the ice-water phase transition. As the sphere's surface is covered by water throughout, this value will not depend on location. The numerical values for the parameters used in this thesis, can be found in Appendix A.

2.1. Scaling the model

We will now nondimensionalize (2.1) using T_s as a scale for temperature,

$$T = T_s T'. \tag{2.4}$$

We also want to include a timescale, t_0, in our model. Applying the time scale

$$t = t_0 t' \tag{2.5}$$

to the time derivative,

$$\frac{\partial T}{\partial t} = \frac{1}{t_0}\frac{\partial T}{\partial t'},$$

in equation (2.1), as well as the temperature scaling (2.4), we get the following nondimensional time dependent energy balance equation;

$$\gamma \partial_t T - \frac{1}{\sin\theta}\frac{\partial}{\partial\theta}\big(\sin\theta \frac{\partial T}{\partial\theta}\big) + \beta T = \eta s(\theta)(1 - a(T)) - \alpha, \tag{2.6}$$

where

$$\begin{aligned} \gamma &= \frac{C}{t_0 D}, \\ \beta &= \frac{B}{D}, \\ \alpha &= \frac{A}{T_s D}, \\ \eta &= \frac{Q}{T_s D}. \end{aligned} \tag{2.7}$$

Note that in (2.6), we have dropped the primes on the nondimensional temperature and nondimensional time. Since T_s carries the physical quantity °C, T is now dimensionless. Similarly, t_0 carries physical quantity s and t is therefore dimensionless. The parameters (2.7) are also dimensionless. From this point we will only consider (2.6), the current iteration of our energy balance model on a sphere where the surface is covered entirely by water.

Now we have formulated an energy balance equation on a sphere (2.6), and two accompanying boundary conditions (2.2) and (2.3). In the next section we will proceed by finding stationary solutions to (2.6) using the boundary integral method.

3. Boundary integral method

In this section we are going to apply the boundary integral method to solve the stationary energy balance equation from 2.1,

$$-\frac{1}{\sin\theta}\frac{\partial}{\partial\theta}\big(\sin\theta\frac{\partial T}{\partial\theta}\big)+\beta T=\eta s(\theta)(1-a(T))-\alpha. \tag{3.1}$$

As mentioned in the introduction, we may force the climate system through varying either the incoming or outgoing energy as this would anyway bring about the same radiative imbalance driving a temperature change on the surface. In this thesis we have chosen to vary the incoming radiation, specifically the solar constant Q. This will be the bifurcation parameter. As we will see shortly, for certain values of Q (3.1) will have certain types of solutions corresponding to certain climate states. It is important to identify all possible states the climate system may realize in order to 1) apply the boundary integral method, and 2) to later view the system as a whole. We will start by looking at a water world and developing a framework for finding stationary solutions depending on the state of the climate system. Next, we will introduce a rotationally symmetrical continent that preserves the north-south symmetry and find all the possible stationary states of the climate system on such a sphere. Finally, we will move the continent, breaking the north-south symmetry and find all possible stationary solutions with this continent configuration. By gradually reducing the symmetry properties of the sphere, we hope to identify some form of pattern regarding the presence of multiple stationary solutions and asymmetry down the line.

3.1. Boundary integral method in general

Before proceeding to solve (3.1) using the boundary integral method, we will give a recap of the general procedure when applying this method. The aim of the boundary integral method is to describe the solution to a differential equation in the interior of a given domain, through a relation including certain boundary points of the domain. Let's consider a general equation on the form

$$\mathcal{G}y(\vec{x})=h(\vec{x}),\qquad \vec{x}\ \in\ D, \tag{3.2}$$

where $\mathcal{G}$ is some differential operator. In order to solve (3.2) using the boundary integral method, one must first find the *fundamental integral identity* associated with the operator $\mathcal{G}$. Next step is to find a *Green's function* for the operator $\mathcal{G}$. A Green's function for the operator $\mathcal{G}$, is any solution to the equation

$$\mathcal{G}K(\vec{x},\vec{\xi})=\delta_{\vec{\xi}}(\vec{x}), \tag{3.3}$$

where K is the Green's function and $\delta_{\vec{\xi}}$ is an expression of the the Dirac-delta function on the domain D. The Green's function can be used, in combination with the fundamental integral identity, to derive integral identities for the solution to the (3.2) that relate values of the solution in the interior of the domain, D, to values on the boundary of the domain, ∂D. To illustrate this point, let's consider an example.

Suppose that the fundamental integral identity has been found and that it has the form

$$\int_D dV\ \{u\mathcal{G}v - v\mathcal{G}u\} = \int_{\partial D} dS\ \{u\mathcal{H}v - v\mathcal{H}u\}, \tag{3.4}$$

where u and v are some functions defined on D and $\mathcal{H}$ is some operator that ensures that (3.4) holds. Suppose that we have found a Green's function, K, that solves (3.3). Interchanging

$$u = y$$

and

$$v = K$$

in (3.4) we get

$$\begin{aligned}
\int_D dV\ \{y\mathcal{G}K - K\mathcal{G}y\} &= \int_{\partial D} dS\ \{y\mathcal{H}K - K\mathcal{H}y\} \\
\int_D dV\ \{y\delta_{\vec{\xi}} - Kh\} &= \int_{\partial D} dS\ \{y\mathcal{H}K - K\mathcal{H}y\} \\
y(\vec{\xi}) &= \int_D dV\ Kh + \int_{\partial D} dS\ \{y\mathcal{H}K - K\mathcal{H}y\}.
\end{aligned} \tag{3.5}$$

Equation (3.5) relates values of the solution to (3.2) inside the domain D to values on the boundary ∂D, often referred to as a *boundary integral relation*. This identity will still not give us a solution unless we somehow determine the unknown boundary values. This can be done either through eliminating the unknown values using a specific choice of Green's function, invoking certain boundary conditions, developing a set of *boundary integral equations* or a combination of the above. We will soon see how this might be done in practice by solve (3.1) using the boundary integral method and choosing the latter approach in order to determine the unknown boundary values.

3.2. Boundary integral method for a water world

Let us return to the problem at hand, namely the stationary energy balance equation (3.1). We are now going to find stationary solutions to (3.1) using the boundary integral method for a sphere with no continents and a surface entirely covered by water and/or snow and ice, a water world. Depending on the parameter regime we are in, the water world will realize one of three possible states:

i) The planets surface is entirely covered by ice or snow.

ii) The planets surface is entirely covered by water.

iii) The planets surface is partially covered by ice or snow and partially covered by water.

Using the boundary integral method, we are able to find semi-analytical solutions to (3.1) for the cases i), ii) and iii). We will start by analysing the cases i) and ii) together and later move on to looking at case iii). The presence of a partial ice cover implies that there are certain critical latitudes at which the ice cover ends and begins, we will refer to these critical latitudes as *ice edges*. The governing equation (3.1) will, because of the albedo, slightly differ depending on whether there is ice cover or no ice cover. It is therefore vital to identify these critical latitudes and this ultimately requires a combination of both analytical and numerical methods.

As we now know, the goal of the boundary integral method is to describe the solution to a differential equation in the interior of a given domain, through a relation including certain boundary points of the domain. In order to find such a relation for the solution to (3.1), we must first find the fundamental integral identity for the operator

$$\mathcal{L}(\cdot) = -\frac{1}{\sin\theta}\frac{\partial}{\partial\theta}\big(\sin\theta\frac{\partial}{\partial\theta}(\cdot)\big) + \beta(\cdot). \tag{3.6}$$

Appendix D includes a full derivation of the fundamental integral identity for the operator (3.6) and it is found to be

$$\int_{\theta_1}^{\theta_2} d\theta\ \sin\theta\big\{v\mathcal{L}u - u\mathcal{L}v\big\} = \left\{u\sin\theta\frac{\partial v}{\partial\theta} - v\sin\theta\frac{\partial u}{\partial\theta}\right\}\Bigg|_{\theta_1}^{\theta_2}. \tag{3.7}$$

We must also find a Green's function for the operator (3.6),

$$\mathcal{L}K(\theta,\xi) = \delta_\xi(\theta). \tag{3.8}$$

In Appendix D we find a suitable Green's function,

$$K(\theta,\xi) = \begin{cases} \frac{P_\lambda(\cos\xi)(\pi\cot(\pi\lambda)P_\lambda(\cos\theta) - 2Q_\lambda(\cos\theta))}{2(1+\lambda)(P_\lambda(\cos\xi)Q_{\lambda+1}(\cos\xi) - P_{\lambda+1}(\cos\xi)Q_\lambda(\cos\xi))}, & \theta > \xi \\ \frac{P_\lambda(\cos\theta)(\pi\cot(\pi\lambda)P_\lambda(\cos\xi) - 2Q_\lambda(\cos\xi))}{2(1+\lambda)(P_\lambda(\cos\xi)Q_{\lambda+1}(\cos\xi) - P_{\lambda+1}(\cos\xi)Q_\lambda(\cos\xi))}, & \theta < \xi \end{cases}. \tag{3.9}$$

Here P_λ and Q_λ are Legendre functions of order λ, where

$$\lambda = \frac{1}{2}\left(\sqrt{1-4\beta} - 1\right).$$

This Green's function is continuous and bounded on the domain $\theta \in [0,\pi]$, and its derivative is also bounded at the boundaries $\theta = 0$ and $\theta = \pi$, for a given $\xi \in [0,\pi]$. We choose this to be our Green's function.

Now that we have both the fundamental integral identity and a Green's function for the operator (3.6), we are ready to derive the boundary integral relations for the cases i), ii) and iii). If the boundary integral relations contain unknown boundary values, we will develop a system of equations, the boundary integral equations, that can be solved to find these unknown boundary values. We start by looking at case i) and ii).

3.2.1. The case of no ice edges

The simplest possible cases are ones in which the surface of the sphere is either completely covered in ice, case i), or completely ice free, ii). What's similar for these case is that there are no ice edges and this makes it easier to obtain a temperature profile.

Let

$$h(T,\theta) = \eta s(\theta)(1 - a(T)) - \alpha.$$

We can now write the stationary energy balance equation (3.1) on the compact form

$$\mathcal{L}T = h. \tag{3.10}$$

Interchanging

$$v = T$$
$$u = K$$

in the fundamental integral identity (3.7) we have

$$\int_{\theta_1}^{\theta_2} d\theta \, \sin\theta \, \{T\mathcal{L}K - K\mathcal{L}T\} = \left\{ K\sin\theta\frac{\partial T}{\partial\theta} - T\sin\theta\frac{\partial K}{\partial\theta} \right\}\Bigg|_{\theta_1}^{\theta_2}$$

Applying (3.10) and (3.8) we can express the solution to (3.10) through the relation

$$T(\xi) = \int_{\theta_1}^{\theta_2} d\theta \, \sin\theta \, K(\theta,\xi)h(T,\theta) + \left\{ K\sin\theta\frac{\partial T}{\partial\theta} - T\sin\theta\frac{\partial K}{\partial\theta} \right\}\Bigg|_{\theta_1}^{\theta_2}. \tag{3.11}$$

We are currently looking at the cases where the surface is entirely covered by either ice or water, hence there are no ice edges and the source term, h, will be identical throughout the domain. Based on this, we apply (3.11) on the entire domain, S, letting $\theta_1 \to 0^+$ and $\theta_2 \to \pi^-$,

$$\begin{aligned} T(\xi) = &\int_0^{\pi} d\theta \, \sin\theta \, K(\theta,\xi)h(T,\theta) + \lim_{\theta_2\to\pi^-} K(\theta_2,\xi)\sin\theta_2\frac{\partial T}{\partial\theta}(\theta_2) \\ &- \lim_{\theta_2\to\pi^-} T(\theta_2)\sin\theta_2\frac{\partial K}{\partial\theta}(\theta_2,\xi) - \lim_{\theta_1\to 0^+} K(\theta_1,\xi)\sin\theta_1\frac{\partial T}{\partial\theta}(\theta_1) \\ &+ \lim_{\theta_1\to 0^+} T(\theta_1)\sin\theta_1\frac{\partial K}{\partial\theta}(\theta_1,\xi). \end{aligned} \tag{3.12}$$

The fact that the Green's function, K, and its derivative is bounded at the boundary, in combination with boundary conditions (2.2) and (2.3), ensures that equation (3.12) takes on the simpler form

$$T(\xi) = \int_0^{\pi} d\theta \, \sin\theta \, K(\theta,\xi)h(T,\theta). \tag{3.13}$$

Note that since our Green's function is piecewise, we must necessarily split any relevant integral in order to integrate over the appropriate bounds,

$$T(\xi) = \int_0^{\xi} d\theta \, \sin\theta \, K_-(\theta,\xi)h(T,\theta) + \int_{\xi}^{\pi} d\theta \, \sin\theta \, K_+(\theta,\xi)h(T,\theta),$$

where

$$K(\theta,\xi) = \begin{cases} K_+(\theta,\xi), & \theta > \xi \\ K_-(\theta,\xi), & \theta < \xi \end{cases}. \tag{3.14}$$

In order to arrive at a solution from (3.13), we need to address the function $h(T,\theta)$ inside the integral. When applying the boundary integral method, $h(T,\theta)$ cannot depend on the solution T in some arbitrary way. Therefore, we will in this section use a simpler model for the albedo,

$$a(T) = \begin{cases} a_1, & T > -1 \\ a_2, & T < -1. \end{cases}$$

Note that this albedo is a function of non-dimensional temperature. Applying this albedo, $h(T,\theta)$ becomes

$$h(T,\theta) = \begin{cases} \eta s(\theta)(1-a_1) - \alpha, & T > -1 \\ \eta s(\theta)(1-a_2) - \alpha, & T < -1 \end{cases}$$

and we can now obtain a solution to (3.1) through the boundary integral method. Since we model the albedo as a_1 wherever the is no ice cover and a_2 wherever the is ice cover, we define two functions,

$$h_1(\theta) = \eta s(\theta)(1-a_1) - \alpha, \tag{3.15}$$

wherever there is no ice cover, and

$$h_2(\theta) = \eta s(\theta)(1-a_2) - \alpha, \tag{3.16}$$

wherever the is ice cover. Thus, the boundary integral relation for the case where the surface is entirely cover by water is

$$T(\xi) = \int_0^{\pi} d\theta \, \sin\theta \, K(\theta,\xi)h_1(\theta), \qquad \forall\, \xi \in [0,\pi]. \tag{3.17}$$

Similarly, the boundary integral relation for the case where the surface is entirely cover by ice or snow is

$$T(\xi) = \int_0^{\pi} d\theta \, \sin\theta \, K(\theta,\xi)h_2(\theta), \qquad \forall\, \xi \in [0,\pi]. \tag{3.18}$$

The boundary integral relations (3.17) and (3.18) are trivial to solve, and the corresponding temperature profiles are shown in dimensional form in Figure 19. The parameters used to obtain these solutions are found in Appendix A.

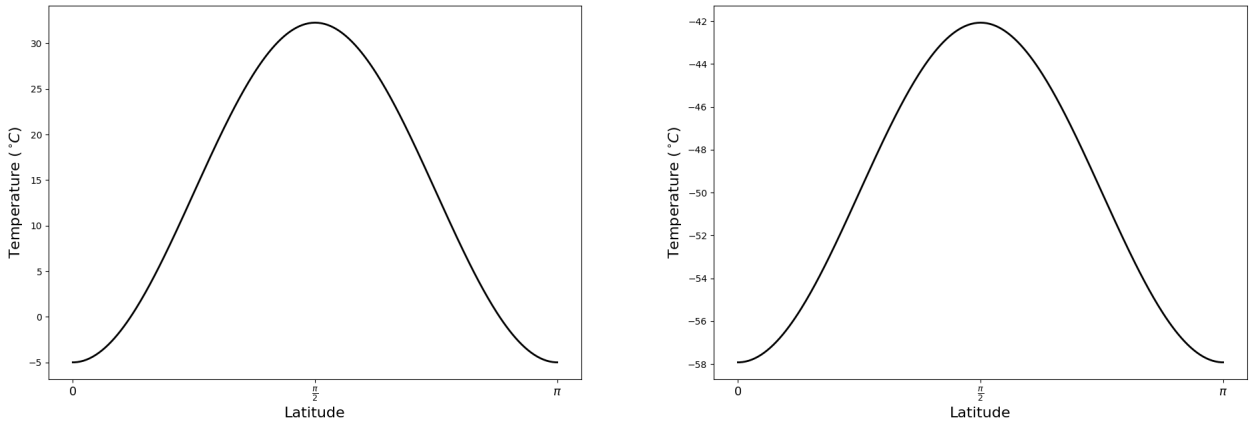

(a) (b)

Figure 2: *Temperature profile of a water world with no ice or snow present on the surface (a) and a water world with its surface entirely covered by ice and/or snow (b).*

3.2.2. The case of two ice edges

Let us now turn our attention to the case where the planet's surface is partially covered by water and partially by ice/snow, and apply the boundary integral method to solve (3.1) for this case. As mentioned in the introduction to this section, there will be certain critical latitudes at which ice cover ends and begins. We will refer to these critical latitudes as θ_{c_1} and θ_{c_2}. Since the latitudinal energy distribution function, $s(\theta)$, is symmetrical about equator and decreasing towards the poles, the ice cover on the surface will stretch from the poles to some unknown latitudes on the northern and southern hemisphere. Our aim will be to derive a system of equations, the boundary integral equations, which can be solved to determine the critical latitudes, θ_{c_1} and θ_{c_2}, the values of which are critical in order to calculate the temperature profile for a given Q.

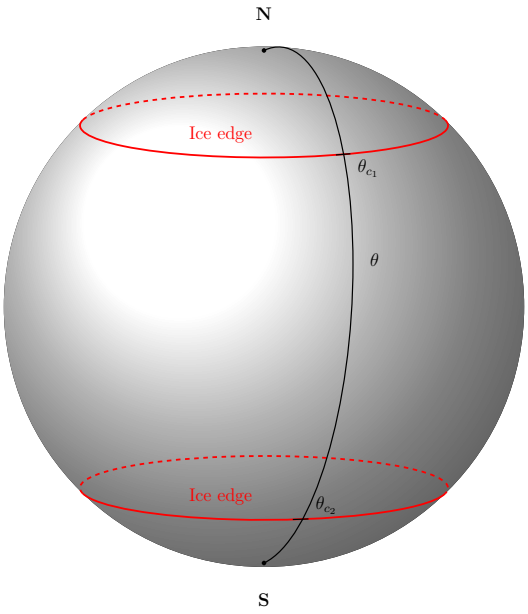

Figure 3: *Schematic of the surface of the water planet with a partial ice cover.*

We divide our domain into three sub-domains based on the ability of the surface to absorb incident radiation,

$$\theta \in (0, \theta_{c_1}), \tag{I}$$

$$\theta \in (\theta_{c_1}, \theta_{c_2}) \tag{II}$$

and

$$\theta \in (\theta_{c_2}, \pi). \tag{III}$$

As there is no ice cover in region (II) we let (3.15) be the source term in the governing equation for region (II),

$$\mathcal{L}T = h_1.$$

In region (I) and (III), where there is ice cover, we let (3.16) be the source term in the governing equation,

$$\mathcal{L}T = h_2.$$

We are going to derive boundary integral relations for the three regions (I), (II) and (III). We apply the general relation (3.11) in the respective regions, letting θ_1 and θ_2 approach the boundaries of the sub-domains. Starting with region (I), we apply (3.11) and let $\theta_1 \to 0^+$ and $\theta_2 \to \theta_{c_1}^-$,

$$
\begin{aligned}
T(\xi) &= \int_0^{\theta_{c_1}} d\theta\ \sin\theta\, K(\theta,\xi)h_2(\theta) + \lim_{\substack{\theta_1\to 0^+\\ \theta_2\to\theta_{c_1}^-}} \left\{ K\sin\theta\frac{\partial T}{\partial\theta} - T\sin\theta\frac{\partial K}{\partial\theta}\right\}\Bigg|_{\theta_1}^{\theta_2} \\
&= \int_0^{\xi} d\theta\ \sin\theta\, K_-(\theta,\xi)h_2(\theta) + \int_{\xi}^{\theta_{c_1}} d\theta\ \sin\theta\, K_+(\theta,\xi)h_2(\theta) \\
&+ \lim_{\theta_2\to\theta_{c_1}^-} K(\theta_2,\xi)\sin(\theta_2)\frac{\partial T}{\partial\theta}(\theta_2) \\
&- \lim_{\theta_2\to\theta_{c_1}^-} T(\theta_2)\sin(\theta_2)\frac{\partial K}{\partial\theta}(\theta_2,\xi) \\
&- \lim_{\theta_1\to 0^+} K(\theta_1,\xi)\sin(\theta_1)\frac{\partial T}{\partial\theta}(\theta_1) \\
&+ \lim_{\theta_1\to 0^+} T(\theta_1)\sin(\theta_1)\frac{\partial K}{\partial\theta}(\theta_1,\xi).
\end{aligned}
\tag{3.19}
$$

We assume that the solution is bounded at $\theta = 0$, thus the last term in (3.19) is zero. The Green's function is also bounded at $\theta = 0$ and therefore the second-to-last term in (3.19) is also zero due to the boundary condition (2.2). Furthermore, we will assume that T is continuous at $\theta = \theta_{c_1}$ and $\theta = \theta_{c_2}$, and the temperature at these critical latitudes must necessarily be $-T_s$. The value of the non-dimensional temperature at the latitudes is therefore

$$T(\theta_{c_1}) = T(\theta_{c_2}) = -1.$$

We apply this, as well as the fact that the Green's function is continuous at $\theta = \theta_{c_1}$, to (3.19),

$$
\begin{aligned}
T(\xi) &= \int_0^{\xi} d\theta\ \sin\theta\, K_-(\theta,\xi)h_2(\theta) + \int_{\xi}^{\theta_{c_1}} d\theta\ \sin\theta\, K_+(\theta,\xi)h_2(\theta) \\
&+ K(\theta_{c_1},\xi)\sin(\theta_{c_1}) \lim_{\theta_2\to\theta_{c_1}^-} \frac{\partial T}{\partial\theta}(\theta_2) + \sin(\theta_{c_1}) \lim_{\theta_2\to\theta_{c_1}^-} \frac{\partial K}{\partial\theta}(\theta_2,\xi).
\end{aligned}
\tag{3.20}
$$

Now we move on to region (II), applying (3.11) and letting $\theta_1 \to \theta_{c_1}^+$ and $\theta_2 \to \theta_{c_2}^-$,

$$
\begin{aligned}
T(\xi) &= \int_{\theta_{c_1}}^{\xi} d\theta\ \sin\theta\, K_-(\theta,\xi)h_1(\theta) + \int_{\xi}^{\theta_{c_2}} d\theta\ \sin\theta\, K_+(\theta,\xi)h_1(\theta) \\
&+ \lim_{\theta_2\to\theta_{c_2}^-} K(\theta_2,\xi)\sin(\theta_2)\frac{\partial T}{\partial\theta}(\theta_2) \\
&- \lim_{\theta_2\to\theta_{c_2}^-} T(\theta_2)\sin(\theta_2)\frac{\partial K}{\partial\theta}(\theta_2,\xi) \\
&- \lim_{\theta_1\to\theta_{c_1}^+} K(\theta_1,\xi)\sin(\theta_1)\frac{\partial T}{\partial\theta}(\theta_1) \\
&+ \lim_{\theta_1\to\theta_{c_1}^+} T(\theta_1)\sin(\theta_1)\frac{\partial K}{\partial\theta}(\theta_1,\xi).
\end{aligned}
\tag{3.21}
$$

Under the assumption that T and K are continuous at $\theta = \theta_{c_1}$ and $\theta = \theta_{c_2}$ (3.21) becomes

$$\begin{aligned} T(\xi) = &\int_{\theta_{c_1}}^{\xi} d\theta \ \sin\theta \, K_-(\theta,\xi)h_1(\theta) + \int_{\xi}^{\theta_{c_2}} d\theta \ \sin\theta \, K_+(\theta,\xi)h_1(\theta) \\ &+ K(\theta_{c_2},\xi)\sin(\theta_{c_2}) \lim_{\theta_2\to\theta_{c_2}^-} \frac{\partial T}{\partial\theta}(\theta_2) \\ &+ \sin(\theta_{c_2}) \lim_{\theta_2\to\theta_{c_2}^-} \frac{\partial K}{\partial\theta}(\theta_2,\xi) \\ &- K(\theta_{c_1},\xi)\sin(\theta_{c_1}) \lim_{\theta_1\to\theta_{c_1}^+} \frac{\partial T}{\partial\theta}(\theta_1) \\ &- \sin(\theta_{c_1}) \lim_{\theta_1\to\theta_{c_1}^+} \frac{\partial K}{\partial\theta}(\theta_1,\xi). \end{aligned} \tag{3.22}$$

Finally, we apply (3.11) in region (III) letting $\theta_1 \to \theta_{c_2}^+$ and $\theta_2 \to \pi^-$,

$$\begin{aligned} T(\xi) = &\int_{\theta_{c_2}}^{\xi} d\theta \ \sin\theta \, K_-(\theta,\xi)h_2(\theta) + \int_{\xi}^{\pi} d\theta \ \sin\theta \, K_+(\theta,\xi)h_2(\theta) \\ &+ \lim_{\theta_2\to\pi^-} K(\theta_2,\xi)\sin(\theta_2)\frac{\partial T}{\partial\theta}(\theta_2) \\ &- \lim_{\theta_2\to\pi^-} T(\theta_2)\sin(\theta_2)\frac{\partial K}{\partial\theta}(\theta_2,\xi) \\ &- \lim_{\theta_1\to\theta_{c_2}^+} K(\theta_1,\xi)\sin(\theta_1)\frac{\partial T}{\partial\theta}(\theta_1) \\ &+ \lim_{\theta_1\to\theta_{c_2}^+} T(\theta_1)\sin(\theta_1)\frac{\partial K}{\partial\theta}(\theta_1,\xi). \end{aligned} \tag{3.23}$$

Assuming that T bounded at $\theta = \pi$ and continuous at $\theta = \theta_{c_2}$, in combination with the boundary condition (2.3) and the known value of $T(\theta_{c_2})$, (3.23) becomes

$$\begin{aligned} T(\xi) = &\int_{\theta_{c_2}}^{\xi} d\theta \ \sin\theta \, K_-(\theta,\xi)h_2(\theta) + \int_{\xi}^{\pi} d\theta \ \sin\theta \, K_+(\theta,\xi)h_2(\theta) \\ &- K(\theta_{c_2},\xi)\sin(\theta_{c_2}) \lim_{\theta_1\to\theta_{c_2}^+} \frac{\partial T}{\partial\theta}(\theta_1) - \sin(\theta_{c_2}) \lim_{\theta_1\to\theta_{c_2}^+} \frac{\partial K}{\partial\theta}(\theta_1,\xi). \end{aligned} \tag{3.24}$$

Equation (3.20), (3.22) and (3.24) gives the solution in region (I), (II) and (III), respectively, expressed through an integral and the unknown values θ_{c_1}, θ_{c_2}, $\lim_{\theta\to\theta_{c_1}^-} \frac{\partial T}{\partial\theta}(\theta)$, $\lim_{\theta\to\theta_{c_1}^+} \frac{\partial T}{\partial\theta}(\theta)$, $\lim_{\theta\to\theta_{c_2}^-} \frac{\partial T}{\partial\theta}(\theta)$ and $\lim_{\theta\to\theta_{c_2}^+} \frac{\partial T}{\partial\theta}(\theta)$. We are obviously seeking T, and consequently do not know its derivative. However, we will assume that heat does not build up at the critical latitudes and

therefore we must have

$$\lim_{\theta\to\theta_{c_1}^-}\frac{\partial T}{\partial\theta}(\theta)=\lim_{\theta\to\theta_{c_1}^+}\frac{\partial T}{\partial\theta}(\theta)=\frac{\partial T}{\partial\theta}(\theta_{c_1})$$
$$\lim_{\theta\to\theta_{c_2}^-}\frac{\partial T}{\partial\theta}(\theta)=\lim_{\theta\to\theta_{c_2}^+}\frac{\partial T}{\partial\theta}(\theta)=\frac{\partial T}{\partial\theta}(\theta_{c_2}).$$

We will now develop a system of equations, the boundary integral equations, in order to determine the unknown values θ_{c_1}, θ_{c_2}, $\frac{\partial T}{\partial\theta}(\theta_{c_1})$ and $\frac{\partial T}{\partial\theta}(\theta_{c_2})$. Our approach will be to let ξ approach the boundaries in each of the sub-domains (I), (II) and (III).

Staring with region (I), we let $\xi\to 0^+$ in equation (3.20),

$$\begin{aligned}T(0)=&\int_0^{\theta_{c_1}}d\theta\ \sin\theta\,K_+(\theta,0)h_2(\theta)\\&+K_+(\theta_{c_1},0)\sin(\theta_{c_1})\frac{\partial T}{\partial\theta}(\theta_{c_1})+\sin(\theta_{c_1})\lim_{\xi\to 0^+}\lim_{\theta\to\theta_{c_1}^-}\frac{\partial K}{\partial\theta}(\theta,\xi),\end{aligned}\tag{i}$$

and $\xi\to\theta_{c_1}^-$ in (3.20),

$$\begin{aligned}-1=&\int_0^{\theta_{c_1}}d\theta\ \sin\theta\,K_-(\theta,\theta_{c_1})h_2(\theta)\\&+K_+(\theta_{c_1},\theta_{c_1})\sin(\theta_{c_1})\frac{\partial T}{\partial\theta}(\theta_{c_1})+\sin(\theta_{c_1})\lim_{\xi\to\theta_{c_1}^-}\lim_{\theta\to\theta_{c_1}^-}\frac{\partial K}{\partial\theta}(\theta,\xi).\end{aligned}\tag{ii}$$

For region (II) we let $\xi\to\theta_{c_1}^+$ in (3.22),

$$\begin{aligned}-1=&\int_{\theta_{c_1}}^{\theta_{c_2}}d\theta\ \sin\theta\,K_+(\theta,\theta_{c_1})h_1(\theta)\\&+K_+(\theta_{c_2},\theta_{c_1})\sin(\theta_{c_2})\frac{\partial T}{\partial\theta}(\theta_{c_2})+\sin(\theta_{c_2})\lim_{\xi\to\theta_{c_1}^+}\lim_{\theta\to\theta_{c_2}^-}\frac{\partial K}{\partial\theta}(\theta,\xi)\\&-K_-(\theta_{c_1},\theta_{c_1})\sin(\theta_{c_1})\frac{\partial T}{\partial\theta}(\theta_{c_1})-\sin(\theta_{c_1})\lim_{\xi\to\theta_{c_1}^+}\lim_{\theta\to\theta_{c_1}^+}\frac{\partial K}{\partial\theta}(\theta,\xi),\end{aligned}\tag{iii}$$

and $\xi\to\theta_{c_2}^-$ in (3.22),

$$\begin{aligned}-1=&\int_{\theta_{c_1}}^{\theta_{c_2}}d\theta\ \sin\theta\,K_-(\theta,\theta_{c_2})h_1(\theta)\\&+K_+(\theta_{c_2},\theta_{c_2})\sin(\theta_{c_2})\frac{\partial T}{\partial\theta}(\theta_{c_2})+\sin(\theta_{c_2})\lim_{\xi\to\theta_{c_2}^-}\lim_{\theta\to\theta_{c_2}^-}\frac{\partial K}{\partial\theta}(\theta,\xi)\\&-K_-(\theta_{c_1},\theta_{c_2})\sin(\theta_{c_1})\frac{\partial T}{\partial\theta}(\theta_{c_1})-\sin(\theta_{c_1})\lim_{\xi\to\theta_{c_2}^-}\lim_{\theta\to\theta_{c_1}^+}\frac{\partial K}{\partial\theta}(\theta,\xi),\end{aligned}\tag{iv}$$

Finally, for region (III) we let $\xi \to \theta_{c_2}^+$ in (3.24),

$$\begin{aligned} -1 = &\int_{\theta_{c_2}}^{\pi} d\theta \, \sin\theta \, K_+(\theta, \theta_{c_2}) h_2(\theta) \\ &- K_-(\theta_{c_2}, \theta_{c_2}) \sin(\theta_{c_2}) \frac{\partial T}{\partial \theta}(\theta_{c_2}) - \sin(\theta_{c_2}) \lim_{\xi \to \theta_{c_2}^+} \lim_{\theta \to \theta_{c_2}^+} \frac{\partial K}{\partial \theta}(\theta, \xi), \end{aligned} \tag{v}$$

and $\xi \to \pi^-$ in (3.24),

$$\begin{aligned} T(\pi) = &\int_{\theta_{c_2}}^{\pi} d\theta \, \sin\theta \, K_-(\theta, \pi) h_2(\theta) \\ &- K_-(\theta_{c_2}, \pi) \sin(\theta_{c_2}) \frac{\partial T}{\partial \theta}(\theta_{c_2}) - \sin(\theta_{c_2}) \lim_{\xi \to \pi^-} \lim_{\theta \to \theta_{c_2}^+} \frac{\partial K}{\partial \theta}(\theta, \xi). \end{aligned} \tag{vi}$$

The system of equations (i)-(vi) is the boundary integral equations for the case of a water world with two ice edges. It is a system of 6 equations for 6 unknown boundary values, θ_{c_1}, θ_{c_2}, $\frac{\partial T}{\partial \theta}(\theta_{c_1})$, $\frac{\partial T}{\partial \theta}(\theta_{c_2})$, $T(0)$ and $T(\pi)$. Solving this system of equations ultimately require a combination of both analytical and numerical methods as the integrals cannot be evaluated analytically. We start by solving equation (iii) and (iv) for $\frac{\partial T}{\partial \theta}(\theta_{c_1})$ and $\frac{\partial T}{\partial \theta}(\theta_{c_2})$. We substitute the expression for $\frac{\partial T}{\partial \theta}(\theta_{c_1})$ and $\frac{\partial T}{\partial \theta}(\theta_{c_2})$ into equation (ii) and (v) to create two functions of θ_{c_1} and θ_{c_2},

$$\begin{aligned} f_1 &= f_1(\theta_{c_1}, \theta_{c_2}), \\ f_2 &= f_2(\theta_{c_1}, \theta_{c_2}). \end{aligned}$$

We wish to find the roots of these functions using Newton's iteration to obtain θ_{c_1} and θ_{c_2}. However, the functions f_1 and f_2 are extremely complicated and involve several integrals, and we therefore evaluate them on a grid and create two interpolation functions representing the functions f_1 and f_2. This will ease the process of finding the roots, θ_{c_1} and θ_{c_2}, as these interpolation functions are less complicated and a Newton's iteration can now be readily applied. Once the approximate roots are found, it is trivial to find numerical values for the remaining boundary values $\frac{\partial T}{\partial \theta}(\theta_{c_1})$, $\frac{\partial T}{\partial \theta}(\theta_{c_2})$, $T(0)$ and $T(\pi)$. The solution in the interior of the three sub-domains, (I), (II) and (III), are given by (3.20), (3.22) and (3.24), respectively. The solution at the boundaries of the sub-domains is naturally $T(0)$ and $T(\pi)$ at the North and South pole, respectively, and at the critical latitudes $T(\theta_{c_1}) = T(\theta_{c_2}) = -1$.

A noteworthy remark is that when solving the system of equations (i)-(vi), one must handle the limits of the derivative of the Green's function with the utmost care. The limits must be taken in the correct order, hence the awkward notation. It merely serves as a remainder to the reader to handle these limits with delicacy.

Using the parameters found in Appendix A, with $Q = 247$, we obtain the solutions shown in dimensional form in Figure 4. The blue vertical lines indicate the critical latitudes. For $Q = 247$ the system of boundary integral equations (i)-(vi) has three solutions, meaning that there are three possible ways the sphere can realize a temperature distribution consistent with two ice edges.

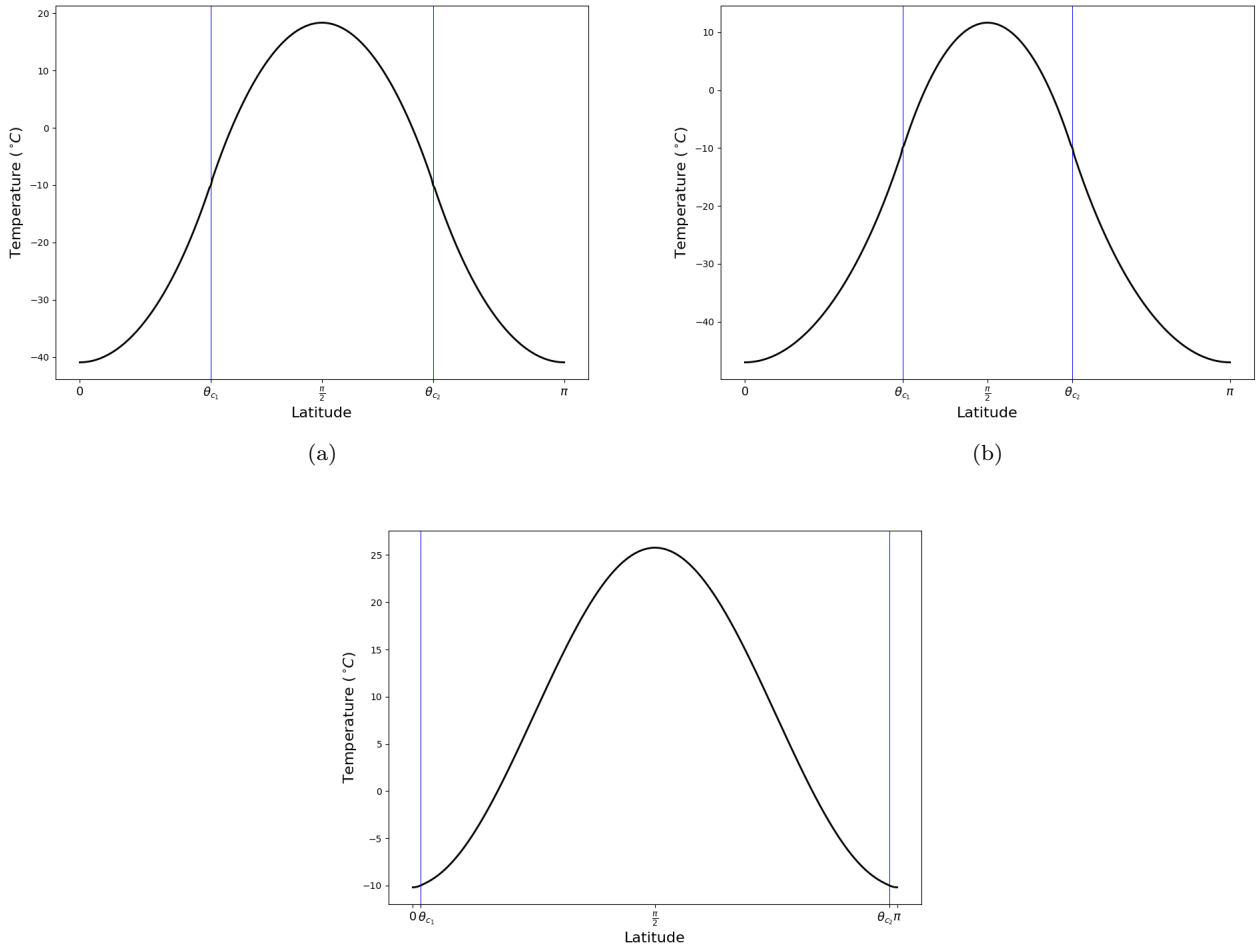

Figure 4: *Temperature profile of a water world with two ice edges. In the relevant parameter regime, two ice edges may be realized in three possible ways, shown in (a), (b) and (c).*

The observant reader may have noticed that the changing of the parameter Q caused a sudden qualitative change in the solution space of (3.1). Namely, the appearance of multiple stationary solutions, a bifurcation phenomena has occurred. In section 5 we will further investigate how bifurcation occurs in the model, and we shall see that for a certain range of parameter values, equation (3.1) has five solutions, and for other ranges there is only one.

3.3. Introducing a continent

We are now going to extend our energy balance model on a sphere to include a continent. We are still going to consider a rotationally symmetrical sphere, such that we can neglect the longitudinal dependence and persist with our one-dimensional analysis. A rotationally symmetrical sphere demands that a continent is a zonal strip stretching from the latitude θ_{l_1} to latitude θ_{l_2}. The following analysis will only include one such continent.

For the area of the surface covered by water, $\theta \in [0, \theta_{l_1}) \cup (\theta_{l_2}, \pi]$, the governing equation is the time-dependent energy balance equation from section 2. The dimensional form can be written as

$$C\partial_t T + D\mathcal{L}T + BT = Qs(\theta)(1 - a(T)) - A, \tag{3.25}$$

where

$$\mathcal{L}(\cdot) = -\frac{1}{\sin x}\frac{\partial}{\partial x}\left(\sin x \frac{\partial}{\partial x}(\cdot)\right). \tag{3.26}$$

For the area of the surface covered by land, $\theta \in [\theta_{l_1}, \theta_{l_2}]$, certain parameters in the governing equation will differ due to the physical properties of soil/bedrock and atmospheric conditions on continents compared to oceans. We let the continent have the average heat capacity

$$C_1$$

and the average thermal diffusion coefficient

$$D_1.$$

Both of these are constants, independent of latitude. Note that by approximating these parameters as two constants, we effectively consider the continent to be one uniform medium with a constant heat capacity and heat diffusion throughout. We model the albedo on the continent as

$$a_{\text{land}} = a_{\text{land}}(T).$$

The form of this albedo can be found in Appendix A. We allow for a separate critical temperature at the continent,

$$T_s(\theta, t) = T_{s_2} \qquad , \theta \in [\theta_{l_1}, \theta_{l_2}].$$

An average annual temperature below this threshold is deemed to induce a snow cover on the surface. The governing equation for continent is therefore

$$C_1\partial_t T + D_1\mathcal{L}T + BT = Qs(\theta)(1 - a_{\text{land}}(T)) - A, \tag{3.27}$$

where $\mathcal{L}$ is the operator (3.26). The numerical values chosen for C_1 and D_1 can be found in Appendix A.2.

Let's nondimensionalize the energy balance equations (3.25) and (3.27) following the approach outlined in section 2.1. Let

$$T(\theta_{c_i}) = -T_s \qquad \forall\, \theta_{c_i} \in [0, \theta_{l_1}) \cup (\theta_{l_2}, \pi]$$

be the critical temperature for the water-ice phase transition on water, and let

$$T(\theta_{c_i}) = -T_{s_2} \qquad \forall\, \theta_{c_i} \in (\theta_{l_1}, \theta_{l_2})$$

be the critical temperature for the water-ice phase transition on land. We use the dimensional constant T_s as a scale for temperature,

$$T = T_s T'. \tag{3.28}$$

Thus, the non-dimensional temperature at the critical latitudes, θ_{c_i}, must be

$$T'(\theta_{c_i}) = -1 \qquad \forall\, \theta_{c_i} \in [0, \theta_{l_1}) \cup (\theta_{l_2}, \pi]$$

on water, and

$$T'(\theta_{c_i}) = -\frac{T_{s_2}}{T_s} = -T_c \qquad \forall\, \theta_{c_i} \in (\theta_{l_1}, \theta_{l_2}) \tag{3.29}$$

on the continent. Note that we will encounter some special cases where $\theta_{c_i} = \theta_{l_1}$ or $\theta_{c_i} = \theta_{l_2}$. For these cases (3.29) does not necessarily hold and the temperature at these latitudes will instead be given by $T(\theta_{l_1})$ or $T(\theta_{l_2})$, found through solving the boundary integral equations. We use t_0 as a scale for time,

$$t = t_0 t'. \tag{3.30}$$

Using the scaling (3.28) and (3.30) we can write (3.25) and (3.27) as

$$\begin{cases} \gamma_1 \partial_t T + \mathcal{L}T + \beta_1 T = \eta_1 s(\theta)(1 - a_{\text{water}}(T)) - \alpha_1, & \theta \in [0, \theta_{l_1}) \cup (\theta_{l_2}, \pi] \\ \gamma_1 \partial_t T + \mathcal{L}T + \beta_2 T = \eta_2 s(\theta)(1 - a_{\text{land}}(T)) - \alpha_2, & \theta \in [\theta_{l_1}, \theta_{l_2}], \end{cases} \tag{3.31}$$

where

$$\begin{aligned} \gamma_1 &= \frac{C}{t_0 D}, & \gamma_2 &= \frac{C_1}{t_0 D_1}, \\ \beta_1 &= \frac{B}{D}, & \beta_2 &= \frac{B}{D_1}, \\ \eta_1 &= \frac{Q}{T_s D}, & \eta_2 &= \frac{Q}{T_s D_1}, \\ \alpha_1 &= \frac{A}{T_s D}, & \alpha_2 &= \frac{A}{T_s D_1}. \end{aligned} \tag{3.32}$$

Here the albedo function $a_{\text{water}}(T)$ is the albedo for water, familiar to us from presiding sections, previously referred to as simply $a(T)$. Note that in (3.31) we have dropped the prime notation on the non-dimensional temperature and time, as we from this point will work exclusively with the non-dimensional form of the governing equations. The solution must necessarily be continuous and differentiable at the interface between water and continent, θ_{l_1} and θ_{l_2}, as we cannot have a discontinuity in the average annual temperature nor do we allow for a build up of heat at these latitudes.

With the necessary modifications to our energy balance model addressed, we are ready to apply the boundary integral method to solve the stationary form of the energy balance equation (3.31) on sphere with a rotationally symmetrical continent.

3.3.1. Symmetrical continent

We are now going to find solutions to the stationary form of (3.31),

$$\begin{cases} \mathcal{L}T + \beta_1 T = \eta_1 s(\theta)(1 - a_{\text{water}}(T)) - \alpha_1, & \theta \in [0, \theta_{l_1}) \cup (\theta_{l_2}, \pi] \\ \mathcal{L}T + \beta_2 T = \eta_2 s(\theta)(1 - a_{\text{land}}(T)) - \alpha_2, & \theta \in [\theta_{l_1}, \theta_{l_2}], \end{cases} \tag{3.33}$$

on a sphere with a continent preserving the north-south symmetry. We let the extent of continent be

$$l = \frac{\pi}{4}.$$

Therefore, the continent must extend from the latitude

$$\theta_{l_1} = \frac{\pi}{2} - \frac{l}{2} = \frac{3\pi}{8}$$

to the latitude

$$\theta_{l_2} = \frac{\pi}{2} + \frac{l}{2} = \frac{5\pi}{8}.$$

Figure 5 shows a schematic of the surface of the sphere with a continent in accordance with these specifications.

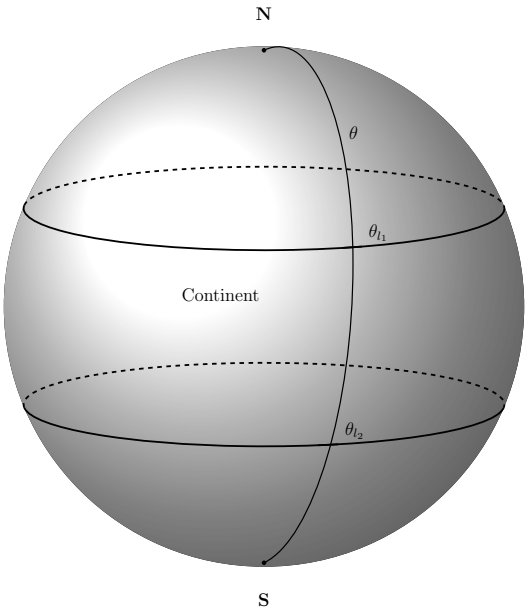

Figure 5: *Schematic of the surface of the sphere with a rotationally symmetrical continent preserving the north-south symmetry.*

Applying the boundary integral method to solve (3.33) will largely follow the procedure outlined in section 3.2, with the added complication of a continent. The most significant difference caused by the introduction of a continent is the appearance of multiple stationary solutions as we vary

the bifurcation parameter. Again, the bifurcation parameter is chosen to be the solar constant Q. As we shall soon see, there will be 4 major categories of solutions, referred to as cases. What's similar for solutions in the same category is the number of critical latitudes or ice edges, and the mathematical procedure for obtaining these solutions will consequently be very similar. In each category we may have up to two sub-categories of solutions, referred to as scenarios. In some of these scenarios there may be two possible solutions for a given Q, this will be further discussed shortly for the relevant scenarios. The cases and scenarios analysed in this section may be summarized as follows:

- The case of no ice edges
  - No ice/snow on the sphere
  - The sphere is fully covered by ice/snow
- The case of two ice edges
- The case of four ice edges
  - The continent is completely covered in ice/snow
  - The continent is partially covered in ice/snow
- The case of six ice edges
  - The northern and southern tips of continent is ice/snow free
  - The northern and southern tips of continent is covered in ice/snow

Recall that the goal of the boundary integral method is to derive integral relations for the solution to a differential equation that relate values of the solution in the interior of the domain to values on the boundary of the domain using a Green's function. In section 3.2 we saw that once we have obtained these integral relations, we can apply boundary integral equations to determine the unknown boundary values. A detailed derivation of the boundary integral relations and the boundary integral equations for the above cases can be found in Appendix E, as well as a description of how we solve the boundary integral equations to obtain stationary solutions. Here we will only present the dimensional form of the resulting temperature distributions for the various scenarios for a given Q. The following results concern a continent that preserves the north-south symmetry, the choice for θ_{l_1} and θ_{l_2} is stated above.

The case of no ice edges

The simplest possible case is one in which the surface is either entirely covered by ice/snow or the surface has no ice/snow-cover at all. Using the parameters found in Appendix A, with $Q = 300$, we obtain the temperature profiles shown in Figure 6 for these two scenarios. The green vertical lines indicate the latitudes at which the continent ends and begins.

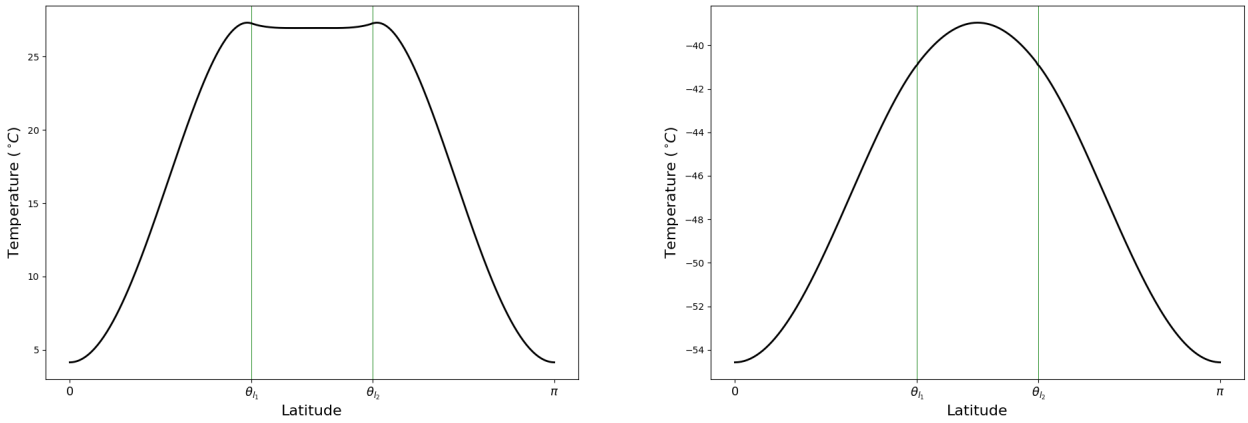

(a) *No ice/snow cover on the surface.*

(b) *The surface entirely covered by ice/snow.*

Figure 6: *Temperature profiles of a planet with a rotationally symmetrical continent preserving the north-south symmetry and no ice edges.*

The case of two ice edges

Let's turn our attention to the case where the sphere has two critical latitudes, θ_{c_1} and θ_{c_2}, or two ice edges. With a continent symmetrical about equator, and with the parameters used in the thesis, the only possible scenario is found to be one in which the critical latitudes appear somewhere on the water-covered part of the surface. The surface of the continent will then be completely ice-free. One could conceivably imagine a scenario where the water is completely frozen over and the critical latitudes appear somewhere on the continent, but this case is never realized with the current continent configuration. This scenario was analysed, but no solution was found.

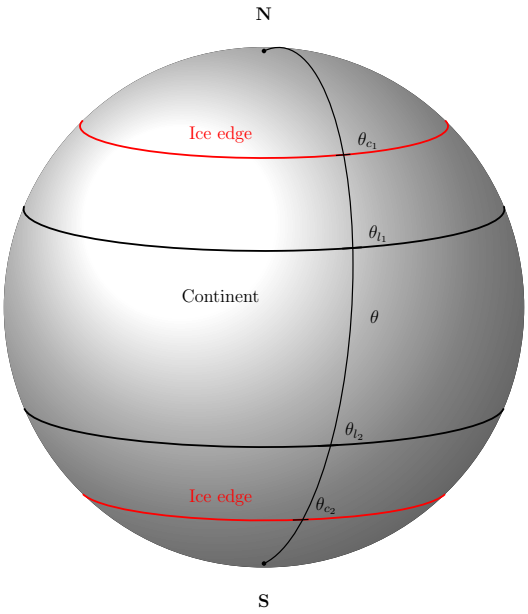

Figure 7: *Schematic of the surface of the sphere with a rotationally symmetrical continent preserving the north-south symmetry and two ice edges.*

Using the parameters found in Appendix A, with $Q = 275$, we obtain the temperature profile shown in Figure 8 for this scenario.

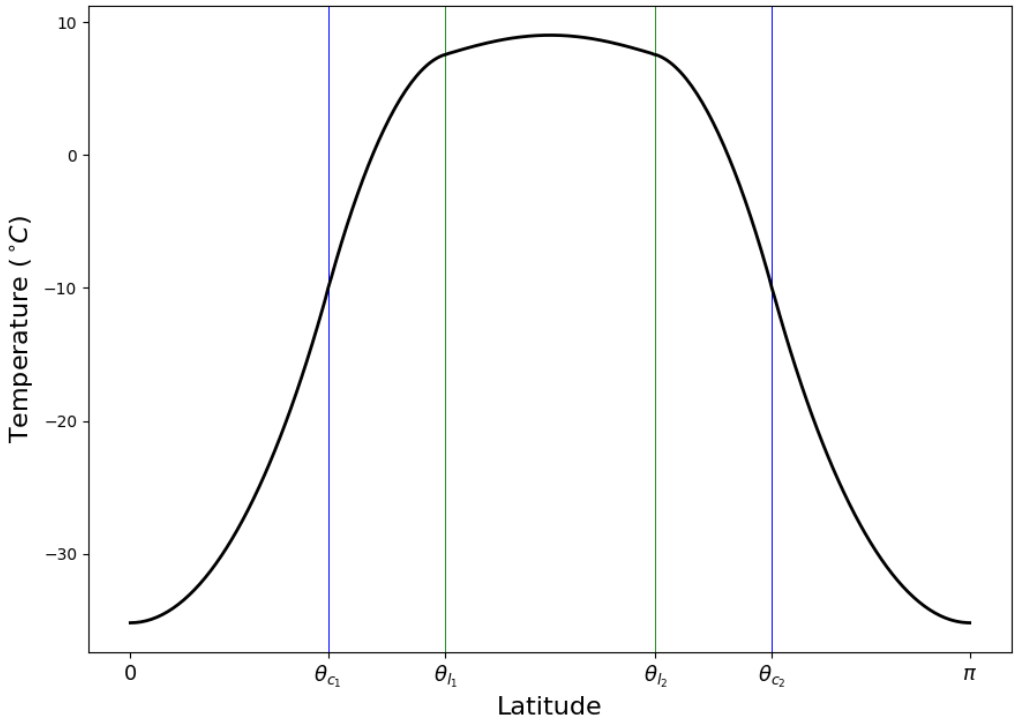

Figure 8: *Temperature profile of a planet with a rotationally symmetrical continent preserving the north-south symmetry and two ice edges.*

The case of four ice edges

The case where the sphere has four critical latitudes, θ_{c_1}, θ_{c_2}, θ_{c_3} and θ_{c_4}, was found to have two scenarios. Thus far we have referred to these scenarios as "the continent is completely covered in ice/snow" and "the continent has a partial ice/snow cover" and an explanation as to how these scenarios are realized might be in order. Figure 9 shows a schematic of the surface of the sphere for the case of four ice edges, and we observe that the surface of the continent is covered by three zonal strips. In the "the continent has a partial ice/snow cover"-scenario the northern and southern strips has no ice/snow cover. In the "the continent is completely covered in ice/snow"-scenario, the two of ice edges are exactly at the interface between continent and ocean,

$$\theta_{c_2} = \theta_{l_1}$$
$$\theta_{c_3} = \theta_{l_2}.$$

This is possible because the continent is chosen to have a higher critical temperature for ice formation than water (see Appendix A).

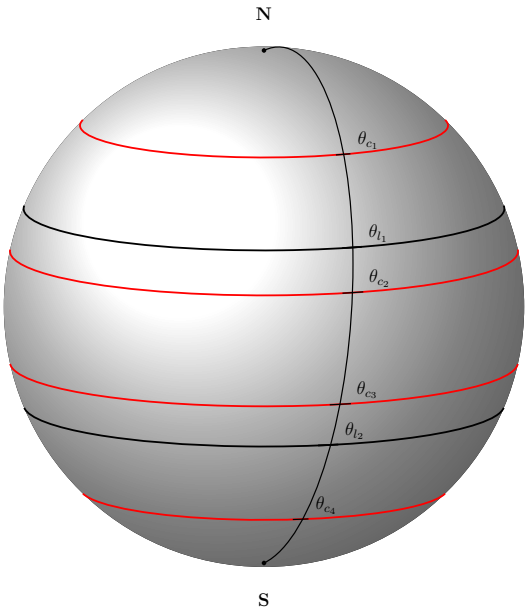

Figure 9: *Schematic of the surface of the sphere with a rotationally symmetrical continent preserving the north-south symmetry and four ice edges.*

Using the parameters found in Appendix A, with $Q = 350$, we obtain the temperature profile shown in Figure 10a for the scenario where the continent is completely covered in ice/snow. Using the parameters found in Appendix A, with $Q = 298$, we obtain the temperature profiles shown in Figure 10b and 10c for the scenario where there is a partial ice cover on the continent. For certain Q values, this scenario may be realized in two separate ways, meaning that the boundary integral equations associated with this scenario has two solutions.

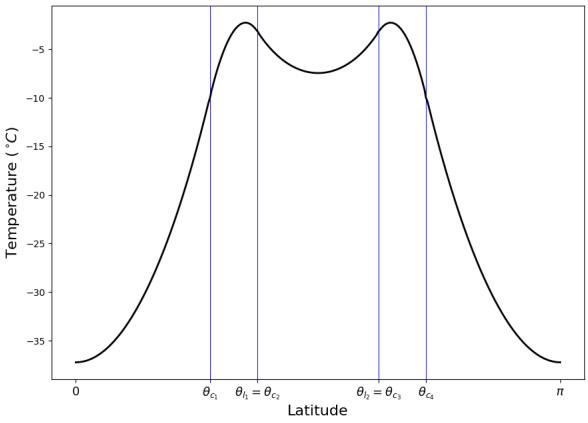

(a) *The continent is completely covered in ice/snow.*

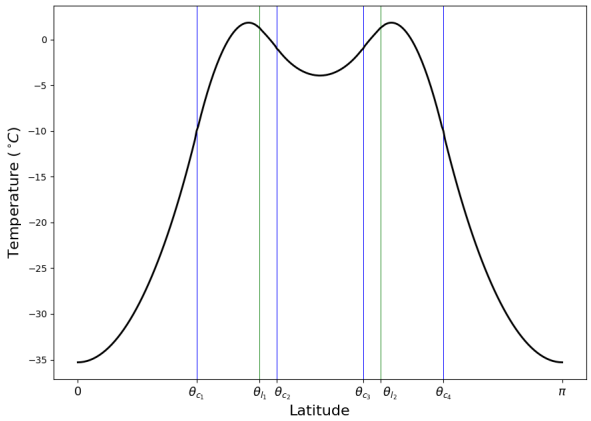

(b) *The continent has a partial ice/snow cover.*

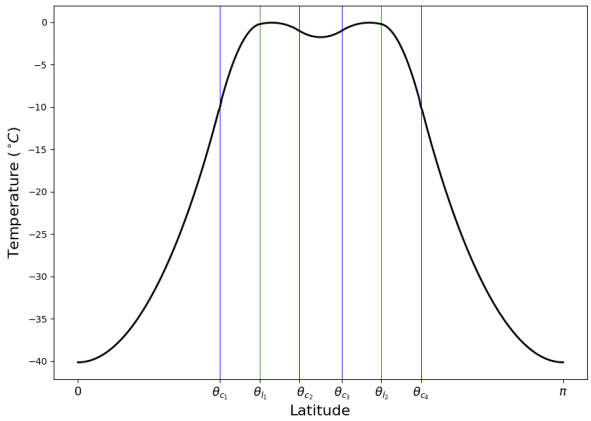

(c) *The continent has a partial ice/snow cover.*

Figure 10: *Temperature profiles of a planet with a rotationally symmetrical continent preserving the north-south symmetry and four ice edges.*

The case of six ice edges

The most complicated case analysed, was one in which the sphere has six critical latitudes, θ_{c_1}, θ_{c_2}, θ_{c_3}, θ_{c_4}, θ_{c_5} and θ_{c_6}. This case may be realized in two ways; either the northern and southern tips of continent is ice/snow free or the northern and southern tips of continent is covered in ice/snow. Figure 11 shows a schematic of the surface of the sphere with six ice edges and we observe that the continent has five zonal strips. If the northern and southern tips of continent is ice/snow free, we evidently must have a situation where the first and last zonal strips are ice/snow free. In order to have six ice edges the middle zonal strip must also be ice/snow free and the two remaining strips must be covered in ice/snow. The other possibility we must consider, is that the first and the last zonal strips covered in ice/snow. This can only be realized if

$$\theta_{c_2} = \theta_{l_1}$$

and

$$\theta_{c_5} = \theta_{l_2}.$$

Then the five zonal strips turns into three and the middle strip is the only ice/snow free strip. This is the "the northern and southern tips of continent is covered in ice/snow"-scenario.

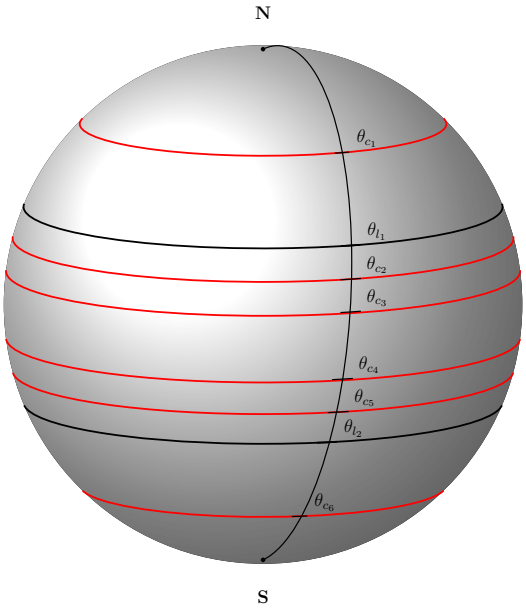

Figure 11: *Schematic of the surface of the sphere with a rotationally symmetrical continent preserving the north-south symmetry and six ice edges.*

Using the parameters found in Appendix A, with $Q = 304$, we obtain the temperature profile shown in Figure 12a for the scenario where the northern and southern tips of continent is ice/snow free. Using these parameters, and $Q = 310$, we obtain the temperature profile shown in Figure 12b and 12c for the scenario where the northern and southern tips of continent is covered in ice/snow. This scenario may be realized in two ways for certain Q values.

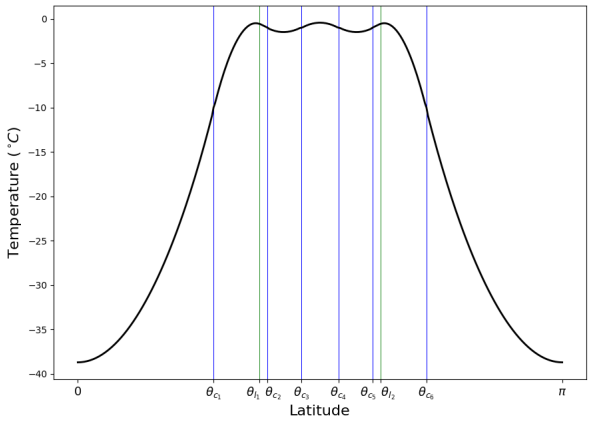

(a) *The northern and southern tips of continent is ice/snow free.*

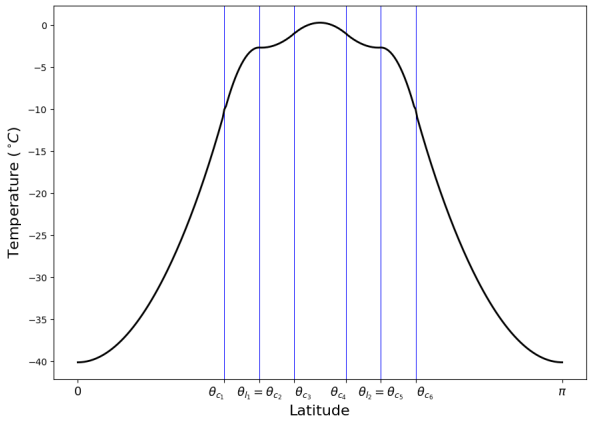

(b) *The northern and southern tips of continent is covered in ice/snow.*

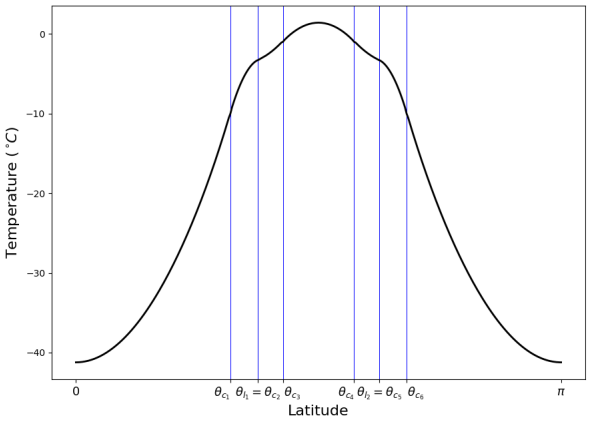

(c) *The northern and southern tips of continent is covered in ice/snow.*

Figure 12: *Temperature profiles of a planet with a a rotationally symmetrical continent preserving the north-south symmetry and six ice edges.*

In an attempt to reduce the computational complexity of the four and six ice edges cases, a symmetry assumption was applied. This symmetry assumption, as well as the resulting boundary integral relations and boundary integral equations, is discussed in detail in Appendix E. The advantage of applying such an assumption is that it reduces the complexity of the problem and it is especially useful in cases where the boundary integral equations has two solutions. The obvious downside is that this assumption is only valid for a continent that is symmetrical about equator.

3.3.2. Continent breaking the north-south symmetry

We are now going to find solutions the stationary energy balance equation (3.33) on a sphere with a continent breaking the north-south symmetry. We want to investigate how symmetry affect the

solution space of (3.33) and it therefore makes sense to initially observe how the climate system on the sphere respond to a minor symmetry violation. The symmetry violation here will be to slightly shift the continent to the north, thus breaking the symmetry about equator. We let the extent of continent remain at $l = \frac{\pi}{4}$, but the continent will now extend from the latitude

$$\theta_{l_1} = \frac{\pi}{2} - \frac{l}{2} - \varepsilon$$

to

$$\theta_{l_2} = \frac{\pi}{2} + \frac{l}{2} - \varepsilon,$$

where

$$\varepsilon = 0.1.$$

We will again use the boundary integral method to find solutions to (3.33) with this continent configuration. We obviously expect this symmetry violation to result in an asymmetrical temperature distributions for a given Q and we might therefore encounter new types of stationary solutions with an odd number of critical latitudes. In fact, our analysis shows that stationary solutions with numerous critical latitudes (four and six) will disappear as a result of this symmetry violation. We will at most have two critical latitudes with this continent configuration and the parameters used in this thesis. Mathematically speaking, this makes our job easier as there will be less unknown boundary values to find in order to obtain a solution.

We will again partition the types of stationary solutions found into categories based on the number of critical latitudes on the sphere. Retaining the case and scenario paradigm for section 3.3.1, we may summarize the types stationary solutions as:

- The case of no ice edges
  - No ice/snow on the sphere
  - The sphere is fully covered by ice/snow
- The case of one ice edge
  - Ice edge on northern ocean
  - Ice edge on continent
  - The northern ocean and the continent is covered by ice/snow
- The case of two ice edges
  - One ice edge on the northern ocean and one ice edge on the continent
  - One ice edge on the continent and one ice edge on the southern ocean

Appendix E includes a detailed description of how to apply the boundary integral method to obtain solutions for the above scenarios. Here we will only present a selection of solutions in dimensional form.

The case of no edges

For the case of no ice edges we naturally have the two scenarios of an ice-free and a totally ice covered surface familiar to us from the preceding sections. Using the parameters found in Appendix A, with $Q = 280$, we obtain the temperature profiles shown in Figure 13 for the two scenarios.

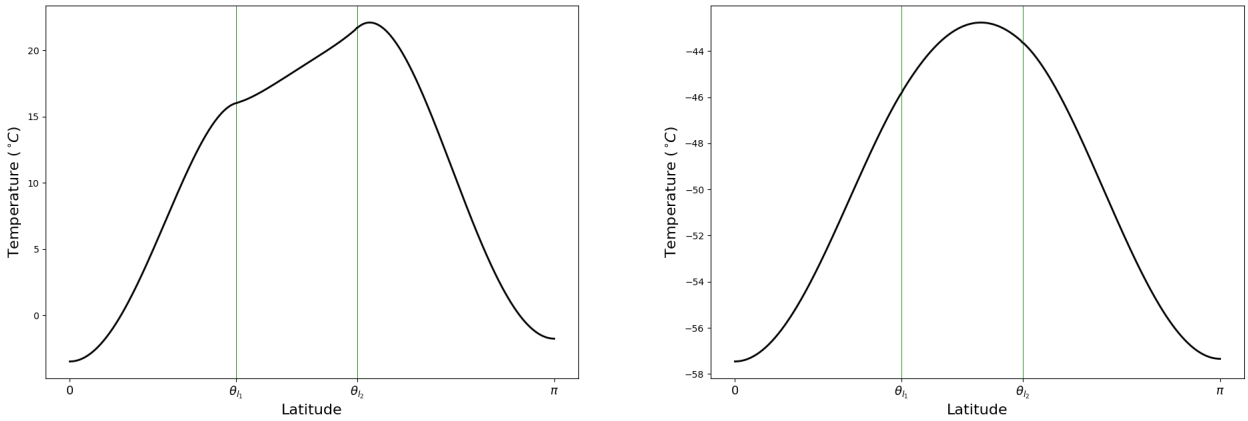

(a) *No ice/snow cover.*

(b) *Total ice/snow cover.*

Figure 13: *Temperature profiles of a planet with an asymmetrical continent with respect to the north-south symmetry,* $\varepsilon = 0.1$ *and no ice edges.*

The case of one edge

The case of one ice edge is an example of the new odd-numbered critical latitudes solutions expected from an asymmetrical continent configuration. In the case of one ice edge, the ice edge may appear either on the northern ocean or on the continent depending on Q. The stationary solutions with one ice edge are further grouped into scenarios based on the location of the ice edge, as the two types of solutions require a separate set of boundary integral relations and boundary integral equations. We have chosen to include the types of stationary solutions where both the northern ocean and the continent is completely ice/snow covered as a separate scenario. The reason for this is that for this type of solution we do not have to locate the ice edge. We know that the ice edge must be a the southern tip of the continent,

$$\theta_{c_1} = \theta_{l_2}.$$

Therefore, the boundary integral relations and boundary integral equations will differ from the "one ice edge on the continent"-scenario and we have three scenarios in the case of one ice edge. Using the parameters found in Appendix A, with $Q = 280$, we obtain the temperature profile shown in Figure 14a for the scenario in which the ice edge is on the northern ocean and the temperature

profile shown in Figure 14b when both the northern ocean and the continent is completely covered in ice/snow and the southern ocean is ice-free. With these parameters, and $Q = 310$, we obtain the temperature profile shown in Figure 14c when the ice edge is on the continent.

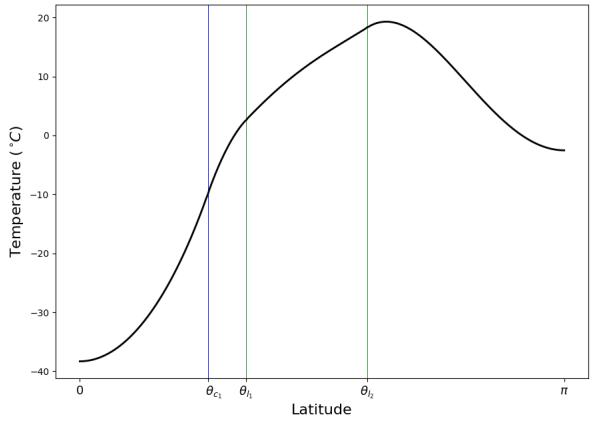

(a) *Ice edge on northern ocean.*

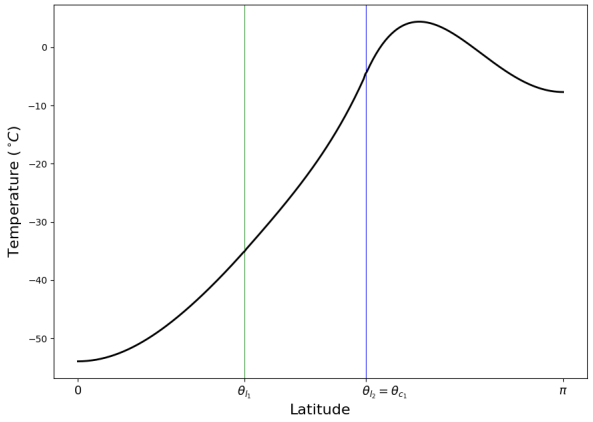

(b) *Ice/snow cover on the northern ocean and the continent.*

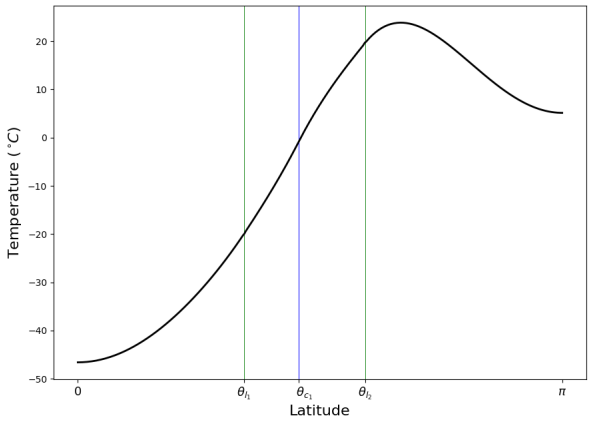

(c) *Ice edge on continent.*

Figure 14: *Temperature profiles of a planet with an asymmetrical continent with respect to the north-south symmetry, $\varepsilon = 0.1$ and one ice edge.*

The case of two edges

Finally, with this continent configuration the sphere may have two ice edges. This case can be realized in two way; either there is one ice edge on the northern ocean and one on the continent or there is one ice edge on the continent and one ice edge on the southern ocean. In the latter scenario the ice edge is always on the southern most tip of the continent,

$$\theta_{c_1} = \theta_{l_2}.$$

Using the parameters found in Appendix A, with $Q = 300$, we obtain the temperature profiles shown in Figure 15 for the two scenarios.

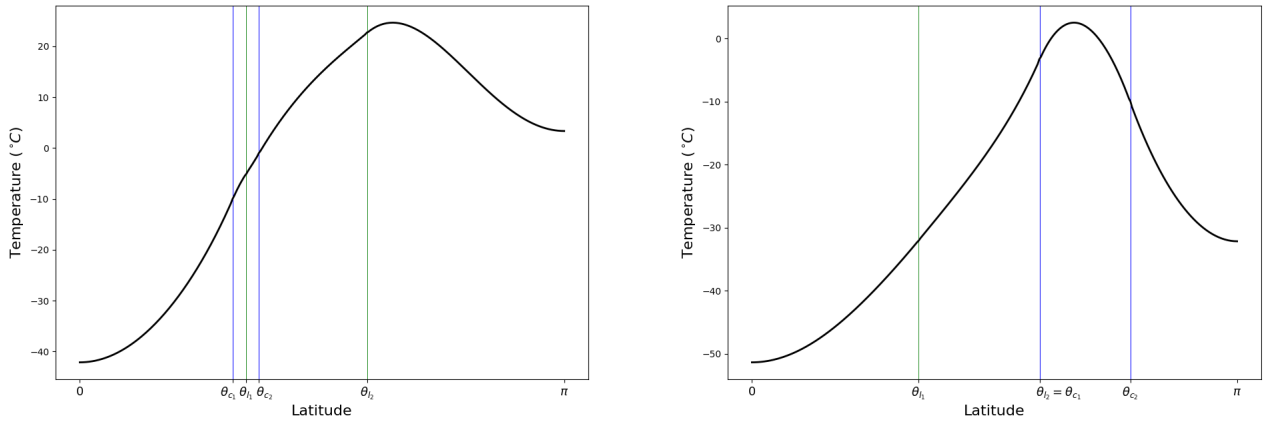

(a) *One ice edge on the northern ocean and one ice edge on the continent.*

(b) *One ice edge on the continent and one ice edge on the southern ocean.*

Figure 15: *Temperature profile of a planet with an asymmetrical continent with respect to the north-south symmetry,* $\varepsilon = 0.1$ *and two ice edges.*

3.3.3. Increasing the asymmetry

We want to further investigate how asymmetry affect the model. Now we are going to find solutions to the stationary energy balance equation (3.33) on a sphere with a continent shifted even further to the north. The continent still has an extent of $l = \frac{\pi}{4}$, but now it extends from the latitude

$$\theta_{l_1} = \frac{\pi}{2} - \frac{l}{2} - \varepsilon$$

to

$$\theta_{l_2} = \frac{\pi}{2} + \frac{l}{2} - \varepsilon,$$

where

$$\varepsilon = 0.5.$$

We use the boundary integral method to find these stationary solutions. The types of stationary solutions we will encounter with this continent configuration will be very similar to the ones found for $\varepsilon = 0.1$. Partitioning the types of stationary solutions into categories based on the number of critical latitudes, we may summarize the types of stationary solutions as:

- The case of no ice edges
  - No ice/snow on the sphere
  - The sphere is fully covered by ice/snow
- The case of one ice edge
  - Ice edge on northern ocean
  - Ice edge on continent

- The case of two ice edges
  - One ice edge on the northern ocean and one ice edge on the continent
  - One ice edge on the continent and one ice edge on the southern ocean

When listing the types of stationary solutions in this manner, there does not seem to be much change following a further shift of the continent, just the disappearance of one type of stationary solution. However, as we will see shorty, one these scenarios may be realized in several ways for the same Q value. Again, we only present a selection of these stationary solutions here, a detailed description of how to apply the boundary integral method to obtain these solutions is included in Appendix E.

The case of no edges

For the case of no ice edges we still have the ice-free and totally ice covered surface scenarios, shown in Figure 16. These solutions were obtained using the parameters found in Appendix A and $Q = 325$.

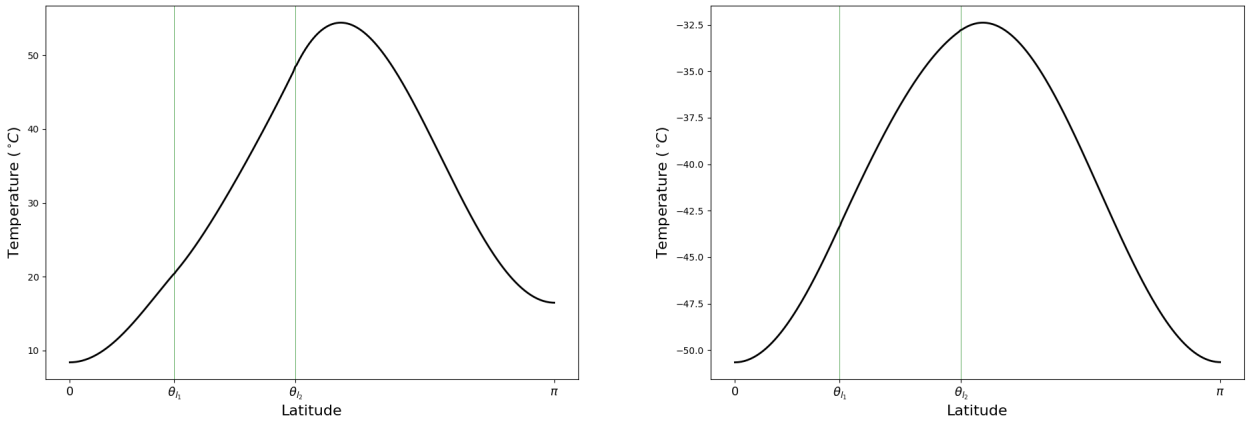

(a) *No ice/snow cover.* (b) *Total ice/snow cover.*

Figure 16: *Temperature profiles of a planet with an asymmetrical continent with respect to the north-south symmetry,* $\varepsilon = 0.5$ *and no ice edges.*

The case of one edge

With this new continent configuration, the sphere may still have one ice edge and that can appear anywhere on the surface depending on Q, apart from on the southern ocean. Figure 17 shows the temperature profile when the ice edge is on the northern ocean (17a) and when the ice edge is on the continent (17b), for $Q = 280$.

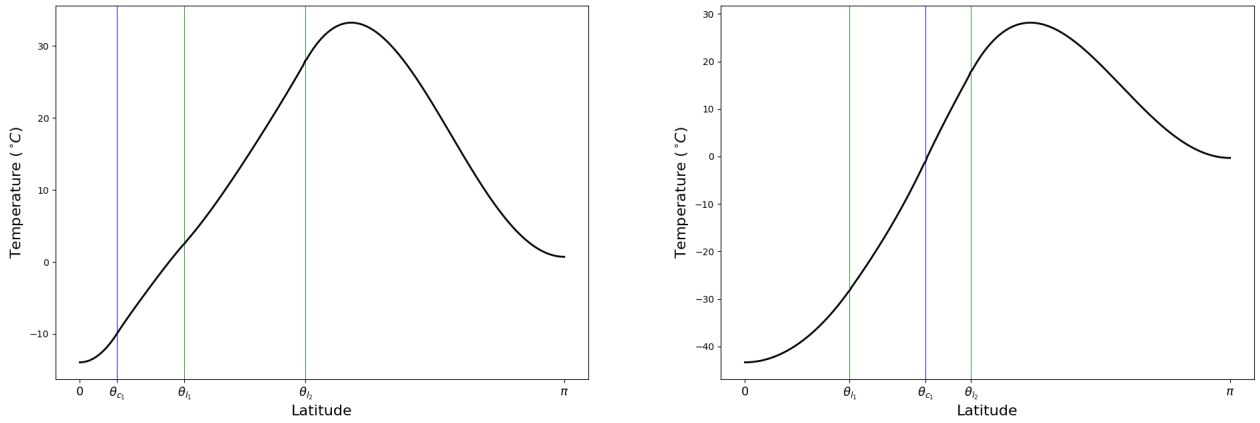

(a) *Ice edge on northern ocean.*

(b) *Ice edge on continent.*

Figure 17: *Temperature profiles of a planet with an asymmetrical continent with respect to the north-south symmetry,* $\varepsilon = 0.5$ *and one ice edge.*

The case of two edges

The last type of stationary solution with this continent configuration, is solutions where the sphere has two ice edges. This may be realised in two ways: The first possibility is that there is one ice edge on the northern ocean and one on the continent. Figure 18a shows the temperature profile on the sphere if this scenario is realized when $Q = 300$. The other possibility is that there is one ice edge on the continent and one ice edge on the southern ocean. Figure 18b-18d shows the three possible temperature profiles for $Q = 264$ when there is one ice edge on the continent and one ice edge on the southern ocean. For this scenario, the associated boundary integral equations has three solutions for certain Q values. Consequently, this type of stationary solution may be realized in three possible ways for the same Q value.

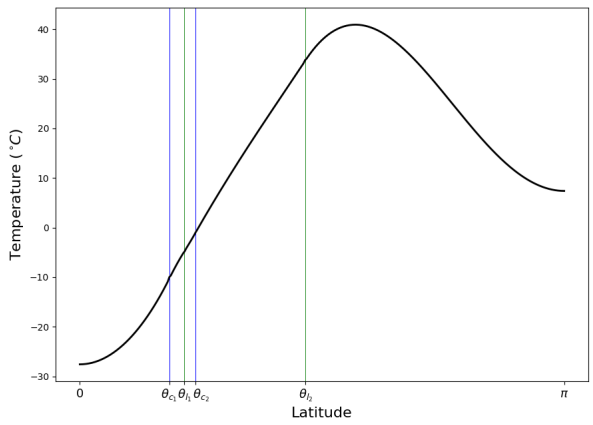

(a) *One ice edge on the northern ocean and one ice edge on the continent.*

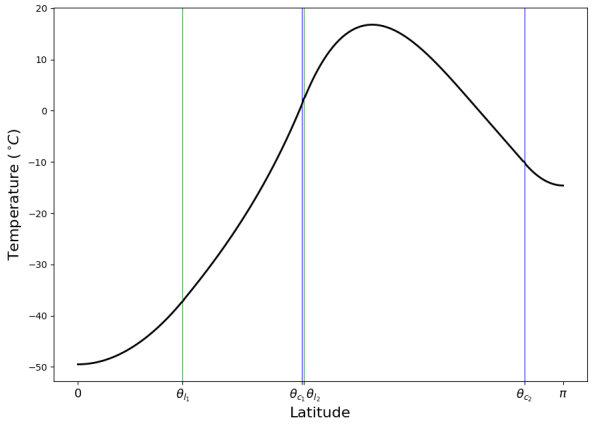

(b) *One ice edge on the continent and one ice edge on the southern ocean.*

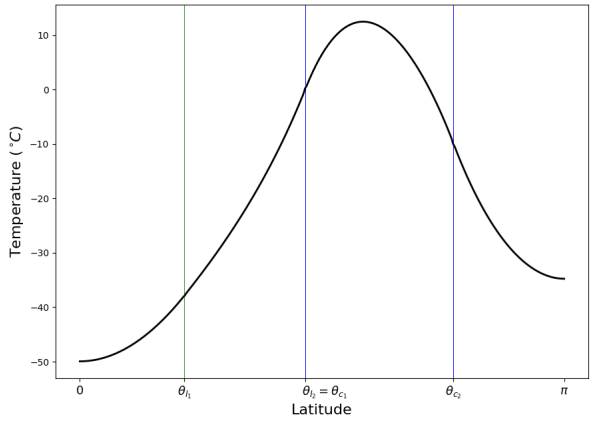

(c) *One ice edge on the continent and one ice edge on the southern ocean.*

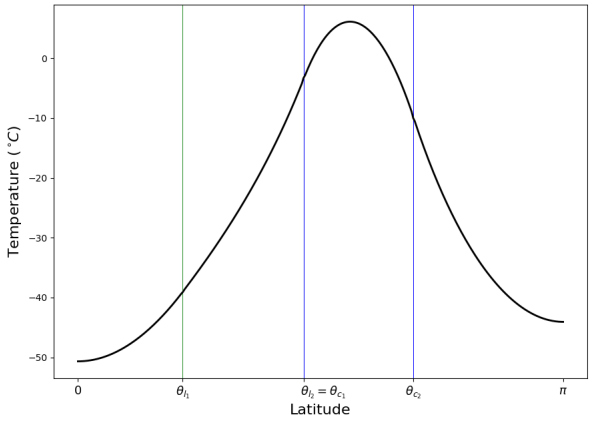

(d) *One ice edge on the continent and one ice edge on the southern ocean.*

Figure 18: *Temperature profile of a planet with an asymmetrical continent with respect to the north-south symmetry,* $\varepsilon = 0.5$ *and two ice edges.*

We have now found stationary solutions to the energy balance equation on a sphere (2.1), both with and without a continent. The stationary solutions are obviously time independent and describe the temperature distribution on the sphere when the climate system is in radiative equilibrium. In the next section we are going to find time dependent solutions, allowing us to observe how the climate system evolves over time from a given initial state.

4. Finite difference method

In this section we are going to apply a finite difference method for solving the nondimensional time dependent energy balance equation from section 2.1,

$$\gamma \partial_t T + \mathcal{L}T + \beta T = \eta s(\theta) a_c(T) - \alpha, \tag{4.1}$$

where $\mathcal{L}$ is the operator (3.6) and the dimensionless parameters are defined in (2.7). The co-albedo, $a_c(T) = 1 - a(T)$, is modelled as a smooth function and the specific form of this function is given in Appendix A. We have previously solved the stationary form of (4.1) using both analytical and numerical methods to obtain semi-analytical stationary solutions. For time dependent solutions to (4.1),

$$T = T(\theta, t),$$

we are content with a numerical solution. We start off by implementing a finite difference algorithm that solves (4.1) and then we apply an *artificial source test* to validate the implemented code.

4.1. Implement a finite difference algorithm

Finite difference methods relies on approximating differential operators using finite differences. Appendix C includes a derivation of a centered difference formula for operator (3.6) applied to a smooth function, f. For the discretized function evaluated on a uniform grid, x_i, where $f_i = f(x_i)$, a discrete approximation of $\mathcal{L}f$ will be

$$\hat{\mathcal{L}} f_i = -\frac{2(f_{i-1} - 2f_i + f_{i+1}) + (f_{i-1} - 4f_i + 3f_{i+1}) h \cot x_i}{2h^2}. \tag{4.2}$$

We will apply this approximation to implement a finite difference algorithm that solves (4.1) numerically. When approximating the term $\mathcal{L}T$ using (4.2), only the time derivative appears in (4.1) turning the problem into a system of ordinary differential equations. Let us first implement an algorithm that solves (4.1) on a water world and later discussing the necessary modifications to the algorithm in order to include a continent on the sphere.

4.1.1. For a water world

We have the discrete approximation (4.2) and we are ready to apply this approximation and develop a finite difference algorithm that solves (4.1) on a water world. We start by discretizing the domain as a uniform angular-time grid,

$$\begin{aligned} \theta_{i+1} &= \theta_i + h, \\ \theta_0 &= 0, \\ \theta_N &= \pi \end{aligned}$$

and

$$t_{j+1} = t_j + k.$$

We introduce the notation

$$T_{i,j} = T(\theta_i, t_j).$$

Using this notation, the discretized form of (2.6) becomes

$$\gamma \partial_t T_{i,j} + \hat{\mathcal{L}} T_{i,j} + \beta T_{i,j} = \eta s(\theta_i) a_c(T_{i,j}) - \alpha. \tag{4.3}$$

We assume that $T(\theta, t)$ is smooth throughout the domain, and can be described in terms of a power series expansion. We can therefore apply the finite difference approximation (4.2), and equation (4.3) takes the form

$$\begin{aligned} \gamma \partial_t T_{i,j} - \frac{2(T_{i-1,j} - 2T_{i,j} + T_{i+1,j}) + (T_{i-1,j} - 4T_{i,j} + 3T_{i+1,j}) h \cot\theta_i}{2h^2} \\ + \beta T_{i,j} = \eta s(\theta_i) a_c(T_{i,j}) - \alpha. \end{aligned} \tag{4.4}$$

Equation (4.4) paired with an initial condition,

$$T(\theta, t = 0) = T_{IC}(\theta),$$

gives rise to the system of initial value problems

$$\begin{aligned} \frac{\partial}{\partial t} T_{i,j} &= f(\theta_i, T_{i-1,j}, T_{i,j}, T_{i+1,j}), \qquad i = 1, 2, 3, ..., N-1, \\ T_{i,0} &= T_{IC}(\theta_i), \end{aligned} \tag{4.5}$$

where

$$\begin{aligned} f(\theta_i, T_{i-1,j}, T_{i,j}, T_{i+1,j}) = \frac{1}{\gamma} \Bigg[\frac{2(T_{i-1,j} - 2T_{i,j} + T_{i+1,j}) + (T_{i-1,j} - 4T_{i,j} + 3T_{i+1,j}) h \cot\theta_i}{2h^2} \\ - \beta T_{i,j} + \eta s(\theta_i) a_c(T_{i,j}) - \alpha \Bigg]. \end{aligned}$$

In order to fully specify the solution we need the values at the endpoints of grid, $T_{0,j}$ and $T_{N,j}$. We get these by invoking the boundary conditions. Recall that we have

$$\lim_{\theta \to 0} \sin\theta \frac{\partial T}{\partial \theta}(\theta) = 0.$$

Assume now that we have chosen an arbitrarily small h. At the second grid point, $\theta_1 = h$, we must therefore have

$$\sin\theta_1 \frac{\partial T}{\partial \theta}(\theta_1) = 0.$$

Applying the centered difference formula for first order derivatives, we can conclude that

$$\sin h \frac{T_2 - T_0}{2h} = 0.$$

For an arbitrarily small $h << 1$,

$$\sin h \approx h,$$

and therefore

$$\frac{T_2 - T_0}{2} = 0 \qquad \Longrightarrow \qquad T_0 = T_2.$$

Following a similar approach for the boundary condition at $\theta = \pi$, we get the analogous condition

$$T_N = T_{N-2}.$$

Thus, the boundary conditions (2.2) and (2.3) gives rise to the following rules in the numerical scheme;

$$\begin{aligned} T_{0,j} &= T_{2,j} \\ T_{N,j} &= T_{N-2,j}. \end{aligned} \tag{4.6}$$

The system of initial value problems (4.5), paired the rules at either end of the angular-time grid (4.6), is easily solved by any IVP-solver. Between every time step, the boundary conditions (4.6) is invoked allowing the algorithm to fill the angular-time grid and this gives us a numerical solution to the nondimensional time dependent energy balance equation (2.6) on a water world.

It is important to note that the rule (4.6) ensures that the finite difference method will only give a valid solution at the boundary if the solution satisfy the condition

$$T(\theta_0, t) \simeq T(\theta_2, t). \tag{4.7}$$

This condition is obviously a peculiar one, since it implies that either $\theta_0 \simeq \theta_2$ or the solution has to be approximately flat in a neighborhood near the boundary. In general we cannot rely on the solution being flat near the boundary, therefore satisfying condition (4.7) should ideally be satisfied through applying a very small spacial step, h.

4.1.2. With a continent

Modifying the algorithm outlined above to include a continent is simply a matter of changing the inhomogeneous term in the system of IVP's (4.5) for an interval of the domain corresponding to the extent of the continent. We are considering a rotationally symmetrical sphere with a continent stretching from θ_{l_1} to θ_{l_2}. Let

$$i_{l_1}$$

be the index of θ_{l_1} and

$$i_{l_2}$$

be the index of θ_{l_2} in the angular grid. Let

$$f_1(\theta_i, T_{i-1,j}, T_{i,j}, T_{i+1,j}) = \frac{1}{\gamma_1}\Bigg[\frac{2(T_{i-1,j} - 2T_{i,j} + T_{i+1,j}) + (T_{i-1,j} - 4T_{i,j} + 3T_{i+1,j})h\cot\theta_i}{2h^2} - \beta_1 T_{i,j} + \eta_1 s(\theta_i)\big(1 - a_{\text{water}}(T_{i,j})\big) - \alpha_1\Bigg] \tag{4.8}$$

and

$$f_2(\theta_i, T_{i-1,j}, T_{i,j}, T_{i+1,j}) = \frac{1}{\gamma_2}\Bigg[\frac{2(T_{i-1,j} - 2T_{i,j} + T_{i+1,j}) + (T_{i-1,j} - 4T_{i,j} + 3T_{i+1,j})h\cot\theta_i}{2h^2} - \beta_2 T_{i,j} + \eta_2 s(\theta_i)\big(1 - a_{\text{land}}(T_{i,j})\big) - \alpha_2\Bigg], \tag{4.9}$$

where the dimensionless parameters $\gamma_1, \beta_1, \eta_1, \alpha_1, \gamma_2, \beta_2, \eta_2$ and α_2 are defined in (3.32). The modified system of initial value problems now takes the form

$$\begin{aligned} \frac{\partial}{\partial t}T_{i,j} &= \tilde{f}(i, \theta_i, T_{i-1,j}, T_{i,j}, T_{i+1,j}) \qquad\qquad i = 1, 2, 3, ..., N-1, \\ T_{i,0} &= T_{IC}(\theta_i), \end{aligned} \tag{4.10}$$

where

$$\tilde{f}(i, \theta_i, T_{i-1,j}, T_{i,j}, T_{i+1,j}) = \begin{cases} f_1(\theta_i, T_{i-1,j}, T_{i,j}, T_{i+1,j}), & i \in [1, i_{l_1}) \cup (i_{l_2}, N-1] \\ f_2(\theta_i, T_{i-1,j}, T_{i,j}, T_{i+1,j}), & i \in [i_{l_1}, i_{l_2}] \end{cases}.$$

The system of IVP's (4.10) is solved by an IVP solver, between every time step in the iteration we must still invoke the discretized boundary condition (4.6). This gives us a numerical solution to the nondimensional time dependent energy balance equation (2.6) on sphere with a rotationally symmetrical continent.

4.2. Artificial source test

We are now going to apply an artificial source test to validate the numerical solution form section 4.1. An artificial source test is a general method for testing the precision of a numerical solution to a differential equation. The procedure when applying an artificial source test is as follows: Consider a general differential equation on the form

$$\mathcal{G}f(\vec{x}, t) = h(\vec{x}, t), \tag{4.11}$$

where $\mathcal{G}$ is some differential operator. Assume that we have implemented some numerical method for solving (4.11). In order to apply the artificial source test we assume an exact solution

$$f_e(\vec{x}, t),$$

such that the exact function

$$\rho(\vec{x}, t) = \mathcal{G} f_e(\vec{x}, t)$$

is known. Let this be the "artificial source", hence the name of the test. Next, we let the implemented numerical method solve the related problem

$$\mathcal{G} f(\vec{x}, t) = \rho(\vec{x}, t). \tag{4.12}$$

The solution, $f(\vec{x}, t)$, produced by the numerical method when solving (4.12), should match the assumed exact solution $f_e(\vec{x}, t)$ perfectly. If so, this validates the implemented numerical method as the exact solution to (4.12) is exactly $f_e(\vec{x}, t)$. Choosing an assortment of assumed exact solutions and running them through the artificial source test procedure, the resulting numerical solutions should all match the corresponding assumed exact solutions. The assumed exact solution must also satisfy any constraints or conditions imposed on the solution of the original problem (4.11).

Now we are going to apply several artificial source tests to the finite difference method developed in section 4.1. We assume some solution to (2.6),

$$T_e = T_e(\theta, t).$$

We make sure that this assumed solution satisfy the boundary conditions (2.2) and (2.3). We find the associated artificial source

$$\rho(\theta, t) = \gamma \partial_t T_e + \mathcal{L} T_e + \beta T_e.$$

This artificial source will be an exact function, and we let the finite difference algorithm solve the modified problem

$$\begin{aligned} \gamma \partial_t T + \mathcal{L} T + \beta T &= \rho(\theta, t) \\ \lim_{\theta \to 0} \sin\theta \frac{\partial T}{\partial \theta}(\theta) &= 0 \\ \lim_{\theta \to \pi} \sin\theta \frac{\partial T}{\partial \theta}(\theta) &= 0. \end{aligned}$$

A variety of assumed solutions were tested. Some plausible solutions based on physical intuition and some solutions chosen specifically to test the robustness of the implemented code. Here we present a selection of two assumed solutions, and the results when these are applied in an artificial source test. For both of these tests were applied to a water world with the angular step $h = 0.01$ and the parameters given in appendix A. Figure 19a and 19b shows the dimensional form of the assumed solution (dotted) and the numerical solution produced by the finite difference algorithm when given the corresponding artificial source (solid).

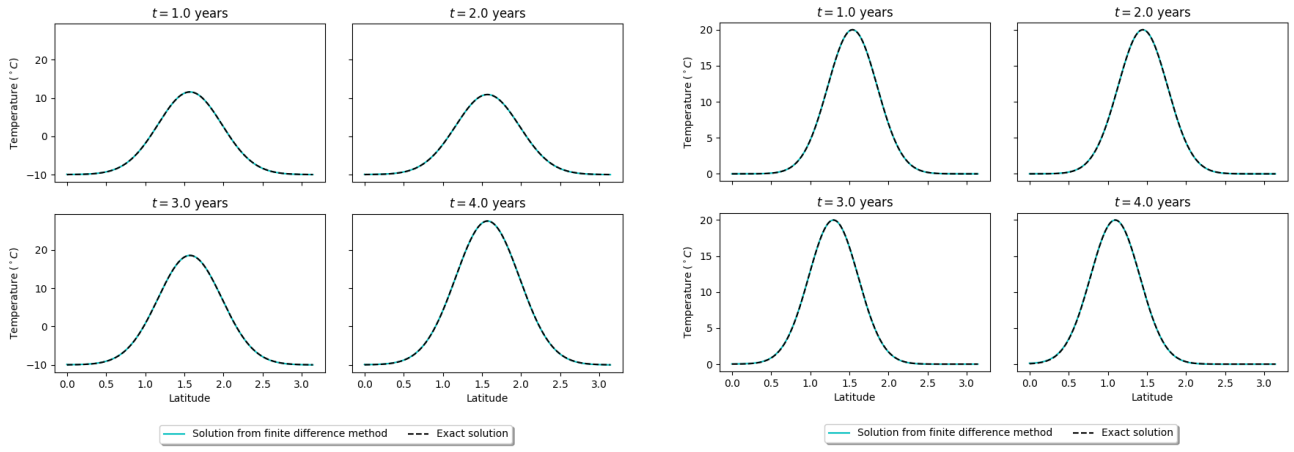

(a) (b)

Figure 19: *Artificial source test.*

In Figure 19a the assumed solution is

$$T_e(\theta, t) = (3 - \sin(t_0 t))e^{-3(\theta - \frac{\pi}{2})^2} - 1 \tag{4.13}$$

and in Figure 19b the assumed solution is

$$T_e(\theta, t) = 2e^{-5(\theta - \frac{\pi}{2}\cos(0.2 t_0 t))^2}. \tag{4.14}$$

The assumed solutions (4.13) and (4.14) are non-dimensional, and chosen such that the dimensional equivalent, $T_s T_e$, has a magnitude within a plausible range based the current state of Earth's climate, and they vary on the timescale t_0. The functions (4.13) and (4.14) are also chosen such that they are approximately flat in a neighborhood around the boundary. This is strictly for convenience, as the rule in the numerical scheme (4.6) implies that the algorithm only gives valid solutions at the boundary either if the spacial step h is sufficiently small or the solution is flat close to the boundary. Reducing h exponentially increases the run time of the code, hence why it is more convenient to choose assumed solutions that are flat near the boundary when one are to apply a multitude of tests.

We have now developed a time dependent numerical solution to (4.1) and validated it using artificial sources. In the next section we are going to apply the finite difference code to investigate how the stationary solutions from section 3 evolve in time given a small perturbation. This will hopefully give us some clues regarding the stability properties of the stationary solutions.

5. Analysis of stationary solutions

In this section we are going to analyse the stationary solutions found in section 3. As we saw in section 3, for a certain type of sphere there are several types of stationary solutions corresponding to certain climate states, each of these will be realized for a certain parameter regime. The parameter we vary in the model is Q, the bifurcation parameter. Varying Q will cause the sudden appearance and disappearance of stationary solutions and in this section we wish to draw bifurcation diagrams associated with the different spheres analysed in section 3. In order to do so, it is vital to identify for which values of Q the different types of stationary solutions are realized. This was done by a trial and error approach where different Q values was tried and the resulting stationary solution was analyzed. If the underlying assumptions of the specific type of stationary solution was not violated, we gradually increased/decreased Q until the underlying assumptions are violated. At that point we repeat the process for the subsequent type of stationary solution. The values in the bifurcation diagram associated with a specific type of stationary solution is often called a *branch*, and the points at which one type of stationary solution transitions into another usually indicate bifurcation points.

Once we have identified the Q values for which the various types of stationary solutions are valid, the next step in order to draw a bifurcation diagram is to choose a state quantity to gauge the change in the climate system on the sphere. Here we are free to choose any state quantity, but we want to choose a state defining quantity, some quantity that represents the state of the climate system for a certain Q. In this thesis we choose this quantity to be maximum global surface temperature.

In order to draw an informative bifurcation diagram, we want it to include indications of stability. We are therefore going to assess the stability of the stationary solutions found in section 3. We start by analysing the stationary solutions found for a water world. For a water world, a heuristic approach will suffice in order to infer the stability properties of the stationary solutions. Next, we analyse the stationary solutions found in the case of a sphere with a continent, apply a stability analysis with an eigenvalue approach and draw the associated bifurcation diagrams. In the latter part of this section we are going to look at our findings as a whole and view them in light of the more complex earth system models.

5.1. Water world

A bifurcation diagram associated with a water world is shown in Figure 20. It shows the maximum global surface temperature as a function of the bifurcation parameter, Q. The solid lines indicate stable states of the climate system, and the dotted line indicate an unstable state. From Figure 20 it is evident that the type of bifurcations present in this system are saddle-node bifurcations, as two stationary solutions come together as the bifurcation parameter is varied and disappear beyond the bifurcation point. On Either side of the bifurcation point we have an unstable stationary solution (saddle) and a stable stationary solution (node). We will shortly address how we draw the conclusions regarding the stability of the stationary solutions, but let's first discuss what the stability means in physical terms.

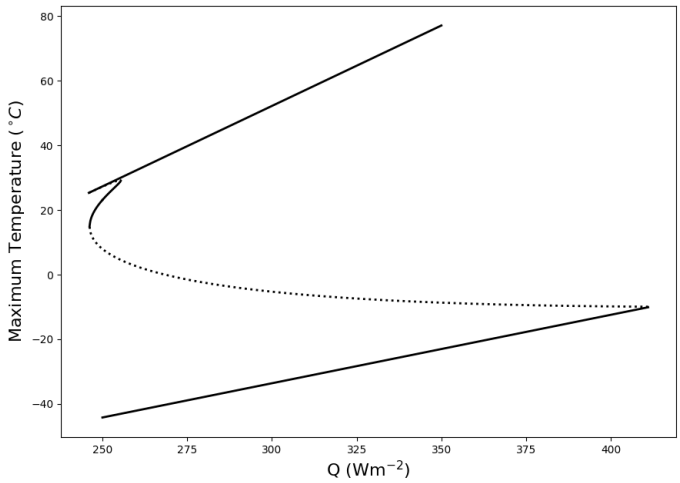

Figure 20: *The bifurcation diagram associated with the stationary energy balance equation (3.1) for a water world.*

The above discussion suggests that the climate system on the water world has multiple states. The lower branch in Figure 20 corresponds to a state of the climate system often referred to as "Snowball Earth". This is a state in which the planet is entirely covered by ice and snow, and due to the reflectiveness of ice and snow, the climate system will remain in this state making it a steady state. As for the intermediate unstable branch in Figure 20, this is a state the climate system will never retain. Since this branch contains unstable stationary solutions to (3.1), these states cannot persist over time and will never by observed in a physical system. The upper branch and the stable, intermediate branch represents steady states akin to the interglacial climate of the Earth today. There is also a small unstable branch between the upper branch and the stable, intermediate branch, better illustrated in Figure 21.

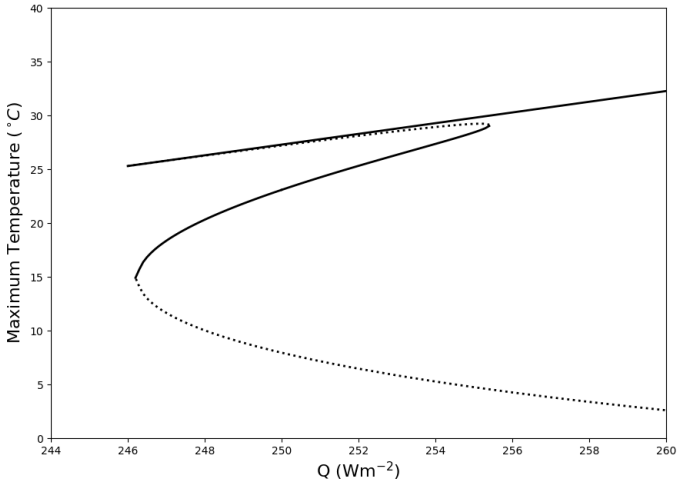

Figure 21: *The bifurcation diagram illustrating the small ice cap instability associated with a water world.*

The bistability observed in Figure 21 has a fascinating consequence. Let's say the climate system on our sphere rests at some equilibrium in the stable, intermediate branch and Q is gradually

increased. This will initially result in a more or less linear response in the temperature profile until a tipping point is reached. Beyond the tipping point, the climate system on the planet will, in time, stabilize at a new equilibrium in the upper branch. For the sphere in question, this will have a dramatic effect on the polar ice caps. The smaller, unstable branch consists of stationary solutions where the ice edges are close to the poles (see Figure 4c) and the sphere has small polar ice caps. Figure 21 suggests that these state cannot persist and the climate system will therefore abruptly transition into an ice-free state if a tipping point is exceeded. In order to return to the initial state, Q must be decreased until another tipping point is reach causing the climate to eventually stabilize at the intermediate branch again. This is the small ice cap instability famous for this model [16].

5.1.1. Heuristic stability analysis

The discussion above highlights the importance of stability in a physical system. We are now going to test the stability of the stationary solutions found in section 3.2 using a heuristic approach. The idea here is to apply the finite difference algorithm developed in section 4.1 to study how the stationary solutions evolve in time. For a given Q value, the stationary solution is found and then added white noise. This perturbed solution is subsequently used as the initial condition in the finite difference algorithm, which is ran until the time dependent numerical solution stabilizes at some temperature profile. The stability criteria here is that the time dependent numerical solution must remain approximately similar to the initial condition for a sufficiently long period of time. Here, $t = 20$ years is deemed to be a sufficiently long time for the time dependent solutions to stabilize, and we are satisfied with approximate similarity considering that the numerical solution uses a smooth albedo function and the stationary solutions are found using a step function albedo.

A stability analysis of this kind was performed on a number of stationary solutions. Stationary solutions corresponding to the upper and lower intermediate branches in the bifurcation diagram (Figure 20) were deemed to be unstable. Solutions corresponding to the upper and lower branches were deemed to be stable, as well as the very intermediate branch. Figure 22 shows a selection of perturbed stationary solutions and the resulting time dependent solution after $t = 20$ years. Note that even though Figure 22 includes dynamical runs of multiple perturbed stationary solutions within the same branch, we do not expect to find differing stability properties within the same branch. The branches are clearly defined and the bifurcation points have been identified. We simply try multiple stationary solutions within the same branch to illustrate the stability properties of the branches with some additional evidence.

We can clearly see that the solutions corresponding to the lower, intermediate branch stabilizes at some temperature profile consistent with an upper or lower branch solution. Solutions in the upper and lower branch remain virtually unchanged after $t = 20$ years, only the initial noise is removed. The finite difference algorithm was ran with the parameters in Appendix A and a the spacial step $h = 0.01$.

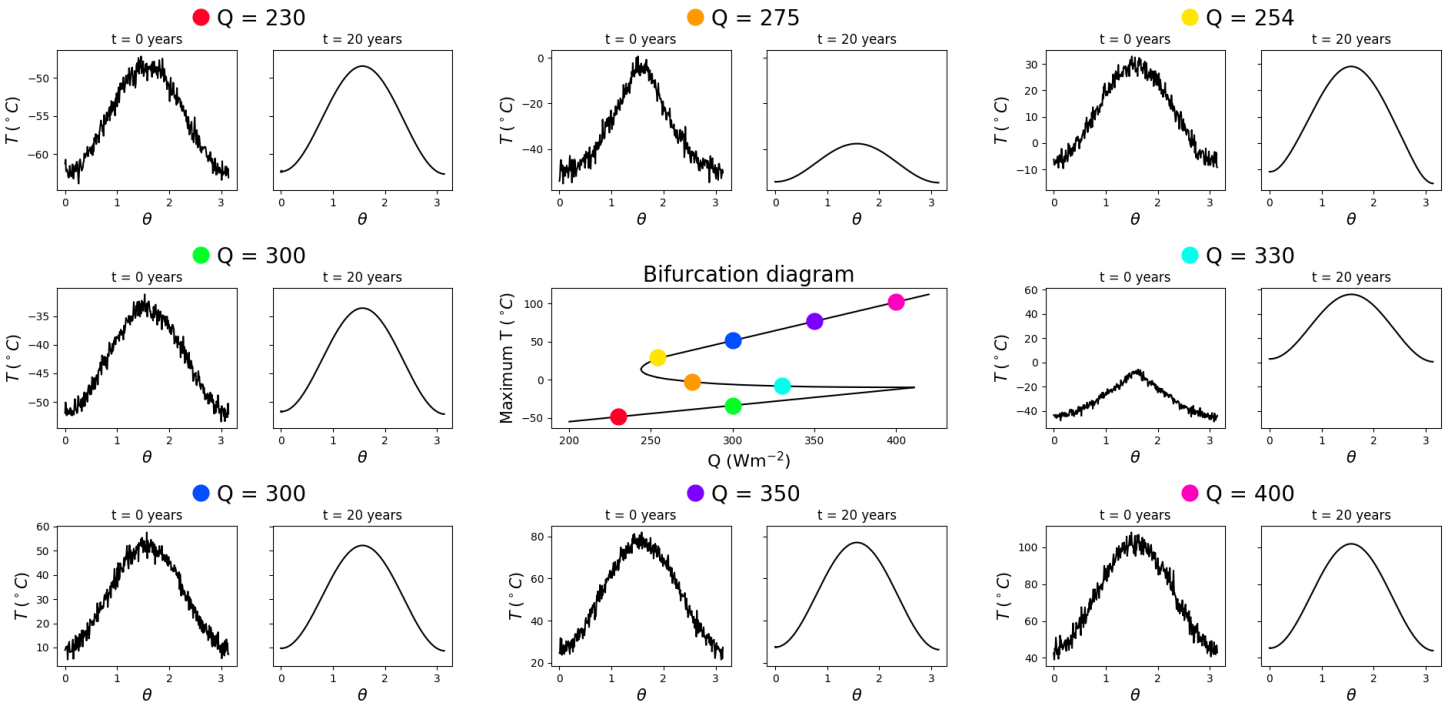

Figure 22: *Heuristic stability analysis of a selection of stationary solutions, with indications of their respective location in the bifurcation diagram.*

This heuristic approach is far from ideal. For one, performing numerical simulations on a number of initial conditions is a time consuming process and we cannot try all possible stationary solutions within a branch. Secondly, we can never know for certain whether the simulation was ran for a sufficiently long time to assess the stability properties of the stationary solutions. Stability requires that the time dependent solution stabilizes and remains unchanged for all future time, which is obviously unfeasible to assess due to computational complexity. Numerical errors will also compile as t grows. The method ultimately require a certain amount of judgement on the part of the user. Is the time dependent solution similar enough to the initial condition to be deemed stable or unstable? And is the simulation ran for a sufficient time to detect a potential divergence away from the stationary solution? In the case of a water world, this method was nevertheless deemed to give enough evidence to infer the stability properties of the stationary solutions. Solutions within the same branch in the bifurcation diagram behaved very similarly, solutions in the upper and lower branch showed no sign of diverging from the initial condition as t grew, and solutions in the intermediate branch stabilized quickly on a form consistent with an upper or lower branch solution.

5.2. North-south symmetrical continent

We are going to draw the bifurcation diagram for the stationary energy balance equation (3.33) with a continent that preserves the north-south symmetry. In section 3.3.1 we saw that the introduction

of a continent gave rise to the appearance of new types of stationary solutions and some of these also had a two solutions for a given Q. Consequently, a bifurcation diagram associated with a sphere with a rotationally symmetrical continent will have more branches than a bifurcation diagram associated with a water world. Figure 23 shows the maximum global surface temperature on the sphere as a function of the bifurcation parameter Q. This bifurcation diagram has no indications of stability, just indications of where the cases analysed in this section belong in the bifurcation diagram. We will shortly analyse the stability of the stationary solutions, and then revisit the bifurcation diagram for a more thorough discussion.

As it turned out, the increased complexity brought about by the introduction of a continent, called for a more robust stability analysis than the heuristic approach discussed above. We will therefore develop an eigenvalue approach to assess the stability of the stationary solutions found in section 3.3.1.

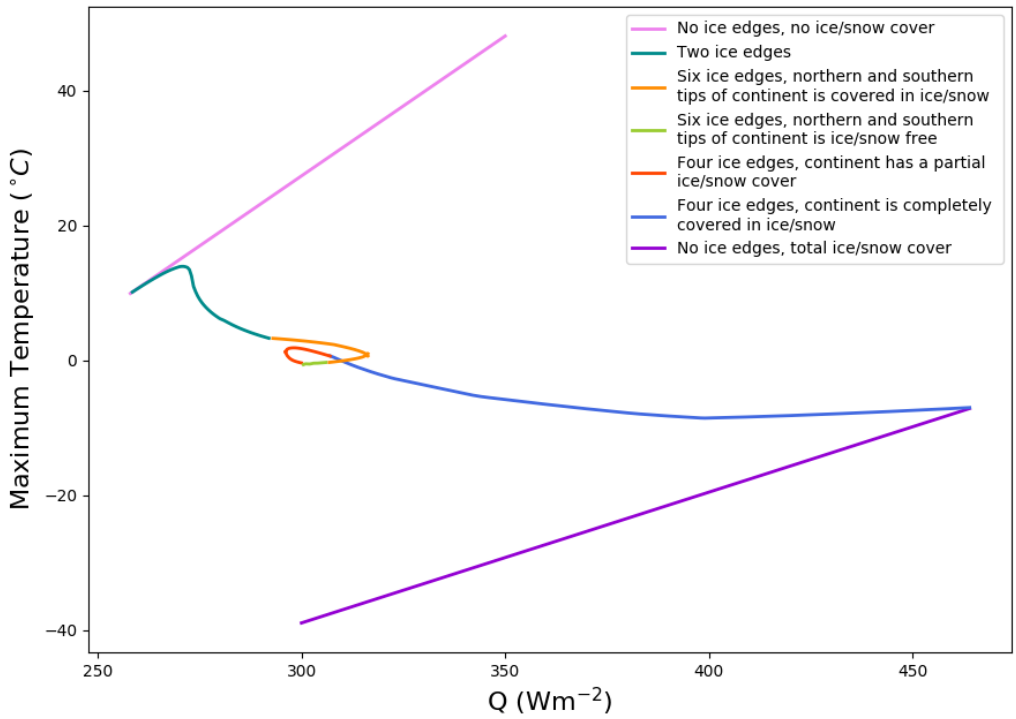

Figure 23: *Bifurcation diagram with indications of the type of solution in each branch.*

This section has an accompanying animation which illustrates how the surface of the sphere and the temperature profile is affected by varying the bifurcation parameter. The reader is encouraged to watch this animation as it highlights how the various cases are realized and the transitions between them. Note that the animation is not meant to depict the time evolution of the climate system on the sphere as a consequence of radiative forcing. The animation simply follows the branches in the bifurcation diagram to illustrate the transition between the cases discussed in this section. As we will see shortly, some branches in the bifurcation diagram might be unstable and

will not persist in a physical system over time. Furthermore, the bifurcation parameter switches between increasing and decreasing in the animation in order to follow the branches. The smooth transitions between climate states depicted in the animation may not necessarily present how a physical planet respond to radiative forcing, we will return to this question ones the branches are tested for stability. The animation is the attached file "*animation.mp4*".

5.2.1. Stability analysis

We are going to test the stationary solutions found in section 3.3 using an eigenvalue approach. Let's start by considering the time dependent energy balance equation,

$$\gamma\partial_t T - \frac{1}{\sin\theta}\frac{\partial}{\partial\theta}\big(\sin\theta\frac{\partial T}{\partial\theta}\big) + \beta T = \eta s(\theta)(1 - a(T)) - \alpha, \tag{5.1}$$

where $a(T)$ is the smooth albedo function. Applying the notation from section 3 we rewrite equation (5.1) as

$$\gamma\partial_t T + \mathcal{L}T = h, \tag{5.2}$$

where

$$h = h(T, \theta)$$

and

$$\mathcal{L}(\cdot) = -\frac{1}{\sin\theta}\frac{\partial}{\partial\theta}\big(\sin\theta\frac{\partial}{\partial\theta}(\cdot)\big) + \beta(\cdot).$$

In section 3 we found a set of stationary solutions,

$$T_0 = T(\theta, t = 0),$$

such that

$$\mathcal{L}T_0 = h \qquad \Longrightarrow \qquad \partial_t T_0 = 0.$$

The stationary solution, T_0, is given a small perturbation,

$$T(\theta, t) = T_0(\theta) + \zeta(\theta, t).$$

The idea here is to investigate if ζ will grow or shrink as t grows. The stationary solution, T_0, is stable if ζ approach 0 as $t \longrightarrow \infty$.

We substitute the perturbed stationary solution back into equation (5.2),

$$\begin{aligned} \gamma\partial_t(T_0 + \zeta) + \mathcal{L}(T_0 + \zeta) &= h(T_0 + \zeta, \theta) \\ \gamma\partial_t\zeta + \mathcal{L}T_0 + \mathcal{L}\zeta &= h(T_0 + \zeta, \theta). \end{aligned} \tag{5.3}$$

The perturbation is initially small, therefore

$$\zeta(\theta, t) \approx 0$$

for $t \sim 0$. Taylor expanding $h(T_0 + \zeta, \theta)$ around (T_0, θ) we get

$$h(T_0 + \zeta, \theta) \approx h(T_0, \theta) + h_T(T_0, \theta)\zeta,$$

neglecting higher order terms since ζ is initially small. Here

$$h_T(T_0, \theta) = \frac{\partial h}{\partial T}(T_0, \theta)$$

and can be found analytically for a given T_0. Substituting this $h(T_0 + \zeta, \theta)$ into (5.3) we get

$$\begin{aligned} \gamma\partial_t\zeta + \mathcal{L}T_0 + \mathcal{L}\zeta &= h(T_0, \theta) + h_T(T_0, \theta)\zeta \\ \partial_t\zeta &= \mathcal{H}\zeta, \end{aligned} \tag{5.4}$$

where

$$\mathcal{H}(\cdot) = \frac{1}{\gamma}\Big[h_T(T_0, \theta)(\cdot) - \mathcal{L}(\cdot)\Big].$$

Suppose ζ has the form

$$\zeta(\theta, t) = e^{\lambda t}\zeta_0(\theta). \tag{5.5}$$

We substitude this ζ into (5.4)

$$\begin{aligned} \lambda e^{\lambda t}\zeta_0 &= e^{\lambda t}\mathcal{H}\zeta_0 \\ \lambda\zeta_0 &= \mathcal{H}\zeta_0 \end{aligned} \tag{5.6}$$

and recognize that we now have an eigenvalue problem. If the eigenvalue λ is real and positive, the perturbation (5.5) will grow exponentially and the stationary solution T_0 is unstable.

We will solve this eigenvalue problem (5.6) with a numerical method that relays on discretizing ζ_0 and $\mathcal{H}\zeta_0$. We introduce a uniform angular grid for θ,

$$\theta_{i+1} = \theta_i + d\theta,$$

where

$$\begin{aligned} \theta_0 &= 0 \\ \theta_N &= \pi \end{aligned}$$

Let

$$T_0^i = T_0(\theta_i)$$

and

$$\zeta_0(\theta_i) = \zeta_0^i.$$

The discrete form of ζ_0, that is ζ_0 evaluated on the grid, is evidently a vector,

$$\vec{\zeta_0} = \begin{bmatrix} \zeta_0^0 \\ \zeta_0^1 \\ \vdots \\ \zeta_0^N \end{bmatrix}.$$

Let

$$f^i = \big(\mathcal{H}\zeta_0\big)^i = \frac{1}{\gamma}\Big[h_T(T_0^i, \theta_i)\zeta_0^i - \hat{\mathcal{L}}\zeta_0^i\Big].$$

be a discrete approximation to the function $\mathcal{H}\zeta_0$. We can now approximate the eigenvalue problem (5.6) as

$$\lambda\vec{\zeta_0} = H\vec{\zeta_0}, \tag{5.7}$$

where the set of the set of linear equations

$$\big\{\lambda\zeta_0^i = f^i\big\}_{i=0}^N \tag{5.8}$$

gives rise to the coefficient matrix H. Solving the discretized eigenvalue problem (5.7) is now a numerical exercise where we are looking for eigenvalues, λ_j, where $\mathrm{Re}\{\lambda_j\} > 0$. If the matrix H, associated with a stationary solution, T_0, has at least one eigenvalue with a positive real part, the stationary solution T_0 is deemed to be unstable.

In order to build the matrix H we must find a discrete approximation, f^i, to the function $\mathcal{H}\zeta_0$. Since $h_T(T, \theta)$ is an analytical function, we only have to approximate $\mathcal{L}\zeta_0$. We are going to approximate $\mathcal{L}\zeta_0$ using finite differences and for $i = 1, 2, 3, ..., N-1$ we can apply the centered difference approximation of the operator $\mathcal{L}$ from section 4,

$$f^i = \frac{1}{\gamma}\Big[h_T(T_0^i, \theta_i)\zeta_0^i - \hat{\mathcal{L}}\zeta_0^i\Big], \tag{5.9}$$

where

$$\hat{\mathcal{L}}\zeta_0^i = \beta\zeta_0^i - \frac{2(\zeta_0^{i-1} - 2\zeta_0^i + \zeta_0^{i+1}) + (\zeta_0^{i-1} - 4\zeta_0^i + 3\zeta_0^{i+1})d\theta\cot\theta_i}{2d\theta^2}.$$

For f^0 and f^N we need an approximation of $\mathcal{L}\zeta_0$ that does not rely on neighboring grid values on both sides of ζ_0^i. We are therefore seeking a forward difference approximation for f^0 and a backward difference approximation for f^N. Appendix C includes a derivation of both a forward and the backward approximation of the operator $\mathcal{L}$ and we will use those to determine f^0 and f^N.

With the appropriate approximations of $\mathcal{L}\zeta_0$, f^0 and f^N takes the form;

$$f^0 = \frac{1}{\gamma}\left[h_T(T_0^0, \theta_0)\zeta_0^0 - \hat{\mathcal{L}}_f\zeta_0^0\right],$$
$$f^N = \frac{1}{\gamma}\left[h_T(T_0^N, \theta_N)\zeta_0^N - \hat{\mathcal{L}}_b\zeta_0^N\right],$$

where

$$\hat{\mathcal{L}}_f\zeta_0^0 = \beta\zeta_0^0 + \frac{-2(\zeta_0^0 - 2\zeta_0^1 + \zeta_0^2) + (5\zeta_0^0 - 8\zeta_0^1 + 3\zeta_0^2)d\theta\cot\theta_0}{2d\theta^2}$$

and

$$\hat{\mathcal{L}}_b\zeta_0^N = \beta\zeta_0^N + \frac{-2(\zeta_0^{N-2} - 2\zeta_0^{N-1} + \zeta_0^N) + (\zeta_0^{N-2} - \zeta_0^N)d\theta\cot\theta_N}{2d\theta^2}.$$

As t grows the perturbation (5.5) must necessarily follow the same boundary conditions as the solution. This is only possible if the discretized form of the function $\zeta_0(\theta)$, ζ_0^i, follow the discrete boundary conditions (4.6) from section 4.1. Therefore, ζ_0^i must satisfy the following condition;

$$\begin{aligned}\zeta_0^0 &= \zeta_0^2\\ \zeta_0^N &= \zeta_0^{N-2}.\end{aligned} \tag{5.10}$$

The approximation f^i will generally have the form

$$f^i = f_1^i\zeta_0^{i-1} + f_2^i\zeta_0^i + f_3^i\zeta_0^{i+1},$$

but for every f^i involving ζ_0^2 and ζ_0^{N-2} we must impose condition (5.10), thus eliminating ζ_0^2 and ζ_0^{N-2} from the system of equations (5.8). With these expression for f^i the matrix H takes the form

$$H = \begin{bmatrix}
f_1^0 & f_2^0 & 0 & 0 & 0 & 0 & 0 & 0 & & & & & & & & 0 \\
f_1^1 & f_2^1 & 0 & 0 & 0 & 0 & 0 & 0 & & & & & & & & 0 \\
f_1^2 & f_2^2 & 0 & f_3^2 & 0 & 0 & 0 & 0 & & & & \dots & & & & 0 \\
f_1^3 & 0 & 0 & f_2^3 & f_3^3 & 0 & 0 & 0 & & & & & & & & 0 \\
0 & 0 & 0 & f_1^4 & f_2^4 & f_3^4 & 0 & 0 & & & & & & & & 0 \\
0 & 0 & 0 & 0 & f_1^5 & f_2^5 & f_3^5 & 0 & & & & & & & & 0 \\
 & & & & & & & \ddots & & & & & & & & \\
0 & & & & & & & 0 & f_1^{N-5} & f_2^{N-5} & f_3^{N-5} & 0 & 0 & 0 & 0 & \\
0 & & & & & & & 0 & 0 & f_1^{N-4} & f_2^{N-4} & f_3^{N-4} & 0 & 0 & 0 & \\
0 & & & & & & & 0 & 0 & 0 & f_1^{N-3} & f_2^{N-3} & 0 & 0 & f_3^{N-3} & \\
0 & & & & \dots & & & 0 & 0 & 0 & 0 & f_1^{N-2} & 0 & f_2^{N-2} & f_3^{N-2} & \\
0 & & & & & & & 0 & 0 & 0 & 0 & 0 & 0 & f_1^{N-1} & f_2^{N-1} & \\
0 & & & & & & & 0 & 0 & 0 & 0 & 0 & 0 & f_1^N & f_2^N &
\end{bmatrix}.$$

An important note here is that the parameters γ and β in (5.9) will vary depending on whether θ_i is in a regime corresponding to water or a regime corresponding to the continent. So, we must vary f^i depending θ_i in the same way as we did in section 4.1.2. Details are left out here, the procedure will be exactly the same as in section 4.1.2, but this is important in order to obtain the correct H and successfully performing this stability analysis.

Given a stationary solution T_0, constructing the matrix H and finding its eigenvalues is a quick process, computationally speaking. We can therefore try a multitude of stationary solutions within a branch in the bifurcation diagram. For every branch in the bifurcation diagram, we apply this stability analysis on every stationary solutions with an integer Q value. For instance, in the "No ice edges, total ice/snow cover"-branch in Figure 23 we try $Q = 300, 301, 302, ..., 460$. If the matrix H associated with a stationary solution T_0 has one or more real, positive eigenvalues, the stationary solution T_0 is deemed unstable. Note that if the stationary solution has a Q value too close to the bifurcation point, this test fails and we must therefore draw conclusions form stationary solutions in the interior of the branch. A stability analysis of this kind was applied on the stationary solutions found in section 3.3.1, and the results are displayed in the bifurcation diagram in Figure 24. Solid lines indicate stable stationary solutions and dashed lines indicate unstable stationary solutions. These results were cross checked with the heuristic approach from earlier as a "sanity check".

Note that this stability analysis has a potential pitfall that warrants some discussion. The discretized eigenvalue problem (5.7) may give rise to "parasitic" eigenvalues. Some of the associated eigenvectors might not describe the discrete form of a differentiable function. The idea here, is that

the perturbation (5.5) should be able to describe the solution $T(\theta, t)$. However, if the eigenvectors do not represent a differentiable function, they can never describe the solution. The associated eigenvalues are therefore uninteresting since the behavior they would exhibit in the perturbation (5.5) would never occur. It is therefore wise to inspect the associated eigenvectors and assess their suitability as eigenfunctions to the original eigenvalue problem (5.6). In this thesis, we instead ran through the above process with numerous stationary solutions within the same branch and viewed the result as a whole. If the vast majority of stationary solutions had no real, positive eigenvalues, the branch was deemed stable. Even though this potential issue with unsuitable eigenvectors did not cause us much trouble in this instance, it is an important thing to keep in mind when applying this method.

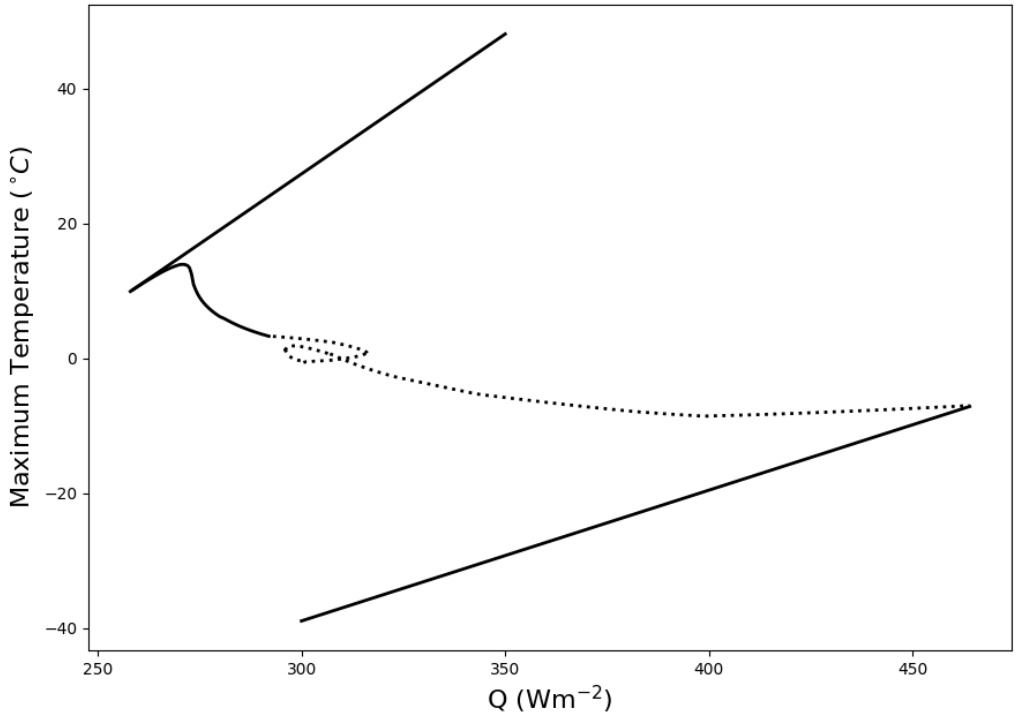

Figure 24: *Bifurcation diagram associated with a sphere with a rotationally symmetrical continent preserving the north-south symmetry.*

From Figure 24 it is evident that for a certain range of Q values, $Q \in [258, 292]$, we have three stable stationary solutions (the lower branch extends linearly until $Q = 0$). In this simple model, it makes sense to focus on the stable stationary solutions since we are investigating the model in light of the complex dynamics of the earth system models. For earth system models, only dynamical runs are available and the solution must, in time, settle at some stable equilibrium or close to some fixed point in solution space. As we have seen, a dynamical run of our model will always settle at some solutions consistent with a stable stationary solution. We want to see if the stable stationary solutions are affected by moving the continent to a configuration that breaks the north-south symmetry. Particularly, we want to investigate if the range of parameter values where we have three stable stationary solutions decrease or even disappear.

5.3. Asymmetrical continent

We are now going to perform the stability analysis introduced above on the stationary solutions to the energy balance equation (3.31) on a sphere with a rotationally symmetrical continent breaking the north-south symmetry. Once the stability properties of the stationary solutions are known, we draw a bifurcation diagram where the results of the stability analysis are the displayed. The stability properties are cross check with numerical simulations using the finite difference algorithm from section 4.

5.3.1. Shift continent of 0.1 latitude

We start by looking at the stationary solutions on a sphere with a minor symmetry violation with respect to the north-south symmetry. These are the stationary solutions found in section 3.3.2. Recall that the first symmetry violation introduced, consisted of slightly shifting the continent to the north such that the continent extends from the latitude

$$\theta_{l_1} = \frac{\pi}{2} - \frac{l}{2} - \varepsilon$$

to

$$\theta_{l_2} = \frac{\pi}{2} + \frac{l}{2} - \varepsilon,$$

where

$$\varepsilon = 0.1.$$

As we saw in section 3.3.2, this minor symmetry violation had a major effect on the climate system on the sphere. Consequently, we expect a bifurcation diagram for a sphere with this continent configuration to look very different from that of a sphere with a north-south symmetrical continent. Figure 25a show a bifurcation diagram for a sphere with a continent satisfying the above specifications, where the maximum surface temperature is plotted as a function of the bifurcation parameter Q. Solid lines indicate stable states and dashed lines indicate unstable states.

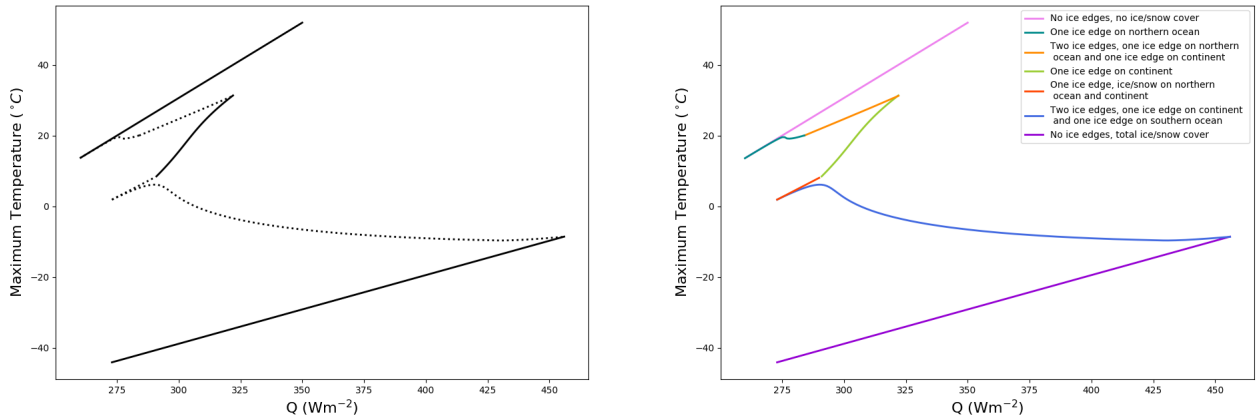

(a) *With stability indications.*

(b) *With indications of the type of stationary solutions.*

Figure 25: *Bifurcation diagram associated with a sphere with a rotationally symmetrical continent breaking the north-south symmetry and* $\varepsilon = 0.1$.

The continent has a higher thermal diffusion coefficient, D_1, than that of water (see Appendix A), and the continent therefore distributes thermal energy more efficiently. In the case of a north-south symmetrical continent, this resulted in a very fine dynamic with several unstable "multiple-ice-edge" solutions, generating a spiral in the bifurcation diagram. In the case of a continent breaking the north-south symmetry, this energy distribution becomes skewed and this very fine dynamic disappears. We still have a range of Q values, $Q \in [290, 322]$, in which there are three stable stationary solutions. However, the symmetry violation caused this range to slightly diminish. We want to investigate if there is a pattern here: Is the symmetry violation responsible for this phenomenological reduction in the range of Q values for which there are three stable stationary solutions? Seeking to answer this question, we are going to draw a similar bifurcation diagram for a sphere with a continent shifted even further to the north.

5.3.2. Shift continent of 0.5 latitude

We are going to draw a similar bifurcation diagram as above for a sphere where the continent is moved even further to the north. In section 3.3.2 we also found stationary solutions to (3.31) for

$$\theta_{l_1} = \frac{\pi}{2} - \frac{l}{2} - \varepsilon$$
$$\theta_{l_2} = \frac{\pi}{2} + \frac{l}{2} - \varepsilon,$$

where

$$\varepsilon = 0.5.$$

We perform the stability analysis from above and the results are displayed in the bifurcation diagram in Figure 26a.

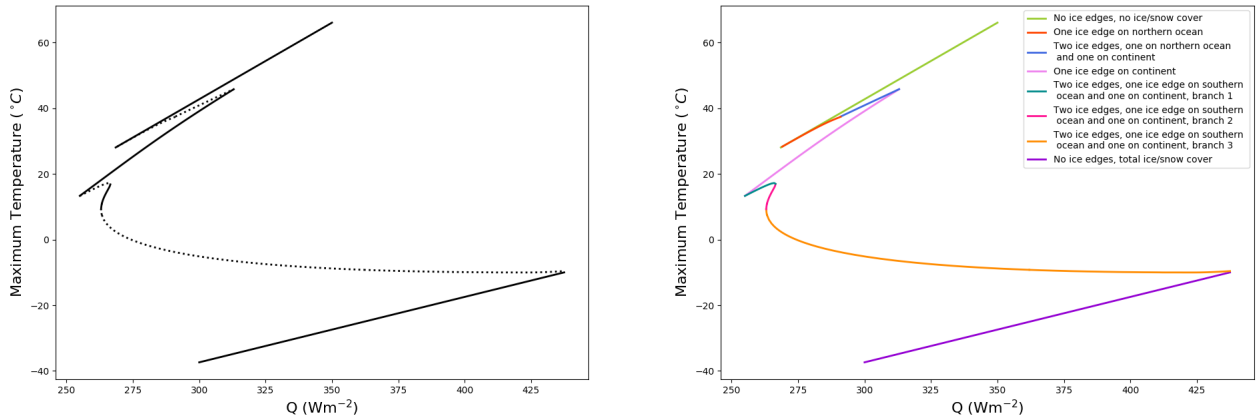

(a) *With stability indications.*

(b) *With indications of the type of stationary solutions.*

Figure 26: *Bifurcation diagram associated with a sphere with a rotationally symmetrical continent breaking the north-south symmetry and* $\varepsilon = 0.5$.

From the bifurcation diagram in Figure 26a it is evident that the range of Q values in which we have three stable stationary solutions has not decreased. In fact, the range of Q values where there are three stable stationary solutions, $Q \in [263, 267] \cup [269, 313]$, has quite markedly increased. Figure 26a does however, display another highly interesting observation. The stable stationary solutions in the intermediate branch has moved towards the upper stable branch. The bifurcation diagram seems to converge, not surprisingly, towards the bifurcation diagram of a water world as we move the continent further and further north. What is interesting here is that the intermediate branch remains stable quite close to the upper branch. The implications of this warrants a some further discussion.

5.4. Discussion

As we have seen in this section, moving the continent further and further north causes the associated bifurcation diagram to converge to that of a water world. As the asymmetry is gradually increased, the stable intermediate branch moves closer and closer to the upper stable branch. It is reasonable to assume that this intermediate branch will remain stable as it approaches the upper branch. Our inkling at the start of this section, that the range of parameter values where there exists three stable stationary solutions will decrease as a consequence of symmetry violations, did evidently not hold. As a consequence, the initial hypothesis that symmetry violations will affect the presence of multiple stationary solutions, is refuted. There seems to be no evidence for a pattern regarding the number of stationary solutions and the degree of the symmetry violation.

Though our initial hypothesis is refuted, we have identified another pattern. Symmetry violations cause the stable branches to move closer, overlooking the extreme "snowball" branch which remains unchanged. A new hypothesis is therefore formulated; symmetry violations in energy balance models cause stable stationary solutions to look more similar.

Let's return to the bifurcation diagram for a sphere with a rotationally symmetrical continent stretching from latitude

$$\theta_{l_1} = \frac{\pi}{2} - \frac{l}{2} - \varepsilon$$

to

$$\theta_{l_2} = \frac{\pi}{2} + \frac{l}{2} - \varepsilon,$$

where

$$\varepsilon = 0.5.$$

It can be argued that a continent configuration similar to this, where the continent is somewhere north of equator, is a reasonable approximation to the continent configuration on the Earth today over long timescales. Since the Earth spins on its axis, an average position of the Earth's continents on the time scale of years would be somewhere on the northern hemisphere. One can imagine this be considering the Earth's surface with a clear distinction between the continents and the ocean and speeding up the rotation on its axis. Then Eurasia and North America would eventually be "moshed" into a zonal strip on the northern hemisphere. The Earth obviously has an obliquity as well, but the point here is not to argue that it is a particularly accurate approximation, only that such a continent configuration captures the asymmetry of the Earth's surface better than a water world. It can therefore be argued that the asymmetry in earth system models is an aspect that the presented energy balance model has an improved ability to capture, with this continent configuration compared to that of a water world. However, the resulting temperature distributions we saw in section 3.3.2 is, at best, a caricature of the Earth's zonal mean temperature, this is down to the choice of the thermal diffusion coefficient on the continent. This will be discussed below, but first let's continue this argument.

Let's say the climate system associated with the bifurcation diagram in Figure 26a rests in some state in the stable intermediate branch. If Q is increased until a tipping point is exceeded, the climate system would eventually settle at some equilibrium in the upper branch. This would obviously result in an abrupt climate change. However, the change would not be of the cataclysmic nature we have seen for other climate systems on spheres with a more symmetrical continent configuration. Figure 27 illustrates this point. From the bifurcation diagram (Figure 26a) we observe that the larger, stable intermediate branch has a tipping point around $310 \lesssim Q \lesssim 320$, the exact location of it is at $Q = 313$. If this tipping point is exceeded, the climate system will eventually stabilize at a state consistent with that of Figure 27b. The change would largely occur north of the center of the continent and other regions remain virtually unchanged. This change would obviously be drastic, resulting in a disappearance of the northern ice cap, but it is markedly less severe than the change resulting from surpassing similar tipping points in more symmetrical cases. In fact, the preceding analysis indicate that move the continent further north will reduce the severity of this change. As the bifurcation diagram is, in all likelihood, converging to the bifurcation diagram of a water world, the intermediate branch and the upper branch will gradually become more and more similar as the continent is shifted north.

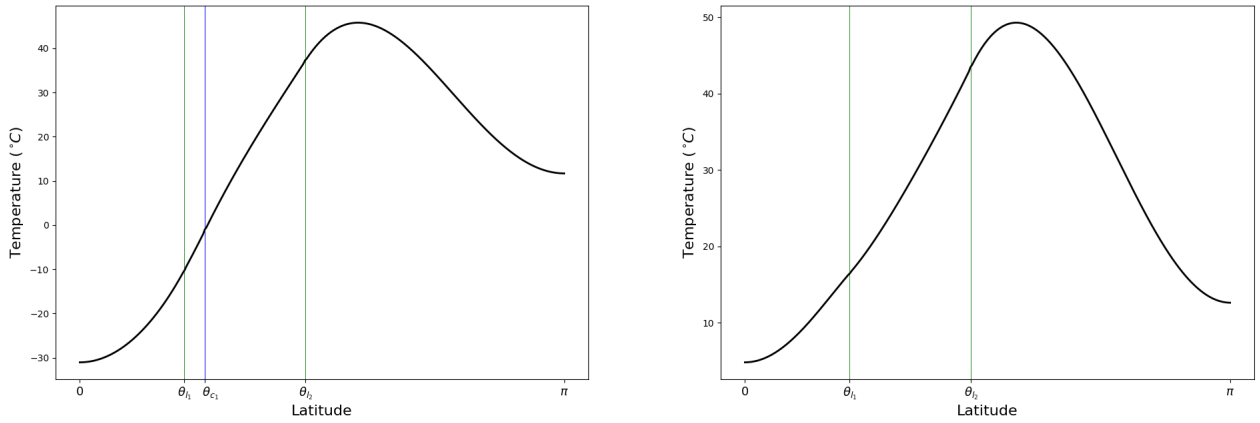

(a) *Intermediate branch,* $Q = 313$.

(b) *Upper branch,* $Q = 314$.

Figure 27: *The temperature change associated with exceeding the tipping point at* $Q = 313$*, for a rotationally symmetrical continent breaking the north-south symmetry and* $\varepsilon = 0.5$.

The above discussion indicate a possible explanation of why multiple equilibria and tipping points are difficult to detect in earth system models. If stable equilibria are stacked closely together, jumping between equilibria would not induce large scale climate change. In fact, exceeding tipping points could be difficult to detect in a dynamical run. It is important to keep in mind that an earth system model is essentially a system of coupled partial differential equations and it is extremely likely that both multiple equilibria and bifurcation points exists. Tipping points are usually associated with large scale climate change, so for the sake of this discussion, let's instead refer to tipping points that does not induce large scale change as simply bifurcation points. Say one designs an experiment looking for hysteresis in an earth system model, like the ones discussed in the introduction to this thesis. If the model has several, similar equilibria, a sweeping increase in forcing could then possibly enclose several bifurcation points. An equivalent reduction in forcing would see the climate system settle at another equilibrium. However, if this equilibrium is very similar to the initial state one could easily conclude that no bifurcation points where identified. One could argue that no "tipping point" exists here, in the sense of thresholds that, when exceed, induce large, irreversible climate change, that would be a matter of definition. Furthermore, if several equilibria are very similar, cascading bifurcation points would hardly induce the catastrophic events many fear.

Our analysis has showed that stable stationary solutions do become more similar in this model as a result of symmetry violations. We must however, acknowledge some of the shortcomings of the model presented. The minor symmetry violation that involved shifting the continent slightly to the north ($\varepsilon = 0.1$), had a major effect on the climate system on the sphere. In the context of the Earth's continent, this temperature response is, at best, a caricature. We would not expect such a minor change in the continent configuration to produce such a radically different temperature profile. The issue here is the thermal diffusion coefficient for the continent. The value chosen for this parameter in this thesis cannot be given much validity in terms of approximating the thermal diffusion that occurs on the Earth's continents. The parameters for a water world, adopted from [11], are empirically chosen to fit the Earth's current climate. These parameters are intended to be

approximate values for the Earth's surface in its entirety, continents and oceans. When introducing a continent, one should ideally modify all parameters, both for the oceans and continent, if one wishes to adequately approximate the temperature distribution on the Earth today. This was not done in this thesis, nor was the point of this thesis to approximate the Earth's current temperature distribution for an analysis including continents. This is a crude model to begin with. The reason for placing a continent in this thesis was to investigate the effects of breaking the symmetry in this simple climate model. As mentioned above, some aspects of the asymmetry in the Earth's climate system can, however, be captured with a continent configuration similar to the latter continent arrangement ($\varepsilon = 0.5$). This configuration can be used as a staring point, but in order to improve the models ability to approximate the Earth's zonal mean temperature, some modifications to the parameters should be made: For one, the extent and placement of the zonal strip continent should be carefully chosen in order for it to be an acceptable approximation to the Earth's continents over long timescales. Secondly, the thermal diffusion coefficients for the continent and the oceans should be reevaluated and the numerical values of these two coefficients should be more similar. The thermal diffusion constant chosen for the continent in this thesis is simply too different from that of the oceans (see Appendix A), resulting in a very skewed zonal mean temperature distribution. Another possibility to consider would be to include a smaller continent around the South pole. It is well known that the annual mean temperature of the South pole is significantly lower than that of the North pole. Placing a continent around the South pole will lower its temperature as this continent should be given special parameters to capture the South pole's thick ice layer and atmospheric conditions.

6. Concluding remarks

This thesis started with posing a hypothesis; that asymmetry affects the presence of multiple equilibria in a simple climate model. We have investigated this hypothesis in light of complex, fully coupled earth system models and why tipping points, that are common in simple, low-dimensional models, have proved difficult to detect in these complex models. The simple climate model we have been studying, the energy balance model on a sphere (2.1), has multiple stable stationary solutions for renditions both with and without a continent. The climate system on the sphere exhibits the possibility of abrupt climate change if forced beyond various tipping points. We initially explored a water world and later introduced a rotationally symmetrical continent to the sphere. The continent was first placed in a north-south symmetrical configuration, then gradually moved north to investigate how symmetry violations affected the bifurcation diagram. We focused our attention on the steady state solutions, as these states are the ones a dynamical run is able to capture. The behavior of earth system models are available exclusively through performing dynamical runs and analysing the output. Our investigation found no evidence for a pattern regarding the presence of multiple stationary solutions and the degree of the symmetry violation. The initial hypothesis was subsequently refuted. Instead another pattern emerged; the stable branches in the bifurcation diagram moved ever closer following a gradual shifting of the continent to the north (shifting the continent to the south would result in the same pattern). In light of this realization, a new hypothesis was formulated: Symmetry violations in energy balance models cause stable stationary solutions to look more similar. Evidence supporting this hypothesis was presented, as well as an argument for why this pattern would continue following a further shift of the continent.

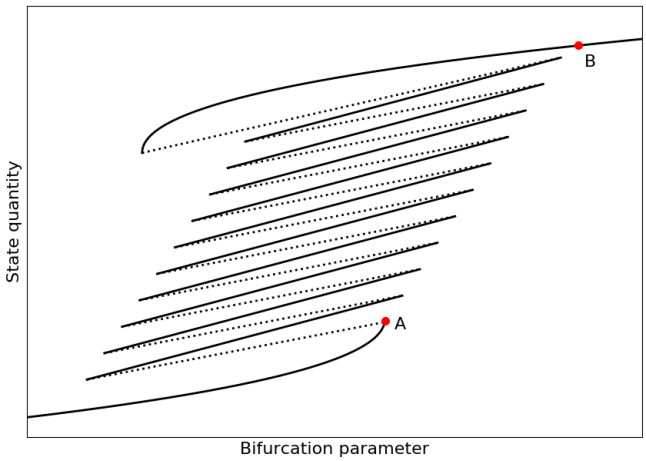

Figure 28: *Bifurcation diagram with uninteresting tipping points.*

The new hypothesis was discussed in light of earth system models in section 5.4. If symmetry violations cause stationary solutions to become more similar, this could serve as a partial explanation of why tipping points and multiple equilibria are difficult to detect in earth system models. Exceeding a tipping point causes the climate system to transition into another state, but if this other state is extremely similar to the initial state, the tipping point is not very interesting. Figure 28 illustrates how closely stacked stable branches in the bifurcation diagram can result in uninteresting tipping

points. In order to transition from state A to state B as a consequence of gradually increasing the bifurcation parameter, the system will make several intermediate jumps between equilibria before reaching state B. None of these intermediate jumps will induce large scale changes to the system compared to that of a jump straight from state A to state B. Introducing a continent breaking the north-south symmetry to the model presented caused a similar phenomenon to occur, albeit with less branches. Whether or not this aspect of the simple model replicates a behavior of the earth system models, is left an unanswered question. Based on the evidence presented, drawing any such conclusions would ultimately become highly speculative. Instead this is presented as a possibility, open to be further investigated.

The possibility of several similar equilibrium states can never serve as a complete explanation of the difficulty in detecting tipping points in earth system models. Though it can muddy the water, so to speak, making the detection of tipping points and early warning signals more difficult. As we know, geological records has provided overwhelming evidence that the Earth has historically been in numerous states very different from its current state, including the "snowball" state we have seen in this thesis. Earth system models are however, tuned to stay within a scope similar to the Earth's current climate [13], potentially causing extreme states to be difficult to obtain. Simple models has historically served a purpose in explaining how such states could be reached, as the climate system can enter a positive feedback loop. Only in the presence of a sufficient forcing could the climate system escape this state, such as a flurry of volcanic activity. In the modern development of climate dynamics, simple climate models have increasingly been useful in understanding complex climate models. This is likely to continue as the behavior of earth system models is extremely complicated and not easily studied due to the computational infrastructure required to perform experiments. Simple climate models are therefore not a thing of the past and the study of them still comes with the possibility of gaining important insights in a crucial time for the Earth's climate.

6.1. Future work

A natural extension of this study would be to extend the analysis to two dimensions and investigate if the results of this thesis still holds. That is, does gradually violating the symmetry properties of the sphere result in gradually more similar, stable stationary solutions. Ideally, one would start with a continent configuration that ensures some kind of symmetry on the sphere, for instance a rotationally symmetrical continent that preserves the north-south symmetry. Then gradually break apart and move the continent until the sphere has a continent configuration similar to that of the Earth today. This would obviously require a substantial amount of work, especially to find analytical/semi-analytical stationary solutions, but it could be a valuable endeavor if it highlights some pattern that aids in the understanding of earth system models.

The simple climate model studied in this thesis is only capable of replicating one feedback mechanism in the climate system, the ice-albedo feedback. In a simple, low-dimensional model with one

feedback mechanism, there is often a possibility that the feedback is pushed to the extreme as it neglects the intricate dynamics between feedback mechanisms that a complex, fully coupled climate model is able to capture. There are no other feedbacks to counteract the positive feedback loop in the model presented and, as a consequence, there will always be two extreme states for a parameter regime that closely resembles that of the Earth today. If other feedbacks were implemented, the extreme states could possibly be balanced out by other climate mechanism, or amplified to increase the rate of the positive feedback loop. Take for instance the "snowball Earth" state. If the model had included mechanisms such as state dependent ocean circulations, the bifurcation diagram is likely to radically change. Implementing other important climate mechanisms, and coupling that to the system, would be an important next step to investigate whether the pattern regarding asymmetry and the similarity of different equilibria, persists as the complexity of the model increase.

Appendices

Appendix A Parameter values

In this thesis we have used the following parameters, unless stated otherwise in the relevant section. We adopt the latitudinal energy distribution function, s, from [11];

$$s(\theta) = s_0 + s_1 \cos^2(\theta - \frac{\pi}{2}),$$

where

$$s_0 = 0.523$$
$$s_1 = 0.716.$$

This is an approximation to the average latitudinal energy distribution on Earth over one year, with the Earth's current obliquity.

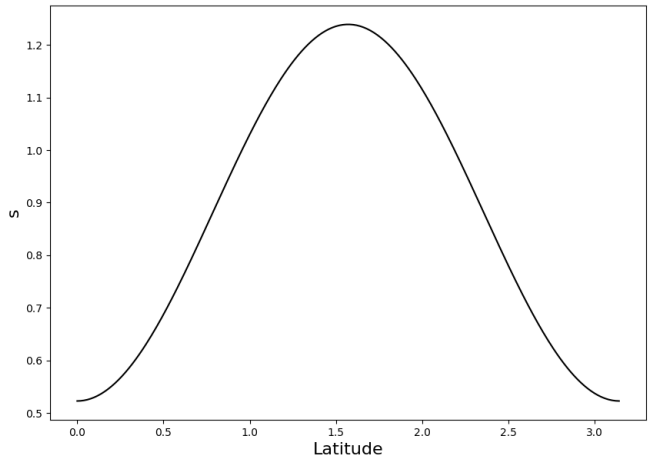

Figure 29: *Graph of the approximated average annual latitudinal energy distribution function, $s(\theta)$.*

Since s is averaged over one year, we choose our time scale to be one year,

$$t_0 = 31556926\,\text{s}.$$

We use the following parameters in the outgoing radiation (B.17);

$$A = 203\,\text{W m}^{-2}$$

and

$$B = 2.09\,\text{W m}^{-2}(^\circ\text{C})^{-1}.$$

The material specific parameters for water and continent are listed below.

A.1 Water

For the part of the surface covered by water we use the following thermal diffusion coefficient;

$$D = 0.208 \cdot B,$$

adopted from [11]. We want our model to reasonably represent the current state of the Earth's climate system, hence we empirically choose

$$C = 13.2\,\mathrm{W\ s\ m^{-2}(^{\circ}C)^{-1}}$$

and

$$Q = 260\,\mathrm{W\ m^{-2}}.$$

With this C and Q, along with the parameter values above, the resulting temperature profile on a water world is an acceptable approximation to the present day annual, zonal mean surface temperature on the Earth.

We choose the critical temperature for the water-ice phase transition to be

$$T_s = 10\,^{\circ}\mathrm{C}.$$

We let

$$a_1 = 0.06$$

be the albedo for water, and

$$a_2 = 0.6$$

be the albedo for ice and/or snow cover. An emphasis is put on snow cover, as the surface is assumed to accumulate a snow cover over a timescale of years due to precipitation. We want the model for the albedo to retain the general behavior

$$a(T) \sim \begin{cases} a_1, & T > -T_s \\ a_2, & T < -T_s \end{cases}.$$

Therefore, we introduce a function

$$a(T) = a_1 + \frac{a_2 - a_1}{2}(1 + \tanh(-\sigma(T + 1))), \tag{A.1}$$

to replicate this behavior. This model allows us better capture subtleties in the ice-albedo feedback mechanism as there is likely to be a partial ice cover around the critical temperature for ice formation. This is now reflected in the model for the albedo. The parameter σ determines the slope of the albedo at the transition between ice cover and water.

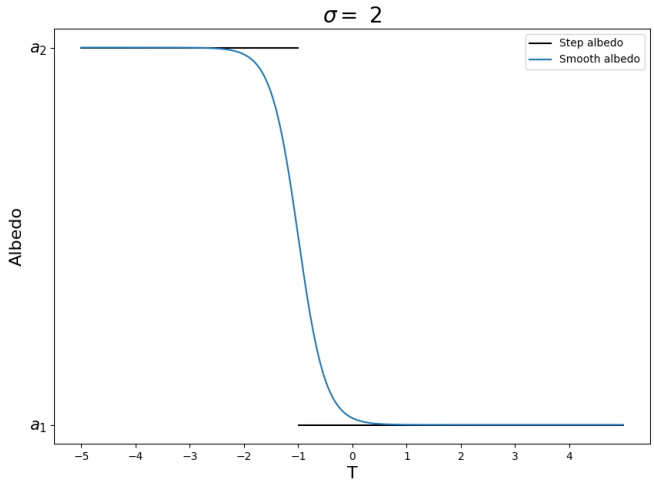

Figure 30: *A plot of the albedo given in (A.2) for $\sigma = 2$, as a function of non-dimensional temperature.*

Note that the albedo given in (A.2) is a function of non-dimensional temperature. We use $\sigma = 2$.

A.2 Continent

The top layer of the continent is deemed to consist of soil and the parameters for the continent is intended to partly capture the physical properties of soil, as well as the atmosphere above the continent. The thermal conductivity of semi-saturated soil is generally higher than that of water [1] and atmospheric effects are also likely to contribute to a higher thermal diffusion on a continent than on an ocean. We therefore use

$$D_1 = 0.75 \text{ W m}^{-2}(^\circ\text{C})^{-1}$$

as the thermal diffusion coefficient on the continent. For the heat capacity of the continent we use

$$C_1 = 12 \text{ W s m}^{-2}(^\circ\text{C})^{-1}.$$

With these parameters, the temperature distribution on a sphere with a rotationally symmetrical continent will be a reasonable approximation to the Earth's current climate when $Q = 260$.

We choose the critical temperature for ice and snow formation on the continent to be

$$T_{s_2} = 1\,^\circ\text{C}.$$

We let

$$a_3 = 0.3$$

be the albedo for the surface of the continent, and

$$a_4 = 0.6$$

be the albedo for ice and/or snow cover. We model the albedo on the continent through a continuous function of non-dimensional temperature,

$$a_{\text{land}}(T) = a_3 + \frac{a_4 - a_3}{2}(1 + \tanh(-\sigma(T + T_c))), \tag{A.2}$$

where $T_c = \frac{T_{s_2}}{T_s}$. We use $\sigma = 2$.

The finite difference algorithm is implemented in Python and for the IVP-solver referred to in section 4.1, we use the "*solve_ivp*"-module from the "*scipy.integrate*" library. The IVP-solver uses an explicit Runge-Kutta method of order 5, and we let the solver choose the time step k.

Appendix B Deriving the energy balance model

In this appendix we are going to derive a 1D energy balance model on a sphere. The sphere under consideration will be rotationally symmetrical, either with or without continents. We start by formulating an energy balance equation for a general surface in $\mathbb{R}^2$, before proceeding to specify this energy balance equation to the domain of interest, namely a sphere. Finally, we will develop a set of boundary conditions for the energy balance equation on this sphere.

B.1 General energy balance equation

We are going to derive an energy balance equation on a general domain in $\mathbb{R}^2$, following the work of Jakobsen [8]. In order to formulate an energy balance model for a given system one has to adequately model the amount of energy entering and leaving the system. Inspired by this let's start by introducing three key quantities. The first is the energy density, e. For any infinitesimal area element, dA, centered at a point $p \in \mathbb{R}^2$, we have

$$e(p,t)\,dA - \text{the total energy residing inside } dA \text{ at time } t.$$

The second is the energy flux density, $\vec{q}$. For any directed line element, $\vec{n}dl$, centered at a point p, we have

$$\vec{q}(p,t)\cdot\vec{n}dl - \text{the total amount of energy flowing through } dl \text{ ,in the direction of } \vec{n}\text{, pr. unit time.}$$

The third is the energy source density, h. For any infinitesimal area element, dA, centered at a point p, we have

$$h(p,t)\,dA - \text{the net energy injected into } dA,\ (h>0),\text{ or the net energy extracted from } dA,\ (h<0),\text{ pr. unit time.}$$

Consider now some domain $S \subset \mathbb{R}^2$, with boundary ∂S.

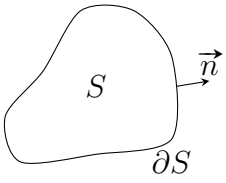

The total amount of energy inside S at time t is then

$$E(t) = \int_S dA\, e(p,t).$$

The total amount of energy extracted or injected from S pr. unit time is

$$H(t) = \int_S dA\, h(p,t),$$

and the total amount of energy entering S through the boundary, ∂S, pr. unit time is

$$-\oint_{\partial S} dl\ \vec{q}\cdot\vec{n}.$$

Thus, the change in energy inside S pr. unit time is

$$\frac{dE}{dt} = -\oint_{\partial S} dl\ \vec{q}\cdot\vec{n} + H. \tag{B.1}$$

This is a basic energy balance law on integral form for some arbitrary domain S. We may write this equation on differential form,

$$\begin{aligned}
\frac{d}{dt}\int_S dA\, e &= -\oint_{\partial S} dl\ \vec{q}\cdot\vec{n} + \int_S dA\, h \\
&\Downarrow \text{ Gauss theorem} \\
\int_S dA\, \partial_t e &= -\int_S dA\, \nabla\cdot\vec{q} + \int_S dA\, h \\
&\Downarrow \\
\int_S dA\, \left\{\partial_t e + \nabla\cdot\vec{q} - h\right\} &= 0.
\end{aligned} \tag{B.2}$$

Equation (B.2) holds for any domain S, we must therefore have that

$$\partial_t e + \nabla\cdot\vec{q} = h. \tag{B.3}$$

This is the basic energy balance equation on differential form. Note however, that in order to go from (B.1) to (B.3) we must ensure that 1) e and h are bounded, and 2) that $\vec{q}$ is continuously differentiable. We will return to these conditions once we have established the form of e, h and $\vec{q}$.

Next, we will specify e, h and $\vec{q}$ using thermodynamic assumptions. We assume that our energy balance model describe a system in local thermodynamic equilibrium. We therefore approximate the equations of state as

$$\begin{aligned}
e(p,t) &= C(p)T(p,t), \\
\vec{q}(p,t) &= -k(p)\nabla T(p,t),
\end{aligned}$$

where C is the heat capacity and k is the thermal conductivity of the medium under consideration. Our energy balance model now takes the form

$$C\,\partial_t T = \nabla\cdot(k\nabla T) + h.$$

We will assume that the surface under consideration is enclosed by an atmosphere, and receives energy in the form of radiation from an external source. We will refer to this external source as a

sun. We write the source term, h, as

$$h = h_+(1-a) - h_-,$$

where h_+ is the incident solar radiation, which is scaled by the absorption rate of the surface, $(1-a)$, where a is the albedo. h_- is the energy returned to outer space through thermal radiation. For the incident solar radiation we have

$$h_+(p) = Qs(p)$$

where Q is the flux density of solar radiation at the surface and $s(p)$ describe how the solar radiation distributes across the surface of interest. The albedo measures the diffuse reflection of the incident radiation and the value will depend on the properties of the surface at point p. The albedo will also depends on the temperature at point p, as the presence of ice or snow at point p will increase the local reflection of incident radiation. Therefore, we model the albedo as

$$a = a(p, T).$$

The loss of energy through thermal radiation occurs at a given height in the atmosphere. This height, and consequently the exact amount of energy lost, will depend on the temperature and the concentration of gases in the atmosphere at a given location. Given a constant lapse rate, the surface temperature and the temperature in the upper atmosphere will be linearly related [14]. Furthermore, the surface temperature will also affect gas concentrations in the atmosphere, particularly water vapor. We will therefore model the outgoing radiation as

$$h_- = h_-(p, T).$$

Our energy balance model now takes the form

$$C\,\partial_t T = \nabla \cdot (k\nabla T) + Qs(1-a) - h_-. \tag{B.4}$$

B.2 Energy balance on a sphere

We will apply (B.4) to derive an energy balance model on a spherical planet. We start by considering a spherical planet with a surface S. We will describe the surface, S, using spherical coordinates,

$$\begin{aligned} x &= r\sin\theta\cos\varphi \\ y &= r\sin\theta\sin\varphi \\ z &= r\cos\theta, \end{aligned}$$

where θ is the polar angle and φ is the azimuthal angle. We let

$$\theta \in [0, \pi]$$

where $\theta = 0$ is the North pole and $\theta = \pi$ is the South pole. Furthermore, we will only concern ourselves with matters on the surface, so we keep r constant,

$$r = R.$$

This reduces the problem to two-dimensions, and we will later further reduce the problem to a one-dimensional one by considering a rotationally symmetrical sphere. Let's start by deriving the gradient of a function and the divergence of a vector field in spherical coordinates, which is vital in order to formulate the model (B.4) on a sphere. The metric coefficients of the Riemanninan metric tensor associated with the coordinates,

$$\begin{aligned} x &= R\sin\theta\cos\varphi \\ y &= R\sin\theta\sin\varphi \\ z &= R\cos\theta, \end{aligned} \tag{B.5}$$

where R is constant, are:

$$\begin{aligned} g_{\theta\theta} &= \frac{\partial x}{\partial\theta}\frac{\partial x}{\partial\theta} + \frac{\partial y}{\partial\theta}\frac{\partial y}{\partial\theta} + \frac{\partial z}{\partial\theta}\frac{\partial z}{\partial\theta} \\ &= R^2\cos^2\varphi\cos^2\theta + R^2\sin^2\varphi\cos^2\theta + R^2\sin^2\theta \\ &= R^2 \end{aligned} \tag{B.6}$$

$$\begin{aligned} g_{\theta\varphi} &= \frac{\partial x}{\partial\theta}\frac{\partial x}{\partial\varphi} + \frac{\partial y}{\partial\theta}\frac{\partial y}{\partial\varphi} + \frac{\partial z}{\partial\theta}\frac{\partial z}{\partial\varphi} \\ &= -R^2\cos\varphi\cos\theta\sin\theta\sin\varphi + R^2\cos\theta\sin\varphi\sin\theta\cos\varphi \\ &= 0 \end{aligned} \tag{B.7}$$

$$g_{\theta\varphi} = 0 \tag{B.8}$$

$$\begin{aligned} g_{\varphi\varphi} &= \frac{\partial x}{\partial\varphi}\frac{\partial x}{\partial\varphi} + \frac{\partial y}{\partial\varphi}\frac{\partial y}{\partial\varphi} + \frac{\partial z}{\partial\varphi}\frac{\partial z}{\partial\varphi} \\ &= R^2\sin^2\theta\sin^2\varphi + R^2\sin^2\theta\cos^2\varphi \\ &= R^2\sin^2\theta \end{aligned} \tag{B.9}$$

The above considerations (B.6)-(B.9) follows from the formula for the metric tensor with respect to arbitrary coordinates, q^i,

$$g_{ij} = \frac{\partial x^k}{\partial q^i}\frac{\partial x^k}{\partial q^j}. \tag{B.10}$$

In (B.10) we have used Einstein notation and we will do so in the following discussion. We now wish to reinstate the gradient as a vector field on the Riemannian manifold of interest, a sphere. For any smooth real-valued function, f, on a Riemannian manifold, we have that the gradient of f is defined by

$$\nabla f = \hat{g}^{-1}(df)$$

where

$$\hat{g}^{-1}(\omega) = \omega^i \frac{\partial}{\partial x^i}$$

and

$$\omega^i = g^{ij}\omega_j.$$

In smooth coordinates, we have the expression

$$\nabla f = g^{ij}\frac{\partial f}{\partial x^i}\frac{\partial}{\partial x^j}. \tag{B.11}$$

Applying (B.11) to our sphere we find that

$$\begin{aligned}\nabla f &= g^{\theta\theta}\frac{\partial f}{\partial \theta}\frac{\partial}{\partial \theta} + g^{\varphi\varphi}\frac{\partial f}{\partial \varphi}\frac{\partial}{\partial \varphi} \\ &= \frac{1}{R^2}\frac{\partial f}{\partial \theta}\frac{\partial}{\partial \theta} + \frac{1}{R^2\sin^2\theta}\frac{\partial f}{\partial \varphi}\frac{\partial}{\partial \varphi}.\end{aligned}$$

Thus, the gradient of f with respect to the Euclidean metric in spherical coordinates is

$$\nabla f = \frac{1}{R^2}\frac{\partial f}{\partial \theta}\hat{\theta} + \frac{1}{R^2\sin^2\theta}\frac{\partial f}{\partial \varphi}\hat{\varphi}, \tag{B.12}$$

where $\hat{\theta}$ and $\hat{\varphi}$ is the unit vector in the direction of θ and φ, respectively.

Next, we wish to define the divergence of a vector field on the surface of the sphere. We consider vector fields on the form

$$\vec{f} = f^\theta\hat{\theta} + f^\varphi\hat{\varphi}. \tag{B.13}$$

The divergence of a vector field, $\vec{f}$, in general coordinates, x^i, can be expressed through the Voss-Weyl formula;

$$\nabla \cdot \vec{f} = \frac{1}{\rho}\frac{\partial \rho f^i}{\partial x^i},$$

where the volume coefficient is

$$\rho = \sqrt{|\det g|}.$$

In our coordinates (B.5), the metric tensor takes the form

$$g = \begin{pmatrix} R^2 & 0 \\ 0 & R^2\sin^2\theta \end{pmatrix} \tag{B.14}$$

$$\Downarrow$$

$$\det g = R^4\sin^2\theta, \tag{B.15}$$

with the associated volume coefficient

$$\rho = R^2 \sin\theta.$$

The divergence of a vector field on the form (B.13), on the sphere is therefore

$$\begin{aligned}\nabla \cdot \vec{f} &= \frac{1}{\rho}\frac{\partial \rho f^\theta}{\partial \theta} + \frac{1}{\rho}\frac{\partial \rho f^\varphi}{\partial \varphi} \\ &= \frac{1}{R^2 \sin\theta}\frac{\partial}{\partial \theta}\big(R^2 \sin\theta f^\theta\big) + \frac{1}{R^2 \sin\theta}\frac{\partial}{\partial \varphi}\big(R^2 \sin\theta f^\varphi\big) \\ &= \frac{1}{\sin\theta}\frac{\partial}{\partial \theta}\big(\sin\theta f^\theta\big) + \frac{\partial}{\partial \varphi} f^\varphi. \end{aligned} \tag{B.16}$$

Now that we have formulated a framework for evaluating the gradient of functions and the divergence of vector fields on our Riemannian manifold of interest, we can return to the general equation for our energy balance model (B.4). We adopt Budyko's linear model [4] for the outgoing energy,

$$h_- = A + BT, \tag{B.17}$$

where A and B are constants. For a given φ, the area of the disk capturing solar radiation will be 4 times less than the total area of the sphere, hence the incident solar radiation will be

$$Q = \frac{S_o}{4},$$

where S_o is the solar constant. We do however, retain Q and our model now looks like

$$C\partial_t T - \nabla \cdot (k \nabla T) + BT = Qs(1-a) - A \tag{B.18}$$

where

$$\begin{aligned} T &= T(\theta, \varphi) \\ k &= k(\theta, \varphi) \\ s &= s(\theta, \varphi). \end{aligned}$$

Applying (B.12) and (B.16) to the first term in (B.18) we get

$$\begin{aligned} -\nabla \cdot (k \nabla T) &= -\nabla \cdot k\left(\frac{1}{R^2}\partial_\theta T \hat{\theta} + \frac{1}{R^2 \sin^2\theta}\partial_\varphi T \hat{\varphi}\right) \\ &= -\frac{1}{\sin\theta}\partial_\theta\big(\sin\theta \frac{k}{R^2}\partial_\theta T\big) - \partial_\varphi\big(\frac{k}{R^2 \sin^2\theta}\partial_\varphi T\big). \end{aligned}$$

The general equation for our energy balance model is therefore

$$C\partial_t T - \frac{1}{R^2 \sin\theta}\partial_\theta\big(\sin\theta k \partial_\theta T\big) - \frac{1}{R^2 \sin^2\theta}\partial_\varphi\big(k\partial_\varphi T\big) + BT = Qs(1-a) - A. \tag{B.19}$$

For now we will only consider a planet where the entire surface is covered by water. In this thesis we will investigated a planet with a continent, but for now our sphere is totally symmetrical as we are looking at a case where the entire surface of the sphere is covered by water. For this situation we model the heat conductivity parameter,

$$k(\theta, \varphi) = k_0,$$

as a constant. Our energy balance model (B.19) takes on a simpler form

$$C\partial_t T - \frac{k_0}{R^2}\left[\frac{1}{\sin\theta}\partial_\theta\big(\sin\theta\partial_\theta T\big) - \frac{1}{\sin^2\theta}\partial_{\varphi\varphi}T\right] + BT = Qs(1-a) - A. \tag{B.20}$$

Furthermore, we will assume that the planet under consideration rotates on its axis, hence

$$T = T(\theta, \varphi)$$
$$s = s(\theta, \varphi).$$

However, averaging s over long timescales we may neglect the dependence on φ,

$$s = s(\theta).$$

The night and day cycle on our planet will be irrelevant on long timescales as the planet is rotationally symmetrical. We will also assume that the planet has an obliquity, however this seasonality is also built into $s(\theta)$. Because of the invariance of s with respect to φ, we seek solutions with the same kind of invariance,

$$T = T(\theta).$$

Given these restrictions on s and T, our energy balance model (B.20) becomes

$$C\partial_t T - D\frac{1}{\sin\theta}\partial_\theta\big(\sin\theta\partial_\theta T\big) + BT = Qs(\theta)(1-a) - A,$$

where $D = \frac{k_0}{R^2}$. This is the energy balance model formulated by North in 1975 [14].

B.3 Boundary condition

We want to derive a boundary condition for the domain under consideration, namely a sphere. Recall the energy balance equation on integral form

$$\int_S dA\,\partial_t e = -\int_S dA\,\nabla\cdot\vec{q} + \int_S dA\,h.$$

Let's consider the stationary case,

$$\int_S dA\,\nabla\cdot\vec{q} = \int_S dA\,h$$
$$\oint_{\partial S} dl\,\vec{q}\cdot\vec{n} = \int_S dA\,h.$$

Consider now a small domain, S_ε, on the surface of the sphere. For this domain the following general equation holds

$$\oint_{C_\varepsilon} dl\ \vec{q} \cdot \vec{n} = \int_{S_\varepsilon} dA\, h,$$

where C_ε is the boundary of S_ε. Let S_ε be a circle on the surface of the sphere with radius ε. Since h is bounded, as $\varepsilon \longrightarrow 0$ we must have that

$$\oint_{C_\varepsilon} dl\ \vec{q} \cdot \vec{n} \longrightarrow 0.$$

Now let the domain S_ε encircle the North pole, with the center of S_ε at $\theta = 0$.

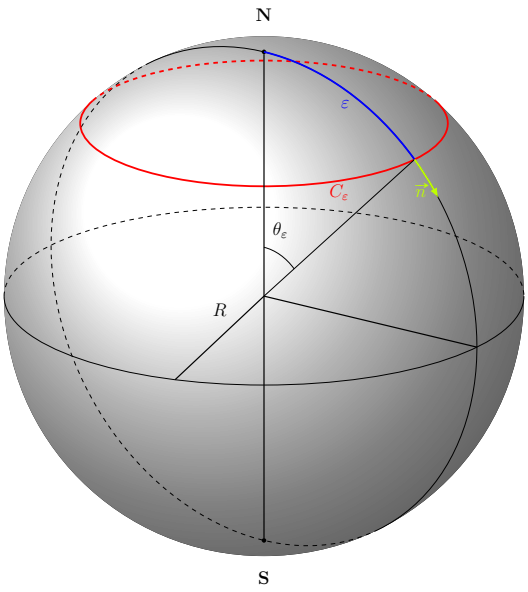

Figure 31: *Schematic of the domain* S_ε.

In order to evaluate the scalar line integral

$$\oint_{C_\varepsilon} dl\ \vec{q} \cdot \vec{n}, \tag{B.21}$$

we parameterize C_ε as a curve on the surface of the sphere,

$$C_\varepsilon(t) = \begin{cases} r = R \\ \theta = \theta_\varepsilon \\ \varphi = t \end{cases}, \qquad t \in [0, 2\pi].$$

The angle θ_ε is depicted in Figure 31, and described by the relation

$$\varepsilon = R\theta_\varepsilon.$$

Recall that we have

$$\vec{q} = -k_0 \nabla T \tag{B.22}$$

$$= -k_0 \left[\frac{1}{R^2} \frac{\partial T}{\partial \theta} \hat{\theta} + \frac{1}{R^2 \sin^2 \theta} \frac{\partial T}{\partial \varphi} \hat{\varphi} \right]. \tag{B.23}$$

The unit normal, $\vec{n}$, is perpendicular on C_ε, pointing out from S_ε, therefore

$$\vec{n} = \hat{\theta}.$$

Finally, we must determine the line element, dl, which is an infinitesimal displacement along the curve C_ε.

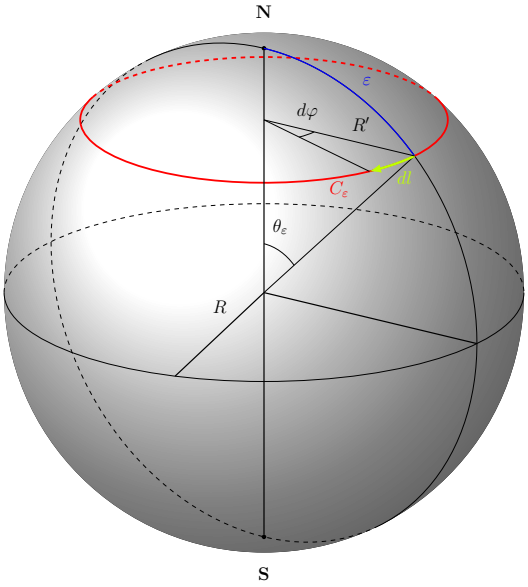

Figure 32: *Schematic of the line element dl.*

From Figure 32 it is evident that the line element is determined by the relation

$$dl = R' d\varphi.$$

The radius of the curve C_ε, R', will be determined by ε through

$$R' = R \sin \theta_\varepsilon.$$

Therefore, we can express the line element as

$$dl = R \sin \theta_\varepsilon d\varphi.$$

Applying this we can evaluate (B.21),

$$\begin{aligned}\oint_{C_\varepsilon} dl\ \vec{q}\cdot\vec{n} &= \oint_{C_\varepsilon} dl\left\{-\frac{k_0}{R^2}\frac{\partial T}{\partial\theta}\right\}\\ &= -\frac{k_0}{R^2}\int_0^{2\pi} dt\ R\sin\theta_\varepsilon\frac{\partial T}{\partial\theta}(R,\theta_\varepsilon,t)\\ &= -\frac{k_0}{R}\int_0^{2\pi} dt\ \sin\theta_\varepsilon\frac{\partial T}{\partial\theta}(\theta_\varepsilon)\\ &= -\frac{2\pi k_0}{R}\sin\theta_\varepsilon\frac{\partial T}{\partial\theta}(\theta_\varepsilon).\end{aligned}$$

As $\varepsilon\longrightarrow 0\iff\theta_\varepsilon\longrightarrow 0$, we have

$$\sin\theta_\varepsilon\frac{\partial T}{\partial\theta}(\theta_\varepsilon)\longrightarrow 0.$$

following a similar approach for the South pole, $\theta=\pi$, we get the boundary conditions

$$\lim_{\theta\to 0}\sin\theta\frac{\partial T}{\partial\theta}(\theta)=0$$

and

$$\lim_{\theta\to\pi}\sin\theta\frac{\partial T}{\partial\theta}(\theta)=0.$$

Appendix C Approximate the differential operator

In this appendix we are going to find discrete approximations to

$$\mathcal{L}f(x),$$

for the operator

$$\mathcal{L}(\cdot) = -\frac{1}{\sin x}\frac{\partial}{\partial x}\left(\sin x \frac{\partial}{\partial x}(\cdot)\right) \tag{C.1}$$

using finite differences. Let's assume that f is smooth enough to be expressed in terms of a power series expansion around a point x_0 sufficiently close to x,

$$f(x) \approx a_1 + a_2(x - x_0) + a_3(x - x_0)^2. \tag{C.2}$$

Applying the operator (C.1) to f we get

$$\mathcal{L}f(x) = -\frac{\cos x}{\sin x}a_2 + \left(-2 - 2(x - x_0)\frac{\cos x}{\sin x}\right)a_3. \tag{C.3}$$

Now we introduce a uniform grid for x,

$$x_{i+1} = x_i + h \qquad \Longrightarrow \qquad h = x_{i+1} - x_i, \tag{C.4}$$

and let

$$f_i = f(x_i). \tag{C.5}$$

The discretized form of equation (C.3) is

$$\hat{\mathcal{L}}f_i = -\frac{\cos x_i}{\sin x_i}a_2 + \left(-2 - 2h\frac{\cos x_i}{\sin x_i}\right)a_3. \tag{C.6}$$

The coefficients a_2 and a_3 will depend on how we choose to describe f in the first place, in other words what point we choose x_0 to be. The coefficients a_2 and a_3 will differ depending on whether we want a centered, a forward or a backward difference approximation. In this appendix we are going to find all of these approximations, starting with the centered difference approximation. In the latter part of this appendix we develop a framework for dealing with functions f, where $\mathcal{L}f$ is singular at $x = 0$, and propose a method for approximating f around the singularity.

C.1 Centered difference approximation

In order to develop a centered difference approximation to $\mathcal{L}f$ we assume that f can be expressed in terms of a power series expansion around a point x_i,

$$f(x) \approx a_1 + a_2(x - x_i) + a_3(x - x_i)^2.$$

Evaluating f on the grid (C.4) and using the notation (C.5), for some arbitrarily small h we must have

$$\begin{aligned} f_{i-1} &= a_1 + a_2(x_{i-1} - x_i) + a_3(x_{i-1} - x_i)^2 \\ &= a_1 - a_2 h + a_3 h^2 \qquad \text{(C.7)} \\ f_i &= a_1 + a_2(x_i - x_i) + a_3(x_i - x_i)^2 \\ &= a_1 \qquad \text{(C.8)} \\ f_{i+1} &= a_1 + a_2(x_{i+1} - x_i) + a_3(x_{i+1} - x_i)^2 \\ &= a_1 + a_2 h + a_3 h^2. \qquad \text{(C.9)} \end{aligned}$$

For non-zero h, the solution to the linear system (C.7)-(C.9) is

$$a_1 = f_i \qquad \text{(C.10)}$$

$$a_2 = \frac{f_{i+1} - f_{i-1}}{2h} \qquad \text{(C.11)}$$

$$a_3 = \frac{f_{i-1} - 2f_i + f_{i+1}}{2h^2}. \qquad \text{(C.12)}$$

Applying the coefficients (C.10)-(C.12) to (C.6) we get

$$\hat{\mathcal{L}} f_i = -\frac{2(f_{i-1} - 2f_i + f_{i+1}) + (f_{i-1} - 4f_i + 3f_{i+1}) h \cot x_i}{2h^2}. \qquad \text{(C.13)}$$

The formula (C.13) gives a centered difference approximation of $\mathcal{L}f$ for a function, f_i, evaluated on a uniform grid, x_i.

C.2 Forward difference approximation

In order to develop a forward difference approximation to $\mathcal{L}f$ we assume that f can be expressed in terms of a power series expansion around a point x_{i-1},

$$f(x) \approx a_1 + a_2(x - x_{i-1}) + a_3(x - x_{i-1})^2.$$

Evaluating f on the grid (C.4) and using the notation (C.5), for some arbitrarily small h we must have

$$\begin{aligned} f_{i-1} &= a_1 + a_2(x_{i-1} - x_{i-1}) + a_3(x_{i-1} - x_{i-1})^2 \\ &= a_1 \qquad \text{(C.14)} \\ f_i &= a_1 + a_2(x_i - x_{i-1}) + a_3(x_i - x_{i-1})^2 \\ &= a_1 + a_2 h + a_3 h^2 \qquad \text{(C.15)} \\ f_{i+1} &= a_1 + a_2(x_{i+1} - x_{i-1}) + a_3(x_{i+1} - x_{i-1})^2 \\ &= a_1 + 2a_2 h + 4a_3 h^2. \qquad \text{(C.16)} \end{aligned}$$

For non-zero h, the solution to the linear system (C.14)-(C.16) is

$$a_1 = f_{i-1} \tag{C.17}$$
$$a_2 = -\frac{3f_{i-1} - 4f_i + f_{i+1}}{2h} \tag{C.18}$$
$$a_3 = \frac{f_{i-1} - 2f_i + f_{i+1}}{2h^2}. \tag{C.19}$$

Applying the coefficients (C.17)-(C.19) to (C.6) we get

$$\hat{\mathcal{L}} f_{i-1} = \frac{-2(f_{i-1} - 2f_i + f_{i+1}) + (5f_{i-1} - 8f_i + 3f_{i+1})h\cot x_i}{2h^2}. \tag{C.20}$$

The formula (C.20) gives a forward difference approximation of $\mathcal{L}f$ for a function, f_i, evaluated on a uniform grid, x_i.

C.3 Backward difference approximation

In order to develop a backward difference approximation to $\mathcal{L}f$ we assume that f can be expressed in terms of a power series expansion around a point x_{i+1},

$$f(x) \approx a_1 + a_2(x - x_{i+1}) + a_3(x - x_{i+1})^2.$$

Evaluating f on the grid (C.4) and using the notation (C.5), for some arbitrarily small h we must have

$$\begin{aligned} f_{i-1} &= a_1 + a_2(x_{i-1} - x_{i+1}) + a_3(x_{i-1} - x_{i+1})^2 \\ &= a_1 - 2a_2h + 4a_3h^2 \end{aligned} \tag{C.21}$$
$$\begin{aligned} f_i &= a_1 + a_2(x_i - x_{i+1}) + a_3(x_i - x_{i+1})^2 \\ &= a_1 - a_2h + a_3h^2 \end{aligned} \tag{C.22}$$
$$\begin{aligned} f_{i+1} &= a_1 + a_2(x_{i+1} - x_{i+1}) + a_3(x_{i+1} - x_{i+1})^2 \\ &= a_1. \end{aligned} \tag{C.23}$$

For non-zero h, the solution to the linear system (C.21)-(C.23) is

$$a_1 = f_{i+1} \tag{C.24}$$
$$a_2 = \frac{f_{i-1} - 4f_i + 3f_{i+1}}{2h} \tag{C.25}$$
$$a_3 = \frac{f_{i-1} - 2f_i + f_{i+1}}{2h^2}. \tag{C.26}$$

Applying the coefficients (C.24)-(C.26) to (C.6) we get

$$\hat{\mathcal{L}} f_{i+1} = \frac{-2(f_{i-1} - 2f_i + f_{i+1}) + (f_{i-1} - f_{i+1})h\cot x_i}{2h^2}. \tag{C.27}$$

The formula (C.27) gives a backward difference approximation of $\mathcal{L}f$ for a function, f_i, evaluated on a uniform grid, x_i.

C.4 Alternative finite difference approximation

Generally, we expect any function we wish to approximate in this thesis, the average zonal temperature, to behave regularly thus a power series model will suffice in order to describe a given solution. Given some function, $T(\theta)$, that is smooth and twice differentiable at every gridpoint, θ_i, we expect the approximations (C.13), (C.20) and (C.27) to give reasonably precise description of the $\mathcal{L}T$, given a sufficiently small $h = \theta_{i+1} - \theta_i$. We might however, encounter solutions to the time dependent energy balance equation (2.6) without this regular behavior. Specifically, solutions where $\mathcal{L}T$ is singular at $\theta = 0$. In such cases, a power series model for the solution will not suffice and the numerical solution will become increasingly imprecise as we approach the singularity. Therefore, we will have to develop a framework for handling solutions with a singularity of this type.

The standard finite difference method, where we model the solution through a power series, will in certain cases break down and produce solutions with unsatisfactory precision. In such cases we need an alternative method for approximating the solution near the singularity. In this alternative finite difference method we instead use

$$T(\theta) = \alpha_1 + \alpha_2 \theta^{\alpha_3} \tag{C.28}$$

as a model for the solution. This model is specifically chosen to better approximate singular functions of the kind described above. However, this method will be a more computationally expensive one. As we shall see, there will arise a nonlinear system of equations that we will have to solve numerically for each iteration, thus we would prefer to only apply this method near the singularity. Having said that, let's start by developing this method. Just like before, we want to approximate

$$\mathcal{L}T,$$

where $\mathcal{L}$ is the operator (C.1) and T is the unknown solution. We introduce a uniform grid for the spacial domain,

$$\theta_{i+1} = \theta_i + h \qquad \Longrightarrow \qquad h = \theta_{i+1} - \theta_i,$$

and let

$$T_i = T(\theta_i).$$

In combination with (C.28), this gives raise to the system of equations

$$T_{i-1} = \alpha_1 + \alpha_2 \theta_{i-1}^{\alpha_3} \tag{C.29}$$
$$T_i = \alpha_1 + \alpha_2 \theta_i^{\alpha_3} \tag{C.30}$$
$$T_{i+1} = \alpha_1 + \alpha_2 \theta_{i+1}^{\alpha_3}. \tag{C.31}$$

Solving (C.29) and (C.31) for α_1 and α_2 we get

$$\alpha_1 = \frac{T_{i+1}\theta_{i-1}^{\alpha_3} - T_{i-1}\theta_{i+1}^{\alpha_3}}{\theta_{i-1}^{\alpha_3} - \theta_{i+1}^{\alpha_3}} \tag{C.32}$$
$$\alpha_2 = \frac{T_{i-1} - T_{i+1}}{\theta_{i-1}^{\alpha_3} - \theta_{i+1}^{\alpha_3}}. \tag{C.33}$$

We apply the operator (C.1) to (C.28),

$$\mathcal{L}T = -\alpha_2\alpha_3\theta^{\alpha_3-2}(\alpha_3 - 1 + \theta\cot\theta). \tag{C.34}$$

The dicretized form of (C.34),

$$\mathcal{L}T_i = -\alpha_2\alpha_3\theta_i^{\alpha_3-2}(\alpha_3 - 1 + \theta_i\cot\theta_i), \tag{C.35}$$

together with the coefficients (C.32) and (C.33), gives us an approximation to $\mathcal{L}T$ when T is modelled on the form (C.28),

$$\mathcal{L}T_i = -\frac{(T_{i-1} - T_{i+1})\theta_i^{\alpha_3-2}(\alpha_3 - 1 + \theta_i\cot\theta_i)}{\theta_{i-1}^{\alpha_3} - \theta_{i+1}^{\alpha_3}}. \tag{C.36}$$

Equation (C.36) still contains the unknown exponent α_3 and therefore we must solve a nonlinear system of equations numerically for every iteration in this numerical scheme. The exact system will depend on the specific structure of the implementation, but it will involve variations of equation (C.29)-(C.31) and (C.36). Let's now test the precision of this approximation scheme in the case of a singular solution.

C.4.1 Test the precision of the alternative approximation

We have now developed an alternative approximation scheme for the operator (C.1). As mentioned above, the standard finite difference method will be our go-to for any solution that is not expected to be singular at $\theta = 0$. For solutions with the kind of singularity previously described, we hypothesized that the standard method will be highly imprecise and hence developed the alternative method. Now we to test this hypotheses by considering a known singular solution of the form

$$\tilde{T}(\theta) = a + \theta^{\alpha}\cos\theta. \tag{C.37}$$

For a given solution on the form (C.37), the exact solution to $\mathcal{L}\tilde{T}$ is known. We want to test the capability of the centered difference approximation and the new alternative approximation scheme to replicate the exact value $\mathcal{L}\tilde{T}$ for some θ close to 0. More specifically, we will consider a spacial

grid with uniform intervals of $\Delta\theta$,

$$\theta_i = i\Delta\theta, \qquad i = 0, 1, 2, ... \tag{C.38}$$

and compare the approximated value for the two approximation schemes in the first grid point, θ_1, against the exact value $\mathcal{L}\tilde{T}(\theta_1)$. We will do this for several spacial grids with various $\Delta\theta$, testing the precision as well as giving us an indication of what step size we should choose in order to remain within an acceptable percentage error margin.

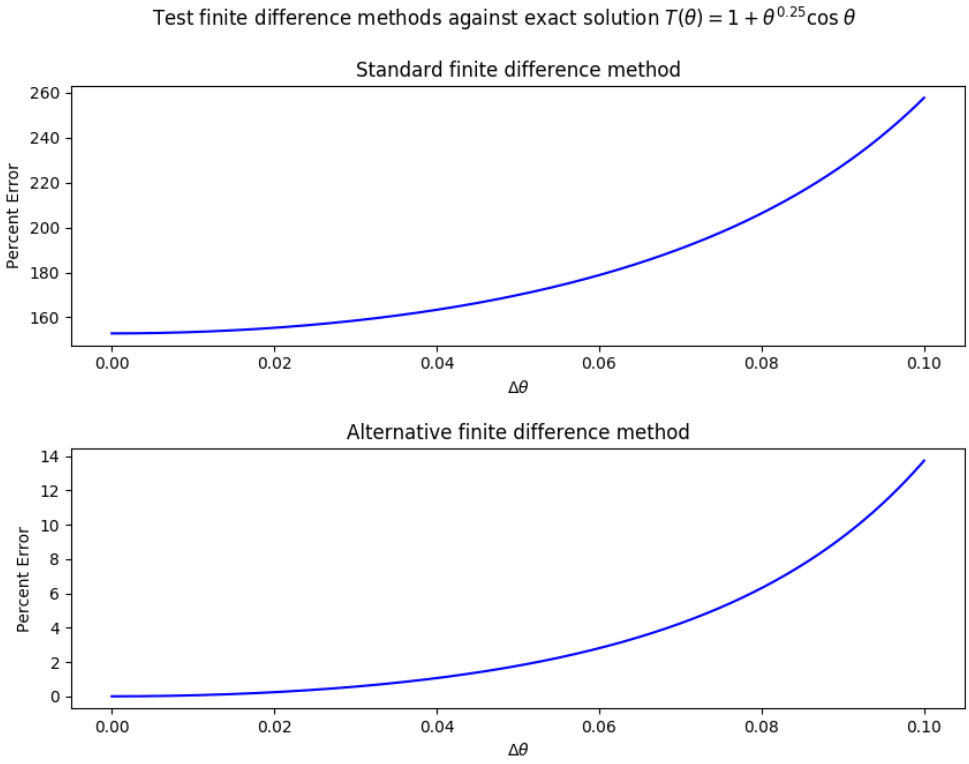

Figure 33: *Plot of the percentage error of $\mathcal{L}T$ in the first grid point, θ_1, against a selection of $\Delta\theta$, for an exact solution $T(\theta) = 1 + \theta^{0.25}\cos\theta$.*

From Figure 33 it is evident that for solutions of the form (C.37), the alternative finite difference method gives a better approximation than the standard centered difference approximation. If we encounter singular solutions of the type described above, we should apply this alternative method in a small neighbourhood around the singularity and with a step size $\Delta\theta = 0.1$ we are likely to remain within a 1% error margin.

Appendix D Fundamental integral identity and a Green's function for the operator $\mathcal{L}$

In this appendix we are going to derive the fundamental integral identity and a Green's function for the operator

$$\mathcal{L}(\cdot) = -\frac{1}{\sin\theta}\frac{\partial}{\partial\theta}\big(\sin\theta\frac{\partial}{\partial\theta}(\cdot)\big) + \beta(\cdot). \tag{D.1}$$

D.1 The fundamental integral identity

In order to derive the integral identity we need to clarify how to integrate on the surface of a sphere. More specifically, we need to find an expression for the integration element, a surface element, dA, corresponding to the induced metric on the sphere introduced in Appendix B.2. For an oriented Riemannian manifold with oriented smooth coordinates (x^i), the Riemannian volume form has the local expression

$$\omega_g = \sqrt{\det(g_{ij})}\, dx^1 \wedge \cdots \wedge dx^n,$$

where g_{ij} are the components of the Riemannian metric in these coordinates.

Let dA denote the Riemannian volume form on our surface, S, with respect to the induced metric. Our domain, S, is an oriented Riemannian manifold with oriented smooth coordinates (θ, φ), hence the Riemannian volume form has the local expression

$$dA = \sqrt{\det(g)}\, d\theta \wedge d\varphi,$$

where g is the metric tensor (B.14) [12]. Thus, by equation (B.15) we have

$$dA = R^2 \sin\theta\, d\theta \wedge d\varphi. \tag{D.2}$$

We are now ready to derive the integral identity. In Appendix B.2 we saw that by considering a rotationally symmetrical sphere and averaging over long timescales, we may disregard the dependence on φ,

$$T = T(\theta).$$

Bering this in mind, we introduce two functions defined on the sphere;

$$v = v(\theta)$$
$$u = u(\theta).$$

For these functions we have

$$\begin{aligned}
\int_{\varphi_1}^{\varphi_2}\int_{\theta_1}^{\theta_2} dA\, v\mathcal{L}u &= \int_{\varphi_1}^{\varphi_2}\int_{\theta_1}^{\theta_2} d\varphi d\theta\, R^2\sin\theta\, v\mathcal{L}u \\
&= R^2(\varphi_2-\varphi_1)\int_{\theta_1}^{\theta_2} d\theta\ \sin\theta\, v\left\{-\frac{1}{\sin\theta}\frac{\partial}{\partial\theta}\big(\sin\theta\frac{\partial u}{\partial\theta}\big)+\beta u\right\} \\
&= R^2(\varphi_2-\varphi_1)\left[-\int_{\theta_1}^{\theta_2} d\theta\, v\frac{\partial}{\partial\theta}\big(\sin\theta\frac{\partial u}{\partial\theta}\big)+\beta\int_{\theta_1}^{\theta_2} d\theta\ \sin\theta\, vu\right] \\
&= R^2(\varphi_2-\varphi_1)\left[-v\sin\theta\frac{\partial u}{\partial\theta}\bigg|_{\theta_1}^{\theta_2}+\int_{\theta_1}^{\theta_2} d\theta\ \frac{\partial v}{\partial\theta}\sin\theta\frac{\partial u}{\partial\theta}+\beta\int_{\theta_1}^{\theta_2} d\theta\ \sin\theta\, vu\right] \\
&= R^2(\varphi_2-\varphi_1)\left[-v\sin\theta\frac{\partial u}{\partial\theta}\bigg|_{\theta_1}^{\theta_2}+\frac{\partial v}{\partial\theta}\sin\theta\, u\bigg|_{\theta_1}^{\theta_2}-\int_{\theta_1}^{\theta_2} d\theta\, u\frac{\partial}{\partial\theta}\big(\sin\theta\frac{\partial v}{\partial\theta}\big)\right. \\
&\qquad\left.+\beta\int_{\theta_1}^{\theta_2} d\theta\ \sin\theta\, vu\right] \\
&= R^2(\varphi_2-\varphi_1)\left[\left\{-v\sin\theta\frac{\partial u}{\partial\theta}+\frac{\partial v}{\partial\theta}\sin\theta\, u\right\}\bigg|_{\theta_1}^{\theta_2}\right. \\
&\qquad\left.+\int_{\theta_1}^{\theta_2} d\theta\ \sin\theta\, u\left\{-\frac{1}{\sin\theta}\frac{\partial}{\partial\theta}\big(\sin\theta\frac{\partial v}{\partial\theta}\big)+\beta v\right\}\right].
\end{aligned}$$

From the above calculations we see that we have

$$R^2(\varphi_2-\varphi_1)\int_{\theta_1}^{\theta_2} d\theta\ \sin\theta\, v\mathcal{L}u = R^2(\varphi_2-\varphi_1)\left[\left\{-v\sin\theta\frac{\partial u}{\partial\theta}+\frac{\partial v}{\partial\theta}\sin\theta\, u\right\}\bigg|_{\theta_1}^{\theta_2}+\int_{\theta_1}^{\theta_2} d\theta\ \sin\theta\, u\mathcal{L}v\right],$$

and we can conclude that the fundamental integral identity is

$$\int_{\theta_1}^{\theta_2} d\theta\ \sin\theta\big\{v\mathcal{L}u-u\mathcal{L}v\big\}=\left\{u\sin\theta\frac{\partial v}{\partial\theta}-v\sin\theta\frac{\partial u}{\partial\theta}\right\}\bigg|_{\theta_1}^{\theta_2}.$$

D.2 Find a Green's function

A Green's function, $K(\theta,\xi)$, for the operator (D.1) is a solution to the equation

$$\mathcal{L}K(\theta,\xi)=\delta_\xi(\theta), \tag{D.3}$$

where $\delta_\xi(\theta)$ is the Dirac-delta function. In order to find a Green's function we must first find an expression for the Dirac-delta function, $\delta_\xi(\theta)$, on our surface S. The two defining properties of the Dirac-delta function is;

1) for any surface of interest, S, we must have

$$\int_S dA\, \delta_{\vec{\xi}} = 1, \tag{D.4}$$

2) for any function, $f(\vec{x})$, defined on S we must have

$$\int_S dA\, \delta_{\vec{\xi}} f = f(\vec{\xi}). \tag{D.5}$$

For our surface of interest, S, with its induced metric, the properties (D.4) and (D.5) becomes

$$\int_0^{2\pi} \int_0^{\pi} d\theta d\varphi\, R^2 \sin\theta\, \delta_{\vec{\xi}}(\theta, \varphi) = 1$$

and

$$\int_0^{2\pi} \int_0^{\pi} d\theta d\varphi\, R^2 \sin\theta\, \delta_{\vec{\xi}}(\theta, \varphi) f(\theta, \varphi) = f(\vec{\xi}).$$

We are seeking a solution to (3.1) that is independent of φ, therefore it makes sense to seek a Green's function, and consequently a Dirac-delta function, with the same independence. Thus, for the Dirac-delta function we are seeking, the following properties must hold

$$2\pi R^2 \int_0^{\pi} d\theta\ \sin\theta\, \delta_\xi(\theta) = 1 \tag{D.6}$$

and

$$2\pi R^2 \int_0^{\pi} d\theta\ \sin\theta\, \delta_\xi(\theta) f(\theta) = f(\xi). \tag{D.7}$$

Observe that choosing

$$\delta_\xi(\theta) = \frac{\delta(\theta - \xi)}{2\pi R^2 \sin\theta}, \tag{D.8}$$

where $\delta(\theta - \xi)$ is the usual delayed Dirac-delta function on the line, will ensure that (D.6) and (D.7) are satisfied. We will therefore express the Dirac-delta function as (D.8).

Now we are ready to find a Green's function for the operator (D.1). We start by choosing a scale, $\overline{K}$, for the Green's function,

$$K = \overline{K} K', \tag{D.9}$$

and for that we temporarily return to the dimensional form of (D.1). Applying the Dirac-delta function (D.8), the dimensional form of (D.3) becomes

$$-\frac{k_0}{R^2} \frac{1}{\sin\theta} \frac{\partial}{\partial\theta} \Big(\sin\theta \frac{\partial K}{\partial\theta} \Big) + BK = \frac{\delta(\theta - \xi)}{2\pi R^2 \sin\theta}.$$

We apply the scaling (D.9),

$$-\frac{1}{\sin\theta}\frac{\partial}{\partial\theta}\Big(\sin\theta\frac{\partial K'}{\partial\theta}\Big)+\beta K'=\frac{1}{2\pi k_0\overline{K}}\frac{\delta(\theta-\xi)}{\sin\theta}, \tag{D.10}$$

and observe that choosing

$$\overline{K}=\frac{1}{2\pi k_0}$$

equation (D.10) becomes

$$\mathcal{L}K=\frac{\delta(\theta-\xi)}{\sin\theta}. \tag{D.11}$$

In equation (D.11) we have dropped the prime notation on the dimensionless Green's function since only dimensionless Green's functions will appear from this point onward. Now, let's find a Green's function that solves (D.11).

We start by assuming that the Green's function, $K(\theta,\xi)$, is continuous across $\theta=\xi$. Therefore we must have

$$\lim_{\theta\to\xi^+}K(\theta,\xi)=\lim_{\theta\to\xi^-}K(\theta,\xi). \tag{D.12}$$

Introducing the short hand notation

$$\begin{aligned}\lim_{\theta\to\xi^+}K(\theta,\xi)&=K(\xi^+,\xi)\\ \lim_{\theta\to\xi^-}K(\theta,\xi)&=K(\xi^-,\xi)\end{aligned} \tag{D.13}$$

we can rewrite (D.12) as

$$K(\xi^+,\xi)-K(\xi^-,\xi)=0. \tag{D.14}$$

This is the first condition on the Green's function.

Next, we integrate (D.11) over a small interval centered on $\theta=\xi$,

$$\int_{\xi-\varepsilon}^{\xi+\varepsilon}d\theta\ \sin\theta\left\{-\frac{1}{\sin\theta}\frac{\partial}{\partial\theta}\Big(\sin\theta\frac{\partial K}{\partial\theta}\Big)+\beta K\right\}=\int_{\xi-\varepsilon}^{\xi+\varepsilon}d\theta\ \sin\theta\,\frac{\delta(\theta-\xi)}{\sin\theta}$$

$$-\int_{\xi-\varepsilon}^{\xi+\varepsilon}d\theta\,\frac{\partial}{\partial\theta}\Big(\sin\theta\frac{\partial}{\partial\theta}K(\theta,\xi)\Big)+\beta\int_{\xi-\varepsilon}^{\xi+\varepsilon}d\theta\ \sin\theta\,K(\theta,\xi)=1$$

$$-\sin\theta\frac{\partial}{\partial\theta}K(\theta,\xi)\Big|_{\xi-\varepsilon}^{\xi+\varepsilon}+\beta\int_{\xi-\varepsilon}^{\xi+\varepsilon}d\theta\ \sin\theta\,K(\theta,\xi)=1.$$

Since $K(\theta,\xi)$ is continuous at $\theta=\xi$, letting $\varepsilon\to0$ we must have

$$\begin{aligned}-\sin\xi\left[\frac{\partial}{\partial\theta}K(\xi^+,\xi)-\frac{\partial}{\partial\theta}K(\xi^-,\xi)\right]&=1\\ \frac{\partial}{\partial\theta}K(\xi^+,\xi)-\frac{\partial}{\partial\theta}K(\xi^-,\xi)&=-\frac{1}{\sin\xi},\end{aligned} \tag{D.15}$$

where we have applied the short hand notation (D.13). This is the second condition on the Green's function.

At $\theta \neq \xi$ we evidently have

$$\mathcal{L}K(\theta, \xi) = 0. \tag{D.16}$$

We can therefore conclude that $K(\theta, \xi)$ must satisfy the necessary conditions (D.14), (D.15) and (D.16). In order to find a Green's function that solves (D.11) we need to find a basis of solutions for an equation on the form

$$-\frac{1}{\sin\theta}\frac{\partial}{\partial\theta}\big(\sin\theta\frac{\partial}{\partial\theta}y(\theta)\big) + \beta y(\theta) = 0. \tag{D.17}$$

Let's introduce the change of variables;

$$x = \cos\theta.$$

Observe that

$$\sin\theta = \sqrt{1-\cos^2\theta} = \sqrt{1-x^2}. \tag{D.18}$$

Applying (D.18) in combination with the chain rule we have

$$\frac{\partial}{\partial\theta} = \frac{\partial x}{\partial\theta}\frac{\partial}{\partial x} = -\sin\theta\frac{\partial}{\partial x} = -\sqrt{1-x^2}\frac{\partial}{\partial x}. \tag{D.19}$$

We introduce a function, u, such that

$$u(\cos\theta) = y(\theta). \tag{D.20}$$

Applying (D.19) and (D.20) we can rewrite (D.17) as

$$\begin{aligned}
-\frac{1}{\sqrt{1-x^2}}\left[-\sqrt{1-x^2}\frac{\partial}{\partial x}\left(\sqrt{1-x^2}\left(-\sqrt{1-x^2}\frac{\partial}{\partial x}u(x)\right)\right)\right] + \beta u(x) &= 0 \\
-\frac{\partial}{\partial x}\left((1-x^2)\frac{\partial}{\partial x}u(x)\right) + \beta u(x) &= 0 \\
(1-x^2)\frac{\partial^2}{\partial x^2}u(x) + 2x\frac{\partial}{\partial x}u(x) - \beta u(x) &= 0.
\end{aligned} \tag{D.21}$$

Let λ be a number such that

$$-\beta = \lambda(\lambda+1).$$

Now we can write (D.21) as a Legendre equation,

$$(1-x^2)\frac{\partial^2}{\partial x^2}u(x) + 2x\frac{\partial}{\partial x}u(x) + \lambda(\lambda+1)u(x) = 0. \tag{D.22}$$

The general Legendre equation is

$$(1-x^2)\frac{d^2}{dx^2}P_l^m(x) - 2x\frac{d}{dx}P_l^m(x) + \left[l(l+1) - \frac{m^2}{1-x^2}\right]P_l^m(x) = 0$$

and when $m = 0$ and $l = \lambda$ is some arbitrary real or complex value, the solutions are the Legendre

functions P_λ and Q_λ. Thus, a basis of solutions for (D.22) is

$$\{P_\lambda,\, Q_\lambda\}.$$

By relation (D.20) we can therefore conclude that

$$\{P_\lambda(\cos\theta),\, Q_\lambda(\cos\theta)\}, \tag{D.23}$$

where

$$\lambda = \frac{1}{2}\left(\sqrt{1-4\beta}-1\right),$$

is a basis for the solution space of (D.17). Using this basis, the general solution to (D.16) is

$$K(\theta,\xi) = \begin{cases} a(\xi)P_\lambda(\cos\theta) + b(\xi)Q_\lambda(\cos\theta), & \theta > \xi \\ c(\xi)P_\lambda(\cos\theta) + d(\xi)Q_\lambda(\cos\theta), & \theta < \xi \end{cases}. \tag{D.24}$$

The parameterdependent coefficients $a(\xi), b(\xi), c(\xi)$ and $d(\xi)$ can be determined through the conditions (D.14) and (D.15). Any choice of these coefficients satisfying (D.14) and (D.15) will give a Green's function for the operator (D.1).

We are solving the stationary energy balance equation (3.10) on the domain $\theta \in [0,\pi]$, it therefore makes sense to seek a Green's function that is non-singular in this domain. We expect the Legendre functions (D.23) to have singularities at the boundaries of the domain, at $\theta = 0$ and $\theta = \pi$, for a given $\lambda \in \mathbb{C}$. Thus, we want to to develop a set of conditions on the coefficients $a(\xi), b(\xi), c(\xi)$ and $d(\xi)$ to ensure that the Green's function (D.24) is non-singular when $\theta \to 0$ and $\theta \to \pi$. Before we proceed with finding these conditions, let's introduce the notation

$$\begin{aligned} K_+(\theta,\xi) &= a(\xi)P_\lambda(\cos\theta) + b(\xi)Q_\lambda(\cos\theta) \\ K_-(\theta,\xi) &= c(\xi)P_\lambda(\cos\theta) + d(\xi)Q_\lambda(\cos\theta) \end{aligned} \tag{D.25}$$

such that

$$K(\theta,\xi) = \begin{cases} K_+(\theta,\xi), & \theta > \xi \\ K_-(\theta,\xi), & \theta < \xi \end{cases}.$$

Using a computer algebra system, we find a series expansion of K_+ around $\theta = \pi$, and recognize that there is a term in this expansion containing $\log(\pi-\theta)$ with a coefficient $c_{+0}(a(\xi), b(\xi))$. We want to ensure that K_+ is non-singular at $\theta = \pi$ and therefore demand that

$$c_{+0}(a(\xi), b(\xi)) = 0 \qquad \forall\, \xi \in [0,\pi]. \tag{D.26}$$

Similarly, we find a series expansion of K_- around $\theta = 0$. In this expansion there is a term containing $\log(\theta)$ with a coefficient $c_{-0}(c(\xi), d(\xi))$, and we demand that

$$c_{-0}(c(\xi), d(\xi)) = 0 \qquad \forall\, \xi \in [0,\pi]. \tag{D.27}$$

Using the notation (D.25) we can rewrite the conditions (D.14) and (D.15) on the Green's function

as

$$K_+(\xi,\xi) - K_-(\xi,\xi) = 0 \tag{D.28}$$

and

$$\frac{\partial}{\partial\theta}K_+(\xi,\xi) - \frac{\partial}{\partial\theta}K_-(\xi,\xi) = -\frac{1}{\sin\xi}. \tag{D.29}$$

We solve the system of equations (D.26)-(D.29) for $a(\xi), b(\xi), c(\xi)$ and $d(\xi)$, and find the following Green's function;

$$K(\theta,\xi) = \begin{cases} \frac{P_\lambda(\cos\xi)(\pi\cot(\pi\lambda)P_\lambda(\cos\theta)-2Q_\lambda(\cos\theta))}{2(1+\lambda)(P_\lambda(\cos\xi)Q_{\lambda+1}(\cos\xi)-P_{\lambda+1}(\cos\xi)Q_\lambda(\cos\xi))}, & \theta > \xi \\ \frac{P_\lambda(\cos\theta)(\pi\cot(\pi\lambda)P_\lambda(\cos\xi)-2Q_\lambda(\cos\xi))}{2(1+\lambda)(P_\lambda(\cos\xi)Q_{\lambda+1}(\cos\xi)-P_{\lambda+1}(\cos\xi)Q_\lambda(\cos\xi))}, & \theta < \xi \end{cases}. \tag{D.30}$$

The Green's function (D.30) is non-singular and bounded at $\theta = 0$ and $\theta = \pi$. The derivative of the Green's function (D.30) is also bounded at the boundary and actually tends to zero,

$$\begin{aligned} \lim_{\theta\to 0}\frac{\partial K}{\partial\theta} &= 0 \qquad \forall\,\xi\in[0,\pi] \\ \lim_{\theta\to\pi}\frac{\partial K}{\partial\theta} &= 0 \qquad \forall\,\xi\in[0,\pi]. \end{aligned} \tag{D.31}$$

Appendix E Boundary integral method with a continent

In this appendix we are going to apply the boundary integral method to solve the stationary form of the energy balance equation (3.31) for the cases outlined in section 3.3,

$$\begin{cases} \mathcal{L}T + \beta_1 T = \eta_1 s(\theta)(1 - a_{\text{water}}(T)) - \alpha_1, & \theta \in [0, \theta_{l_1}) \cup (\theta_{l_2}, \pi] \\ \mathcal{L}T + \beta_2 T = \eta_2 s(\theta)(1 - a_{\text{land}}(T)) - \alpha_2, & \theta \in [\theta_{l_1}, \theta_{l_2}]. \end{cases}$$

The first part of this appendix will consist of laying the necessary groundwork for extending the application of the boundary integral method to include a continent. The latter part of this appendix will include the boundary integral relations and boundary integral equations associated with the various cases, rendered more or less in full for the sake of reproducibility. Readers uninterested in reproducing these results may skip the latter part of this appendix as the methodology for arriving at these stationary solutions will be analogous to the procedure outlined in section 3. At the very end of this appendix we will discuss the symmetry assumption mentioned section 3.3.1 and how the application of this assumption greatly reduces the computational complexity of the most complicated cases encountered in this thesis.

We start by imposing some conditions on the solution. The solution has to be continuous and must therefore satisfy the following conditions across the boundary between water and continent,

$$\begin{aligned} \lim_{\theta \to \theta_{l_1}^-} T(\theta) &= \lim_{\theta \to \theta_{l_1}^+} T(\theta) = T(\theta_{l_1}) \\ \lim_{\theta \to \theta_{l_2}^-} T(\theta) &= \lim_{\theta \to \theta_{l_2}^+} T(\theta) = T(\theta_{l_2}). \end{aligned}$$

Furthermore, we can have no build up of heat at the boundary between water and continent, nor at the critical latitudes. We therefore demand that the solution is differentiable across these latitudes,

$$\begin{aligned} \lim_{\theta \to \theta_{l_1}^-} \frac{\partial T}{\partial \theta}(\theta) &= \lim_{\theta \to \theta_{l_1}^+} \frac{\partial T}{\partial \theta}(\theta) = T(\theta_{l_1}) \\ \lim_{\theta \to \theta_{l_2}^-} \frac{\partial T}{\partial \theta}(\theta) &= \lim_{\theta \to \theta_{l_2}^+} \frac{\partial T}{\partial \theta}(\theta) = T(\theta_{l_2}) \\ \lim_{\theta \to \theta_{c_i}^-} \frac{\partial T}{\partial \theta}(\theta) &= \lim_{\theta \to \theta_{c_i}^+} \frac{\partial T}{\partial \theta}(\theta) = T(\theta_{c_i}). \end{aligned}$$

At the poles, the solution must still satisfy the boundary conditions developed in Appendix B.3,

$$\lim_{\theta \to 0} \sin\theta \frac{\partial T}{\partial \theta}(\theta) = 0$$

and

$$\lim_{\theta \to \pi} \sin\theta \frac{\partial T}{\partial \theta}(\theta) = 0.$$

In order to apply the boundary integral method we need a simpler model for the albedo. Just like in section 3, we will use the following albedo for water,

$$a_{\text{water}}(T) = \begin{cases} a_1, & T > -1 \\ a_2, & T < -1 \end{cases}.$$

For the continent we use the albedo

$$a_{\text{land}}(T) = \begin{cases} a_3, & T > -T_c \\ a_4, & T < -T_c \end{cases},$$

where $T_c = \frac{T_{s_2}}{T_s}$. The numerical values of a_1, a_2, a_3, a_4, T_s and T_{s_2} can be found in Appendix A. Defining

$$\mathcal{L}_1(\cdot) = -\frac{1}{\sin\theta}\frac{\partial}{\partial\theta}\big(\sin\theta\frac{\partial}{\partial\theta}(\cdot)\big) + \beta_1(\cdot)$$

we can write the governing equation for part of the surface covered by water on the compact form

$$\mathcal{L}_1 T = h_j.$$

Similarly, defining

$$\mathcal{L}_2(\cdot) = -\frac{1}{\sin\theta}\frac{\partial}{\partial\theta}\big(\sin\theta\frac{\partial}{\partial\theta}(\cdot)\big) + \beta_2(\cdot)$$

we can write the governing equation for the continent on the compact form

$$\mathcal{L}_2 T = h_j.$$

The source term, h_j, will depend on whether or not the surface has a snow/ice-cover. Therefore we let

$$h_1 = \eta_1 s(\theta)(1 - a_1) - \alpha_1 \tag{E.1}$$

be defined for water with no snow/ice cover and let

$$h_2 = \eta_1 s(\theta)(1 - a_2) - \alpha_1 \tag{E.2}$$

be defined for water with snow/ice cover. Similarly, let

$$h_3 = \eta_2 s(\theta)(1 - a_3) - \alpha_2 \tag{E.3}$$

be defined for the continent with no snow/ice cover and let

$$h_4 = \eta_2 s(\theta)(1 - a_4) - \alpha_2 \tag{E.4}$$

be defined for the continent with snow/ice-cover.

Recall that the aim of the boundary integral method is to derive integral identities for the solution to a differential equation that relate values of the solution in the interior of the domain to values

on the boundary of the domain using a Green's function. In section 3 we developed the general relation

$$T(\xi) = \int_{\theta_1}^{\theta_2} d\theta \, \sin\theta \, K(\theta,\xi) h(T,\theta) + \left\{ K \sin\theta \frac{\partial T}{\partial \theta} - T \sin\theta \frac{\partial K}{\partial \theta} \right\} \Bigg|_{\theta_1}^{\theta_2}, \tag{E.5}$$

which we will once again use, but with some minor modifications in order for it to fit with the current case. Recall also that a Green's function for an operator $\mathcal{G}$ is any solution to the equation

$$\mathcal{G}K(\vec{x}, \vec{\xi}) = \delta_{\vec{\xi}}(\vec{x}).$$

Thus, we will have to choose a slightly different Green's function depending whether the surface is covered by water or land. Let $K_1(\theta,\xi)$ be a solution to the equation

$$\mathcal{L}_1 K_1(\theta,\xi) = \delta_\xi(\theta),$$

and let $K_2(\theta,\xi)$ be a solution to the equation

$$\mathcal{L}_2 K_2(\theta,\xi) = \delta_\xi(\theta),$$

where $\delta_\xi(\theta)$ is the expression for the Dirac-delta function from Appendix D.2. Following the approach described in detail in Appendix D.2, we let

$$K_1(\theta,\xi) = \begin{cases} \frac{P_{\lambda_1}(\cos\xi)(\pi\cot(\pi\lambda_1)P_{\lambda_1}(\cos\theta) - 2Q_{\lambda_1}(\cos\theta))}{2(1+\lambda_1)(P_{\lambda_1}(\cos\xi)Q_{\lambda_1+1}(\cos\xi) - P_{\lambda_1+1}(\cos\xi)Q_{\lambda_1}(\cos\xi))}, & \theta > \xi \\ \frac{P_{\lambda_1}(\cos\theta)(\pi\cot(\pi\lambda_1)P_{\lambda_1}(\cos\xi) - 2Q_{\lambda_1}(\cos\xi))}{2(1+\lambda_1)(P_{\lambda_1}(\cos\xi)Q_{\lambda_1+1}(\cos\xi) - P_{\lambda_1+1}(\cos\xi)Q_{\lambda_1}(\cos\xi))}, & \theta < \xi \end{cases},$$

where

$$\lambda_1 = \frac{1}{2}\left(\sqrt{1-4\beta_1} - 1\right),$$

be our choice of Green's function for the interval on the surface covered by water, $\theta \in [0, \theta_{l_1}) \cup (\theta_{l_2}, \pi]$. Similarly, we let

$$K_2(\theta,\xi) = \begin{cases} \frac{P_{\lambda_2}(\cos\xi)(\pi\cot(\pi\lambda_2)P_{\lambda_2}(\cos\theta) - 2Q_{\lambda_2}(\cos\theta))}{2(1+\lambda_2)(P_{\lambda_2}(\cos\xi)Q_{\lambda_2+1}(\cos\xi) - P_{\lambda_2+1}(\cos\xi)Q_{\lambda_2}(\cos\xi))}, & \theta > \xi \\ \frac{P_{\lambda_2}(\cos\theta)(\pi\cot(\pi\lambda_2)P_{\lambda_2}(\cos\xi) - 2Q_{\lambda_2}(\cos\xi))}{2(1+\lambda_2)(P_{\lambda_2}(\cos\xi)Q_{\lambda_2+1}(\cos\xi) - P_{\lambda_2+1}(\cos\xi)Q_{\lambda_2}(\cos\xi))}, & \theta < \xi \end{cases},$$

where

$$\lambda_2 = \frac{1}{2}\left(\sqrt{1-4\beta_2} - 1\right),$$

be our choice of Green's function for the interval on the surface covered by the continent, $\theta \in [\theta_{l_1}, \theta_{l_2}]$. The Green's function $K_1(\theta,\xi)$ must necessarily retain the properties discussed in Appendix D.2 and the same goes for $K_2(\theta,\xi)$. With these choices of Green's functions, the general relation (E.5) becomes

$$T(\xi) = \int_{\theta_1}^{\theta_2} d\theta \, \sin\theta \, K_1(\theta,\xi) h_j + \left\{ K_1 \sin\theta \frac{\partial T}{\partial \theta} - T \sin\theta \frac{\partial K_1}{\partial \theta} \right\} \Bigg|_{\theta_1}^{\theta_2}, \quad \xi \in [0, \theta_{l_1}) \cup (\theta_{l_2}, \pi] \tag{E.6}$$

for water-covered part of the surface, and

$$T(\xi) = \int_{\theta_1}^{\theta_2} d\theta \, \sin\theta \, K_2(\theta, \xi) h_j + \left\{ K_2 \sin\theta \frac{\partial T}{\partial \theta} - T \sin\theta \frac{\partial K_2}{\partial \theta} \right\} \Bigg|_{\theta_1}^{\theta_2}, \qquad \xi \in [\theta_{l_1}, \theta_{l_2}] \quad \text{(E.7)}$$

for the continent. The function h_j, where $j = 1, 2, 3, 4$, will take the form (E.1)-(E.4) depending on the properties of the surface on interval in which we apply (E.6) and (E.7). Now we have laid the groundwork our proceeding analysis, it's time apply these results to find stationary solutions for the cases outlined section 3.3.

E.1 The case of no ice edges

Let's first consider the simplest possible case, one in which the sphere is either completely covered by ice/snow or no ice/snow cover at all. For this case we have three relevant region,

$$\theta \in (0, \theta_{l_1}) \qquad \text{(I)}$$

$$\theta \in (\theta_{l_1}, \theta_{l_2}) \qquad \text{(II)}$$

$$\theta \in (\theta_{l_2}, \pi). \qquad \text{(III)}$$

Let's concentrate on the scenario with no ice/snow-cover first. The governing equation in region I is therefore

$$\mathcal{L}_1 T = h_1.$$

In region II we have

$$\mathcal{L}_2 T = h_3$$

and in region III we have

$$\mathcal{L}_1 T = h_1.$$

Starting with region I, let's apply (E.6) letting $\theta_1 \to 0^+$ and $\theta_2 \to \theta_{l_1}^-$

$$\begin{aligned} T(\xi) = &\int_0^{\theta_{l_1}} d\theta \ \sin\theta \, K_1(\theta,\xi) h_1(\theta) \\ &+ \lim_{\theta_2 \to \theta_{l_1}^-} K_1(\theta_2,\xi)\sin(\theta_2)\frac{\partial T}{\partial \theta}(\theta_2) \\ &- \lim_{\theta_2 \to \theta_{l_1}^-} T(\theta_2)\sin(\theta_2)\frac{\partial K_1}{\partial \theta}(\theta_2,\xi) \\ &- \lim_{\theta_1 \to 0^+} K_1(\theta_1,\xi)\sin(\theta_1)\frac{\partial T}{\partial \theta}(\theta_1) \\ &+ \lim_{\theta_1 \to 0^+} T(\theta_1)\sin(\theta_1)\frac{\partial K_1}{\partial \theta}(\theta_1,\xi). \end{aligned}$$

Applying the boundary condition, as well as the fact that the Green's function is bounded at the boundary, we get the following relation for the solution in region I;

$$\begin{aligned} T(\xi) = &\int_0^{\theta_{l_1}} d\theta \ \sin\theta \, K_1(\theta,\xi) h_1(\theta) + K_1(\theta_{l_1},\xi)\sin(\theta_{l_1})\frac{\partial T}{\partial \theta}(\theta_{l_1}) \\ &- T(\theta_{l_1})\sin(\theta_{l_1}) \lim_{\theta \to \theta_{l_1}^-} \frac{\partial K_1}{\partial \theta}(\theta,\xi). \end{aligned} \tag{E.8}$$

Next, we apply (E.7) in region II letting $\theta_1 \to \theta_{l_1}^+$ and $\theta_2 \to \theta_{l_2}^-$ to obtain a relation for the solution in region II,

$$\begin{aligned} T(\xi) = &\int_{\theta_{l_1}}^{\theta_{l_2}} d\theta \ \sin\theta \, K_2(\theta,\xi) h_3(\theta) + K_2(\theta_{l_2},\xi)\sin(\theta_{l_2})\frac{\partial T}{\partial \theta}(\theta_{l_2}) \\ &- T(\theta_{l_2})\sin(\theta_{l_2}) \lim_{\theta \to \theta_{l_2}^-} \frac{\partial K_2}{\partial \theta}(\theta,\xi) - K_2(\theta_{l_1},\xi)\sin(\theta_{l_1})\frac{\partial T}{\partial \theta}(\theta_{l_1}) \\ &+ T(\theta_{l_1})\sin(\theta_{l_1}) \lim_{\theta \to \theta_{l_1}^+} \frac{\partial K_1}{\partial \theta}(\theta,\xi). \end{aligned} \tag{E.9}$$

Finally, to obtain a relation for the solution in region III we apply (E.6) in region III letting $\theta_1 \to \theta_{l_2}^+$ and $\theta_2 \to \pi^-$,

$$\begin{aligned} T(\xi) = &\int_{\theta_{l_2}}^{\pi} d\theta \ \sin\theta \, K_1(\theta,\xi) h_1(\theta) - K_1(\theta_{l_2},\xi)\sin(\theta_{l_2})\frac{\partial T}{\partial \theta}(\theta_{l_2}) \\ &+ T(\theta_{l_2})\sin(\theta_{l_2}) \lim_{\theta \to \theta_{l_2}^+} \frac{\partial K_1}{\partial \theta}(\theta,\xi). \end{aligned} \tag{E.10}$$

Here we applied the boundary condition and the fact that the Green's function is bounded at the boundary. Now we let ξ approach the boundaries of the sub-domains I, II and III in the same

fashion as in section 3.2.2. Starting with (E.8) we let $\xi \to 0^+$,

$$\begin{aligned} T(0) = &\int_0^{\theta_{l_1}} d\theta \, \sin\theta \, K_1(\theta,0)h_1(\theta) + K_1(\theta_{l_1},0)\sin(\theta_{l_1})\frac{\partial T}{\partial\theta}(\theta_{l_1}) \\ &- T(\theta_{l_1})\sin(\theta_{l_1}) \lim_{\xi\to 0^+}\lim_{\theta\to\theta_{l_1}^-}\frac{\partial K_1}{\partial\theta}(\theta,\xi), \end{aligned} \tag{E.11}$$

and $\xi \to \theta_{l_1}^-$,

$$\begin{aligned} T(\theta_{l_1}) = &\int_0^{\theta_{l_1}} d\theta \, \sin\theta \, K_1(\theta,\theta_{l_1})h_1(\theta) + \lim_{\xi\to\theta_{l_1}^-} K_1(\theta_{l_1},\xi)\sin(\theta_{l_1})\frac{\partial T}{\partial\theta}(\theta_{l_1}) \\ &- T(\theta_{l_1})\sin(\theta_{l_1}) \lim_{\xi\to\theta_{l_1}^-}\lim_{\theta\to\theta_{l_1}^-}\frac{\partial K_1}{\partial\theta}(\theta,\xi). \end{aligned} \tag{E.12}$$

Similarly, in (E.9) we let $\xi \to \theta_{l_1}^+$,

$$\begin{aligned} T(\theta_{l_1}) = &\int_{\theta_{l_1}}^{\theta_{l_2}} d\theta \, \sin\theta \, K_2(\theta,\theta_{l_1})h_3(\theta) + K_2(\theta_{l_2},\theta_{l_1})\sin(\theta_{l_2})\frac{\partial T}{\partial\theta}(\theta_{l_2}) \\ &- T(\theta_{l_2})\sin(\theta_{l_2}) \lim_{\xi\to\theta_{l_1}^+}\lim_{\theta\to\theta_{l_2}^-}\frac{\partial K_2}{\partial\theta}(\theta,\xi) - \lim_{\xi\to\theta_{l_1}^+} K_2(\theta_{l_1},\xi)\sin(\theta_{l_1})\frac{\partial T}{\partial\theta}(\theta_{l_1}) \\ &+ T(\theta_{l_1})\sin(\theta_{l_1}) \lim_{\xi\to\theta_{l_1}^+}\lim_{\theta\to\theta_{l_1}^+}\frac{\partial K_1}{\partial\theta}(\theta,\xi), \end{aligned} \tag{E.13}$$

and $\xi \to \theta_{l_2}^-$,

$$\begin{aligned} T(\theta_{l_2}) = &\int_{\theta_{l_1}}^{\theta_{l_2}} d\theta \, \sin\theta \, K_2(\theta,\theta_{l_2})h_3(\theta) + \lim_{\xi\to\theta_{l_2}^-} K_2(\theta_{l_2},\xi)\sin(\theta_{l_2})\frac{\partial T}{\partial\theta}(\theta_{l_2}) \\ &- T(\theta_{l_2})\sin(\theta_{l_2}) \lim_{\xi\to\theta_{l_2}^-}\lim_{\theta\to\theta_{l_2}^-}\frac{\partial K_2}{\partial\theta}(\theta,\xi) - K_2(\theta_{l_1},\theta_{l_2})\sin(\theta_{l_1})\frac{\partial T}{\partial\theta}(\theta_{l_1}) \\ &+ T(\theta_{l_1})\sin(\theta_{l_1}) \lim_{\xi\to\theta_{l_2}^-}\lim_{\theta\to\theta_{l_1}^+}\frac{\partial K_1}{\partial\theta}(\theta,\xi). \end{aligned} \tag{E.14}$$

Finally, in (E.10) we let $\xi \to \theta_{l_2}^+$,

$$\begin{aligned} T(\theta_{l_2}) = &\int_{\theta_{l_2}}^{\pi} d\theta \, \sin\theta \, K_1(\theta,\theta_{l_2})h_1(\theta) - \lim_{\xi\to\theta_{l_2}^+} K_1(\theta_{l_2},\xi)\sin(\theta_{l_2})\frac{\partial T}{\partial\theta}(\theta_{l_2}) \\ &+ T(\theta_{l_2})\sin(\theta_{l_2}) \lim_{\xi\to\theta_{l_2}^+}\lim_{\theta\to\theta_{l_2}^+}\frac{\partial K_1}{\partial\theta}(\theta,\xi), \end{aligned} \tag{E.15}$$

and $\xi \to \pi^-$,

$$\begin{aligned} T(\pi) = &\int_{\theta_{l_2}}^{\pi} d\theta \ \sin\theta \, K_1(\theta,\pi)h_1(\theta) - K_1(\theta_{l_2},\pi)\sin(\theta_{l_2})\frac{\partial T}{\partial\theta}(\theta_{l_2}) \\ &+ T(\theta_{l_2})\sin(\theta_{l_2}) \lim_{\xi\to\pi^-}\lim_{\theta\to\theta_{l_2}^+}\frac{\partial K_1}{\partial\theta}(\theta,\xi). \end{aligned} \tag{E.16}$$

The system of equations (E.11)-(E.16) is the boundary integral equations for the case of a sphere with a continent and no ice/snow-cover. It is a system of 6 equations for 6 unknowns, $T(0)$, $T(\theta_{l_1})$, $T(\theta_{l_2})$, $\frac{\partial T}{\partial\theta}(\theta_{l_1})$, $\frac{\partial T}{\partial\theta}(\theta_{l_2})$ and $T(\pi)$. These unknown boundary values appear linearly in this system of equations, making the system trivial to solve with a computer algebra system. Once these boundary values are obtained the relations (E.8), (E.9) and (E.10) will give us the solution inside the regions I, II and III, respectively.

We must also consider the scenario where the sphere is completely ice/snow-covered. The approach here will be analogous to the above process, it's simply a matter of changing the function h_j in the relevant regions. Hence, the boundary integral relations in region I, II and III will be;

$$\begin{aligned} T(\xi) = &\int_0^{\theta_{l_1}} d\theta \ \sin\theta \, K_1(\theta,\xi)h_2(\theta) + K_1(\theta_{l_1},\xi)\sin(\theta_{l_1})\frac{\partial T}{\partial\theta}(\theta_{l_1}) \\ &- T(\theta_{l_1})\sin(\theta_{l_1}) \lim_{\theta\to\theta_{l_1}^-}\frac{\partial K_1}{\partial\theta}(\theta,\xi), \end{aligned} \tag{E.17}$$

$$\begin{aligned} T(\xi) = &\int_{\theta_{l_1}}^{\theta_{l_2}} d\theta \ \sin\theta \, K_2(\theta,\xi)h_4(\theta) + K_2(\theta_{l_2},\xi)\sin(\theta_{l_2})\frac{\partial T}{\partial\theta}(\theta_{l_2}) \\ &- T(\theta_{l_2})\sin(\theta_{l_2}) \lim_{\theta\to\theta_{l_2}^-}\frac{\partial K_2}{\partial\theta}(\theta,\xi) - K_2(\theta_{l_1},\xi)\sin(\theta_{l_1})\frac{\partial T}{\partial\theta}(\theta_{l_1}) \\ &+ T(\theta_{l_1})\sin(\theta_{l_1}) \lim_{\theta\to\theta_{l_1}^+}\frac{\partial K_1}{\partial\theta}(\theta,\xi) \end{aligned} \tag{E.18}$$

and

$$\begin{aligned} T(\xi) = &\int_{\theta_{l_2}}^{\pi} d\theta \ \sin\theta \, K_1(\theta,\xi)h_2(\theta) - K_1(\theta_{l_2},\xi)\sin(\theta_{l_2})\frac{\partial T}{\partial\theta}(\theta_{l_2}) \\ &+ T(\theta_{l_2})\sin(\theta_{l_2}) \lim_{\theta\to\theta_{l_2}^+}\frac{\partial K_1}{\partial\theta}(\theta,\xi), \end{aligned} \tag{E.19}$$

respectively. Subsequently, the boundary integral equations will be;

$$\begin{aligned} T(0) = &\int_0^{\theta_{l_1}} d\theta\ \sin\theta\, K_1(\theta,0)h_2(\theta) + K_1(\theta_{l_1},0)\sin(\theta_{l_1})\frac{\partial T}{\partial\theta}(\theta_{l_1}) \\ &- T(\theta_{l_1})\sin(\theta_{l_1})\lim_{\xi\to 0^+}\lim_{\theta\to\theta_{l_1}^-}\frac{\partial K_1}{\partial\theta}(\theta,\xi) \end{aligned} \tag{E.20}$$

$$\begin{aligned} T(\theta_{l_1}) = &\int_0^{\theta_{l_1}} d\theta\ \sin\theta\, K_1(\theta,\theta_{l_1})h_2(\theta) + \lim_{\xi\to\theta_{l_1}^-} K_1(\theta_{l_1},\xi)\sin(\theta_{l_1})\frac{\partial T}{\partial\theta}(\theta_{l_1}) \\ &- T(\theta_{l_1})\sin(\theta_{l_1})\lim_{\xi\to\theta_{l_1}^-}\lim_{\theta\to\theta_{l_1}^-}\frac{\partial K_1}{\partial\theta}(\theta,\xi). \end{aligned} \tag{E.21}$$

$$\begin{aligned} T(\theta_{l_1}) = &\int_{\theta_{l_1}}^{\theta_{l_2}} d\theta\ \sin\theta\, K_2(\theta,\theta_{l_1})h_4(\theta) + K_2(\theta_{l_2},\theta_{l_1})\sin(\theta_{l_2})\frac{\partial T}{\partial\theta}(\theta_{l_2}) \\ &- T(\theta_{l_2})\sin(\theta_{l_2})\lim_{\xi\to\theta_{l_1}^+}\lim_{\theta\to\theta_{l_2}^-}\frac{\partial K_2}{\partial\theta}(\theta,\xi) - \lim_{\xi\to\theta_{l_1}^+} K_2(\theta_{l_1},\xi)\sin(\theta_{l_1})\frac{\partial T}{\partial\theta}(\theta_{l_1}) \\ &+ T(\theta_{l_1})\sin(\theta_{l_1})\lim_{\xi\to\theta_{l_1}^+}\lim_{\theta\to\theta_{l_1}^+}\frac{\partial K_1}{\partial\theta}(\theta,\xi) \end{aligned} \tag{E.22}$$

$$\begin{aligned} T(\theta_{l_2}) = &\int_{\theta_{l_1}}^{\theta_{l_2}} d\theta\ \sin\theta\, K_2(\theta,\theta_{l_2})h_4(\theta) + \lim_{\xi\to\theta_{l_2}^-} K_2(\theta_{l_2},\xi)\sin(\theta_{l_2})\frac{\partial T}{\partial\theta}(\theta_{l_2}) \\ &- T(\theta_{l_2})\sin(\theta_{l_2})\lim_{\xi\to\theta_{l_2}^-}\lim_{\theta\to\theta_{l_2}^-}\frac{\partial K_2}{\partial\theta}(\theta,\xi) - K_2(\theta_{l_1},\theta_{l_2})\sin(\theta_{l_1})\frac{\partial T}{\partial\theta}(\theta_{l_1}) \\ &+ T(\theta_{l_1})\sin(\theta_{l_1})\lim_{\xi\to\theta_{l_2}^-}\lim_{\theta\to\theta_{l_1}^+}\frac{\partial K_1}{\partial\theta}(\theta,\xi). \end{aligned} \tag{E.23}$$

$$\begin{aligned} T(\theta_{l_2}) = &\int_{\theta_{l_2}}^{\pi} d\theta\ \sin\theta\, K_1(\theta,\theta_{l_2})h_2(\theta) - \lim_{\xi\to\theta_{l_2}^+} K_1(\theta_{l_2},\xi)\sin(\theta_{l_2})\frac{\partial T}{\partial\theta}(\theta_{l_2}) \\ &+ T(\theta_{l_2})\sin(\theta_{l_2})\lim_{\xi\to\theta_{l_2}^+}\lim_{\theta\to\theta_{l_2}^+}\frac{\partial K_1}{\partial\theta}(\theta,\xi) \end{aligned} \tag{E.24}$$

$$\begin{aligned} T(\pi) = &\int_{\theta_{l_2}}^{\pi} d\theta\ \sin\theta\, K_1(\theta,\pi)h_2(\theta) - K_1(\theta_{l_2},\pi)\sin(\theta_{l_2})\frac{\partial T}{\partial\theta}(\theta_{l_2}) \\ &+ T(\theta_{l_2})\sin(\theta_{l_2})\lim_{\xi\to\pi^-}\lim_{\theta\to\theta_{l_2}^+}\frac{\partial K_1}{\partial\theta}(\theta,\xi). \end{aligned} \tag{E.25}$$

E.2 The case of one ice edge

For the case of one ice edge, the ice edge may be either on the northern ocean or on the continent. Let us first consider the scenario where the ice edge is on the northern ocean. For this scenario we have four relevant regions,

$$\theta \in (0, \theta_{c_1}), \tag{I}$$

$$\theta \in (\theta_{c_1}, \theta_{l_1}), \tag{II}$$

$$\theta \in (\theta_{l_1}, \theta_{l_2}), \tag{III}$$

$$\theta \in (\theta_{l_2}, \pi). \tag{IV}$$

The governing equations in the four regions are;

$$\mathcal{L}_1 T = h_2$$

in region I,

$$\mathcal{L}_1 T = h_1$$

in region II,

$$\mathcal{L}_2 T = h_4$$

in region III and

$$\mathcal{L}_1 T = h_1$$

in region IV. We have seen the following procedure repeatedly throughout this thesis, hence details are omitted and we present instead the most important equations that will eventually lead us to a solution. Applying the general integral relations (E.6) and (E.7) in the respective regions we get

$$\begin{aligned} T(\xi) = &\int_0^{\theta_{c_1}} d\theta \ \sin\theta \, K_1(\theta,\xi) h_2(\theta) + K_1(\theta_{c_1},\xi)\sin(\theta_{c_1})\frac{\partial T}{\partial \theta}(\theta_{c_1}) \\ &+ \sin(\theta_{c_1}) \lim_{\theta \to \theta_{c_1}^-} \frac{\partial K_1}{\partial \theta}(\theta,\xi) \end{aligned} \tag{E.26}$$

in region I,

$$\begin{aligned} T(\xi) = &\int_{\theta_{c_1}}^{\theta_{l_1}} d\theta \ \sin\theta \, K_1(\theta,\xi) h_1(\theta) + K_1(\theta_{l_1},\xi)\sin(\theta_{l_1})\frac{\partial T}{\partial \theta}(\theta_{l_1}) \\ &- T(\theta_{l_1})\sin(\theta_{l_1}) \lim_{\theta \to \theta_{l_1}^-} \frac{\partial K_1}{\partial \theta}(\theta,\xi) - K_1(\theta_{c_1},\xi)\sin(\theta_{c_1})\frac{\partial T}{\partial \theta}(\theta_{c_1}) \\ &- \sin(\theta_{c_1}) \lim_{\theta \to \theta_{c_1}^+} \frac{\partial K_1}{\partial \theta}(\theta,\xi) \end{aligned} \tag{E.27}$$

in region II,

$$\begin{aligned} T(\xi) = &\int_{\theta_{l_1}}^{\theta_{l_2}} d\theta \ \sin\theta \, K_2(\theta,\xi) h_3(\theta) + K_2(\theta_{l_2},\xi)\sin(\theta_{l_2})\frac{\partial T}{\partial\theta}(\theta_{l_2}) \\ &- T(\theta_{l_2})\sin(\theta_{l_2}) \lim_{\theta\to\theta_{l_2}^-} \frac{\partial K_2}{\partial\theta}(\theta,\xi) - K_2(\theta_{l_1},\xi)\sin(\theta_{l_1})\frac{\partial T}{\partial\theta}(\theta_{l_1}) \\ &+ T(\theta_{l_1})\sin(\theta_{l_1}) \lim_{\theta\to\theta_{l_1}^+} \frac{\partial K_1}{\partial\theta}(\theta,\xi) \end{aligned} \tag{E.28}$$

in region III and

$$\begin{aligned} T(\xi) = &\int_{\theta_{l_2}}^{\pi} d\theta \ \sin\theta \, K_1(\theta,\xi) h_1(\theta) - K_1(\theta_{l_2},\xi)\sin(\theta_{l_2})\frac{\partial T}{\partial\theta}(\theta_{l_2}) \\ &+ T(\theta_{l_2})\sin(\theta_{l_2}) \lim_{\theta\to\theta_{l_2}^+} \frac{\partial K_1}{\partial\theta}(\theta,\xi) \end{aligned} \tag{E.29}$$

in region IV. Here we have applied the demand that $T(\theta_{c_1}) = -1$, as well as the boundary conditions and the aforementioned properties of the Green's functions. Equation (E.26)-(E.29) relates values of the solution inside the four regions to certain unknown boundary values. These boundary values may once again be obtained through boundary integral equations. We derive the boundary integral equations by letting ξ approach the boundaries of the-sub domains I-IV, and the resulting boundary integral equations are;

$$\begin{aligned} T(0) = &\int_0^{\theta_{c_1}} d\theta \ \sin\theta \, K_1(\theta,0) h_2(\theta) + K_1(\theta_{c_1},0)\sin(\theta_{c_1})\frac{\partial T}{\partial\theta}(\theta_{c_1}) \\ &+ \sin(\theta_{c_1}) \lim_{\xi\to 0^+} \lim_{\theta\to\theta_{c_1}^-} \frac{\partial K_1}{\partial\theta}(\theta,\xi) \end{aligned} \tag{E.30}$$

$$\begin{aligned} -1 = &\int_0^{\theta_{c_1}} d\theta \ \sin\theta \, K_1(\theta,\theta_{c_1}) h_2(\theta) + \lim_{\xi\to\theta_{c_1}^-} K_1(\theta_{c_1},\xi)\sin(\theta_{c_1})\frac{\partial T}{\partial\theta}(\theta_{c_1}) \\ &+ \sin(\theta_{c_1}) \lim_{\xi\to\theta_{c_1}^-} \lim_{\theta\to\theta_{c_1}^-} \frac{\partial K_1}{\partial\theta}(\theta,\xi) \end{aligned} \tag{E.31}$$

$$\begin{aligned} -1 = &\int_{\theta_{c_1}}^{\theta_{l_1}} d\theta \ \sin\theta \, K_1(\theta,\theta_{c_1}) h_1(\theta) + K_1(\theta_{l_1},\theta_{c_1})\sin(\theta_{l_1})\frac{\partial T}{\partial\theta}(\theta_{l_1}) \\ &- T(\theta_{l_1})\sin(\theta_{l_1}) \lim_{\xi\to\theta_{c_1}^+} \lim_{\theta\to\theta_{l_1}^-} \frac{\partial K_1}{\partial\theta}(\theta,\xi) - \lim_{\xi\to\theta_{c_1}^+} K_1(\theta_{c_1},\xi)\sin(\theta_{c_1})\frac{\partial T}{\partial\theta}(\theta_{c_1}) \\ &- \sin(\theta_{c_1}) \lim_{\xi\to\theta_{c_1}^+} \lim_{\theta\to\theta_{c_1}^+} \frac{\partial K_1}{\partial\theta}(\theta,\xi) \end{aligned} \tag{E.32}$$

$$
\begin{aligned}
T(\theta_{l_1}) = &\int_{\theta_{c_1}}^{\theta_{l_1}} d\theta\ \sin\theta\, K_1(\theta,\theta_{l_1})h_1(\theta) + \lim_{\xi\to\theta_{l_1}^-} K_1(\theta_{l_1},\xi)\sin(\theta_{l_1})\frac{\partial T}{\partial\theta}(\theta_{l_1}) \\
&- T(\theta_{l_1})\sin(\theta_{l_1}) \lim_{\xi\to\theta_{l_1}^-}\lim_{\theta\to\theta_{l_1}^-} \frac{\partial K_1}{\partial\theta}(\theta,\xi) - K_1(\theta_{c_1},\theta_{l_1})\sin(\theta_{c_1})\frac{\partial T}{\partial\theta}(\theta_{c_1}) \\
&- \sin(\theta_{c_1}) \lim_{\xi\to\theta_{l_1}^-}\lim_{\theta\to\theta_{c_1}^+} \frac{\partial K_1}{\partial\theta}(\theta,\xi)
\end{aligned} \tag{E.33}
$$

$$
\begin{aligned}
T(\theta_{l_1}) = &\int_{\theta_{l_1}}^{\theta_{l_2}} d\theta\ \sin\theta\, K_2(\theta,\theta_{l_1})h_4(\theta) + K_2(\theta_{l_2},\theta_{l_1})\sin(\theta_{l_2})\frac{\partial T}{\partial\theta}(\theta_{l_2}) \\
&- T(\theta_{l_2})\sin(\theta_{l_2}) \lim_{\xi\to\theta_{l_1}^+}\lim_{\theta\to\theta_{l_2}^-} \frac{\partial K_2}{\partial\theta}(\theta,\xi) - \lim_{\xi\to\theta_{l_1}^+} K_2(\theta_{l_1},\xi)\sin(\theta_{l_1})\frac{\partial T}{\partial\theta}(\theta_{l_1}) \\
&+ T(\theta_{l_1})\sin(\theta_{l_1}) \lim_{\xi\to\theta_{l_1}^+}\lim_{\theta\to\theta_{l_1}^+} \frac{\partial K_1}{\partial\theta}(\theta,\xi)
\end{aligned} \tag{E.34}
$$

$$
\begin{aligned}
T(\theta_{l_2}) = &\int_{\theta_{l_1}}^{\theta_{l_2}} d\theta\ \sin\theta\, K_2(\theta,\theta_{l_2})h_4(\theta) + \lim_{\xi\to\theta_{l_2}^-} K_2(\theta_{l_2},\xi)\sin(\theta_{l_2})\frac{\partial T}{\partial\theta}(\theta_{l_2}) \\
&- T(\theta_{l_2})\sin(\theta_{l_2}) \lim_{\xi\to\theta_{l_2}^-}\lim_{\theta\to\theta_{l_2}^-} \frac{\partial K_2}{\partial\theta}(\theta,\xi) - K_2(\theta_{l_1},\theta_{l_2})\sin(\theta_{l_1})\frac{\partial T}{\partial\theta}(\theta_{l_1}) \\
&+ T(\theta_{l_1})\sin(\theta_{l_1}) \lim_{\xi\to\theta_{l_2}^-}\lim_{\theta\to\theta_{l_1}^+} \frac{\partial K_1}{\partial\theta}(\theta,\xi).
\end{aligned} \tag{E.35}
$$

$$
\begin{aligned}
T(\theta_{l_2}) = &\int_{\theta_{l_2}}^{\pi} d\theta\ \sin\theta\, K_1(\theta,\theta_{l_2})h_2(\theta) - \lim_{\xi\to\theta_{l_2}^+} K_1(\theta_{l_2},\xi)\sin(\theta_{l_2})\frac{\partial T}{\partial\theta}(\theta_{l_2}) \\
&+ T(\theta_{l_2})\sin(\theta_{l_2}) \lim_{\xi\to\theta_{l_2}^+}\lim_{\theta\to\theta_{l_2}^+} \frac{\partial K_1}{\partial\theta}(\theta,\xi)
\end{aligned} \tag{E.36}
$$

$$
\begin{aligned}
T(\pi) = &\int_{\theta_{l_2}}^{\pi} d\theta\ \sin\theta\, K_1(\theta,\pi)h_2(\theta) - K_1(\theta_{l_2},\pi)\sin(\theta_{l_2})\frac{\partial T}{\partial\theta}(\theta_{l_2}) \\
&+ T(\theta_{l_2})\sin(\theta_{l_2}) \lim_{\xi\to\pi^-}\lim_{\theta\to\theta_{l_2}^+} \frac{\partial K_1}{\partial\theta}(\theta,\xi).
\end{aligned} \tag{E.37}
$$

The boundary integral equations (E.30)-(E.37) is a system of 8 equations for the 8 unknown boundary values $T(0)$, θ_{c_1}, $\frac{\partial T}{\partial\theta}(\theta_{c_1})$, $\frac{\partial T}{\partial\theta}(\theta_{l_1})$, $\frac{\partial T}{\partial\theta}(\theta_{l_2})$ and $T(\pi)$. To solve this system we algebraically combine equation (E.30)-(E.37) to create a function,

$$f_1 = f_1(\theta_{c_1}).$$

We wish to find the root of this function using Newton's iteration. The functions f_1 is, however, extremely complicated, and we therefore evaluate it on a grid to create an interpolation function. We then use this interpolation function in a Newton's iteration to obtain the approximate root θ_{c_1}. Once θ_{c_1} is known, it is trivial to find the remaining boundary values $T(0)$, $\frac{\partial T}{\partial\theta}(\theta_{c_1})$, $\frac{\partial T}{\partial\theta}(\theta_{l_1})$, $\frac{\partial T}{\partial\theta}(\theta_{l_2})$ and $T(\pi)$. The solution in the interior of region I-IV is given by the integral relations (E.26)-(E.29), respectively. The solution is naturally $T(0)$ and $T(\pi)$ at the poles and $T(\theta_{c_1}) = -1$, $T(\theta_{l_1})$ and $T(\theta_{l_2})$ at the boundaries between the regions.

We follow the same procedure for the scenario in which the ice edge is at the continent, changing the function h_j in the relevant regions. We get the following boundary integral relations;

$$\begin{aligned} T(\xi) = &\int_0^{\theta_{l_1}} d\theta \ \sin\theta \, K_1(\theta,\xi) h_2(\theta) + K_1(\theta_{l_1},\xi)\sin(\theta_{l_1})\frac{\partial T}{\partial\theta}(\theta_{l_1}) \\ &- T(\theta_{l_1})\sin(\theta_{l_1}) \lim_{\theta\to\theta_{l_1}^-} \frac{\partial K_1}{\partial\theta}(\theta,\xi) \end{aligned} \tag{E.38}$$

in region I,

$$\begin{aligned} T(\xi) = &\int_{\theta_{l_1}}^{\theta_{c_1}} d\theta \ \sin\theta \, K_2(\theta,\xi) h_4(\theta) + K_2(\theta_{c_1},\xi)\sin(\theta_{c_1})\frac{\partial T}{\partial\theta}(\theta_{c_1}) \\ &+ T_c \sin(\theta_{c_1}) \lim_{\theta\to\theta_{c_1}^-} \frac{\partial K_2}{\partial\theta}(\theta,\xi) - K_2(\theta_{l_1},\xi)\sin(\theta_{l_1})\frac{\partial T}{\partial\theta}(\theta_{l_1}) \\ &+ T(\theta_{l_1})\sin(\theta_{l_1}) \lim_{\theta\to\theta_{l_1}^+} \frac{\partial K_2}{\partial\theta}(\theta,\xi) \end{aligned} \tag{E.39}$$

in region II,

$$\begin{aligned} T(\xi) = &\int_{\theta_{c_1}}^{\theta_{l_2}} d\theta \ \sin\theta \, K_2(\theta,\xi) h_3(\theta) + K_2(\theta_{l_2},\xi)\sin(\theta_{l_2})\frac{\partial T}{\partial\theta}(\theta_{l_2}) \\ &- T(\theta_{l_2})\sin(\theta_{l_2}) \lim_{\theta\to\theta_{l_2}^-} \frac{\partial K_2}{\partial\theta}(\theta,\xi) - K_2(\theta_{c_1},\xi)\sin(\theta_{c_1})\frac{\partial T}{\partial\theta}(\theta_{c_1}) \\ &- T_c \sin(\theta_{c_1}) \lim_{\theta\to\theta_{c_1}^+} \frac{\partial K_2}{\partial\theta}(\theta,\xi) \end{aligned} \tag{E.40}$$

in region III and

$$\begin{aligned} T(\xi) = &\int_{\theta_{l_2}}^{\pi} d\theta \ \sin\theta \, K_1(\theta,\xi) h_1(\theta) - K_1(\theta_{l_2},\xi)\sin(\theta_{l_2})\frac{\partial T}{\partial\theta}(\theta_{l_2}) \\ &+ T(\theta_{l_2})\sin(\theta_{l_2}) \lim_{\theta\to\theta_{l_2}^+} \frac{\partial K_1}{\partial\theta}(\theta,\xi) \end{aligned} \tag{E.41}$$

in region IV. In (E.39) and (E.40) we have applied the demand that the non-dimensional critical temperature on the continent is $T(\theta_{c_1}) = -T_c$. The associated boundary integral equations are;

$$\begin{aligned} T(0) = &\int_0^{\theta_{l_1}} d\theta \ \sin\theta \, K_1(\theta,0) h_2(\theta) + K_1(\theta_{l_1},0)\sin(\theta_{l_1})\frac{\partial T}{\partial\theta}(\theta_{l_1}) \\ &- T(\theta_{l_1})\sin(\theta_{l_1}) \lim_{\xi\to 0^+} \lim_{\theta\to\theta_{l_1}^-} \frac{\partial K_1}{\partial\theta}(\theta,\xi), \end{aligned} \tag{E.42}$$

$$T(\theta_{l_1}) = \int_0^{\theta_{l_1}} d\theta\ \sin\theta\, K_1(\theta,\theta_{l_1})h_2(\theta) + \lim_{\xi\to\theta_{l_1}^-} K_1(\theta_{l_1},\xi)\sin(\theta_{l_1})\frac{\partial T}{\partial\theta}(\theta_{l_1}) - T(\theta_{l_1})\sin(\theta_{l_1})\lim_{\xi\to\theta_{l_1}^-}\lim_{\theta\to\theta_{l_1}^-}\frac{\partial K_1}{\partial\theta}(\theta,\xi), \tag{E.43}$$

$$T(\theta_{l_1}) = \int_{\theta_{l_1}}^{\theta_{c_1}} d\theta\ \sin\theta\, K_2(\theta,\theta_{l_1})h_4(\theta) + K_2(\theta_{c_1},\theta_{l_1})\sin(\theta_{c_1})\frac{\partial T}{\partial\theta}(\theta_{c_1}) + T_c\sin(\theta_{c_1})\lim_{\xi\to\theta_{l_1}^+}\lim_{\theta\to\theta_{l_2}^-}\frac{\partial K_2}{\partial\theta}(\theta,\xi) - \lim_{\xi\to\theta_{l_1}^+} K_2(\theta_{l_1},\xi)\sin(\theta_{l_1})\frac{\partial T}{\partial\theta}(\theta_{l_1}) + T(\theta_{l_1})\sin(\theta_{l_1})\lim_{\xi\to\theta_{l_1}^+}\lim_{\theta\to\theta_{l_1}^+}\frac{\partial K_2}{\partial\theta}(\theta,\xi), \tag{E.44}$$

$$-T_c = \int_{\theta_{l_1}}^{\theta_{c_1}} d\theta\ \sin\theta\, K_2(\theta,\theta_{c_1})h_4(\theta) + \lim_{\xi\to\theta_{c_1}^-} K_2(\theta_{c_1},\xi)\sin(\theta_{c_1})\frac{\partial T}{\partial\theta}(\theta_{c_1}) + T_c\sin(\theta_{c_1})\lim_{\xi\to\theta_{c_1}^-}\lim_{\theta\to\theta_{c_1}^-}\frac{\partial K_2}{\partial\theta}(\theta,\xi) - K_2(\theta_{l_1},\theta_{c_1})\sin(\theta_{l_1})\frac{\partial T}{\partial\theta}(\theta_{l_1}) + T(\theta_{l_1})\sin(\theta_{l_1})\lim_{\xi\to\theta_{c_1}^-}\lim_{\theta\to\theta_{l_1}^+}\frac{\partial K_2}{\partial\theta}(\theta,\xi), \tag{E.45}$$

$$-T_c = \int_{\theta_{c_1}}^{\theta_{l_2}} d\theta\ \sin\theta\, K_2(\theta,\theta_{c_1})h_3(\theta) + K_2(\theta_{l_2},\theta_{c_1})\sin(\theta_{l_2})\frac{\partial T}{\partial\theta}(\theta_{l_2}) - T(\theta_{l_2})\sin(\theta_{l_2})\lim_{\xi\to\theta_{c_1}^+}\lim_{\theta\to\theta_{l_2}^-}\frac{\partial K_2}{\partial\theta}(\theta,\xi) - \lim_{\xi\to\theta_{c_1}^+} K_2(\theta_{c_1},\xi)\sin(\theta_{c_1})\frac{\partial T}{\partial\theta}(\theta_{c_1}) - T_c\sin(\theta_{c_1})\lim_{\xi\to\theta_{c_1}^+}\lim_{\theta\to\theta_{c_1}^+}\frac{\partial K_2}{\partial\theta}(\theta,\xi), \tag{E.46}$$

$$T(\theta_{l_2}) = \int_{\theta_{c_1}}^{\theta_{l_2}} d\theta\ \sin\theta\, K_2(\theta,\theta_{l_2})h_3(\theta) + \lim_{\xi\to\theta_{l_2}^-} K_2(\theta_{l_2},\xi)\sin(\theta_{l_2})\frac{\partial T}{\partial\theta}(\theta_{l_2}) - T(\theta_{l_2})\sin(\theta_{l_2})\lim_{\xi\to\theta_{l_2}^-}\lim_{\theta\to\theta_{l_2}^-}\frac{\partial K_2}{\partial\theta}(\theta,\xi) - K_2(\theta_{c_1},\theta_{l_2})\sin(\theta_{c_1})\frac{\partial T}{\partial\theta}(\theta_{c_1}) - T_c\sin(\theta_{c_1})\lim_{\xi\to\theta_{l_2}^-}\lim_{\theta\to\theta_{c_1}^+}\frac{\partial K_2}{\partial\theta}(\theta,\xi), \tag{E.47}$$

$$T(\theta_{l_2}) = \int_{\theta_{l_2}}^{\pi} d\theta\ \sin\theta\, K_1(\theta,\theta_{l_2})h_2(\theta) - \lim_{\xi\to\theta_{l_2}^+} K_1(\theta_{l_2},\xi)\sin(\theta_{l_2})\frac{\partial T}{\partial\theta}(\theta_{l_2}) + T(\theta_{l_2})\sin(\theta_{l_2})\lim_{\xi\to\theta_{l_2}^+}\lim_{\theta\to\theta_{l_2}^+}\frac{\partial K_1}{\partial\theta}(\theta,\xi), \tag{E.48}$$

$$T(\pi) = \int_{\theta_{l_2}}^{\pi} d\theta\ \sin\theta\, K_1(\theta,\pi)h_2(\theta) - K_1(\theta_{l_2},\pi)\sin(\theta_{l_2})\frac{\partial T}{\partial\theta}(\theta_{l_2}) + T(\theta_{l_2})\sin(\theta_{l_2})\lim_{\xi\to\pi^-}\lim_{\theta\to\theta_{l_2}^+}\frac{\partial K_1}{\partial\theta}(\theta,\xi). \tag{E.49}$$

The boundary integral equations (E.42)-(E.49) is a system of 8 equations for the 8 unknown boundary values $T(0)$, θ_{c_1}, $\frac{\partial T}{\partial\theta}(\theta_{c_1})$, $\frac{\partial T}{\partial\theta}(\theta_{l_1})$, $\frac{\partial T}{\partial\theta}(\theta_{l_2})$ and $T(\pi)$. We solve this system using the

exact same procure outline above for the one ice edge on the northern ocean.

For the one ice edge scenario from section 3.3.2 where the northern ocean and the continent is covered by ice/snow we know that

$$\theta_{c_1} = \theta_{l_2}.$$

Therefore, we do not have to locate this ice edge through solving the boundary integral equations and can use the procedure outline for the case with no ice edges and a complete ice/snow cover. Consequently, the boundary integral relations will be (E.17)-(E.19), but interchanging $h_2 \to h_1$ in (E.19) since the southern ocean will be ice-free. Similarly, the boundary integral equations will be (E.20)-(E.25), but interchanging $h_2 \to h_1$ in (E.24) and (E.25).

E.3 The case of two ice edges

For the case of two ice edges we will have five relevant regions,

$$\theta \in (0, \theta_{c_1}), \tag{I}$$

$$\theta \in (\theta_{c_1}, \theta_{l_1}), \tag{II}$$

$$\theta \in (\theta_{l_1}, \theta_{l_2}), \tag{III}$$

$$\theta \in (\theta_{l_2}, \theta_{c_2}), \tag{IV}$$

$$\theta \in (\theta_{c_2}, \pi). \tag{V}$$

The governing equations in the five regions are

$$\mathcal{L}_1 T = h_2$$

in region I,

$$\mathcal{L}_1 T = h_1$$

in region II,

$$\mathcal{L}_2 T = h_3$$

in region III,

$$\mathcal{L}_1 T = h_1$$

in region IV and

$$\mathcal{L}_1 T = h_2$$

in region V. Applying the general integral relations (E.6) and (E.7) in the respective regions we get

$$\begin{aligned} T(\xi) = &\int_0^{\theta_{c_1}} d\theta \ \sin\theta \, K_1(\theta,\xi) h_2(\theta) + K_1(\theta_{c_1},\xi)\sin(\theta_{c_1})\frac{\partial T}{\partial\theta}(\theta_{c_1}) \\ &+ \sin(\theta_{c_1}) \lim_{\theta\to\theta_{c_1}^-} \frac{\partial K_1}{\partial\theta}(\theta,\xi) \end{aligned} \tag{E.50}$$

in region I,

$$\begin{aligned} T(\xi) = &\int_{\theta_{c_1}}^{\theta_{l_1}} d\theta \ \sin\theta \, K_1(\theta,\xi) h_1(\theta) + K_1(\theta_{l_1},\xi)\sin(\theta_{l_1})\frac{\partial T}{\partial\theta}(\theta_{l_1}) \\ &- T(\theta_{l_1})\sin(\theta_{l_1}) \lim_{\theta\to\theta_{l_1}^-} \frac{\partial K_1}{\partial\theta}(\theta,\xi) - K_1(\theta_{c_1},\xi)\sin(\theta_{c_1})\frac{\partial T}{\partial\theta}(\theta_{c_1}) \\ &- \sin(\theta_{c_1}) \lim_{\theta\to\theta_{c_1}^+} \frac{\partial K_1}{\partial\theta}(\theta,\xi) \end{aligned} \tag{E.51}$$

in region II,

$$\begin{aligned} T(\xi) = &\int_{\theta_{l_1}}^{\theta_{l_2}} d\theta \ \sin\theta \, K_2(\theta,\xi) h_3(\theta) + K_2(\theta_{l_2},\xi)\sin(\theta_{l_2})\frac{\partial T}{\partial\theta}(\theta_{l_2}) \\ &- T(\theta_{l_2})\sin(\theta_{l_2}) \lim_{\theta\to\theta_{l_2}^-} \frac{\partial K_2}{\partial\theta}(\theta,\xi) - K_2(\theta_{l_1},\xi)\sin(\theta_{l_1})\frac{\partial T}{\partial\theta}(\theta_{l_1}) \\ &+ T(\theta_{l_1})\sin(\theta_{l_1}) \lim_{\theta\to\theta_{l_1}^+} \frac{\partial K_1}{\partial\theta}(\theta,\xi) \end{aligned} \tag{E.52}$$

in region III,

$$\begin{aligned} T(\xi) = &\int_{\theta_{l_2}}^{\theta_{c_2}} d\theta \ \sin\theta \, K_1(\theta,\xi) h_1(\theta) + K_1(\theta_{c_2},\xi)\sin(\theta_{c_2})\frac{\partial T}{\partial\theta}(\theta_{c_2}) \\ &+ \sin(\theta_{c_2}) \lim_{\theta\to\theta_{c_2}^-} \frac{\partial K_1}{\partial\theta}(\theta,\xi) - K_1(\theta_{l_2},\xi)\sin(\theta_{l_1})\frac{\partial T}{\partial\theta}(\theta_{l_2}) \\ &+ T(\theta_{l_2})\sin(\theta_{l_2}) \lim_{\theta\to\theta_{l_2}^+} \frac{\partial K_1}{\partial\theta}(\theta,\xi) \end{aligned} \tag{E.53}$$

in region IV and

$$\begin{aligned} T(\xi) = &\int_{\theta_{c_2}}^{\pi} d\theta \ \sin\theta \, K_1(\theta,\xi) h_2(\theta) - K_1(\theta_{c_2},\xi)\sin(\theta_{c_2})\frac{\partial T}{\partial\theta}(\theta_{c_2}) \\ &- \sin(\theta_{c_2}) \lim_{\theta\to\theta_{c_2}^+} \frac{\partial K_1}{\partial\theta}(\theta,\xi). \end{aligned} \tag{E.54}$$

in region V. Equation (E.50)-(E.54) relates values of the solution inside the five regions to certain unknown boundary values. These boundary values are, once again, found through solving the associated boundary integral equations. We derive the boundary integral equations by letting ξ approach the boundaries of the-sub domains I-V, and the resulting boundary integral equations are;

$$\begin{aligned} T(0) = &\int_0^{\theta_{c_1}} d\theta\ \sin\theta\, K_1(\theta,0)h_2(\theta) + K_1(\theta_{c_1},0)\sin(\theta_{c_1})\frac{\partial T}{\partial\theta}(\theta_{c_1}) \\ &+ \sin(\theta_{c_1}) \lim_{\xi\to 0^+}\lim_{\theta\to\theta_{c_1}^-}\frac{\partial K_1}{\partial\theta}(\theta,\xi) \end{aligned} \tag{E.55}$$

$$\begin{aligned} -1 = &\int_0^{\theta_{c_1}} d\theta\ \sin\theta\, K_1(\theta,\theta_{c_1})h_2(\theta) + \lim_{\xi\to\theta_{c_1}^-} K_1(\theta_{c_1},\xi)\sin(\theta_{c_1})\frac{\partial T}{\partial\theta}(\theta_{c_1}) \\ &+ \sin(\theta_{c_1}) \lim_{\xi\to\theta_{c_1}^-}\lim_{\theta\to\theta_{c_1}^-}\frac{\partial K_1}{\partial\theta}(\theta,\xi) \end{aligned} \tag{E.56}$$

$$\begin{aligned} -1 = &\int_{\theta_{c_1}}^{\theta_{l_1}} d\theta\ \sin\theta\, K_1(\theta,\theta_{c_1})h_1(\theta) + K_1(\theta_{l_1},\theta_{c_1})\sin(\theta_{l_1})\frac{\partial T}{\partial\theta}(\theta_{l_1}) \\ &- T(\theta_{l_1})\sin(\theta_{l_1}) \lim_{\xi\to\theta_{c_1}^+}\lim_{\theta\to\theta_{l_1}^-}\frac{\partial K_1}{\partial\theta}(\theta,\xi) - \lim_{\xi\to\theta_{c_1}^+} K_1(\theta_{c_1},\xi)\sin(\theta_{c_1})\frac{\partial T}{\partial\theta}(\theta_{c_1}) \\ &- \sin(\theta_{c_1}) \lim_{\xi\to\theta_{c_1}^+}\lim_{\theta\to\theta_{c_1}^+}\frac{\partial K_1}{\partial\theta}(\theta,\xi) \end{aligned} \tag{E.57}$$

$$\begin{aligned} T(\theta_{l_1}) = &\int_{\theta_{c_1}}^{\theta_{l_1}} d\theta\ \sin\theta\, K_1(\theta,\theta_{l_1})h_1(\theta) + \lim_{\xi\to\theta_{l_1}^-} K_1(\theta_{l_1},\xi)\sin(\theta_{l_1})\frac{\partial T}{\partial\theta}(\theta_{l_1}) \\ &- T(\theta_{l_1})\sin(\theta_{l_1}) \lim_{\xi\to\theta_{l_1}^-}\lim_{\theta\to\theta_{l_1}^-}\frac{\partial K_1}{\partial\theta}(\theta,\xi) - K_1(\theta_{c_1},\theta_{l_1})\sin(\theta_{c_1})\frac{\partial T}{\partial\theta}(\theta_{c_1}) \\ &- \sin(\theta_{c_1}) \lim_{\xi\to\theta_{l_1}^-}\lim_{\theta\to\theta_{c_1}^+}\frac{\partial K_1}{\partial\theta}(\theta,\xi) \end{aligned} \tag{E.58}$$

$$\begin{aligned} T(\theta_{l_1}) = &\int_{\theta_{l_1}}^{\theta_{l_2}} d\theta\ \sin\theta\, K_2(\theta,\theta_{l_1})h_3(\theta) + K_2(\theta_{l_2},\theta_{l_1})\sin(\theta_{l_2})\frac{\partial T}{\partial\theta}(\theta_{l_2}) \\ &- T(\theta_{l_2})\sin(\theta_{l_2}) \lim_{\xi\to\theta_{l_1}^+}\lim_{\theta\to\theta_{l_2}^-}\frac{\partial K_2}{\partial\theta}(\theta,\xi) - \lim_{\xi\to\theta_{l_1}^+} K_2(\theta_{l_1},\xi)\sin(\theta_{l_1})\frac{\partial T}{\partial\theta}(\theta_{l_1}) \\ &+ T(\theta_{l_1})\sin(\theta_{l_1}) \lim_{\xi\to\theta_{l_1}^+}\lim_{\theta\to\theta_{l_1}^+}\frac{\partial K_1}{\partial\theta}(\theta,\xi) \end{aligned} \tag{E.59}$$

$$
\begin{aligned}
T(\theta_{l_2}) = &\int_{\theta_{l_1}}^{\theta_{l_2}} d\theta\ \sin\theta\, K_2(\theta,\theta_{l_2})h_3(\theta) + \lim_{\xi\to\theta_{l_2}^-} K_2(\theta_{l_2},\xi)\sin(\theta_{l_2})\frac{\partial T}{\partial\theta}(\theta_{l_2}) \\
&- T(\theta_{l_2})\sin(\theta_{l_2}) \lim_{\xi\to\theta_{l_2}^-}\lim_{\theta\to\theta_{l_2}^-} \frac{\partial K_2}{\partial\theta}(\theta,\xi) - K_2(\theta_{l_1},\theta_{l_2})\sin(\theta_{l_1})\frac{\partial T}{\partial\theta}(\theta_{l_1}) \\
&+ T(\theta_{l_1})\sin(\theta_{l_1}) \lim_{\xi\to\theta_{l_2}^-}\lim_{\theta\to\theta_{l_1}^+} \frac{\partial K_1}{\partial\theta}(\theta,\xi)
\end{aligned} \tag{E.60}
$$

$$
\begin{aligned}
T(\theta_{l_2}) = &\int_{\theta_{l_2}}^{\theta_{c_2}} d\theta\ \sin\theta\, K_1(\theta,\theta_{l_2})h_1(\theta) + K_1(\theta_{c_2},\theta_{l_2})\sin(\theta_{c_2})\frac{\partial T}{\partial\theta}(\theta_{c_2}) \\
&+ \sin(\theta_{c_2}) \lim_{\xi\to\theta_{l_2}^+}\lim_{\theta\to\theta_{c_2}^-} \frac{\partial K_1}{\partial\theta}(\theta,\xi) - \lim_{\xi\to\theta_{l_2}^+} K_1(\theta_{l_2},\xi)\sin(\theta_{l_1})\frac{\partial T}{\partial\theta}(\theta_{l_2}) \\
&+ T(\theta_{l_2})\sin(\theta_{l_2}) \lim_{\xi\to\theta_{l_2}^+}\lim_{\theta\to\theta_{l_2}^+} \frac{\partial K_1}{\partial\theta}(\theta,\xi)
\end{aligned} \tag{E.61}
$$

$$
\begin{aligned}
-1 = &\int_{\theta_{l_2}}^{\theta_{c_2}} d\theta\ \sin\theta\, K_1(\theta,\theta_{c_2})h_1(\theta) + \lim_{\xi\to\theta_{c_2}^-} K_1(\theta_{c_2},\xi)\sin(\theta_{c_2})\frac{\partial T}{\partial\theta}(\theta_{c_2}) \\
&+ \sin(\theta_{c_2}) \lim_{\xi\to\theta_{c_2}^-}\lim_{\theta\to\theta_{c_2}^-} \frac{\partial K_1}{\partial\theta}(\theta,\xi) - K_1(\theta_{l_2},\theta_{c_2})\sin(\theta_{l_1})\frac{\partial T}{\partial\theta}(\theta_{l_2}) \\
&+ T(\theta_{l_2})\sin(\theta_{l_2}) \lim_{\xi\to\theta_{c_2}^-}\lim_{\theta\to\theta_{l_2}^+} \frac{\partial K_1}{\partial\theta}(\theta,\xi)
\end{aligned} \tag{E.62}
$$

$$
\begin{aligned}
-1 = &\int_{\theta_{c_2}}^{\pi} d\theta\ \sin\theta\, K_1(\theta,\theta_{c_2})h_2(\theta) - \lim_{\xi\to\theta_{c_2}^+} K_1(\theta_{c_2},\xi)\sin(\theta_{c_2})\frac{\partial T}{\partial\theta}(\theta_{c_2}) \\
&- \sin(\theta_{c_2}) \lim_{\xi\to\theta_{c_2}^+}\lim_{\theta\to\theta_{c_2}^+} \frac{\partial K_1}{\partial\theta}(\theta,\xi)
\end{aligned} \tag{E.63}
$$

$$
\begin{aligned}
T(\pi) = &\int_{\theta_{c_2}}^{\pi} d\theta\ \sin\theta\, K_1(\theta,\pi)h_2(\theta) - K_1(\theta_{c_2},\pi)\sin(\theta_{c_2})\frac{\partial T}{\partial\theta}(\theta_{c_2}) \\
&- \sin(\theta_{c_2}) \lim_{\xi\to\pi^-}\lim_{\theta\to\theta_{c_2}^+} \frac{\partial K_1}{\partial\theta}(\theta,\xi).
\end{aligned} \tag{E.64}
$$

The boundary integral equations (E.55)-(E.64) is a system of 10 equations for the 10 unknown boundary values $T(0)$, θ_{c_1}, $\frac{\partial T}{\partial\theta}(\theta_{c_1})$, $\frac{\partial T}{\partial\theta}(\theta_{l_1})$, $\frac{\partial T}{\partial\theta}(\theta_{l_2})$, θ_{c_2}, $\frac{\partial T}{\partial\theta}(\theta_{c_2})$ and $T(\pi)$. To solve this system we algebraically combine equation (E.55)-(E.64) to create two functions,

$$f_1 = f_1(\theta_{c_1},\theta_{c_2})$$

and

$$f_2 = f_2(\theta_{c_1},\theta_{c_2}).$$

We wish to find the roots of these functions using Newton's iteration to obtain θ_{c_1} and θ_{c_2}. However, the functions f_1 and f_2 are extremely complicated and involve several integrals, we will therefore evaluate them on a grid and create two interpolation functions. We then use these interpolation functions in a Newton's iteration and obtain approximate values for θ_{c_1} and θ_{c_2}. Once θ_{c_1} and

θ_{c_2} are known, it is trivial to find the remaining boundary values $T(0)$, $\frac{\partial T}{\partial \theta}(\theta_{c_1})$, $\frac{\partial T}{\partial \theta}(\theta_{l_1})$, $\frac{\partial T}{\partial \theta}(\theta_{l_2})$, $\frac{\partial T}{\partial \theta}(\theta_{c_2})$ and $T(\pi)$. The solution in the regions I-V is given by the integral relations (E.50)-(E.54), respectively.

With a continent configuration that violates the north-south symmetry we may have a scenario where there is one ice edge on the northern ocean and one ice edge on the continent. For such a scenario we must divide the domain into a different set of sub-domains,

$$\theta \in (0, \theta_{c_1}), \tag{I}$$

$$\theta \in (\theta_{c_1}, \theta_{l_1}), \tag{II}$$

$$\theta \in (\theta_{l_1}, \theta_{c_2}), \tag{III}$$

$$\theta \in (\theta_{c_2}, \theta_{l_2}), \tag{IV}$$

$$\theta \in (\theta_{l_2}, \pi). \tag{V}$$

The governing equations in the five regions are

$$\mathcal{L}_1 T = h_2$$

in region I,

$$\mathcal{L}_1 T = h_1$$

in region II,

$$\mathcal{L}_2 T = h_4$$

in region III,

$$\mathcal{L}_1 T = h_3$$

in region IV and

$$\mathcal{L}_1 T = h_1$$

in region V. Applying the general relations (E.6) and (E.7) in the respective regions we get following set of boundary integral relations;

$$\begin{aligned} T(\xi) = &\int_0^{\theta_{c_1}} d\theta \, \sin\theta \, K_1(\theta, \xi) h_2(\theta) + K_1(\theta_{c_1}, \xi) \sin(\theta_{c_1}) \frac{\partial T}{\partial \theta}(\theta_{c_1}) \\ &+ \sin(\theta_{c_1}) \lim_{\theta \to \theta_{c_1}^-} \frac{\partial K_1}{\partial \theta}(\theta, \xi), \end{aligned} \tag{E.65}$$

in region I,

$$\begin{aligned} T(\xi) = & \int_{\theta_{c_1}}^{\theta_{l_1}} d\theta \ \sin\theta \, K_1(\theta,\xi) h_1(\theta) + K_1(\theta_{l_1},\xi)\sin(\theta_{l_1})\frac{\partial T}{\partial\theta}(\theta_{l_1}) \\ & - T(\theta_{l_1})\sin(\theta_{l_1}) \lim_{\theta\to\theta_{l_1}^-} \frac{\partial K_1}{\partial\theta}(\theta,\xi) - K_1(\theta_{c_1},\xi)\sin(\theta_{c_1})\frac{\partial T}{\partial\theta}(\theta_{c_1}) \\ & - \sin(\theta_{c_1}) \lim_{\theta\to\theta_{c_1}^+} \frac{\partial K_1}{\partial\theta}(\theta,\xi), \end{aligned} \tag{E.66}$$

in region II,

$$\begin{aligned} T(\xi) = & \int_{\theta_{l_1}}^{\theta_{c_2}} d\theta \ \sin\theta \, K_2(\theta,\xi) h_4(\theta) + K_2(\theta_{c_2},\xi)\sin(\theta_{c_2})\frac{\partial T}{\partial\theta}(\theta_{c_2}) \\ & + T_c \sin(\theta_{c_2}) \lim_{\theta\to\theta_{c_2}^-} \frac{\partial K_2}{\partial\theta}(\theta,\xi) - K_2(\theta_{l_1},\xi)\sin(\theta_{l_1})\frac{\partial T}{\partial\theta}(\theta_{l_1}) \\ & + T(\theta_{l_1})\sin(\theta_{l_1}) \lim_{\theta\to\theta_{l_1}^+} \frac{\partial K_2}{\partial\theta}(\theta,\xi), \end{aligned} \tag{E.67}$$

in region III,

$$\begin{aligned} T(\xi) = & \int_{\theta_{c_2}}^{\theta_{l_2}} d\theta \ \sin\theta \, K_2(\theta,\xi) h_3(\theta) + K_2(\theta_{l_2},\xi)\sin(\theta_{l_2})\frac{\partial T}{\partial\theta}(\theta_{l_2}) \\ & - T(\theta_{l_2})\sin(\theta_{l_2}) \lim_{\theta\to\theta_{l_2}^-} \frac{\partial K_2}{\partial\theta}(\theta,\xi) - K_2(\theta_{c_2},\xi)\sin(\theta_{c_2})\frac{\partial T}{\partial\theta}(\theta_{c_2}) \\ & - T_c \sin(\theta_{c_2}) \lim_{\theta\to\theta_{c_2}^+} \frac{\partial K_2}{\partial\theta}(\theta,\xi) \end{aligned} \tag{E.68}$$

and

$$\begin{aligned} T(\xi) = & \int_{\theta_{l_2}}^{\pi} d\theta \ \sin\theta \, K_1(\theta,\xi) h_1(\theta) - K_1(\theta_{l_2},\xi)\sin(\theta_{l_2})\frac{\partial T}{\partial\theta}(\theta_{l_2}) \\ & + T(\theta_{l_2})\sin(\theta_{l_2}) \lim_{\theta\to\theta_{l_2}^+} \frac{\partial K_1}{\partial\theta}(\theta,\xi). \end{aligned} \tag{E.69}$$

in region IV. Equation (E.65)-(E.69) gives the solution in the interior of the five sub-domains I-V. The unknown boundary values are obtained though solving the associated boundary integral

equations;

$$T(0) = \int_0^{\theta_{c_1}} d\theta\ \sin\theta\, K_1(\theta,0)h_2(\theta) + K_1(\theta_{c_1},0)\sin(\theta_{c_1})\frac{\partial T}{\partial\theta}(\theta_{c_1}) + \sin(\theta_{c_1})\lim_{\xi\to 0^+}\lim_{\theta\to\theta_{c_1}^-}\frac{\partial K_1}{\partial\theta}(\theta,\xi), \tag{E.70}$$

$$-1 = \int_0^{\theta_{c_1}} d\theta\ \sin\theta\, K_1(\theta,\theta_{c_1})h_2(\theta) + \lim_{\xi\to\theta_{c_1}^-} K_1(\theta_{c_1},\xi)\sin(\theta_{c_1})\frac{\partial T}{\partial\theta}(\theta_{c_1}) + \sin(\theta_{c_1})\lim_{\xi\to\theta_{c_1}^-}\lim_{\theta\to\theta_{c_1}^-}\frac{\partial K_1}{\partial\theta}(\theta,\xi), \tag{E.71}$$

$$\begin{aligned}-1 = &\int_{\theta_{c_1}}^{\theta_{l_1}} d\theta\ \sin\theta\, K_1(\theta,\theta_{c_1})h_1(\theta) + K_1(\theta_{l_1},\theta_{c_1})\sin(\theta_{l_1})\frac{\partial T}{\partial\theta}(\theta_{l_1}) \\ &- T(\theta_{l_1})\sin(\theta_{l_1})\lim_{\xi\to\theta_{c_1}^+}\lim_{\theta\to\theta_{l_1}^-}\frac{\partial K_1}{\partial\theta}(\theta,\xi) - \lim_{\xi\to\theta_{c_1}^+} K_1(\theta_{c_1},\xi)\sin(\theta_{c_1})\frac{\partial T}{\partial\theta}(\theta_{c_1}) \\ &- \sin(\theta_{c_1})\lim_{\xi\to\theta_{c_1}^+}\lim_{\theta\to\theta_{c_1}^+}\frac{\partial K_1}{\partial\theta}(\theta,\xi),\end{aligned} \tag{E.72}$$

$$\begin{aligned}T(\theta_{l_1}) = &\int_{\theta_{c_1}}^{\theta_{l_1}} d\theta\ \sin\theta\, K_1(\theta,\theta_{l_1})h_1(\theta) + \lim_{\xi\to\theta_{l_1}^-} K_1(\theta_{l_1},\xi)\sin(\theta_{l_1})\frac{\partial T}{\partial\theta}(\theta_{l_1}) \\ &- T(\theta_{l_1})\sin(\theta_{l_1})\lim_{\xi\to\theta_{l_1}^-}\lim_{\theta\to\theta_{l_1}^-}\frac{\partial K_1}{\partial\theta}(\theta,\xi) - K_1(\theta_{c_1},\theta_{l_1})\sin(\theta_{c_1})\frac{\partial T}{\partial\theta}(\theta_{c_1}) \\ &- \sin(\theta_{c_1})\lim_{\xi\to\theta_{l_1}^-}\lim_{\theta\to\theta_{c_1}^+}\frac{\partial K_1}{\partial\theta}(\theta,\xi),\end{aligned} \tag{E.73}$$

$$\begin{aligned}T(\theta_{l_1}) = &\int_{\theta_{l_1}}^{\theta_{c_2}} d\theta\ \sin\theta\, K_2(\theta,\theta_{l_1})h_4(\theta) + K_2(\theta_{c_2},\theta_{l_1})\sin(\theta_{c_2})\frac{\partial T}{\partial\theta}(\theta_{c_2}) \\ &+ T_c\sin(\theta_{c_2})\lim_{\xi\to\theta_{l_1}^+}\lim_{\theta\to\theta_{l_2}^-}\frac{\partial K_2}{\partial\theta}(\theta,\xi) - \lim_{\xi\to\theta_{l_1}^+} K_2(\theta_{l_1},\xi)\sin(\theta_{l_1})\frac{\partial T}{\partial\theta}(\theta_{l_1}) \\ &+ T(\theta_{l_1})\sin(\theta_{l_1})\lim_{\xi\to\theta_{l_1}^+}\lim_{\theta\to\theta_{l_1}^+}\frac{\partial K_2}{\partial\theta}(\theta,\xi),\end{aligned} \tag{E.74}$$

$$\begin{aligned}-T_c = &\int_{\theta_{l_1}}^{\theta_{c_2}} d\theta\ \sin\theta\, K_2(\theta,\theta_{c_2})h_4(\theta) + \lim_{\xi\to\theta_{c_2}^-} K_2(\theta_{c_2},\xi)\sin(\theta_{c_2})\frac{\partial T}{\partial\theta}(\theta_{c_2}) \\ &+ T_c\sin(\theta_{c_2})\lim_{\xi\to\theta_{c_2}^-}\lim_{\theta\to\theta_{c_2}^-}\frac{\partial K_2}{\partial\theta}(\theta,\xi) - K_2(\theta_{l_1},\theta_{c_2})\sin(\theta_{l_1})\frac{\partial T}{\partial\theta}(\theta_{l_1}) \\ &+ T(\theta_{l_1})\sin(\theta_{l_1})\lim_{\xi\to\theta_{c_2}^-}\lim_{\theta\to\theta_{l_1}^+}\frac{\partial K_2}{\partial\theta}(\theta,\xi),\end{aligned} \tag{E.75}$$

$$
\begin{aligned}
-T_c = &\int_{\theta_{c_2}}^{\theta_{l_2}} d\theta\ \sin\theta\, K_2(\theta,\theta_{c_2})h_3(\theta) + K_2(\theta_{l_2},\theta_{c_2})\sin(\theta_{l_2})\frac{\partial T}{\partial\theta}(\theta_{l_2}) \\
&- T(\theta_{l_2})\sin(\theta_{l_2})\lim_{\xi\to\theta_{c_2}^+}\lim_{\theta\to\theta_{l_2}^-}\frac{\partial K_2}{\partial\theta}(\theta,\xi) - \lim_{\xi\to\theta_{c_2}^+}K_2(\theta_{c_2},\xi)\sin(\theta_{c_2})\frac{\partial T}{\partial\theta}(\theta_{c_2}) \\
&- T_c\sin(\theta_{c_2})\lim_{\xi\to\theta_{c_2}^+}\lim_{\theta\to\theta_{c_2}^+}\frac{\partial K_2}{\partial\theta}(\theta,\xi),
\end{aligned}
\tag{E.76}
$$

$$
\begin{aligned}
T(\theta_{l_2}) = &\int_{\theta_{c_2}}^{\theta_{l_2}} d\theta\ \sin\theta\, K_2(\theta,\theta_{l_2})h_3(\theta) + \lim_{\xi\to\theta_{l_2}^-}K_2(\theta_{l_2},\xi)\sin(\theta_{l_2})\frac{\partial T}{\partial\theta}(\theta_{l_2}) \\
&- T(\theta_{l_2})\sin(\theta_{l_2})\lim_{\xi\to\theta_{l_2}^-}\lim_{\theta\to\theta_{l_2}^-}\frac{\partial K_2}{\partial\theta}(\theta,\xi) - K_2(\theta_{c_2},\theta_{l_2})\sin(\theta_{c_2})\frac{\partial T}{\partial\theta}(\theta_{c_2}) \\
&- T_c\sin(\theta_{c_2})\lim_{\xi\to\theta_{l_2}^-}\lim_{\theta\to\theta_{c_2}^+}\frac{\partial K_2}{\partial\theta}(\theta,\xi),
\end{aligned}
\tag{E.77}
$$

$$
\begin{aligned}
T(\theta_{l_2}) = &\int_{\theta_{l_2}}^{\pi} d\theta\ \sin\theta\, K_1(\theta,\theta_{l_2})h_1(\theta) - \lim_{\xi\to\theta_{l_2}^+}K_1(\theta_{l_2},\xi)\sin(\theta_{l_2})\frac{\partial T}{\partial\theta}(\theta_{l_2}) \\
&+ T(\theta_{l_2})\sin(\theta_{l_2})\lim_{\xi\to\theta_{l_2}^+}\lim_{\theta\to\theta_{l_2}^+}\frac{\partial K_1}{\partial\theta}(\theta,\xi)
\end{aligned}
\tag{E.78}
$$

and

$$
\begin{aligned}
T(\pi) = &\int_{\theta_{l_2}}^{\pi} d\theta\ \sin\theta\, K_1(\theta,\pi)h_1(\theta) - K_1(\theta_{l_2},\pi)\sin(\theta_{l_2})\frac{\partial T}{\partial\theta}(\theta_{l_2}) \\
&+ T(\theta_{l_2})\sin(\theta_{l_2})\lim_{\xi\to\pi^-}\lim_{\theta\to\theta_{l_2}^+}\frac{\partial K_1}{\partial\theta}(\theta,\xi).
\end{aligned}
\tag{E.79}
$$

We solve the system of boundary integral equations (E.70)-(E.79) using the same combination of analytical and numerical methods outlined above for the symmetrical two ice edges scenario.

For the scenario where there is one ice edge on the continent and one ice edge on the southern ocean, the process of finding a stationary solution will benefit from the fact that we know the location of one ice edge. This scenario will only be realized when

$$\theta_{c_1} = \theta_{l_2}.$$

Therefore, we can apply a similar procedure as we did for the one ice edge case and the boundary

integral relations will be;

$$\begin{aligned} T(\xi) = &\int_0^{\theta_{l_1}} d\theta\ \sin\theta\, K_1(\theta,\xi)h_2(\theta) + K_1(\theta_{l_1},\xi)\sin(\theta_{l_1})\frac{\partial T}{\partial\theta}(\theta_{l_1}) \\ &- T(\theta_{l_1})\sin(\theta_{l_1})\lim_{\theta\to\theta_{l_1}^-}\frac{\partial K_1}{\partial\theta}(\theta,\xi), \end{aligned} \tag{E.80}$$

$$\begin{aligned} T(\xi) = &\int_{\theta_{l_1}}^{\theta_{l_2}} d\theta\ \sin\theta\, K_2(\theta,\xi)h_4(\theta) + K_2(\theta_{l_2},\xi)\sin(\theta_{l_2})\frac{\partial T}{\partial\theta}(\theta_{l_2}) \\ &- T(\theta_{l_2})\sin(\theta_{l_2})\lim_{\theta\to\theta_{l_2}^-}\frac{\partial K_2}{\partial\theta}(\theta,\xi) - K_2(\theta_{l_1},\xi)\sin(\theta_{l_1})\frac{\partial T}{\partial\theta}(\theta_{l_1}) \\ &+ T(\theta_{l_1})\sin(\theta_{l_1})\lim_{\theta\to\theta_{l_1}^+}\frac{\partial K_1}{\partial\theta}(\theta,\xi), \end{aligned} \tag{E.81}$$

$$\begin{aligned} T(\xi) = &\int_{\theta_{l_2}}^{\theta_{c_2}} d\theta\ \sin\theta\, K_1(\theta,\xi)h_1(\theta) + K_1(\theta_{c_2},\xi)\sin(\theta_{c_2})\frac{\partial T}{\partial\theta}(\theta_{c_2}) \\ &+ \sin(\theta_{c_2})\lim_{\theta\to\theta_{c_2}^-}\frac{\partial K_1}{\partial\theta}(\theta,\xi) - K_1(\theta_{l_2},\xi)\sin(\theta_{l_1})\frac{\partial T}{\partial\theta}(\theta_{l_2}) \\ &+ T(\theta_{l_2})\sin(\theta_{l_2})\lim_{\theta\to\theta_{l_2}^+}\frac{\partial K_1}{\partial\theta}(\theta,\xi) \end{aligned} \tag{E.82}$$

and

$$\begin{aligned} T(\xi) = &\int_{\theta_{c_2}}^{\pi} d\theta\ \sin\theta\, K_1(\theta,\xi)h_2(\theta) - K_1(\theta_{c_2},\xi)\sin(\theta_{c_2})\frac{\partial T}{\partial\theta}(\theta_{c_2}) \\ &- \sin(\theta_{c_1})\lim_{\theta\to\theta_{c_1}^+}\frac{\partial K_1}{\partial\theta}(\theta,\xi). \end{aligned} \tag{E.83}$$

The associated boundary integral equations are;

$$\begin{aligned} T(0) = &\int_0^{\theta_{l_1}} d\theta\ \sin\theta\, K_1(\theta,0)h_2(\theta) + K_1(\theta_{l_1},0)\sin(\theta_{l_1})\frac{\partial T}{\partial\theta}(\theta_{l_1}) \\ &- T(\theta_{l_1})\sin(\theta_{l_1})\lim_{\xi\to 0^+}\lim_{\theta\to\theta_{l_1}^-}\frac{\partial K_1}{\partial\theta}(\theta,\xi), \end{aligned} \tag{E.84}$$

$$\begin{aligned} T(\theta_{l_1}) = &\int_0^{\theta_{l_1}} d\theta\ \sin\theta\, K_1(\theta,\theta_{l_1})h_2(\theta) + \lim_{\xi\to\theta_{l_1}^-} K_1(\theta_{l_1},\xi)\sin(\theta_{l_1})\frac{\partial T}{\partial\theta}(\theta_{l_1}) \\ &- T(\theta_{l_1})\sin(\theta_{l_1})\lim_{\xi\to\theta_{l_1}^-}\lim_{\theta\to\theta_{l_1}^-}\frac{\partial K_1}{\partial\theta}(\theta,\xi), \end{aligned} \tag{E.85}$$

$$
\begin{aligned}
T(\theta_{l_1}) = &\int_{\theta_{l_1}}^{\theta_{l_2}} d\theta\ \sin\theta\, K_2(\theta,\theta_{l_1})h_4(\theta) + K_2(\theta_{l_2},\theta_{l_1})\sin(\theta_{l_2})\frac{\partial T}{\partial\theta}(\theta_{l_2}) \\
&- T(\theta_{l_2})\sin(\theta_{l_2})\lim_{\xi\to\theta_{l_1}^+}\lim_{\theta\to\theta_{l_2}^-}\frac{\partial K_2}{\partial\theta}(\theta,\xi) - \lim_{\xi\to\theta_{l_1}^+}K_2(\theta_{l_1},\xi)\sin(\theta_{l_1})\frac{\partial T}{\partial\theta}(\theta_{l_1}) \\
&+ T(\theta_{l_1})\sin(\theta_{l_1})\lim_{\xi\to\theta_{l_1}^+}\lim_{\theta\to\theta_{l_1}^+}\frac{\partial K_1}{\partial\theta}(\theta,\xi),
\end{aligned} \tag{E.86}
$$

$$
\begin{aligned}
T(\theta_{l_2}) = &\int_{\theta_{l_1}}^{\theta_{l_2}} d\theta\ \sin\theta\, K_2(\theta,\theta_{l_2})h_4(\theta) + \lim_{\xi\to\theta_{l_2}^-}K_2(\theta_{l_2},\xi)\sin(\theta_{l_2})\frac{\partial T}{\partial\theta}(\theta_{l_2}) \\
&- T(\theta_{l_2})\sin(\theta_{l_2})\lim_{\xi\to\theta_{l_2}^-}\lim_{\theta\to\theta_{l_2}^-}\frac{\partial K_2}{\partial\theta}(\theta,\xi) - K_2(\theta_{l_1},\theta_{l_2})\sin(\theta_{l_1})\frac{\partial T}{\partial\theta}(\theta_{l_1}) \\
&+ T(\theta_{l_1})\sin(\theta_{l_1})\lim_{\xi\to\theta_{l_2}^-}\lim_{\theta\to\theta_{l_1}^+}\frac{\partial K_1}{\partial\theta}(\theta,\xi),
\end{aligned} \tag{E.87}
$$

$$
\begin{aligned}
T(\theta_{l_2}) = &\int_{\theta_{l_2}}^{\theta_{c_2}} d\theta\ \sin\theta\, K_1(\theta,\theta_{l_2})h_1(\theta) + K_1(\theta_{c_2},\theta_{l_2})\sin(\theta_{c_2})\frac{\partial T}{\partial\theta}(\theta_{c_2}) \\
&+ \sin(\theta_{c_2})\lim_{\xi\to\theta_{l_2}^+}\lim_{\theta\to\theta_{c_2}^-}\frac{\partial K_1}{\partial\theta}(\theta,\xi) - \lim_{\xi\to\theta_{l_2}^+}K_1(\theta_{l_2},\xi)\sin(\theta_{l_1})\frac{\partial T}{\partial\theta}(\theta_{l_2}) \\
&+ T(\theta_{l_2})\sin(\theta_{l_2})\lim_{\xi\to\theta_{l_2}^+}\lim_{\theta\to\theta_{l_2}^+}\frac{\partial K_1}{\partial\theta}(\theta,\xi),
\end{aligned} \tag{E.88}
$$

$$
\begin{aligned}
-1 = &\int_{\theta_{l_2}}^{\theta_{c_2}} d\theta\ \sin\theta\, K_1(\theta,\theta_{c_2})h_1(\theta) + \lim_{\xi\to\theta_{c_2}^-}K_1(\theta_{c_2},\xi)\sin(\theta_{c_2})\frac{\partial T}{\partial\theta}(\theta_{c_2}) \\
&+ \sin(\theta_{c_2})\lim_{\xi\to\theta_{c_2}^-}\lim_{\theta\to\theta_{c_2}^-}\frac{\partial K_1}{\partial\theta}(\theta,\xi) - K_1(\theta_{l_2},\theta_{c_2})\sin(\theta_{l_1})\frac{\partial T}{\partial\theta}(\theta_{l_2}) \\
&+ T(\theta_{l_2})\sin(\theta_{l_2})\lim_{\xi\to\theta_{c_2}^-}\lim_{\theta\to\theta_{l_2}^+}\frac{\partial K_1}{\partial\theta}(\theta,\xi),
\end{aligned} \tag{E.89}
$$

$$
\begin{aligned}
-1 = &\int_{\theta_{c_2}}^{\pi} d\theta\ \sin\theta\, K_1(\theta,\theta_{c_2})h_2(\theta) - \lim_{\xi\to\theta_{c_1}^+}K_1(\theta_{c_2},\xi)\sin(\theta_{c_2})\frac{\partial T}{\partial\theta}(\theta_{c_2}) \\
&- \sin(\theta_{c_2})\lim_{\xi\to\theta_{c_2}^+}\lim_{\theta\to\theta_{c_2}^+}\frac{\partial K_1}{\partial\theta}(\theta,\xi)
\end{aligned} \tag{E.90}
$$

and

$$
\begin{aligned}
T(\pi) = &\int_{\theta_{c_2}}^{\pi} d\theta\ \sin\theta\, K_1(\theta,\pi)h_2(\theta) - K_1(\theta_{c_2},\pi)\sin(\theta_{c_2})\frac{\partial T}{\partial\theta}(\theta_{c_2}) \\
&- \sin(\theta_{c_2})\lim_{\xi\to\pi^-}\lim_{\theta\to\theta_{c_2}^+}\frac{\partial K_1}{\partial\theta}(\theta,\xi).
\end{aligned} \tag{E.91}
$$

The boundary integral equations (E.84)-(E.91) is a system of 8 equations for the 8 unknown boundary values $T(0)$, θ_{c_2}, $\frac{\partial T}{\partial\theta}(\theta_{c_2})$, $\frac{\partial T}{\partial\theta}(\theta_{l_1})$, $\frac{\partial T}{\partial\theta}(\theta_{l_2})$ and $T(\pi)$. We solve this system using the exact same procure as above for the "one ice edge on the northern ocean"-scenario.

E.4 The case of four ice edges

In the case of four ice edges we have two scenarios; either the continent is completely covered in ice/snow or the continent has a partial ice/snow cover. Let us first consider the case where the continent is completely covered in ice/snow. This will be the easier scenario since we know the location of two ice edges,

$$\theta_{c_2} = \theta_{l_1}$$
$$\theta_{c_3} = \theta_{l_2}.$$

We will not have to locate these ice edges and that makes the process of finding a solution a lot easier. For one, we will only have five relevant regions,

$$\theta \in (0, \theta_{c_1}), \tag{I}$$

$$\theta \in (\theta_{c_1}, \theta_{l_1}), \tag{II}$$

$$\theta \in (\theta_{l_1}, \theta_{l_2}), \tag{III}$$

$$\theta \in (\theta_{l_2}, \theta_{c_4}), \tag{IV}$$

$$\theta \in (\theta_{c_4}, \pi). \tag{V}$$

Consequently, the boundary integral equations will be a system of 10 equations for the 10 unknown boundary values just like in the case of two ice edges. So let us find the boundary integral equations!

The governing equations in the five regions are

$$\mathcal{L}_1 T = h_2$$

in region I,

$$\mathcal{L}_1 T = h_1$$

in region II,

$$\mathcal{L}_2 T = h_4$$

in region III,

$$\mathcal{L}_1 T = h_1$$

in region IV and

$$\mathcal{L}_1 T = h_2$$

in region V. Applying the general integral relations (E.6) and (E.7) in the respective regions we get

$$\begin{aligned} T(\xi) = &\int_0^{\theta_{c_1}} d\theta \ \sin\theta \, K_1(\theta,\xi) h_2(\theta) + K_1(\theta_{c_1},\xi)\sin(\theta_{c_1})\frac{\partial T}{\partial\theta}(\theta_{c_1}) \\ &+ \sin(\theta_{c_1}) \lim_{\theta\to\theta_{c_1}^-} \frac{\partial K_1}{\partial\theta}(\theta,\xi) \end{aligned} \tag{E.92}$$

in region I,

$$\begin{aligned} T(\xi) = &\int_{\theta_{c_1}}^{\theta_{l_1}} d\theta \ \sin\theta \, K_1(\theta,\xi) h_1(\theta) + K_1(\theta_{l_1},\xi)\sin(\theta_{l_1})\frac{\partial T}{\partial\theta}(\theta_{l_1}) \\ &- T(\theta_{l_1})\sin(\theta_{l_1}) \lim_{\theta\to\theta_{l_1}^-} \frac{\partial K_1}{\partial\theta}(\theta,\xi) - K_1(\theta_{c_1},\xi)\sin(\theta_{c_1})\frac{\partial T}{\partial\theta}(\theta_{c_1}) \\ &- \sin(\theta_{c_1}) \lim_{\theta\to\theta_{c_1}^+} \frac{\partial K_1}{\partial\theta}(\theta,\xi) \end{aligned} \tag{E.93}$$

in region II,

$$\begin{aligned} T(\xi) = &\int_{\theta_{l_1}}^{\theta_{l_2}} d\theta \ \sin\theta \, K_2(\theta,\xi) h_4(\theta) + K_2(\theta_{l_2},\xi)\sin(\theta_{l_2})\frac{\partial T}{\partial\theta}(\theta_{l_2}) \\ &- T(\theta_{l_2})\sin(\theta_{l_2}) \lim_{\theta\to\theta_{l_2}^-} \frac{\partial K_2}{\partial\theta}(\theta,\xi) - K_2(\theta_{l_1},\xi)\sin(\theta_{l_1})\frac{\partial T}{\partial\theta}(\theta_{l_1}) \\ &+ T(\theta_{l_1})\sin(\theta_{l_1}) \lim_{\theta\to\theta_{l_1}^+} \frac{\partial K_1}{\partial\theta}(\theta,\xi) \end{aligned} \tag{E.94}$$

in region III,

$$\begin{aligned} T(\xi) = &\int_{\theta_{l_2}}^{\theta_{c_4}} d\theta \ \sin\theta \, K_1(\theta,\xi) h_1(\theta) + K_1(\theta_{c_4},\xi)\sin(\theta_{c_4})\frac{\partial T}{\partial\theta}(\theta_{c_4}) \\ &+ \sin(\theta_{c_4}) \lim_{\theta\to\theta_{c_4}^-} \frac{\partial K_1}{\partial\theta}(\theta,\xi) - K_1(\theta_{l_2},\xi)\sin(\theta_{l_1})\frac{\partial T}{\partial\theta}(\theta_{l_2}) \\ &+ T(\theta_{l_2})\sin(\theta_{l_2}) \lim_{\theta\to\theta_{l_2}^+} \frac{\partial K_1}{\partial\theta}(\theta,\xi) \end{aligned} \tag{E.95}$$

in region IV and

$$\begin{aligned} T(\xi) = &\int_{\theta_{c_4}}^{\pi} d\theta \ \sin\theta \, K_1(\theta,\xi) h_2(\theta) - K_1(\theta_{c_4},\xi)\sin(\theta_{c_4})\frac{\partial T}{\partial\theta}(\theta_{c_2}) \\ &- \sin(\theta_{c_4}) \lim_{\theta\to\theta_{c_4}^+} \frac{\partial K_1}{\partial\theta}(\theta,\xi). \end{aligned} \tag{E.96}$$

in region V. Equation (E.92)-(E.96) relates values of the solution inside the five regions to certain unknown boundary values. These boundary values are found through solving the associated

boundary integral equations;

$$T(0) = \int_0^{\theta_{c_1}} d\theta\ \sin\theta\, K_1(\theta,0)h_2(\theta) + K_1(\theta_{c_1},0)\sin(\theta_{c_1})\frac{\partial T}{\partial\theta}(\theta_{c_1}) + \sin(\theta_{c_1})\lim_{\xi\to 0^+}\lim_{\theta\to\theta_{c_1}^-}\frac{\partial K_1}{\partial\theta}(\theta,\xi) \tag{E.97}$$

$$-1 = \int_0^{\theta_{c_1}} d\theta\ \sin\theta\, K_1(\theta,\theta_{c_1})h_2(\theta) + \lim_{\xi\to\theta_{c_1}^-} K_1(\theta_{c_1},\xi)\sin(\theta_{c_1})\frac{\partial T}{\partial\theta}(\theta_{c_1}) + \sin(\theta_{c_1})\lim_{\xi\to\theta_{c_1}^-}\lim_{\theta\to\theta_{c_1}^-}\frac{\partial K_1}{\partial\theta}(\theta,\xi) \tag{E.98}$$

$$-1 = \int_{\theta_{c_1}}^{\theta_{l_1}} d\theta\ \sin\theta\, K_1(\theta,\theta_{c_1})h_1(\theta) + K_1(\theta_{l_1},\theta_{c_1})\sin(\theta_{l_1})\frac{\partial T}{\partial\theta}(\theta_{l_1}) - T(\theta_{l_1})\sin(\theta_{l_1})\lim_{\xi\to\theta_{c_1}^+}\lim_{\theta\to\theta_{l_1}^-}\frac{\partial K_1}{\partial\theta}(\theta,\xi) - \lim_{\xi\to\theta_{c_1}^+} K_1(\theta_{c_1},\xi)\sin(\theta_{c_1})\frac{\partial T}{\partial\theta}(\theta_{c_1}) - \sin(\theta_{c_1})\lim_{\xi\to\theta_{c_1}^+}\lim_{\theta\to\theta_{c_1}^+}\frac{\partial K_1}{\partial\theta}(\theta,\xi) \tag{E.99}$$

$$T(\theta_{l_1}) = \int_{\theta_{c_1}}^{\theta_{l_1}} d\theta\ \sin\theta\, K_1(\theta,\theta_{l_1})h_1(\theta) + \lim_{\xi\to\theta_{l_1}^-} K_1(\theta_{l_1},\xi)\sin(\theta_{l_1})\frac{\partial T}{\partial\theta}(\theta_{l_1}) - T(\theta_{l_1})\sin(\theta_{l_1})\lim_{\xi\to\theta_{l_1}^-}\lim_{\theta\to\theta_{l_1}^-}\frac{\partial K_1}{\partial\theta}(\theta,\xi) - K_1(\theta_{c_1},\theta_{l_1})\sin(\theta_{c_1})\frac{\partial T}{\partial\theta}(\theta_{c_1}) - \sin(\theta_{c_1})\lim_{\xi\to\theta_{l_1}^-}\lim_{\theta\to\theta_{c_1}^+}\frac{\partial K_1}{\partial\theta}(\theta,\xi) \tag{E.100}$$

$$T(\theta_{l_1}) = \int_{\theta_{l_1}}^{\theta_{l_2}} d\theta\ \sin\theta\, K_2(\theta,\theta_{l_1})h_4(\theta) + K_2(\theta_{l_2},\theta_{l_1})\sin(\theta_{l_2})\frac{\partial T}{\partial\theta}(\theta_{l_2}) - T(\theta_{l_2})\sin(\theta_{l_2})\lim_{\xi\to\theta_{l_1}^+}\lim_{\theta\to\theta_{l_2}^-}\frac{\partial K_2}{\partial\theta}(\theta,\xi) - \lim_{\xi\to\theta_{l_1}^+} K_2(\theta_{l_1},\xi)\sin(\theta_{l_1})\frac{\partial T}{\partial\theta}(\theta_{l_1}) + T(\theta_{l_1})\sin(\theta_{l_1})\lim_{\xi\to\theta_{l_1}^+}\lim_{\theta\to\theta_{l_1}^+}\frac{\partial K_1}{\partial\theta}(\theta,\xi) \tag{E.101}$$

$$T(\theta_{l_2}) = \int_{\theta_{l_1}}^{\theta_{l_2}} d\theta\ \sin\theta\, K_2(\theta,\theta_{l_2})h_4(\theta) + \lim_{\xi\to\theta_{l_2}^-} K_2(\theta_{l_2},\xi)\sin(\theta_{l_2})\frac{\partial T}{\partial\theta}(\theta_{l_2}) - T(\theta_{l_2})\sin(\theta_{l_2})\lim_{\xi\to\theta_{l_2}^-}\lim_{\theta\to\theta_{l_2}^-}\frac{\partial K_2}{\partial\theta}(\theta,\xi) - K_2(\theta_{l_1},\theta_{l_2})\sin(\theta_{l_1})\frac{\partial T}{\partial\theta}(\theta_{l_1}) + T(\theta_{l_1})\sin(\theta_{l_1})\lim_{\xi\to\theta_{l_2}^-}\lim_{\theta\to\theta_{l_1}^+}\frac{\partial K_1}{\partial\theta}(\theta,\xi) \tag{E.102}$$

$$
\begin{aligned}
T(\theta_{l_2}) = &\int_{\theta_{l_2}}^{\theta_{c_4}} d\theta\ \sin\theta\, K_1(\theta,\theta_{l_2})h_1(\theta) + K_1(\theta_{c_4},\theta_{l_2})\sin(\theta_{c_4})\frac{\partial T}{\partial\theta}(\theta_{c_4}) \\
&+ \sin(\theta_{c_4}) \lim_{\xi\to\theta_{l_2}^+}\lim_{\theta\to\theta_{c_4}^-} \frac{\partial K_1}{\partial\theta}(\theta,\xi) - \lim_{\xi\to\theta_{l_2}^+} K_1(\theta_{l_2},\xi)\sin(\theta_{l_1})\frac{\partial T}{\partial\theta}(\theta_{l_2}) \\
&+ T(\theta_{l_2})\sin(\theta_{l_2}) \lim_{\xi\to\theta_{l_2}^+}\lim_{\theta\to\theta_{l_2}^+} \frac{\partial K_1}{\partial\theta}(\theta,\xi)
\end{aligned} \tag{E.103}
$$

$$
\begin{aligned}
-1 = &\int_{\theta_{l_2}}^{\theta_{c_4}} d\theta\ \sin\theta\, K_1(\theta,\theta_{c_4})h_1(\theta) + \lim_{\xi\to\theta_{c_4}^-} K_1(\theta_{c_4},\xi)\sin(\theta_{c_4})\frac{\partial T}{\partial\theta}(\theta_{c_4}) \\
&+ \sin(\theta_{c_4}) \lim_{\xi\to\theta_{c_4}^-}\lim_{\theta\to\theta_{c_4}^-} \frac{\partial K_1}{\partial\theta}(\theta,\xi) - K_1(\theta_{l_2},\theta_{c_4})\sin(\theta_{l_1})\frac{\partial T}{\partial\theta}(\theta_{l_2}) \\
&+ T(\theta_{l_2})\sin(\theta_{l_2}) \lim_{\xi\to\theta_{c_4}^-}\lim_{\theta\to\theta_{l_2}^+} \frac{\partial K_1}{\partial\theta}(\theta,\xi)
\end{aligned} \tag{E.104}
$$

$$
\begin{aligned}
-1 = &\int_{\theta_{c_4}}^{\pi} d\theta\ \sin\theta\, K_1(\theta,\theta_{c_4})h_2(\theta) - \lim_{\xi\to\theta_{c_4}^+} K_1(\theta_{c_4},\xi)\sin(\theta_{c_4})\frac{\partial T}{\partial\theta}(\theta_{c_4}) \\
&- \sin(\theta_{c_4}) \lim_{\xi\to\theta_{c_4}^+}\lim_{\theta\to\theta_{c_4}^+} \frac{\partial K_1}{\partial\theta}(\theta,\xi)
\end{aligned} \tag{E.105}
$$

$$
\begin{aligned}
T(\pi) = &\int_{\theta_{c_4}}^{\pi} d\theta\ \sin\theta\, K_1(\theta,\pi)h_2(\theta) - K_1(\theta_{c_4},\pi)\sin(\theta_{c_4})\frac{\partial T}{\partial\theta}(\theta_{c_4}) \\
&- \sin(\theta_{c_4}) \lim_{\xi\to\pi^-}\lim_{\theta\to\theta_{c_4}^+} \frac{\partial K_1}{\partial\theta}(\theta,\xi).
\end{aligned} \tag{E.106}
$$

The boundary integral equations (E.97)-(E.106) is a system of 10 equations for the 10 unknown boundary values $T(0)$, θ_{c_1}, $\frac{\partial T}{\partial\theta}(\theta_{c_1})$, $\frac{\partial T}{\partial\theta}(\theta_{l_1})$, $\frac{\partial T}{\partial\theta}(\theta_{l_2})$, θ_{c_4}, $\frac{\partial T}{\partial\theta}(\theta_{c_4})$ and $T(\pi)$. We solve this system of equation following the exact same procedure as outlined above for the two ice edges case. Once we have found the unknown boundary values, the solution in the regions I-V is given by the integral relations (E.92)-(E.96), respectively.

For the scenario where we have four ice edges and the continent has a partial ice cover and we have to locate all four ice edges using the boundary integral equations. For this scenario we have seven relevant regions;

$$\theta \in (0, \theta_{c_1}), \tag{I}$$

$$\theta \in (\theta_{c_1}, \theta_{l_1}), \tag{II}$$

$$\theta \in (\theta_{l_1}, \theta_{c_2}), \tag{III}$$

$$\theta \in (\theta_{c_2}, \theta_{c_3}), \tag{IV}$$

$$\theta \in (\theta_{c_3}, \theta_{l_2}), \tag{V}$$

$$\theta \in (\theta_{l_2}, \theta_{c_4}), \tag{VI}$$

$$\theta \in (\theta_{c_4}, \pi). \tag{VII}$$

The governing equations in the seven regions are

$$\mathcal{L}_1 T = h_2$$

in region I,

$$\mathcal{L}_1 T = h_1$$

in region II,

$$\mathcal{L}_2 T = h_3$$

in region III,

$$\mathcal{L}_2 T = h_4$$

in region IV,

$$\mathcal{L}_2 T = h_3$$

in region V,

$$\mathcal{L}_1 T = h_1$$

in region VI and

$$\mathcal{L}_1 T = h_2$$

in region VII. Applying the general integral relations (E.6) and (E.7) in the respective regions we get

$$\begin{aligned} T(\xi) = \int_0^{\theta_{c_1}} d\theta \, \sin\theta \, K_1(\theta, \xi) h_2(\theta) + K_1(\theta_{c_1}, \xi) \sin(\theta_{c_1}) \frac{\partial T}{\partial \theta}(\theta_{c_1}) \\ + \sin(\theta_{c_1}) \lim_{\theta \to \theta_{c_1}^-} \frac{\partial K_1}{\partial \theta}(\theta, \xi) \end{aligned} \tag{E.107}$$

in region I,

$$\begin{aligned} T(\xi) = &\int_{\theta_{c_1}}^{\theta_{l_1}} d\theta \ \sin\theta \, K_1(\theta,\xi) h_1(\theta) + K_1(\theta_{l_1},\xi)\sin(\theta_{l_1})\frac{\partial T}{\partial\theta}(\theta_{l_1}) \\ &- T(\theta_{l_1})\sin(\theta_{l_1}) \lim_{\theta\to\theta_{l_1}^-} \frac{\partial K_1}{\partial\theta}(\theta,\xi) - K_1(\theta_{c_1},\xi)\sin(\theta_{c_1})\frac{\partial T}{\partial\theta}(\theta_{c_1}) \\ &- \sin(\theta_{c_1}) \lim_{\theta\to\theta_{c_1}^+} \frac{\partial K_1}{\partial\theta}(\theta,\xi) \end{aligned} \tag{E.108}$$

in region II,

$$\begin{aligned} T(\xi) = &\int_{\theta_{l_1}}^{\theta_{c_2}} d\theta \ \sin\theta \, K_2(\theta,\xi) h_3(\theta) + K_2(\theta_{c_2},\xi)\sin(\theta_{c_2})\frac{\partial T}{\partial\theta}(\theta_{c_2}) \\ &+ T_c \sin(\theta_{c_2}) \lim_{\theta\to\theta_{c_2}^-} \frac{\partial K_2}{\partial\theta}(\theta,\xi) - K_2(\theta_{l_1},\xi)\sin(\theta_{l_1})\frac{\partial T}{\partial\theta}(\theta_{l_1}) \\ &+ T(\theta_{l_1})\sin(\theta_{l_1}) \lim_{\theta\to\theta_{l_1}^+} \frac{\partial K_2}{\partial\theta}(\theta,\xi) \end{aligned} \tag{E.109}$$

in region III,

$$\begin{aligned} T(\xi) = &\int_{\theta_{c_2}}^{\theta_{c_3}} d\theta \ \sin\theta \, K_2(\theta,\xi) h_4(\theta) + K_2(\theta_{c_3},\xi)\sin(\theta_{c_3})\frac{\partial T}{\partial\theta}(\theta_{c_3}) \\ &+ T_c \sin(\theta_{c_3}) \lim_{\theta\to\theta_{c_3}^-} \frac{\partial K_2}{\partial\theta}(\theta,\xi) - K_2(\theta_{c_2},\xi)\sin(\theta_{c_2})\frac{\partial T}{\partial\theta}(\theta_{c_2}) \\ &- T_c \sin(\theta_{c_2}) \lim_{\theta\to\theta_{c_2}^+} \frac{\partial K_2}{\partial\theta}(\theta,\xi) \end{aligned} \tag{E.110}$$

in region IV,

$$\begin{aligned} T(\xi) = &\int_{\theta_{c_3}}^{\theta_{l_2}} d\theta \ \sin\theta \, K_2(\theta,\xi) h_3(\theta) + K_2(\theta_{l_2},\xi)\sin(\theta_{l_2})\frac{\partial T}{\partial\theta}(\theta_{l_2}) \\ &- T(\theta_{l_2})\sin(\theta_{l_2}) \lim_{\theta\to\theta_{l_2}^-} \frac{\partial K_2}{\partial\theta}(\theta,\xi) - K_2(\theta_{c_3},\xi)\sin(\theta_{c_3})\frac{\partial T}{\partial\theta}(\theta_{c_3}) \\ &- T_c \sin(\theta_{c_3}) \lim_{\theta\to\theta_{c_3}^+} \frac{\partial K_2}{\partial\theta}(\theta,\xi) \end{aligned} \tag{E.111}$$

in region V,

$$\begin{aligned} T(\xi) = &\int_{\theta_{l_2}}^{\theta_{c_4}} d\theta \ \sin\theta \, K_1(\theta,\xi) h_1(\theta) + K_1(\theta_{c_4},\xi)\sin(\theta_{c_4})\frac{\partial T}{\partial\theta}(\theta_{c_4}) \\ &+ \sin(\theta_{c_4}) \lim_{\theta\to\theta_{c_4}^-} \frac{\partial K_1}{\partial\theta}(\theta,\xi) - K_1(\theta_{l_2},\xi)\sin(\theta_{l_2})\frac{\partial T}{\partial\theta}(\theta_{l_2}) \\ &+ T(\theta_{l_2})\sin(\theta_{l_2}) \lim_{\theta\to\theta_{l_2}^+} \frac{\partial K_1}{\partial\theta}(\theta,\xi) \end{aligned} \tag{E.112}$$

in region VI and

$$\begin{aligned} T(\xi) = &\int_{\theta_{c_4}}^{\pi} d\theta \ \sin\theta \, K_1(\theta,\xi) h_2(\theta) - K_1(\theta_{c_4},\xi)\sin(\theta_{c_4})\frac{\partial T}{\partial\theta}(\theta_{c_4}) \\ &- \sin(\theta_{c_4}) \lim_{\theta\to\theta_{c_4}^+} \frac{\partial K_1}{\partial\theta}(\theta,\xi). \end{aligned} \tag{E.113}$$

in region VII. Here we have demanded that $T(\theta_{c_2}) = T(\theta_{c_3}) = -T_c$. Equation (E.107)-(E.111) relates values of the solution inside the seven regions to certain unknown boundary values. These boundary values are obtained by solving the boundary integral equations. We derive the boundary integral equations by letting ξ approach the boundaries of the sub-domains I-VII, and the resulting boundary integral equations are;

$$\begin{aligned} T(0) = &\int_{0}^{\theta_{c_1}} d\theta \ \sin\theta \, K_1(\theta,0) h_2(\theta) + K_1(\theta_{c_1},0)\sin(\theta_{c_1})\frac{\partial T}{\partial\theta}(\theta_{c_1}) \\ &+ \sin(\theta_{c_1}) \lim_{\xi\to 0^+} \lim_{\theta\to\theta_{c_1}^-} \frac{\partial K_1}{\partial\theta}(\theta,\xi) \end{aligned} \tag{E.114}$$

$$\begin{aligned} -1 = &\int_{0}^{\theta_{c_1}} d\theta \ \sin\theta \, K_1(\theta,\theta_{c_1}) h_2(\theta) + \lim_{\xi\to\theta_{c_1}^-} K_1(\theta_{c_1},\xi)\sin(\theta_{c_1})\frac{\partial T}{\partial\theta}(\theta_{c_1}) \\ &+ \sin(\theta_{c_1}) \lim_{\xi\to\theta_{c_1}^-} \lim_{\theta\to\theta_{c_1}^-} \frac{\partial K_1}{\partial\theta}(\theta,\xi) \end{aligned} \tag{E.115}$$

$$\begin{aligned} -1 = &\int_{\theta_{c_1}}^{\theta_{l_1}} d\theta \ \sin\theta \, K_1(\theta,\theta_{c_1}) h_1(\theta) + K_1(\theta_{l_1},\theta_{c_1})\sin(\theta_{l_1})\frac{\partial T}{\partial\theta}(\theta_{l_1}) \\ &- T(\theta_{l_1})\sin(\theta_{l_1}) \lim_{\xi\to\theta_{c_1}^+} \lim_{\theta\to\theta_{l_1}^-} \frac{\partial K_1}{\partial\theta}(\theta,\xi) - \lim_{\xi\to\theta_{c_1}^+} K_1(\theta_{c_1},\xi)\sin(\theta_{c_1})\frac{\partial T}{\partial\theta}(\theta_{c_1}) \\ &- \sin(\theta_{c_1}) \lim_{\xi\to\theta_{c_1}^+} \lim_{\theta\to\theta_{c_1}^+} \frac{\partial K_1}{\partial\theta}(\theta,\xi) \end{aligned} \tag{E.116}$$

$$
\begin{aligned}
T(\theta_{l_1}) = &\int_{\theta_{c_1}}^{\theta_{l_1}} d\theta\ \sin\theta\, K_1(\theta,\theta_{l_1})h_1(\theta) + \lim_{\xi\to\theta_{l_1}^-} K_1(\theta_{l_1},\xi)\sin(\theta_{l_1})\frac{\partial T}{\partial\theta}(\theta_{l_1}) \\
&- T(\theta_{l_1})\sin(\theta_{l_1}) \lim_{\xi\to\theta_{l_1}^-}\lim_{\theta\to\theta_{l_1}^-} \frac{\partial K_1}{\partial\theta}(\theta,\xi) - K_1(\theta_{c_1},\theta_{l_1})\sin(\theta_{c_1})\frac{\partial T}{\partial\theta}(\theta_{c_1}) \\
&- \sin(\theta_{c_1}) \lim_{\xi\to\theta_{l_1}^-}\lim_{\theta\to\theta_{c_1}^+} \frac{\partial K_1}{\partial\theta}(\theta,\xi)
\end{aligned} \tag{E.117}
$$

$$
\begin{aligned}
T(\theta_{l_1}) = &\int_{\theta_{l_1}}^{\theta_{c_2}} d\theta\ \sin\theta\, K_2(\theta,\theta_{l_1})h_3(\theta) + K_2(\theta_{c_2},\theta_{l_1})\sin(\theta_{c_2})\frac{\partial T}{\partial\theta}(\theta_{c_2}) \\
&+ T_c\sin(\theta_{c_2}) \lim_{\xi\to\theta_{l_1}^+}\lim_{\theta\to\theta_{l_2}^-} \frac{\partial K_2}{\partial\theta}(\theta,\xi) - \lim_{\xi\to\theta_{l_1}^+} K_2(\theta_{l_1},\xi)\sin(\theta_{l_1})\frac{\partial T}{\partial\theta}(\theta_{l_1}) \\
&+ T(\theta_{l_1})\sin(\theta_{l_1}) \lim_{\xi\to\theta_{l_1}^+}\lim_{\theta\to\theta_{l_1}^+} \frac{\partial K_2}{\partial\theta}(\theta,\xi)
\end{aligned} \tag{E.118}
$$

$$
\begin{aligned}
-T_c = &\int_{\theta_{l_1}}^{\theta_{c_2}} d\theta\ \sin\theta\, K_2(\theta,\theta_{c_2})h_3(\theta) + \lim_{\xi\to\theta_{c_2}^-} K_2(\theta_{c_2},\xi)\sin(\theta_{c_2})\frac{\partial T}{\partial\theta}(\theta_{c_2}) \\
&+ T_c\sin(\theta_{c_2}) \lim_{\xi\to\theta_{c_2}^-}\lim_{\theta\to\theta_{c_2}^-} \frac{\partial K_2}{\partial\theta}(\theta,\xi) - K_2(\theta_{l_1},\theta_{c_2})\sin(\theta_{l_1})\frac{\partial T}{\partial\theta}(\theta_{l_1}) \\
&+ T(\theta_{l_1})\sin(\theta_{l_1}) \lim_{\xi\to\theta_{c_2}^-}\lim_{\theta\to\theta_{l_1}^+} \frac{\partial K_2}{\partial\theta}(\theta,\xi)
\end{aligned} \tag{E.119}
$$

$$
\begin{aligned}
-T_c = &\int_{\theta_{c_2}}^{\theta_{c_3}} d\theta\ \sin\theta\, K_2(\theta,\theta_{c_2})h_4(\theta) + K_2(\theta_{c_3},\theta_{c_2})\sin(\theta_{c_3})\frac{\partial T}{\partial\theta}(\theta_{c_3}) \\
&+ T_c\sin(\theta_{c_3}) \lim_{\xi\to\theta_{c_2}^+}\lim_{\theta\to\theta_{c_3}^-} \frac{\partial K_2}{\partial\theta}(\theta,\xi) - \lim_{\xi\to\theta_{c_2}^+} K_2(\theta_{c_2},\xi)\sin(\theta_{c_2})\frac{\partial T}{\partial\theta}(\theta_{c_2}) \\
&- T_c\sin(\theta_{c_2}) \lim_{\xi\to\theta_{c_2}^+}\lim_{\theta\to\theta_{c_2}^+} \frac{\partial K_2}{\partial\theta}(\theta,\xi)
\end{aligned} \tag{E.120}
$$

$$
\begin{aligned}
-T_c = &\int_{\theta_{c_2}}^{\theta_{c_3}} d\theta\ \sin\theta\, K_2(\theta,\theta_{c_3})h_4(\theta) + \lim_{\xi\to\theta_{c_3}^-} K_2(\theta_{c_3},\xi)\sin(\theta_{c_3})\frac{\partial T}{\partial\theta}(\theta_{c_3}) \\
&+ T_c\sin(\theta_{c_3}) \lim_{\xi\to\theta_{c_3}^-}\lim_{\theta\to\theta_{c_3}^-} \frac{\partial K_2}{\partial\theta}(\theta,\xi) - K_2(\theta_{c_2},\theta_{c_3})\sin(\theta_{c_2})\frac{\partial T}{\partial\theta}(\theta_{c_2}) \\
&- T_c\sin(\theta_{c_2}) \lim_{\xi\to\theta_{c_3}^-}\lim_{\theta\to\theta_{c_2}^+} \frac{\partial K_2}{\partial\theta}(\theta,\xi)
\end{aligned} \tag{E.121}
$$

$$
\begin{aligned}
-T_c = &\int_{\theta_{c_3}}^{\theta_{l_2}} d\theta\ \sin\theta\, K_2(\theta,\theta_{c_3})h_3(\theta) + K_2(\theta_{l_2},\theta_{c_3})\sin(\theta_{l_2})\frac{\partial T}{\partial\theta}(\theta_{l_2}) \\
&- T(\theta_{l_2})\sin(\theta_{l_2}) \lim_{\xi\to\theta_{c_3}^+}\lim_{\theta\to\theta_{l_2}^-} \frac{\partial K_2}{\partial\theta}(\theta,\xi) - \lim_{\xi\to\theta_{c_3}^+} K_2(\theta_{c_3},\xi)\sin(\theta_{c_3})\frac{\partial T}{\partial\theta}(\theta_{c_3}) \\
&- T_c\sin(\theta_{c_3}) \lim_{\xi\to\theta_{c_3}^+}\lim_{\theta\to\theta_{c_3}^+} \frac{\partial K_2}{\partial\theta}(\theta,\xi)
\end{aligned} \tag{E.122}
$$

$$
\begin{aligned}
T(\theta_{l_2}) = &\int_{\theta_{c_3}}^{\theta_{l_2}} d\theta\ \sin\theta\, K_2(\theta,\theta_{l_2})h_3(\theta) + \lim_{\xi\to\theta_{l_2}^-} K_2(\theta_{l_2},\xi)\sin(\theta_{l_2})\frac{\partial T}{\partial\theta}(\theta_{l_2}) \\
&- T(\theta_{l_2})\sin(\theta_{l_2}) \lim_{\xi\to\theta_{l_2}^-}\lim_{\theta\to\theta_{l_2}^-} \frac{\partial K_2}{\partial\theta}(\theta,\xi) - K_2(\theta_{c_3},\theta_{l_2})\sin(\theta_{c_3})\frac{\partial T}{\partial\theta}(\theta_{c_3}) \\
&- T_c\sin(\theta_{c_3}) \lim_{\xi\to\theta_{l_2}^-}\lim_{\theta\to\theta_{c_3}^+} \frac{\partial K_2}{\partial\theta}(\theta,\xi)
\end{aligned} \tag{E.123}
$$

$$
\begin{aligned}
T(\theta_{l_2}) = &\int_{\theta_{l_2}}^{\theta_{c_4}} d\theta\ \sin\theta\, K_1(\theta,\theta_{l_2})h_1(\theta) + K_1(\theta_{c_4},\theta_{l_2})\sin(\theta_{c_4})\frac{\partial T}{\partial\theta}(\theta_{c_4}) \\
&+ \sin(\theta_{c_4}) \lim_{\xi\to\theta_{l_2}^+}\lim_{\theta\to\theta_{c_4}^-} \frac{\partial K_1}{\partial\theta}(\theta,\xi) - \lim_{\xi\to\theta_{l_2}^+} K_1(\theta_{l_2},\xi)\sin(\theta_{l_2})\frac{\partial T}{\partial\theta}(\theta_{l_2}) \\
&+ T(\theta_{l_2})\sin(\theta_{l_2}) \lim_{\xi\to\theta_{l_2}^+}\lim_{\theta\to\theta_{l_2}^+} \frac{\partial K_1}{\partial\theta}(\theta,\xi)
\end{aligned} \tag{E.124}
$$

$$
\begin{aligned}
-1 = &\int_{\theta_{l_2}}^{\theta_{c_4}} d\theta\ \sin\theta\, K_1(\theta,\theta_{c_4})h_1(\theta) + \lim_{\xi\to\theta_{c_4}^-} K_1(\theta_{c_4},\xi)\sin(\theta_{c_4})\frac{\partial T}{\partial\theta}(\theta_{c_4}) \\
&+ \sin(\theta_{c_4}) \lim_{\xi\to\theta_{c_4}^-}\lim_{\theta\to\theta_{c_4}^-} \frac{\partial K_1}{\partial\theta}(\theta,\xi) - K_1(\theta_{l_2},\theta_{c_4})\sin(\theta_{l_2})\frac{\partial T}{\partial\theta}(\theta_{l_2}) \\
&+ T(\theta_{l_2})\sin(\theta_{l_2}) \lim_{\xi\to\theta_{c_4}^-}\lim_{\theta\to\theta_{l_2}^+} \frac{\partial K_1}{\partial\theta}(\theta,\xi)
\end{aligned} \tag{E.125}
$$

$$
\begin{aligned}
-1 = &\int_{\theta_{c_4}}^{\pi} d\theta\ \sin\theta\, K_1(\theta,\theta_{c_4})h_2(\theta) - \lim_{\xi\to\theta_{c_4}^+} K_1(\theta_{c_4},\xi)\sin(\theta_{c_4})\frac{\partial T}{\partial\theta}(\theta_{c_4}) \\
&- \sin(\theta_{c_4}) \lim_{\xi\to\theta_{c_4}^+}\lim_{\theta\to\theta_{c_4}^+} \frac{\partial K_1}{\partial\theta}(\theta,\xi)
\end{aligned} \tag{E.126}
$$

$$
\begin{aligned}
T(\pi) = &\int_{\theta_{c_4}}^{\pi} d\theta\ \sin\theta\, K_1(\theta,\pi)h_2(\theta) - K_1(\theta_{c_4},\pi)\sin(\theta_{c_4})\frac{\partial T}{\partial\theta}(\theta_{c_4}) \\
&- \sin(\theta_{c_4}) \lim_{\xi\to\pi^-}\lim_{\theta\to\theta_{c_4}^+} \frac{\partial K_1}{\partial\theta}(\theta,\xi).
\end{aligned} \tag{E.127}
$$

The boundary integral equations (E.114)-(E.127) is a system of 14 equations for the 14 unknown boundary values $T(0)$, θ_{c_1}, $\frac{\partial T}{\partial\theta}(\theta_{c_1})$, $T(\theta_{l_1})$, $\frac{\partial T}{\partial\theta}(\theta_{l_1})$, θ_{c_2}, $\frac{\partial T}{\partial\theta}(\theta_{c_2})$, θ_{c_3}, $\frac{\partial T}{\partial\theta}(\theta_{c_3})$, $T(\theta_{l_2})$, $\frac{\partial T}{\partial\theta}(\theta_{l_2})$, θ_{c_4}, $\frac{\partial T}{\partial\theta}(\theta_{c_3})$ and $T(\pi)$. To solve this system we algebraically combine equation (E.114)-(E.127) to create four functions;

$$
\begin{aligned}
f_1 &= f_1(\theta_{c_1},\theta_{c_2},\theta_{c_3},\theta_{c_4}), \\
f_2 &= f_2(\theta_{c_1},\theta_{c_2},\theta_{c_3},\theta_{c_4}), \\
f_3 &= f_3(\theta_{c_1},\theta_{c_2},\theta_{c_3},\theta_{c_4}), \\
f_4 &= f_4(\theta_{c_1},\theta_{c_2},\theta_{c_3},\theta_{c_4}).
\end{aligned} \tag{E.128}
$$

These functions are extremely complicated and in order to find the four roots, θ_{c_1}, θ_{c_2}, θ_{c_3} and θ_{c_4}, we evaluate the functions on a grid to create four interpolation functions and then apply Newton's iteration. Once θ_{c_1}, θ_{c_2}, θ_{c_3} and θ_{c_4} are known, it is trivial to find the remaining boundary values $T(0)$, $\frac{\partial T}{\partial\theta}(\theta_{c_1})$, $T(\theta_{l_1})$, $\frac{\partial T}{\partial\theta}(\theta_{l_1})$, $\frac{\partial T}{\partial\theta}(\theta_{c_2})$, $\frac{\partial T}{\partial\theta}(\theta_{c_3})$, $T(\theta_{l_2})$, $\frac{\partial T}{\partial\theta}(\theta_{l_2})$, $\frac{\partial T}{\partial\theta}(\theta_{c_3})$ and $T(\pi)$. The solution in the regions I-VII is given by the integral relations (E.107)-(E.113), respectively.

E.5 The case of six ice edges

The case of six ice edges is realized in one of two ways; either the northern and southern tips of the continent is covered in ice/snow or the northern and southern tips of the continent is ice/snow free. Let us first consider the scenario where the northern and southern tips of the continent is covered in ice/snow. For this scenario two of the ice edges must necessarily be at

$$\theta_{c_2} = \theta_{l_1}$$

and

$$\theta_{c_5} = \theta_{l_2}.$$

As we have see above, knowing the location of some of the ice edges greatly reduced the complexity of the problem and in no other case is that more apparent than in the six ice edges case. As we will soon discover, having to locate six ice edges is complicated and requires solving a system of 18 nonlinear equations.

For the scenario where the northern and southern tips of the continent is covered in ice/snow we have to locate four ice edges and the process of finding a stationary solution will therefore be analogous to what we saw above for the four ice edges case. We divide the domain into seven regions;

$$\theta \in (0, \theta_{c_1}), \tag{I}$$

$$\theta \in (\theta_{c_1}, \theta_{l_1}), \tag{II}$$

$$\theta \in (\theta_{l_1}, \theta_{c_3}), \tag{III}$$

$$\theta \in (\theta_{c_3}, \theta_{c_4}), \tag{IV}$$

$$\theta \in (\theta_{c_4}, \theta_{l_2}), \tag{V}$$

$$\theta \in (\theta_{l_2}, \theta_{c_6}), \tag{VI}$$

$$\theta \in (\theta_{c_6}, \pi). \tag{VII}$$

The governing equations in the seven regions are

$$\mathcal{L}_1 T = h_2$$

in region I,

$$\mathcal{L}_1 T = h_1$$

in region II,

$$\mathcal{L}_2 T = h_4$$

in region III,

$$\mathcal{L}_2 T = h_3$$

in region IV,

$$\mathcal{L}_2 T = h_4$$

in region V,

$$\mathcal{L}_1 T = h_1$$

in region VI and

$$\mathcal{L}_1 T = h_2$$

in region VII. Applying the general integral relations (E.6) and (E.7) in the respective regions we get

$$\begin{aligned} T(\xi) = &\int_0^{\theta_{c_1}} d\theta \ \sin\theta \, K_1(\theta,\xi) h_2(\theta) + K_1(\theta_{c_1},\xi)\sin(\theta_{c_1})\frac{\partial T}{\partial\theta}(\theta_{c_1}) \\ &+ \sin(\theta_{c_1}) \lim_{\theta\to\theta_{c_1}^-} \frac{\partial K_1}{\partial\theta}(\theta,\xi) \end{aligned} \tag{E.129}$$

in region I,

$$\begin{aligned} T(\xi) = &\int_{\theta_{c_1}}^{\theta_{l_1}} d\theta \ \sin\theta \, K_1(\theta,\xi) h_1(\theta) + K_1(\theta_{l_1},\xi)\sin(\theta_{l_1})\frac{\partial T}{\partial\theta}(\theta_{l_1}) \\ &- T(\theta_{l_1})\sin(\theta_{l_1}) \lim_{\theta\to\theta_{l_1}^-} \frac{\partial K_1}{\partial\theta}(\theta,\xi) - K_1(\theta_{c_1},\xi)\sin(\theta_{c_1})\frac{\partial T}{\partial\theta}(\theta_{c_1}) \\ &- \sin(\theta_{c_1}) \lim_{\theta\to\theta_{c_1}^+} \frac{\partial K_1}{\partial\theta}(\theta,\xi) \end{aligned} \tag{E.130}$$

in region II,

$$\begin{aligned} T(\xi) = &\int_{\theta_{l_1}}^{\theta_{c_3}} d\theta \ \sin\theta \, K_2(\theta,\xi) h_4(\theta) + K_2(\theta_{c_3},\xi)\sin(\theta_{c_3})\frac{\partial T}{\partial\theta}(\theta_{c_3}) \\ &+ T_c \sin(\theta_{c_3}) \lim_{\theta\to\theta_{c_3}^-} \frac{\partial K_2}{\partial\theta}(\theta,\xi) - K_2(\theta_{l_1},\xi)\sin(\theta_{l_1})\frac{\partial T}{\partial\theta}(\theta_{l_1}) \\ &+ T(\theta_{l_1})\sin(\theta_{l_1}) \lim_{\theta\to\theta_{l_1}^+} \frac{\partial K_2}{\partial\theta}(\theta,\xi) \end{aligned} \tag{E.131}$$

in region III,

$$\begin{aligned} T(\xi) = &\int_{\theta_{c_3}}^{\theta_{c_4}} d\theta \ \sin\theta \, K_2(\theta,\xi) h_3(\theta) + K_2(\theta_{c_4},\xi)\sin(\theta_{c_4})\frac{\partial T}{\partial\theta}(\theta_{c_4}) \\ &+ T_c \sin(\theta_{c_4}) \lim_{\theta\to\theta_{c_4}^-} \frac{\partial K_2}{\partial\theta}(\theta,\xi) - K_2(\theta_{c_3},\xi)\sin(\theta_{c_3})\frac{\partial T}{\partial\theta}(\theta_{c_3}) \\ &- T_c \sin(\theta_{c_3}) \lim_{\theta\to\theta_{c_3}^+} \frac{\partial K_2}{\partial\theta}(\theta,\xi) \end{aligned} \tag{E.132}$$

in region IV,

$$\begin{aligned} T(\xi) = &\int_{\theta_{c_4}}^{\theta_{l_2}} d\theta \ \sin\theta \, K_2(\theta,\xi) h_4(\theta) + K_2(\theta_{l_2},\xi)\sin(\theta_{l_2})\frac{\partial T}{\partial\theta}(\theta_{l_2}) \\ &- T(\theta_{l_2})\sin(\theta_{l_2}) \lim_{\theta\to\theta_{l_2}^-} \frac{\partial K_2}{\partial\theta}(\theta,\xi) - K_2(\theta_{c_4},\xi)\sin(\theta_{c_4})\frac{\partial T}{\partial\theta}(\theta_{c_4}) \\ &- T_c \sin(\theta_{c_4}) \lim_{\theta\to\theta_{c_4}^+} \frac{\partial K_2}{\partial\theta}(\theta,\xi) \end{aligned} \tag{E.133}$$

in region V,

$$\begin{aligned} T(\xi) = &\int_{\theta_{l_2}}^{\theta_{c_6}} d\theta \ \sin\theta \, K_1(\theta,\xi) h_1(\theta) + K_1(\theta_{c_6},\xi)\sin(\theta_{c_6})\frac{\partial T}{\partial\theta}(\theta_{c_6}) \\ &+ \sin(\theta_{c_6}) \lim_{\theta\to\theta_{c_6}^-} \frac{\partial K_1}{\partial\theta}(\theta,\xi) - K_1(\theta_{l_2},\xi)\sin(\theta_{l_2})\frac{\partial T}{\partial\theta}(\theta_{l_2}) \\ &+ T(\theta_{l_2})\sin(\theta_{l_2}) \lim_{\theta\to\theta_{l_2}^+} \frac{\partial K_1}{\partial\theta}(\theta,\xi) \end{aligned} \tag{E.134}$$

in region VI and

$$\begin{aligned} T(\xi) = &\int_{\theta_{c_6}}^{\pi} d\theta \ \sin\theta \, K_1(\theta,\xi) h_2(\theta) - K_1(\theta_{c_6},\xi)\sin(\theta_{c_6})\frac{\partial T}{\partial\theta}(\theta_{c_6}) \\ &- \sin(\theta_{c_6}) \lim_{\theta\to\theta_{c_6}^+} \frac{\partial K_1}{\partial\theta}(\theta,\xi). \end{aligned} \tag{E.135}$$

in region VII. Equation (E.129)-(E.133) relates values of the solution inside the seven regions to several unknown boundary values. It should come as no surprise that we intend to find these

boundary values through solving the associated boundary integral equations;

$$T(0) = \int_0^{\theta_{c_1}} d\theta\ \sin\theta\, K_1(\theta,0)h_2(\theta) + K_1(\theta_{c_1},0)\sin(\theta_{c_1})\frac{\partial T}{\partial\theta}(\theta_{c_1}) + \sin(\theta_{c_1})\lim_{\xi\to 0^+}\lim_{\theta\to\theta_{c_1}^-}\frac{\partial K_1}{\partial\theta}(\theta,\xi) \tag{E.136}$$

$$-1 = \int_0^{\theta_{c_1}} d\theta\ \sin\theta\, K_1(\theta,\theta_{c_1})h_2(\theta) + \lim_{\xi\to\theta_{c_1}^-} K_1(\theta_{c_1},\xi)\sin(\theta_{c_1})\frac{\partial T}{\partial\theta}(\theta_{c_1}) + \sin(\theta_{c_1})\lim_{\xi\to\theta_{c_1}^-}\lim_{\theta\to\theta_{c_1}^-}\frac{\partial K_1}{\partial\theta}(\theta,\xi) \tag{E.137}$$

$$-1 = \int_{\theta_{c_1}}^{\theta_{l_1}} d\theta\ \sin\theta\, K_1(\theta,\theta_{c_1})h_1(\theta) + K_1(\theta_{l_1},\theta_{c_1})\sin(\theta_{l_1})\frac{\partial T}{\partial\theta}(\theta_{l_1}) - T(\theta_{l_1})\sin(\theta_{l_1})\lim_{\xi\to\theta_{c_1}^+}\lim_{\theta\to\theta_{l_1}^-}\frac{\partial K_1}{\partial\theta}(\theta,\xi) - \lim_{\xi\to\theta_{c_1}^+} K_1(\theta_{c_1},\xi)\sin(\theta_{c_1})\frac{\partial T}{\partial\theta}(\theta_{c_1}) - \sin(\theta_{c_1})\lim_{\xi\to\theta_{c_1}^+}\lim_{\theta\to\theta_{c_1}^+}\frac{\partial K_1}{\partial\theta}(\theta,\xi) \tag{E.138}$$

$$T(\theta_{l_1}) = \int_{\theta_{c_1}}^{\theta_{l_1}} d\theta\ \sin\theta\, K_1(\theta,\theta_{l_1})h_1(\theta) + \lim_{\xi\to\theta_{l_1}^-} K_1(\theta_{l_1},\xi)\sin(\theta_{l_1})\frac{\partial T}{\partial\theta}(\theta_{l_1}) - T(\theta_{l_1})\sin(\theta_{l_1})\lim_{\xi\to\theta_{l_1}^-}\lim_{\theta\to\theta_{l_1}^-}\frac{\partial K_1}{\partial\theta}(\theta,\xi) - K_1(\theta_{c_1},\theta_{l_1})\sin(\theta_{c_1})\frac{\partial T}{\partial\theta}(\theta_{c_1}) - \sin(\theta_{c_1})\lim_{\xi\to\theta_{l_1}^-}\lim_{\theta\to\theta_{c_1}^+}\frac{\partial K_1}{\partial\theta}(\theta,\xi) \tag{E.139}$$

$$T(\theta_{l_1}) = \int_{\theta_{l_1}}^{\theta_{c_3}} d\theta\ \sin\theta\, K_2(\theta,\theta_{l_1})h_4(\theta) + K_2(\theta_{c_3},\theta_{l_1})\sin(\theta_{c_3})\frac{\partial T}{\partial\theta}(\theta_{c_3}) + T_c\sin(\theta_{c_3})\lim_{\xi\to\theta_{l_1}^+}\lim_{\theta\to\theta_{l_2}^-}\frac{\partial K_2}{\partial\theta}(\theta,\xi) - \lim_{\xi\to\theta_{l_1}^+} K_2(\theta_{l_1},\xi)\sin(\theta_{l_1})\frac{\partial T}{\partial\theta}(\theta_{l_1}) + T(\theta_{l_1})\sin(\theta_{l_1})\lim_{\xi\to\theta_{l_1}^+}\lim_{\theta\to\theta_{l_1}^+}\frac{\partial K_2}{\partial\theta}(\theta,\xi) \tag{E.140}$$

$$-T_c = \int_{\theta_{l_1}}^{\theta_{c_3}} d\theta\ \sin\theta\, K_2(\theta,\theta_{c_3})h_4(\theta) + \lim_{\xi\to\theta_{c_3}^-} K_2(\theta_{c_3},\xi)\sin(\theta_{c_3})\frac{\partial T}{\partial\theta}(\theta_{c_3}) + T_c\sin(\theta_{c_3})\lim_{\xi\to\theta_{c_3}^-}\lim_{\theta\to\theta_{c_3}^-}\frac{\partial K_2}{\partial\theta}(\theta,\xi) - K_2(\theta_{l_1},\theta_{c_3})\sin(\theta_{l_1})\frac{\partial T}{\partial\theta}(\theta_{l_1}) + T(\theta_{l_1})\sin(\theta_{l_1})\lim_{\xi\to\theta_{c_3}^-}\lim_{\theta\to\theta_{l_1}^+}\frac{\partial K_2}{\partial\theta}(\theta,\xi) \tag{E.141}$$

$$
\begin{aligned}
-T_c = &\int_{\theta_{c_3}}^{\theta_{c_4}} d\theta\ \sin\theta\, K_2(\theta,\theta_{c_3})h_3(\theta) + K_2(\theta_{c_4},\theta_{c_3})\sin(\theta_{c_4})\frac{\partial T}{\partial\theta}(\theta_{c_4}) \\
&+ T_c\sin(\theta_{c_4})\lim_{\xi\to\theta_{c_3}^+}\lim_{\theta\to\theta_{c_4}^-}\frac{\partial K_2}{\partial\theta}(\theta,\xi) - \lim_{\xi\to\theta_{c_3}^+}K_2(\theta_{c_3},\xi)\sin(\theta_{c_3})\frac{\partial T}{\partial\theta}(\theta_{c_3}) \\
&- T_c\sin(\theta_{c_3})\lim_{\xi\to\theta_{c_3}^+}\lim_{\theta\to\theta_{c_3}^+}\frac{\partial K_2}{\partial\theta}(\theta,\xi)
\end{aligned}
\tag{E.142}
$$

$$
\begin{aligned}
-T_c = &\int_{\theta_{c_3}}^{\theta_{c_4}} d\theta\ \sin\theta\, K_2(\theta,\theta_{c_4})h_3(\theta) + \lim_{\xi\to\theta_{c_4}^-}K_2(\theta_{c_4},\xi)\sin(\theta_{c_4})\frac{\partial T}{\partial\theta}(\theta_{c_4}) \\
&+ T_c\sin(\theta_{c_4})\lim_{\xi\to\theta_{c_4}^-}\lim_{\theta\to\theta_{c_4}^-}\frac{\partial K_2}{\partial\theta}(\theta,\xi) - K_2(\theta_{c_3},\theta_{c_4})\sin(\theta_{c_3})\frac{\partial T}{\partial\theta}(\theta_{c_3}) \\
&- T_c\sin(\theta_{c_3})\lim_{\xi\to\theta_{c_4}^-}\lim_{\theta\to\theta_{c_3}^+}\frac{\partial K_2}{\partial\theta}(\theta,\xi)
\end{aligned}
\tag{E.143}
$$

$$
\begin{aligned}
-T_c = &\int_{\theta_{c_4}}^{\theta_{l_2}} d\theta\ \sin\theta\, K_2(\theta,\theta_{c_4})h_4(\theta) + K_2(\theta_{l_2},\theta_{c_4})\sin(\theta_{l_2})\frac{\partial T}{\partial\theta}(\theta_{l_2}) \\
&- T(\theta_{l_2})\sin(\theta_{l_2})\lim_{\xi\to\theta_{c_4}^+}\lim_{\theta\to\theta_{l_2}^-}\frac{\partial K_2}{\partial\theta}(\theta,\xi) - \lim_{\xi\to\theta_{c_4}^+}K_2(\theta_{c_4},\xi)\sin(\theta_{c_4})\frac{\partial T}{\partial\theta}(\theta_{c_4}) \\
&- T_c\sin(\theta_{c_4})\lim_{\xi\to\theta_{c_4}^+}\lim_{\theta\to\theta_{c_4}^+}\frac{\partial K_2}{\partial\theta}(\theta,\xi)
\end{aligned}
\tag{E.144}
$$

$$
\begin{aligned}
T(\theta_{l_2}) = &\int_{\theta_{c_4}}^{\theta_{l_2}} d\theta\ \sin\theta\, K_2(\theta,\theta_{l_2})h_4(\theta) + \lim_{\xi\to\theta_{l_2}^-}K_2(\theta_{l_2},\xi)\sin(\theta_{l_2})\frac{\partial T}{\partial\theta}(\theta_{l_2}) \\
&- T(\theta_{l_2})\sin(\theta_{l_2})\lim_{\xi\to\theta_{l_2}^-}\lim_{\theta\to\theta_{l_2}^-}\frac{\partial K_2}{\partial\theta}(\theta,\xi) - K_2(\theta_{c_4},\theta_{l_2})\sin(\theta_{c_4})\frac{\partial T}{\partial\theta}(\theta_{c_4}) \\
&- T_c\sin(\theta_{c_4})\lim_{\xi\to\theta_{l_2}^-}\lim_{\theta\to\theta_{c_4}^+}\frac{\partial K_2}{\partial\theta}(\theta,\xi)
\end{aligned}
\tag{E.145}
$$

$$
\begin{aligned}
T(\theta_{l_2}) = &\int_{\theta_{l_2}}^{\theta_{c_6}} d\theta\ \sin\theta\, K_1(\theta,\theta_{l_2})h_1(\theta) + K_1(\theta_{c_6},\theta_{l_2})\sin(\theta_{c_6})\frac{\partial T}{\partial\theta}(\theta_{c_6}) \\
&+ \sin(\theta_{c_6})\lim_{\xi\to\theta_{l_2}^+}\lim_{\theta\to\theta_{c_6}^-}\frac{\partial K_1}{\partial\theta}(\theta,\xi) - \lim_{\xi\to\theta_{l_2}^+}K_1(\theta_{l_2},\xi)\sin(\theta_{l_2})\frac{\partial T}{\partial\theta}(\theta_{l_2}) \\
&+ T(\theta_{l_2})\sin(\theta_{l_2})\lim_{\xi\to\theta_{l_2}^+}\lim_{\theta\to\theta_{l_2}^+}\frac{\partial K_1}{\partial\theta}(\theta,\xi)
\end{aligned}
\tag{E.146}
$$

$$
\begin{aligned}
-1 = &\int_{\theta_{l_2}}^{\theta_{c_6}} d\theta\ \sin\theta\, K_1(\theta,\theta_{c_6})h_1(\theta) + \lim_{\xi\to\theta_{c_6}^-}K_1(\theta_{c_6},\xi)\sin(\theta_{c_6})\frac{\partial T}{\partial\theta}(\theta_{c_6}) \\
&+ \sin(\theta_{c_6})\lim_{\xi\to\theta_{c_6}^-}\lim_{\theta\to\theta_{c_6}^-}\frac{\partial K_1}{\partial\theta}(\theta,\xi) - K_1(\theta_{l_2},\theta_{c_6})\sin(\theta_{l_2})\frac{\partial T}{\partial\theta}(\theta_{l_2}) \\
&+ T(\theta_{l_2})\sin(\theta_{l_2})\lim_{\xi\to\theta_{c_6}^-}\lim_{\theta\to\theta_{l_2}^+}\frac{\partial K_1}{\partial\theta}(\theta,\xi)
\end{aligned}
\tag{E.147}
$$

$$
\begin{aligned}
-1 = &\int_{\theta_{c_6}}^{\pi} d\theta\ \sin\theta\, K_1(\theta,\theta_{c_6})h_2(\theta) - \lim_{\xi\to\theta_{c_6}^+}K_1(\theta_{c_6},\xi)\sin(\theta_{c_6})\frac{\partial T}{\partial\theta}(\theta_{c_6}) \\
&- \sin(\theta_{c_6})\lim_{\xi\to\theta_{c_6}^+}\lim_{\theta\to\theta_{c_6}^+}\frac{\partial K_1}{\partial\theta}(\theta,\xi)
\end{aligned}
\tag{E.148}
$$

$$T(\pi) = \int_{\theta_{c_6}}^{\pi} d\theta \, \sin\theta \, K_1(\theta,\pi)h_2(\theta) - K_1(\theta_{c_6},\pi)\sin(\theta_{c_6})\frac{\partial T}{\partial\theta}(\theta_{c_6}) \\ - \sin(\theta_{c_6}) \lim_{\xi\to\pi^-} \lim_{\theta\to\theta_{c_6}^+} \frac{\partial K_1}{\partial\theta}(\theta,\xi). \tag{E.149}$$

The boundary integral equations (E.136)-(E.149) is a system of 14 equations for the 14 unknown boundary values $T(0)$, θ_{c_1}, $\frac{\partial T}{\partial\theta}(\theta_{c_1})$, $T(\theta_{l_1})$, $\frac{\partial T}{\partial\theta}(\theta_{l_1})$, θ_{c_3}, $\frac{\partial T}{\partial\theta}(\theta_{c_3})$, θ_{c_4}, $\frac{\partial T}{\partial\theta}(\theta_{c_4})$, $T(\theta_{l_2})$, $\frac{\partial T}{\partial\theta}(\theta_{l_2})$, θ_{c_6}, $\frac{\partial T}{\partial\theta}(\theta_{c_6})$ and $T(\pi)$. We solve this system of equations in the exact same way as we did above for the four ice edge case. Once we have found all the unknown boundary values the solution in the regions I-VII is given by the integral relations (E.129)-(E.135), respectively.

For the scenario where the northern and southern tips of the continent is ice/snow free we have to locate all six ice edges through solving the boundary integral equations. For this scenario we have nine relevant regions;

$$\theta \in (0, \theta_{c_1}) \tag{I}$$

$$\theta \in (\theta_{c_1}, \theta_{l_1}) \tag{II}$$

$$\theta \in (\theta_{l_1}, \theta_{c_2}) \tag{III}$$

$$\theta \in (\theta_{c_2}, \theta_{c_3}) \tag{IV}$$

$$\theta \in (\theta_{c_3}, \theta_{c_4}) \tag{V}$$

$$\theta \in (\theta_{c_4}, \theta_{c_5}) \tag{VI}$$

$$\theta \in (\theta_{c_5}, \theta_{l_2}) \tag{VII}$$

$$\theta \in (\theta_{l_2}, \theta_{c_6}) \tag{VIII}$$

$$\theta \in (\theta_{c_4}, \pi). \tag{IX}$$

The governing equations in these regions are

$$\mathcal{L}_1 T = h_2$$

in region I,

$$\mathcal{L}_1 T = h_1$$

in region II,

$$\mathcal{L}_2 T = h_3$$

in region III,

$$\mathcal{L}_2 T = h_4$$

in region IV,

$$\mathcal{L}_2 T = h_3$$

in region V,

$$\mathcal{L}_2 T = h_4$$

in region VI and

$$\mathcal{L}_2 T = h_3$$

in region VII,

$$\mathcal{L}_1 T = h_1$$

in region VIII and

$$\mathcal{L}_1 T = h_2$$

in region IX. Applying the general integral relations (E.6) and (E.7) in the respective regions we get

$$\begin{aligned} T(\xi) = &\int_0^{\theta_{c_1}} d\theta \ \sin\theta \, K_1(\theta,\xi) h_2(\theta) + K_1(\theta_{c_1},\xi)\sin(\theta_{c_1})\frac{\partial T}{\partial \theta}(\theta_{c_1}) \\ &+ \sin(\theta_{c_1}) \lim_{\theta \to \theta_{c_1}^-} \frac{\partial K_1}{\partial \theta}(\theta,\xi) \end{aligned} \tag{E.150}$$

in region I,

$$\begin{aligned} T(\xi) = &\int_{\theta_{c_1}}^{\theta_{l_1}} d\theta \ \sin\theta \, K_1(\theta,\xi) h_1(\theta) + K_1(\theta_{l_1},\xi)\sin(\theta_{l_1})\frac{\partial T}{\partial \theta}(\theta_{l_1}) \\ &- T(\theta_{l_1})\sin(\theta_{l_1}) \lim_{\theta \to \theta_{l_1}^-} \frac{\partial K_1}{\partial \theta}(\theta,\xi) - K_1(\theta_{c_1},\xi)\sin(\theta_{c_1})\frac{\partial T}{\partial \theta}(\theta_{c_1}) \\ &- \sin(\theta_{c_1}) \lim_{\theta \to \theta_{c_1}^+} \frac{\partial K_1}{\partial \theta}(\theta,\xi) \end{aligned} \tag{E.151}$$

in region II,

$$\begin{aligned} T(\xi) = &\int_{\theta_{l_1}}^{\theta_{c_2}} d\theta\ \sin\theta\, K_2(\theta,\xi)h_3(\theta) + K_2(\theta_{c_2},\xi)\sin(\theta_{c_2})\frac{\partial T}{\partial\theta}(\theta_{c_2}) \\ &+ T_c\sin(\theta_{c_2})\lim_{\theta\to\theta_{c_2}^-}\frac{\partial K_2}{\partial\theta}(\theta,\xi) - K_2(\theta_{l_1},\xi)\sin(\theta_{l_1})\frac{\partial T}{\partial\theta}(\theta_{l_1}) \\ &+ T(\theta_{l_1})\sin(\theta_{l_1})\lim_{\theta\to\theta_{l_1}^+}\frac{\partial K_2}{\partial\theta}(\theta,\xi) \end{aligned} \tag{E.152}$$

in region III,

$$\begin{aligned} T(\xi) = &\int_{\theta_{c_2}}^{\theta_{c_3}} d\theta\ \sin\theta\, K_2(\theta,\xi)h_4(\theta) + K_2(\theta_{c_3},\xi)\sin(\theta_{c_3})\frac{\partial T}{\partial\theta}(\theta_{c_3}) \\ &+ T_c\sin(\theta_{c_3})\lim_{\theta\to\theta_{c_3}^-}\frac{\partial K_2}{\partial\theta}(\theta,\xi) - K_2(\theta_{c_2},\xi)\sin(\theta_{c_2})\frac{\partial T}{\partial\theta}(\theta_{c_2}) \\ &- T_c\sin(\theta_{c_2})\lim_{\theta\to\theta_{c_2}^+}\frac{\partial K_2}{\partial\theta}(\theta,\xi) \end{aligned} \tag{E.153}$$

in region IV,

$$\begin{aligned} T(\xi) = &\int_{\theta_{c_3}}^{\theta_{c_4}} d\theta\ \sin\theta\, K_2(\theta,\xi)h_3(\theta) + K_2(\theta_{c_4},\xi)\sin(\theta_{c_4})\frac{\partial T}{\partial\theta}(\theta_{c_4}) \\ &+ T_c\sin(\theta_{c_4})\lim_{\theta\to\theta_{c_4}^-}\frac{\partial K_2}{\partial\theta}(\theta,\xi) - K_2(\theta_{c_3},\xi)\sin(\theta_{c_3})\frac{\partial T}{\partial\theta}(\theta_{c_3}) \\ &- T_c\sin(\theta_{c_3})\lim_{\theta\to\theta_{c_3}^+}\frac{\partial K_2}{\partial\theta}(\theta,\xi) \end{aligned} \tag{E.154}$$

in region V,

$$\begin{aligned} T(\xi) = &\int_{\theta_{c_4}}^{\theta_{c_5}} d\theta\ \sin\theta\, K_2(\theta,\xi)h_4(\theta) + K_2(\theta_{c_5},\xi)\sin(\theta_{c_5})\frac{\partial T}{\partial\theta}(\theta_{c_5}) \\ &+ T_c\sin(\theta_{c_5})\lim_{\theta\to\theta_{c_5}^-}\frac{\partial K_2}{\partial\theta}(\theta,\xi) - K_2(\theta_{c_4},\xi)\sin(\theta_{c_4})\frac{\partial T}{\partial\theta}(\theta_{c_4}) \\ &- T_c\sin(\theta_{c_4})\lim_{\theta\to\theta_{c_4}^+}\frac{\partial K_2}{\partial\theta}(\theta,\xi) \end{aligned} \tag{E.155}$$

in region VI,

$$\begin{aligned} T(\xi) = &\int_{\theta_{c_5}}^{\theta_{l_2}} d\theta \ \sin\theta \, K_2(\theta,\xi) h_3(\theta) + K_2(\theta_{l_2},\xi)\sin(\theta_{l_2})\frac{\partial T}{\partial\theta}(\theta_{l_2}) \\ &- T(\theta_{l_2})\sin(\theta_{l_2}) \lim_{\theta\to\theta_{l_2}^-} \frac{\partial K_2}{\partial\theta}(\theta,\xi) - K_2(\theta_{c_5},\xi)\sin(\theta_{c_5})\frac{\partial T}{\partial\theta}(\theta_{c_5}) \\ &- T_c \sin(\theta_{c_5}) \lim_{\theta\to\theta_{c_5}^+} \frac{\partial K_2}{\partial\theta}(\theta,\xi) \end{aligned} \tag{E.156}$$

in region VII,

$$\begin{aligned} T(\xi) = &\int_{\theta_{l_2}}^{\theta_{c_6}} d\theta \ \sin\theta \, K_1(\theta,\xi) h_1(\theta) + K_1(\theta_{c_6},\xi)\sin(\theta_{c_6})\frac{\partial T}{\partial\theta}(\theta_{c_6}) \\ &+ \sin(\theta_{c_6}) \lim_{\theta\to\theta_{c_6}^-} \frac{\partial K_1}{\partial\theta}(\theta,\xi) - K_1(\theta_{l_2},\xi)\sin(\theta_{l_2})\frac{\partial T}{\partial\theta}(\theta_{l_2}) \\ &+ T(\theta_{l_2})\sin(\theta_{l_2}) \lim_{\theta\to\theta_{l_2}^+} \frac{\partial K_1}{\partial\theta}(\theta,\xi) \end{aligned} \tag{E.157}$$

in region VIII and

$$\begin{aligned} T(\xi) = &\int_{\theta_{c_6}}^{\pi} d\theta \ \sin\theta \, K_1(\theta,\xi) h_2(\theta) - K_1(\theta_{c_6},\xi)\sin(\theta_{c_6})\frac{\partial T}{\partial\theta}(\theta_{c_6}) \\ &- \sin(\theta_{c_6}) \lim_{\theta\to\theta_{c_6}^+} \frac{\partial K_1}{\partial\theta}(\theta,\xi). \end{aligned} \tag{E.158}$$

in region IX. Equation (E.107)-(E.111) relates values of the solution inside the nine regions to certain unknown boundary values. These boundary values are once again obtained by solving the boundary integral equations. We derive the boundary integral equations by letting ξ approach the boundaries of the-sub domains I-IX, and the resulting boundary integral equations are;

$$\begin{aligned} T(0) = &\int_0^{\theta_{c_1}} d\theta \ \sin\theta \, K_1(\theta,0) h_2(\theta) + K_1(\theta_{c_1},0)\sin(\theta_{c_1})\frac{\partial T}{\partial\theta}(\theta_{c_1}) \\ &+ \sin(\theta_{c_1}) \lim_{\xi\to 0^+} \lim_{\theta\to\theta_{c_1}^-} \frac{\partial K_1}{\partial\theta}(\theta,\xi) \end{aligned} \tag{E.159}$$

$$\begin{aligned} -1 = &\int_0^{\theta_{c_1}} d\theta \ \sin\theta \, K_1(\theta,\theta_{c_1}) h_2(\theta) + \lim_{\xi\to\theta_{c_1}^-} K_1(\theta_{c_1},\xi)\sin(\theta_{c_1})\frac{\partial T}{\partial\theta}(\theta_{c_1}) \\ &+ \sin(\theta_{c_1}) \lim_{\xi\to\theta_{c_1}^-} \lim_{\theta\to\theta_{c_1}^-} \frac{\partial K_1}{\partial\theta}(\theta,\xi) \end{aligned} \tag{E.160}$$

$$
\begin{aligned}
-1 = &\int_{\theta_{c_1}}^{\theta_{l_1}} d\theta\ \sin\theta\, K_1(\theta,\theta_{c_1})h_1(\theta) + K_1(\theta_{l_1},\theta_{c_1})\sin(\theta_{l_1})\frac{\partial T}{\partial\theta}(\theta_{l_1}) \\
&- T(\theta_{l_1})\sin(\theta_{l_1}) \lim_{\xi\to\theta_{c_1}^+}\lim_{\theta\to\theta_{l_1}^-}\frac{\partial K_1}{\partial\theta}(\theta,\xi) - \lim_{\xi\to\theta_{c_1}^+} K_1(\theta_{c_1},\xi)\sin(\theta_{c_1})\frac{\partial T}{\partial\theta}(\theta_{c_1}) \\
&- \sin(\theta_{c_1}) \lim_{\xi\to\theta_{c_1}^+}\lim_{\theta\to\theta_{c_1}^+}\frac{\partial K_1}{\partial\theta}(\theta,\xi)
\end{aligned} \tag{E.161}
$$

$$
\begin{aligned}
T(\theta_{l_1}) = &\int_{\theta_{c_1}}^{\theta_{l_1}} d\theta\ \sin\theta\, K_1(\theta,\theta_{l_1})h_1(\theta) + \lim_{\xi\to\theta_{l_1}^-} K_1(\theta_{l_1},\xi)\sin(\theta_{l_1})\frac{\partial T}{\partial\theta}(\theta_{l_1}) \\
&- T(\theta_{l_1})\sin(\theta_{l_1}) \lim_{\xi\to\theta_{l_1}^-}\lim_{\theta\to\theta_{l_1}^-}\frac{\partial K_1}{\partial\theta}(\theta,\xi) - K_1(\theta_{c_1},\theta_{l_1})\sin(\theta_{c_1})\frac{\partial T}{\partial\theta}(\theta_{c_1}) \\
&- \sin(\theta_{c_1}) \lim_{\xi\to\theta_{l_1}^-}\lim_{\theta\to\theta_{c_1}^+}\frac{\partial K_1}{\partial\theta}(\theta,\xi)
\end{aligned} \tag{E.162}
$$

$$
\begin{aligned}
T(\theta_{l_1}) = &\int_{\theta_{l_1}}^{\theta_{c_2}} d\theta\ \sin\theta\, K_2(\theta,\theta_{l_1})h_3(\theta) + K_2(\theta_{c_2},\theta_{l_1})\sin(\theta_{c_2})\frac{\partial T}{\partial\theta}(\theta_{c_2}) \\
&+ T_c\sin(\theta_{c_2}) \lim_{\xi\to\theta_{l_1}^+}\lim_{\theta\to\theta_{l_2}^-}\frac{\partial K_2}{\partial\theta}(\theta,\xi) - \lim_{\xi\to\theta_{l_1}^+} K_2(\theta_{l_1},\xi)\sin(\theta_{l_1})\frac{\partial T}{\partial\theta}(\theta_{l_1}) \\
&+ T(\theta_{l_1})\sin(\theta_{l_1}) \lim_{\xi\to\theta_{l_1}^+}\lim_{\theta\to\theta_{l_1}^+}\frac{\partial K_2}{\partial\theta}(\theta,\xi)
\end{aligned} \tag{E.163}
$$

$$
\begin{aligned}
-T_c = &\int_{\theta_{l_1}}^{\theta_{c_2}} d\theta\ \sin\theta\, K_2(\theta,\theta_{c_2})h_3(\theta) + \lim_{\xi\to\theta_{c_2}^-} K_2(\theta_{c_2},\xi)\sin(\theta_{c_2})\frac{\partial T}{\partial\theta}(\theta_{c_2}) \\
&+ T_c\sin(\theta_{c_2}) \lim_{\xi\to\theta_{c_2}^-}\lim_{\theta\to\theta_{c_2}^-}\frac{\partial K_2}{\partial\theta}(\theta,\xi) - K_2(\theta_{l_1},\theta_{c_2})\sin(\theta_{l_1})\frac{\partial T}{\partial\theta}(\theta_{l_1}) \\
&+ T(\theta_{l_1})\sin(\theta_{l_1}) \lim_{\xi\to\theta_{c_2}^-}\lim_{\theta\to\theta_{l_1}^+}\frac{\partial K_2}{\partial\theta}(\theta,\xi)
\end{aligned} \tag{E.164}
$$

$$
\begin{aligned}
-T_c = &\int_{\theta_{c_2}}^{\theta_{c_3}} d\theta\ \sin\theta\, K_2(\theta,\theta_{c_2})h_4(\theta) + K_2(\theta_{c_3},\theta_{c_2})\sin(\theta_{c_3})\frac{\partial T}{\partial\theta}(\theta_{c_3}) \\
&+ T_c\sin(\theta_{c_3}) \lim_{\xi\to\theta_{c_2}^+}\lim_{\theta\to\theta_{c_3}^-}\frac{\partial K_2}{\partial\theta}(\theta,\xi) - \lim_{\xi\to\theta_{c_2}^+} K_2(\theta_{c_2},\xi)\sin(\theta_{c_2})\frac{\partial T}{\partial\theta}(\theta_{c_2}) \\
&- T_c\sin(\theta_{c_2}) \lim_{\xi\to\theta_{c_2}^+}\lim_{\theta\to\theta_{c_2}^+}\frac{\partial K_2}{\partial\theta}(\theta,\xi)
\end{aligned} \tag{E.165}
$$

$$
\begin{aligned}
-T_c = &\int_{\theta_{c_2}}^{\theta_{c_3}} d\theta\ \sin\theta\, K_2(\theta,\theta_{c_3})h_4(\theta) + \lim_{\xi\to\theta_{c_3}^-} K_2(\theta_{c_3},\xi)\sin(\theta_{c_3})\frac{\partial T}{\partial\theta}(\theta_{c_3}) \\
&+ T_c\sin(\theta_{c_3}) \lim_{\xi\to\theta_{c_3}^-}\lim_{\theta\to\theta_{c_3}^-}\frac{\partial K_2}{\partial\theta}(\theta,\xi) - K_2(\theta_{c_2},\theta_{c_3})\sin(\theta_{c_2})\frac{\partial T}{\partial\theta}(\theta_{c_2}) \\
&- T_c\sin(\theta_{c_2}) \lim_{\xi\to\theta_{c_3}^-}\lim_{\theta\to\theta_{c_2}^+}\frac{\partial K_2}{\partial\theta}(\theta,\xi)
\end{aligned} \tag{E.166}
$$

$$
\begin{aligned}
-T_c = &\int_{\theta_{c_3}}^{\theta_{c_4}} d\theta\ \sin\theta\, K_2(\theta,\theta_{c_3})h_3(\theta) + K_2(\theta_{c_4},\theta_{c_3})\sin(\theta_{c_4})\frac{\partial T}{\partial\theta}(\theta_{c_4}) \\
&+ T_c\sin(\theta_{c_4})\lim_{\xi\to\theta_{c_3}^+}\lim_{\theta\to\theta_{c_4}^-}\frac{\partial K_2}{\partial\theta}(\theta,\xi) - \lim_{\xi\to\theta_{c_3}^+}K_2(\theta_{c_3},\xi)\sin(\theta_{c_3})\frac{\partial T}{\partial\theta}(\theta_{c_3}) \\
&- T_c\sin(\theta_{c_3})\lim_{\xi\to\theta_{c_3}^+}\lim_{\theta\to\theta_{c_3}^+}\frac{\partial K_2}{\partial\theta}(\theta,\xi)
\end{aligned}
\tag{E.167}
$$

$$
\begin{aligned}
-T_c = &\int_{\theta_{c_3}}^{\theta_{c_4}} d\theta\ \sin\theta\, K_2(\theta,\theta_{c_4})h_3(\theta) + \lim_{\xi\to\theta_{c_4}^-}K_2(\theta_{c_4},\xi)\sin(\theta_{c_4})\frac{\partial T}{\partial\theta}(\theta_{c_4}) \\
&+ T_c\sin(\theta_{c_4})\lim_{\xi\to\theta_{c_4}^-}\lim_{\theta\to\theta_{c_4}^-}\frac{\partial K_2}{\partial\theta}(\theta,\xi) - K_2(\theta_{c_3},\theta_{c_4})\sin(\theta_{c_3})\frac{\partial T}{\partial\theta}(\theta_{c_3}) \\
&- T_c\sin(\theta_{c_3})\lim_{\xi\to\theta_{c_4}^-}\lim_{\theta\to\theta_{c_3}^+}\frac{\partial K_2}{\partial\theta}(\theta,\xi)
\end{aligned}
\tag{E.168}
$$

$$
\begin{aligned}
-T_c = &\int_{\theta_{c_4}}^{\theta_{c_5}} d\theta\ \sin\theta\, K_2(\theta,\theta_{c_4})h_4(\theta) + K_2(\theta_{c_5},\theta_{c_4})\sin(\theta_{c_5})\frac{\partial T}{\partial\theta}(\theta_{c_5}) \\
&+ T_c\sin(\theta_{c_5})\lim_{\xi\to\theta_{c_4}^+}\lim_{\theta\to\theta_{c_5}^-}\frac{\partial K_2}{\partial\theta}(\theta,\xi) - \lim_{\xi\to\theta_{c_4}^+}K_2(\theta_{c_4},\xi)\sin(\theta_{c_4})\frac{\partial T}{\partial\theta}(\theta_{c_4}) \\
&- T_c\sin(\theta_{c_4})\lim_{\xi\to\theta_{c_4}^+}\lim_{\theta\to\theta_{c_4}^+}\frac{\partial K_2}{\partial\theta}(\theta,\xi)
\end{aligned}
\tag{E.169}
$$

$$
\begin{aligned}
-T_c = &\int_{\theta_{c_4}}^{\theta_{c_5}} d\theta\ \sin\theta\, K_2(\theta,\theta_{c_5})h_4(\theta) + \lim_{\xi\to\theta_{c_5}^-}K_2(\theta_{c_5},\xi)\sin(\theta_{c_5})\frac{\partial T}{\partial\theta}(\theta_{c_5}) \\
&+ T_c\sin(\theta_{c_5})\lim_{\xi\to\theta_{c_5}^-}\lim_{\theta\to\theta_{c_5}^-}\frac{\partial K_2}{\partial\theta}(\theta,\xi) - K_2(\theta_{c_4},\theta_{c_5})\sin(\theta_{c_4})\frac{\partial T}{\partial\theta}(\theta_{c_4}) \\
&- T_c\sin(\theta_{c_4})\lim_{\xi\to\theta_{c_5}^-}\lim_{\theta\to\theta_{c_4}^+}\frac{\partial K_2}{\partial\theta}(\theta,\xi)
\end{aligned}
\tag{E.170}
$$

$$
\begin{aligned}
-T_c = &\int_{\theta_{c_5}}^{\theta_{l_2}} d\theta\ \sin\theta\, K_2(\theta,\theta_{c_5})h_3(\theta) + K_2(\theta_{l_2},\theta_{c_5})\sin(\theta_{l_2})\frac{\partial T}{\partial\theta}(\theta_{l_2}) \\
&- T(\theta_{l_2})\sin(\theta_{l_2})\lim_{\xi\to\theta_{c_5}^+}\lim_{\theta\to\theta_{l_2}^-}\frac{\partial K_2}{\partial\theta}(\theta,\xi) - \lim_{\xi\to\theta_{c_5}^+}K_2(\theta_{c_5},\xi)\sin(\theta_{c_5})\frac{\partial T}{\partial\theta}(\theta_{c_5}) \\
&- T_c\sin(\theta_{c_5})\lim_{\xi\to\theta_{c_5}^+}\lim_{\theta\to\theta_{c_5}^+}\frac{\partial K_2}{\partial\theta}(\theta,\xi)
\end{aligned}
\tag{E.171}
$$

$$
\begin{aligned}
T(\theta_{l_2}) = &\int_{\theta_{c_5}}^{\theta_{l_2}} d\theta\ \sin\theta\, K_2(\theta,\theta_{l_2})h_3(\theta) + \lim_{\xi\to\theta_{l_2}^-}K_2(\theta_{l_2},\xi)\sin(\theta_{l_2})\frac{\partial T}{\partial\theta}(\theta_{l_2}) \\
&- T(\theta_{l_2})\sin(\theta_{l_2})\lim_{\xi\to\theta_{l_2}^-}\lim_{\theta\to\theta_{l_2}^-}\frac{\partial K_2}{\partial\theta}(\theta,\xi) - K_2(\theta_{c_5},\theta_{l_2})\sin(\theta_{c_5})\frac{\partial T}{\partial\theta}(\theta_{c_5}) \\
&- T_c\sin(\theta_{c_5})\lim_{\xi\to\theta_{l_2}^-}\lim_{\theta\to\theta_{c_5}^+}\frac{\partial K_2}{\partial\theta}(\theta,\xi)
\end{aligned}
\tag{E.172}
$$

$$
\begin{aligned}
T(\theta_{l_2}) = &\int_{\theta_{l_2}}^{\theta_{c_6}} d\theta\ \sin\theta\, K_1(\theta,\theta_{l_2})h_1(\theta) + K_1(\theta_{c_6},\theta_{l_2})\sin(\theta_{c_6})\frac{\partial T}{\partial\theta}(\theta_{c_6}) \\
&+ \sin(\theta_{c_6}) \lim_{\xi\to\theta_{l_2}^+}\lim_{\theta\to\theta_{c_6}^-} \frac{\partial K_1}{\partial\theta}(\theta,\xi) - \lim_{\xi\to\theta_{l_2}^+} K_1(\theta_{l_2},\xi)\sin(\theta_{l_1})\frac{\partial T}{\partial\theta}(\theta_{l_2}) \\
&+ T(\theta_{l_2})\sin(\theta_{l_2}) \lim_{\xi\to\theta_{l_2}^+}\lim_{\theta\to\theta_{l_2}^+} \frac{\partial K_1}{\partial\theta}(\theta,\xi)
\end{aligned} \tag{E.173}
$$

$$
\begin{aligned}
-1 = &\int_{\theta_{l_2}}^{\theta_{c_6}} d\theta\ \sin\theta\, K_1(\theta,\theta_{c_6})h_1(\theta) + \lim_{\xi\to\theta_{c_6}^-} K_1(\theta_{c_6},\xi)\sin(\theta_{c_6})\frac{\partial T}{\partial\theta}(\theta_{c_6}) \\
&+ \sin(\theta_{c_6}) \lim_{\xi\to\theta_{c_6}^-}\lim_{\theta\to\theta_{c_6}^-} \frac{\partial K_1}{\partial\theta}(\theta,\xi) - K_1(\theta_{l_2},\theta_{c_6})\sin(\theta_{l_1})\frac{\partial T}{\partial\theta}(\theta_{l_2}) \\
&+ T(\theta_{l_2})\sin(\theta_{l_2}) \lim_{\xi\to\theta_{c_6}^-}\lim_{\theta\to\theta_{l_2}^+} \frac{\partial K_1}{\partial\theta}(\theta,\xi)
\end{aligned} \tag{E.174}
$$

$$
\begin{aligned}
-1 = &\int_{\theta_{c_6}}^{\pi} d\theta\ \sin\theta\, K_1(\theta,\theta_{c_6})h_2(\theta) - \lim_{\xi\to\theta_{c_6}^+} K_1(\theta_{c_6},\xi)\sin(\theta_{c_6})\frac{\partial T}{\partial\theta}(\theta_{c_6}) \\
&- \sin(\theta_{c_6}) \lim_{\xi\to\theta_{c_6}^+}\lim_{\theta\to\theta_{c_6}^+} \frac{\partial K_1}{\partial\theta}(\theta,\xi)
\end{aligned} \tag{E.175}
$$

$$
\begin{aligned}
T(\pi) = &\int_{\theta_{c_6}}^{\pi} d\theta\ \sin\theta\, K_1(\theta,\pi)h_2(\theta) - K_1(\theta_{c_6},\pi)\sin(\theta_{c_6})\frac{\partial T}{\partial\theta}(\theta_{c_6}) \\
&- \sin(\theta_{c_6}) \lim_{\xi\to\pi^-}\lim_{\theta\to\theta_{c_6}^+} \frac{\partial K_1}{\partial\theta}(\theta,\xi).
\end{aligned} \tag{E.176}
$$

The boundary integral equations (E.159)-(E.176) is a system of 18 equations for the 18 unknown boundary values $T(0)$, θ_{c_1}, $\frac{\partial T}{\partial\theta}(\theta_{c_1})$, $T(\theta_{l_1})$, $\frac{\partial T}{\partial\theta}(\theta_{l_1})$, θ_{c_2}, $\frac{\partial T}{\partial\theta}(\theta_{c_2})$, θ_{c_3}, $\frac{\partial T}{\partial\theta}(\theta_{c_3})$, θ_{c_4}, $\frac{\partial T}{\partial\theta}(\theta_{c_4})$, θ_{c_5}, $\frac{\partial T}{\partial\theta}(\theta_{c_5})$, $T(\theta_{l_2})$, $\frac{\partial T}{\partial\theta}(\theta_{l_2})$, θ_{c_6}, $\frac{\partial T}{\partial\theta}(\theta_{c_6})$ and $T(\pi)$. To solve this system we algebraically combine equation (E.159)-(E.176) to create six functions;

$$
\begin{aligned}
f_1 &= f_1(\theta_{c_1},\theta_{c_2},\theta_{c_3},\theta_{c_4},\theta_{c_5},\theta_{c_6}), \\
f_2 &= f_2(\theta_{c_1},\theta_{c_2},\theta_{c_3},\theta_{c_4},\theta_{c_5},\theta_{c_6}), \\
f_3 &= f_3(\theta_{c_1},\theta_{c_2},\theta_{c_3},\theta_{c_4},\theta_{c_5},\theta_{c_6}), \\
f_4 &= f_4(\theta_{c_1},\theta_{c_2},\theta_{c_3},\theta_{c_4},\theta_{c_5},\theta_{c_6}), \\
f_5 &= f_5(\theta_{c_1},\theta_{c_2},\theta_{c_3},\theta_{c_4},\theta_{c_5},\theta_{c_6}), \\
f_6 &= f_6(\theta_{c_1},\theta_{c_2},\theta_{c_3},\theta_{c_4},\theta_{c_5},\theta_{c_6}).
\end{aligned} \tag{E.177}
$$

We evaluate these functions on a grid to create six interpolation functions. Then Newton's iteration is applied to approximate the six roots θ_{c_1}, θ_{c_2}, θ_{c_3}, θ_{c_4}, θ_{c_5} and θ_{c_6}. Once these roots are approximated we find the remaining boundary values and the solution in the regions I-IX is given by the integral relations (E.150)-(E.158), respectively.

E.6 Assumed symmetry

As mentioned in section 3.3 a symmetry assumption was applied for the four and six ice edges cases in the pursuit of a more computationally efficient approach for solving these cases. We have already laid out a framework for solving these cases without any symmetry assumptions. That approach relies on creating interpolation functions, which in turn relies on evaluating the functions f_1-f_4 (E.128) and f_1-f_6 (E.177) on a grid. Evaluating these functions on a four- and six-dimensional grid is a computationally expensive process. Furthermore, a root search with the resulting interpolation functions is also challenging without an initial guess sufficiently close to the roots, often a method of trying an array of initial guesses had to be applied in order to find an acceptable root. An acceptable root refers to a root that results in a smooth solution, and for the analysis with a symmetrical continent this was found to be roots that resulted in a symmetrical solution. The symmetry assumption arises from this realization.

The symmetry here, is a symmetry about equator, $\theta = \frac{\pi}{2}$. With a continent symmetrical about equator, one in which the continent stretches from latitude

$$\theta_{l_1} = \frac{\pi}{2} - \frac{l}{2}$$

to

$$\theta_{l_2} = \frac{\pi}{2} + \frac{l}{2},$$

where l is the length of the continent, we expect to get a temperature distribution that is symmetrical about $\theta = \frac{\pi}{2}$. This is because the latitudinal energy distribution function, $s(\theta)$ is symmetrical about $\theta = \frac{\pi}{2}$, and no other elemants in the model constitutes the appearance of an asymmetrical temperature distribution under these conditions. We will therefore apply the boundary integral method on the truncated domain

$$\theta \in [0, \frac{\pi}{2}]. \tag{E.178}$$

The resulting temperature distribution in this domain will subsequently be mirrored in the remaining domain,

$$\theta \in (\frac{\pi}{2}, \pi].$$

Since we are looking for a solution that is symmetrical about $\theta = \frac{\pi}{2}$ we must have

$$\begin{gathered} T(\theta) = T(\pi - \theta) \\ \Downarrow \\ T'(\theta) = -T'(\pi - \theta). \end{gathered}$$

Inserting $\theta = \frac{\pi}{2}$, it is evident that we must have

$$T'(\frac{\pi}{2}) = 0. \tag{E.179}$$

Imposing this condition will ensure that we can solve the following systems of boundary integral equations. It is important to note that the symmetry assumption can be applied for all cases as

long as the continent preserves the north-south symmetry. However, in this thesis we only utilized this assumption when we had to locate four or six ice edges through solving the boundary integral equations. These cases where the ones in which the procedure outlined in the first part of this appendix was challenging and very time consuming.

E.6.1 The case of four ice edges

In the case of four ice edges, we apply the symmetry assumption only for the scenario where the continent has a partial ice cover. We partition the truncated domain (E.178) into the four sub-domains;

$$\theta \in (0, \theta_{c_1}), \tag{I}$$

$$\theta \in (\theta_{c_1}, \theta_{l_1}), \tag{II}$$

$$\theta \in (\theta_{l_1}, \theta_{c_2}) \tag{III}$$

and

$$\theta \in (\theta_{c_2}, \frac{\pi}{2}). \tag{IV}$$

The boundary integral relations for the regions I-III will essentially be exactly the same as we saw above for the considerations without any symmetry assumption, but we will include them here for completeness. In region IV we must apply the condition (E.179). The boundary integral relations for this will be;

$$\begin{aligned} T(\xi) = &\int_0^{\theta_{c_1}} d\theta \ \sin\theta \, K_1(\theta, \xi) h_2(\theta) + K_1(\theta_{c_1}, \xi) \sin(\theta_{c_1}) \frac{\partial T}{\partial \theta}(\theta_{c_1}) \\ &+ \sin(\theta_{c_1}) \lim_{\theta \to \theta_{c_1}^-} \frac{\partial K_1}{\partial \theta}(\theta, \xi) \end{aligned} \tag{E.180}$$

in region I,

$$\begin{aligned} T(\xi) = &\int_{\theta_{c_1}}^{\theta_{l_1}} d\theta \ \sin\theta \, K_1(\theta, \xi) h_1(\theta) + K_1(\theta_{l_1}, \xi) \sin(\theta_{l_1}) \frac{\partial T}{\partial \theta}(\theta_{l_1}) \\ &- T(\theta_{l_1}) \sin(\theta_{l_1}) \lim_{\theta \to \theta_{l_1}^-} \frac{\partial K_1}{\partial \theta}(\theta, \xi) - K_1(\theta_{c_1}, \xi) \sin(\theta_{c_1}) \frac{\partial T}{\partial \theta}(\theta_{c_1}) \\ &- \sin(\theta_{c_1}) \lim_{\theta \to \theta_{c_1}^+} \frac{\partial K_1}{\partial \theta}(\theta, \xi) \end{aligned} \tag{E.181}$$

in region II,

$$\begin{aligned} T(\xi) = &\int_{\theta_{l_1}}^{\theta_{c_2}} d\theta\ \sin\theta\, K_2(\theta,\xi)h_4(\theta) + K_2(\theta_{c_2},\xi)\sin(\theta_{c_2})\frac{\partial T}{\partial\theta}(\theta_{c_2}) \\ &+ T_c\sin(\theta_{c_2})\lim_{\theta\to\theta_{c_2}^-}\frac{\partial K_2}{\partial\theta}(\theta,\xi) - K_2(\theta_{l_1},\xi)\sin(\theta_{l_1})\frac{\partial T}{\partial\theta}(\theta_{l_1}) \\ &+ T(\theta_{l_1})\sin(\theta_{l_1})\lim_{\theta\to\theta_{l_1}^+}\frac{\partial K_2}{\partial\theta}(\theta,\xi) \end{aligned} \tag{E.182}$$

in region III and

$$\begin{aligned} T(\xi) = &\int_{\theta_{c_2}}^{\frac{\pi}{2}} d\theta\ \sin\theta\, K_2(\theta,\xi)h_3(\theta) - T(\frac{\pi}{2})\lim_{\theta\to\frac{\pi}{2}^-}\frac{\partial K_2}{\partial\theta}(\theta,\xi) \\ &- K_2(\theta_{c_2},\xi)\sin(\theta_{c_2})\frac{\partial T}{\partial\theta}(\theta_{c_2}) - T_c\sin(\theta_{c_2})\lim_{\theta\to\theta_{c_2}^+}\frac{\partial K_2}{\partial\theta}(\theta,\xi) \end{aligned} \tag{E.183}$$

in region IV. The associated boundary integral equations will be;

$$\begin{aligned} T(0) = &\int_0^{\theta_{c_1}} d\theta\ \sin\theta\, K_1(\theta,0)h_2(\theta) + K_1(\theta_{c_1},0)\sin(\theta_{c_1})\frac{\partial T}{\partial\theta}(\theta_{c_1}) \\ &+ \sin(\theta_{c_1})\lim_{\xi\to 0^+}\lim_{\theta\to\theta_{c_1}^-}\frac{\partial K_1}{\partial\theta}(\theta,\xi) \end{aligned} \tag{E.184}$$

$$\begin{aligned} -1 = &\int_0^{\theta_{c_1}} d\theta\ \sin\theta\, K_1(\theta,\theta_{c_1})h_2(\theta) + \lim_{\xi\to\theta_{c_1}^-} K_1(\theta_{c_1},\xi)\sin(\theta_{c_1})\frac{\partial T}{\partial\theta}(\theta_{c_1}) \\ &+ \sin(\theta_{c_1})\lim_{\xi\to\theta_{c_1}^-}\lim_{\theta\to\theta_{c_1}^-}\frac{\partial K_1}{\partial\theta}(\theta,\xi) \end{aligned} \tag{E.185}$$

$$\begin{aligned} -1 = &\int_{\theta_{c_1}}^{\theta_{l_1}} d\theta\ \sin\theta\, K_1(\theta,\theta_{c_1})h_1(\theta) + K_1(\theta_{l_1},\theta_{c_1})\sin(\theta_{l_1})\frac{\partial T}{\partial\theta}(\theta_{l_1}) \\ &- T(\theta_{l_1})\sin(\theta_{l_1})\lim_{\xi\to\theta_{c_1}^+}\lim_{\theta\to\theta_{l_1}^-}\frac{\partial K_1}{\partial\theta}(\theta,\xi) - \lim_{\xi\to\theta_{c_1}^+} K_1(\theta_{c_1},\xi)\sin(\theta_{c_1})\frac{\partial T}{\partial\theta}(\theta_{c_1}) \\ &- \sin(\theta_{c_1})\lim_{\xi\to\theta_{c_1}^+}\lim_{\theta\to\theta_{c_1}^+}\frac{\partial K_1}{\partial\theta}(\theta,\xi) \end{aligned} \tag{E.186}$$

$$\begin{aligned} T(\theta_{l_1}) = &\int_{\theta_{c_1}}^{\theta_{l_1}} d\theta\ \sin\theta\, K_1(\theta,\theta_{l_1})h_1(\theta) + \lim_{\xi\to\theta_{l_1}^-} K_1(\theta_{l_1},\xi)\sin(\theta_{l_1})\frac{\partial T}{\partial\theta}(\theta_{l_1}) \\ &- T(\theta_{l_1})\sin(\theta_{l_1})\lim_{\xi\to\theta_{l_1}^-}\lim_{\theta\to\theta_{l_1}^-}\frac{\partial K_1}{\partial\theta}(\theta,\xi) - K_1(\theta_{c_1},\theta_{l_1})\sin(\theta_{c_1})\frac{\partial T}{\partial\theta}(\theta_{c_1}) \\ &- \sin(\theta_{c_1})\lim_{\xi\to\theta_{l_1}^-}\lim_{\theta\to\theta_{c_1}^+}\frac{\partial K_1}{\partial\theta}(\theta,\xi) \end{aligned} \tag{E.187}$$

$$
\begin{aligned}
T(\theta_{l_1}) = &\int_{\theta_{l_1}}^{\theta_{c_2}} d\theta\ \sin\theta\, K_2(\theta,\theta_{l_1})h_4(\theta) + K_2(\theta_{c_2},\theta_{l_1})\sin(\theta_{c_2})\frac{\partial T}{\partial\theta}(\theta_{c_2}) \\
&+ T_c\sin(\theta_{c_2})\lim_{\xi\to\theta_{l_1}^+}\lim_{\theta\to\theta_{l_2}^-}\frac{\partial K_2}{\partial\theta}(\theta,\xi) - \lim_{\xi\to\theta_{l_1}^+}K_2(\theta_{l_1},\xi)\sin(\theta_{l_1})\frac{\partial T}{\partial\theta}(\theta_{l_1}) \\
&+ T(\theta_{l_1})\sin(\theta_{l_1})\lim_{\xi\to\theta_{l_1}^+}\lim_{\theta\to\theta_{l_1}^+}\frac{\partial K_2}{\partial\theta}(\theta,\xi)
\end{aligned} \tag{E.188}
$$

$$
\begin{aligned}
-T_c = &\int_{\theta_{l_1}}^{\theta_{c_2}} d\theta\ \sin\theta\, K_2(\theta,\theta_{c_2})h_4(\theta) + \lim_{\xi\to\theta_{c_2}^-}K_2(\theta_{c_2},\xi)\sin(\theta_{c_2})\frac{\partial T}{\partial\theta}(\theta_{c_2}) \\
&+ T_c\sin(\theta_{c_2})\lim_{\xi\to\theta_{c_2}^-}\lim_{\theta\to\theta_{c_2}^-}\frac{\partial K_2}{\partial\theta}(\theta,\xi) - K_2(\theta_{l_1},\theta_{c_2})\sin(\theta_{l_1})\frac{\partial T}{\partial\theta}(\theta_{l_1}) \\
&+ T(\theta_{l_1})\sin(\theta_{l_1})\lim_{\xi\to\theta_{c_2}^-}\lim_{\theta\to\theta_{l_1}^+}\frac{\partial K_2}{\partial\theta}(\theta,\xi)
\end{aligned} \tag{E.189}
$$

$$
\begin{aligned}
-T_c = &\int_{\theta_{c_2}}^{\frac{\pi}{2}} d\theta\ \sin\theta\, K_2(\theta,\theta_{c_2})h_3(\theta) - T(\frac{\pi}{2})\lim_{\xi\to\theta_{c_2}^+}\lim_{\theta\to\frac{\pi}{2}^-}\frac{\partial K_2}{\partial\theta}(\theta,\xi) \\
&- \lim_{\xi\to\theta_{c_2}^+}K_2(\theta_{c_2},\xi)\sin(\theta_{c_2})\frac{\partial T}{\partial\theta}(\theta_{c_2}) - T_c\sin(\theta_{c_2})\lim_{\xi\to\theta_{c_2}^+}\lim_{\theta\to\theta_{c_2}^+}\frac{\partial K_2}{\partial\theta}(\theta,\xi)
\end{aligned} \tag{E.190}
$$

$$
\begin{aligned}
T(\frac{\pi}{2}) = &\int_{\theta_{c_2}}^{\frac{\pi}{2}} d\theta\ \sin\theta\, K_2(\theta,\frac{\pi}{2})h_3(\theta) - T(\frac{\pi}{2})\lim_{\xi\to\frac{\pi}{2}^-}\lim_{\theta\to\frac{\pi}{2}^-}\frac{\partial K_2}{\partial\theta}(\theta,\xi) \\
&- K_2(\theta_{c_2},\frac{\pi}{2})\sin(\theta_{c_2})\frac{\partial T}{\partial\theta}(\theta_{c_2}) - T_c\sin(\theta_{c_2})\lim_{\xi\to\frac{\pi}{2}^-}\lim_{\theta\to\theta_{c_2}^+}\frac{\partial K_2}{\partial\theta}(\theta,\xi).
\end{aligned} \tag{E.191}
$$

The boundary integral equations (E.184)-(E.191) is a system of 8 equations for the 8 unknown boundary values $T(0)$, θ_{c_1}, $\frac{\partial T}{\partial\theta}(\theta_{c_1})$, $T(\theta_{l_1})$, $\frac{\partial T}{\partial\theta}(\theta_{l_1})$, θ_{c_2}, $\frac{\partial T}{\partial\theta}(\theta_{c_2})$ and $T(\frac{\pi}{2})$. To solve this system we algebraically combine equation (E.184)-(E.191) to create two functions,

$$f_1 = f_1(\theta_{c_1},\theta_{c_2})$$

and

$$f_2 = f_2(\theta_{c_1},\theta_{c_2}).$$

We wish to find the roots of these functions using Newton's iteration to obtain θ_{c_1} and θ_{c_2}. With the symmetry assumption, we have now turned what was four-dimensional problem into a two-dimensional one. We can now plot the roots and this visual representation was especially useful whenever the boundary integral equations had two solutions. Once θ_{c_1} and θ_{c_2} are known, it is trivial to find the remaining boundary values and the solution in the regions I-IV is given by the integral relations (E.180)-(E.183), respectively.

E.6.2 The case of six ice edges

In the case of six ice edges there are two scenarios and both of these are greatly simplified by applying the symmetry assumption. For the first scenario, where the northern and southern tips of the continent has an ice/snow cover, we can apply the same method as above for the four ice edges. Finding solutions for this scenario will follow the same procedure, but interchanging $h_4 \to h_3$ in (E.182) and $h_3 \to h_4$ in (E.183). Subsequently, we must interchange $h_4 \to h_3$ in (E.188) and (E.189) and $h_3 \to h_4$ in (E.190) and (E.191).

This will obviously not work for the other scenario, where the northern and southern tips of the continent has no ice/snow cover. In this scenario we partition the truncated domain (E.178) into the five sub-domains;

$$\theta \in (0, \theta_{c_1}), \tag{I}$$

$$\theta \in (\theta_{c_1}, \theta_{l_1}), \tag{II}$$

$$\theta \in (\theta_{l_1}, \theta_{c_2}), \tag{III}$$

$$\theta \in (\theta_{c_2}, \theta_{c_3}) \tag{IV}$$

and

$$\theta \in (\theta_{c_3}, \frac{\pi}{2}). \tag{V}$$

The boundary integral relations in these regions will be

$$\begin{aligned} T(\xi) = &\int_0^{\theta_{c_1}} d\theta \ \sin\theta \, K_1(\theta, \xi) h_2(\theta) + K_1(\theta_{c_1}, \xi) \sin(\theta_{c_1}) \frac{\partial T}{\partial \theta}(\theta_{c_1}) \\ &+ \sin(\theta_{c_1}) \lim_{\theta \to \theta_{c_1}^-} \frac{\partial K_1}{\partial \theta}(\theta, \xi) \end{aligned} \tag{E.192}$$

in region I,

$$\begin{aligned} T(\xi) = &\int_{\theta_{c_1}}^{\theta_{l_1}} d\theta \ \sin\theta \, K_1(\theta, \xi) h_1(\theta) + K_1(\theta_{l_1}, \xi) \sin(\theta_{l_1}) \frac{\partial T}{\partial \theta}(\theta_{l_1}) \\ &- T(\theta_{l_1}) \sin(\theta_{l_1}) \lim_{\theta \to \theta_{l_1}^-} \frac{\partial K_1}{\partial \theta}(\theta, \xi) - K_1(\theta_{c_1}, \xi) \sin(\theta_{c_1}) \frac{\partial T}{\partial \theta}(\theta_{c_1}) \\ &- \sin(\theta_{c_1}) \lim_{\theta \to \theta_{c_1}^+} \frac{\partial K_1}{\partial \theta}(\theta, \xi) \end{aligned} \tag{E.193}$$

in region II,

$$\begin{aligned} T(\xi) = &\int_{\theta_{l_1}}^{\theta_{c_2}} d\theta\ \sin\theta\, K_2(\theta,\xi)h_3(\theta) + K_2(\theta_{c_2},\xi)\sin(\theta_{c_2})\frac{\partial T}{\partial\theta}(\theta_{c_2}) \\ &+ T_c\sin(\theta_{c_2})\lim_{\theta\to\theta_{c_2}^-}\frac{\partial K_2}{\partial\theta}(\theta,\xi) - K_2(\theta_{l_1},\xi)\sin(\theta_{l_1})\frac{\partial T}{\partial\theta}(\theta_{l_1}) \\ &+ T(\theta_{l_1})\sin(\theta_{l_1})\lim_{\theta\to\theta_{l_1}^+}\frac{\partial K_2}{\partial\theta}(\theta,\xi) \end{aligned} \tag{E.194}$$

in region III and

$$\begin{aligned} T(\xi) = &\int_{\theta_{c_2}}^{\theta_{c_3}} d\theta\ \sin\theta\, K_2(\theta,\xi)h_4(\theta) + K_2(\theta_{c_3},\xi)\sin(\theta_{c_3})\frac{\partial T}{\partial\theta}(\theta_{c_3}) \\ &+ T_c\sin(\theta_{c_3})\lim_{\theta\to\theta_{c_3}^-}\frac{\partial K_2}{\partial\theta}(\theta,\xi) - K_2(\theta_{c_2},\xi)\sin(\theta_{c_2})\frac{\partial T}{\partial\theta}(\theta_{c_2}) \\ &- T_c\sin(\theta_{c_2})\lim_{\theta\to\theta_{c_2}^+}\frac{\partial K_2}{\partial\theta}(\theta,\xi) \end{aligned} \tag{E.195}$$

in region IV and

$$\begin{aligned} T(\xi) = &\int_{\theta_{c_3}}^{\frac{\pi}{2}} d\theta\ \sin\theta\, K_2(\theta,\xi)h_3(\theta) - T(\frac{\pi}{2})\lim_{\theta\to\frac{\pi}{2}^-}\frac{\partial K_2}{\partial\theta}(\theta,\xi) \\ &- K_2(\theta_{c_3},\xi)\sin(\theta_{c_3})\frac{\partial T}{\partial\theta}(\theta_{c_3}) - T_c\sin(\theta_{c_3})\lim_{\theta\to\theta_{c_3}^+}\frac{\partial K_2}{\partial\theta}(\theta,\xi) \end{aligned} \tag{E.196}$$

in region V. The associated boundary integral equations will be;

$$\begin{aligned} T(0) = &\int_0^{\theta_{c_1}} d\theta\ \sin\theta\, K_1(\theta,0)h_2(\theta) + K_1(\theta_{c_1},0)\sin(\theta_{c_1})\frac{\partial T}{\partial\theta}(\theta_{c_1}) \\ &+ \sin(\theta_{c_1})\lim_{\xi\to 0^+}\lim_{\theta\to\theta_{c_1}^-}\frac{\partial K_1}{\partial\theta}(\theta,\xi) \end{aligned} \tag{E.197}$$

$$\begin{aligned} -1 = &\int_0^{\theta_{c_1}} d\theta\ \sin\theta\, K_1(\theta,\theta_{c_1})h_2(\theta) + \lim_{\xi\to\theta_{c_1}^-} K_1(\theta_{c_1},\xi)\sin(\theta_{c_1})\frac{\partial T}{\partial\theta}(\theta_{c_1}) \\ &+ \sin(\theta_{c_1})\lim_{\xi\to\theta_{c_1}^-}\lim_{\theta\to\theta_{c_1}^-}\frac{\partial K_1}{\partial\theta}(\theta,\xi) \end{aligned} \tag{E.198}$$

$$\begin{aligned} -1 = &\int_{\theta_{c_1}}^{\theta_{l_1}} d\theta\ \sin\theta\, K_1(\theta,\theta_{c_1})h_1(\theta) + K_1(\theta_{l_1},\theta_{c_1})\sin(\theta_{l_1})\frac{\partial T}{\partial\theta}(\theta_{l_1}) \\ &- T(\theta_{l_1})\sin(\theta_{l_1})\lim_{\xi\to\theta_{c_1}^+}\lim_{\theta\to\theta_{l_1}^-}\frac{\partial K_1}{\partial\theta}(\theta,\xi) - \lim_{\xi\to\theta_{c_1}^+} K_1(\theta_{c_1},\xi)\sin(\theta_{c_1})\frac{\partial T}{\partial\theta}(\theta_{c_1}) \\ &- \sin(\theta_{c_1})\lim_{\xi\to\theta_{c_1}^+}\lim_{\theta\to\theta_{c_1}^+}\frac{\partial K_1}{\partial\theta}(\theta,\xi) \end{aligned} \tag{E.199}$$

$$T(\theta_{l_1}) = \int_{\theta_{c_1}}^{\theta_{l_1}} d\theta\ \sin\theta\, K_1(\theta,\theta_{l_1})h_1(\theta) + \lim_{\xi\to\theta_{l_1}^-} K_1(\theta_{l_1},\xi)\sin(\theta_{l_1})\frac{\partial T}{\partial\theta}(\theta_{l_1})$$
$$- T(\theta_{l_1})\sin(\theta_{l_1})\lim_{\xi\to\theta_{l_1}^-}\lim_{\theta\to\theta_{l_1}^-}\frac{\partial K_1}{\partial\theta}(\theta,\xi) - K_1(\theta_{c_1},\theta_{l_1})\sin(\theta_{c_1})\frac{\partial T}{\partial\theta}(\theta_{c_1}) \tag{E.200}$$
$$- \sin(\theta_{c_1})\lim_{\xi\to\theta_{l_1}^-}\lim_{\theta\to\theta_{c_1}^+}\frac{\partial K_1}{\partial\theta}(\theta,\xi)$$

$$T(\theta_{l_1}) = \int_{\theta_{l_1}}^{\theta_{c_2}} d\theta\ \sin\theta\, K_2(\theta,\theta_{l_1})h_3(\theta) + K_2(\theta_{c_2},\theta_{l_1})\sin(\theta_{c_2})\frac{\partial T}{\partial\theta}(\theta_{c_2})$$
$$+ T_c\sin(\theta_{c_2})\lim_{\xi\to\theta_{l_1}^+}\lim_{\theta\to\theta_{l_2}^-}\frac{\partial K_2}{\partial\theta}(\theta,\xi) - \lim_{\xi\to\theta_{l_1}^+} K_2(\theta_{l_1},\xi)\sin(\theta_{l_1})\frac{\partial T}{\partial\theta}(\theta_{l_1}) \tag{E.201}$$
$$+ T(\theta_{l_1})\sin(\theta_{l_1})\lim_{\xi\to\theta_{l_1}^+}\lim_{\theta\to\theta_{l_1}^+}\frac{\partial K_2}{\partial\theta}(\theta,\xi)$$

$$-T_c = \int_{\theta_{l_1}}^{\theta_{c_2}} d\theta\ \sin\theta\, K_2(\theta,\theta_{c_2})h_3(\theta) + \lim_{\xi\to\theta_{c_2}^-} K_2(\theta_{c_2},\xi)\sin(\theta_{c_2})\frac{\partial T}{\partial\theta}(\theta_{c_2})$$
$$+ T_c\sin(\theta_{c_2})\lim_{\xi\to\theta_{c_2}^-}\lim_{\theta\to\theta_{c_2}^-}\frac{\partial K_2}{\partial\theta}(\theta,\xi) - K_2(\theta_{l_1},\theta_{c_2})\sin(\theta_{l_1})\frac{\partial T}{\partial\theta}(\theta_{l_1}) \tag{E.202}$$
$$+ T(\theta_{l_1})\sin(\theta_{l_1})\lim_{\xi\to\theta_{c_2}^-}\lim_{\theta\to\theta_{l_1}^+}\frac{\partial K_2}{\partial\theta}(\theta,\xi)$$

$$-T_c = \int_{\theta_{c_2}}^{\theta_{c_3}} d\theta\ \sin\theta\, K_2(\theta,\theta_{c_2})h_4(\theta) + K_2(\theta_{c_3},\theta_{c_2})\sin(\theta_{c_3})\frac{\partial T}{\partial\theta}(\theta_{c_3})$$
$$+ T_c\sin(\theta_{c_3})\lim_{\xi\to\theta_{c_2}^+}\lim_{\theta\to\theta_{c_3}^-}\frac{\partial K_2}{\partial\theta}(\theta,\xi) - \lim_{\xi\to\theta_{c_2}^+} K_2(\theta_{c_2},\xi)\sin(\theta_{c_2})\frac{\partial T}{\partial\theta}(\theta_{c_2}) \tag{E.203}$$
$$- T_c\sin(\theta_{c_2})\lim_{\xi\to\theta_{c_2}^-}\lim_{\theta\to\theta_{c_2}^+}\frac{\partial K_2}{\partial\theta}(\theta,\xi)$$

$$-T_c = \int_{\theta_{c_2}}^{\theta_{c_3}} d\theta\ \sin\theta\, K_2(\theta,\theta_{c_3})h_4(\theta) + \lim_{\xi\to\theta_{c_3}^-} K_2(\theta_{c_3},\xi)\sin(\theta_{c_3})\frac{\partial T}{\partial\theta}(\theta_{c_3})$$
$$+ T_c\sin(\theta_{c_3})\lim_{\xi\to\theta_{c_2}^-}\lim_{\theta\to\theta_{c_3}^-}\frac{\partial K_2}{\partial\theta}(\theta,\xi) - K_2(\theta_{c_2},\theta_{c_3})\sin(\theta_{c_2})\frac{\partial T}{\partial\theta}(\theta_{c_2}) \tag{E.204}$$
$$- T_c\sin(\theta_{c_2})\lim_{\xi\to\theta_{c_2}^-}\lim_{\theta\to\theta_{c_2}^+}\frac{\partial K_2}{\partial\theta}(\theta,\xi)$$

$$-T_c = \int_{\theta_{c_3}}^{\frac{\pi}{2}} d\theta\ \sin\theta\, K_2(\theta,\theta_{c_3})h_3(\theta) - T(\frac{\pi}{2})\lim_{\xi\to\theta_{c_3}^+}\lim_{\theta\to\frac{\pi}{2}^-}\frac{\partial K_2}{\partial\theta}(\theta,\xi)$$
$$- \lim_{\xi\to\theta_{c_3}^+} K_2(\theta_{c_3},\xi)\sin(\theta_{c_3})\frac{\partial T}{\partial\theta}(\theta_{c_3}) - T_c\sin(\theta_{c_3})\lim_{\xi\to\theta_{c_3}^+}\lim_{\theta\to\theta_{c_3}^+}\frac{\partial K_2}{\partial\theta}(\theta,\xi) \tag{E.205}$$

$$T(\frac{\pi}{2}) = \int_{\theta_{c_3}}^{\frac{\pi}{2}} d\theta\ \sin\theta\, K_2(\theta,\frac{\pi}{2})h_3(\theta) - T(\frac{\pi}{2})\lim_{\xi\to\frac{\pi}{2}^-}\lim_{\theta\to\frac{\pi}{2}^-}\frac{\partial K_2}{\partial\theta}(\theta,\xi)$$
$$- K_2(\theta_{c_3},\frac{\pi}{2})\sin(\theta_{c_3})\frac{\partial T}{\partial\theta}(\theta_{c_3}) - T_c\sin(\theta_{c_3})\lim_{\xi\to\frac{\pi}{2}^-}\lim_{\theta\to\theta_{c_3}^+}\frac{\partial K_2}{\partial\theta}(\theta,\xi). \tag{E.206}$$

The boundary integral equations (E.197)-(E.206) is a system of 10 equations for the 10 unknown boundary values $T(0)$, θ_{c_1}, $\frac{\partial T}{\partial \theta}(\theta_{c_1})$, $T(\theta_{l_1})$, $\frac{\partial T}{\partial \theta}(\theta_{l_1})$, θ_{c_2}, $\frac{\partial T}{\partial \theta}(\theta_{c_2})$, θ_{c_3}, $\frac{\partial T}{\partial \theta}(\theta_{c_3})$ and $T(\frac{\pi}{2})$. To solve this system we algebraically combine equation (E.197)-(E.206) to create three functions,

$$f_1 = f_1(\theta_{c_1}, \theta_{c_2}, \theta_{c_3}),$$
$$f_2 = f_2(\theta_{c_1}, \theta_{c_2}, \theta_{c_3}) and f_3 \quad = f_3(\theta_{c_1}, \theta_{c_2}, \theta_{c_3}).$$

We evaluate these functions on a grid to create three interpolation functions and then apply Newton's iteration. Once θ_{c_1}, θ_{c_2} and θ_{c_3} are known, it is trivial to find the remaining boundary values and the solution in the regions I-V is given by the integral relations (E.192)-(E.196), respectively.

Note that the symmetry assumption applied above, will only hold for a continent that is symmetrical about $\theta = \frac{\pi}{2}$. With an asymmetrical continent, the condition (E.179) will not hold and without knowing the value $\frac{\partial T}{\partial \theta}(\frac{\pi}{2})$, the system of boundary integral equations that arises using the boundary integral method will be underdetermined. The approach outlined in E.4 and E.5 does however, allow for an arbitrary placement of the continent and can thus handle asymmetrical cases as well as symmetrical ones. Though we never encountered multiple (four or more) ice edge solutions for a continent breaking the north south symmetry in this thesis, if one were to encounter such cases, one must simply endure with the more computationally expensive approach. For north-south symmetrical cases, we now have two approaches which allows us to cross reference the solutions obtained with and without a symmetry assumption. Using the critical latitudes found with the application of the symmetry assumption as a starting point in a Newton's iteration for solution without a symmetry assumption, was found to be useful in order to avoid convergence issues.

References

[1] Nidal H Abu-Hamdeh and Randall C Reeder. "Soil thermal conductivity effects of density, moisture, salt concentration, and organic matter". In: *Soil science society of America Journal* 64.4 (2000), pp. 1285–1290.

[2] Sebastian Bathiany et al. "Beyond bifurcation: using complex models to understand and predict abrupt climate change". In: *Dynamics and Statistics of the Climate System* 1.1 (2016).

[3] Victor Brovkin et al. "On the stability of the atmosphere-vegetation system in the Sahara/Sahel region". In: *Journal of Geophysical Research: Atmospheres* 103.D24 (1998), pp. 31613–31624.

[4] M. I. Budyko. "The effect of solar radiation variations on the climate of the Earth". In: *Tellus* 21 (1969), pp. 611–619.

[5] *Earth System Modeling, a definition*. Climateurope. URL: `https://www.climateurope.eu/earth-system-modeling-a-definition/` (visited on 05/08/2022).

[6] Per Kristen Jakobsen. *1D energy balance model for a tidally locked exoplanet*. Technical report. Department of Mathematics and Statistics, UiT The Arctic University of Norway, 2021.

[7] Per Kristen Jakobsen. *An introduction to Green's functions and boundary formulations*. Technical report. Department of Mathematics and Statistics, UiT The Arctic University of Norway, 2021.

[8] Per Kristen Jakobsen. *Boundary formulations for energy balance models in climate science*. Technical report. Department of Mathematics and Statistics, UiT The Arctic University of Norway, 2021.

[9] Per Kristen Jakobsen. *The energy balance model on a spherical planet: The North model*. Technical report. Department of Mathematics and Statistics, UiT The Arctic University of Norway, 2021.

[10] Hans Kaper and Hans Engler. "Climate models". In: *Mathematics & Climate*. Society for Industrial and Applied Mathematics, 2013. Chap. 15, p. 183.

[11] Hans Kaper and Hans Engler. "Zonal Energy Budget". In: *Mathematics & Climate*. Society for Industrial and Applied Mathematics, 2013. Chap. 12, pp. 143–152.

[12] John M. Lee. In: *Introduction to Smooth Manifolds*. 2nd ed. Springer, 2012, pp. 341–343, 388–390.

[13] Thorsten Mauritsen et al. "Tuning the climate of a global model". In: *Journal of advances in modeling Earth systems* 4.3 (2012).

[14] Gerald R North. "Analytical solution to a simple climate model with diffusive heat transport". In: *Journal of Atmospheric Sciences* 32.7 (1975), pp. 1301–1307.

[15] Gerald R North. "Theory of energy-balance climate models". In: *Journal of Atmospheric Sciences* 32.11 (1975), pp. 2033–2043.

[16] Gerald R North. "The small ice cap instability in diffusive climate models". In: *Journal of Atmospheric Sciences* 41.23 (1984), pp. 3390–3395.

[17] Kristoffer Rypdal. *The Earth's Energy Budget*. Presentation. Department of Mathematics and Statistics, UiT The Arctic University of Norway, 2014.

[18] Christopher J Smith et al. "FAIR v1. 3: a simple emissions-based impulse response and carbon cycle model". In: *Geoscientific Model Development* 11.6 (2018), pp. 2273–2297.

[19] Henry Stommel. "Thermohaline convection with two stable regimes of flow". In: *Tellus* 13.2 (1961), pp. 224–230.

[20] Stephen Wiggins. "Local Bifurcations". In: *Introduction to Applied Nonlinear Dynamical Systems and Chaos*. Springer-Verlag, 1990. Chap. 3, pp. 253–263.

[21] Kirsten Zickfeld et al. "Is the Indian summer monsoon stable against global change?" In: *Geophysical Research Letters* 32.15 (2005).